Development and Characterisation of a Novel, Endothelialised *in vitro* Model of Human Atherothrombosis

A DRYSDALE

PhD 2023

Development and Characterisation of a Novel, Endothelialised *in vitro* Model of Human Atherothrombosis

AMELIA DRYSDALE

A thesis submitted in partial fulfilment of the requirements of the Manchester Metropolitan University for the degree of Doctor of Philosophy

Department of Life Sciences

Manchester Metropolitan University

2023

Abstract

Atherothrombosis is a leading cause of mortality worldwide and occurs following rupture or erosion of an atherosclerotic plaque. Current treatments focus on the use of antiplatelet therapy, which reduces but does not eliminate the risk of major vascular events. Historically, research to identify and develop novel antithrombotics has depended heavily on the use of murine *in vivo* models, where the endothelium is artificially damaged, exposing a healthy extracellular matrix. The lack of disease relevance and species variation however, render these models unrepresentative of human atherothrombosis. *In vitro* studies which usually comprise of flow chambers coated with Type I collagen overcome some of these issues by using human blood and relevant haemodynamic conditions, however they do not incorporate the dysfunctional matrices observed in plaque rupture and erosion and are often devoid of endothelial cells. Recent studies investigating the matrices associated with atherosclerosis have shown that matrix components in plaque rupture and erosion differ, as does the composition of thrombi associated with each plaque. Thrombi associated with plaque rupture are often occlusive and appear more fibrin- and erythrocyte-rich. In contrast, erosion thrombi, are platelet-rich and less occlusive. The composition and thrombogenicity of the matrix components in plaque rupture and erosion, and how this affects endothelial cell function and platelet responses, is a novel area of research. The aim of this project was to develop lesion specific, *in vitro* flow models of atherothrombosis, incorporating endothelial cells and the dysfunctional matrices observed in plaque rupture and erosion.

Firstly, recombinant disease-relevant matrices were established and incorporated into a flow model to investigate platelet responses to extracellular matrices associated with plaque rupture and erosion. It was observed that platelet thrombus formation and activation marker expression were significantly enhanced on Types I and III collagen compared with individual proteoglycans associated with plaque rupture and erosion. However, when added to collagen, vascular proteoglycans had a role in regulating thrombus formation on Type I collagen. To further explore the role of a multi-component extracellular matrix in arterial thrombosis, native extracellular matrices, derived from endothelial and smooth muscle cells, were isolated and characterised. Proteomic analysis identified key differences between the composition of endothelial

and smooth muscle cell matrices. Additionally, stimulating cells with common stimuli associated with cardiovascular disease, including cigarette smoke extract and TNF-α, significantly altered the composition and thrombotic properties of extracellular matrices generated from endothelial and smooth muscle cells.

Prior to the incorporation of endothelial cells into the model, comparisons were performed between human umbilical vein endothelial cells (HUVECs) and human coronary artery endothelial cells (HCAECs) to determine the most appropriate cell type to use. Transcript analysis demonstrated similarities in up- and down-regulation of key markers in the regulation of thrombosis in response to inflammatory stimuli, but the resting gene levels of both cell types differed significantly, demonstrating heterogeneity in their capacity to regulate thrombosis. HCAECs were therefore taken forward as the most disease relevant cell type, and successfully incorporated into the flow model under arterial shear stress. Different types of focal damage were evaluated including ferric chloride, needle stick injury and cell dissociation buffer, to enable translation of current *in vivo* protocols and to create a model of plaque erosion.

The final thrombosis model developed throughout the project incorporates vascular endothelial cells, a relevant shear stress and a disease-relevant extracellular matrix to enable investigations into arterial thrombosis as a result of plaque rupture or erosion. The findings from the project demonstrate that a multi-component extracellular matrix can regulate thrombus formation on Type I collagen, and that these components alter in response to different stimuli, demonstrating the importance of using a disease-relevant matrix when performing thrombus formation assays and evaluating antiplatelet efficacy. Uptake of this novel human model of thrombosis as an alternative to current *in vivo* models has the potential to significantly reduce the number of animals used in research, while providing a more relevant model to human atherothrombosis.

Acknowledgements

Firstly, I would like to thank Dr Sarah Jones for trusting me with the success of this project and giving me the autonomy to develop as a scientist throughout my time at MMU, I am endlessly grateful and could not have asked for a better mentor. I would also like to express my gratitude to Dr Amanda Unsworth and Dr Stephen White for their guidance throughout the course of this project, and for being consistent, enthusiastic and supportive throughout.

A special mention to everyone in the Cardiovascular Theme research group, MMU Thrombosis and all colleagues from the PhD/Postdoc offices and technical team who have been there for me when experiments have failed (and succeeded!), offered help with analysis, and lent an ear when I needed one, I have truly enjoyed being a part of such a talented, knowledgeable team and I look forward to working with you all in the future. A special thanks, also, to Dr Jon Humphries and the team at the Biological Mass Spectrometry Facility at the University of Manchester for all of the help and assistance with the ECM proteomics.

Thank you to my friends Nicole and Xenia for all of your support, and a special thanks to my supportive partner Paul and daughter Robyn, who have both suffered through many a presentation and speech! Finally, I would like to dedicate this thesis to the memory of my dearest Nan and greatest support, Ann Bell, I love and miss you every day.

Funding acknowledgements

This project was funded a part of an NC3Rs/BHF PhD studentship. The primary goal is to replace current animal models by creating a representative, humanised model of atherothrombosis and enabling comparability of the model with current *in vivo* models.

Contents

Presentations

2021

Poster presentation - Platelet Society Meeting, Keele

2022

Oral presentation - SVD@TheJeff Symposium, Manchester

Oral and poster presentations – Platelet Society Meeting, Hull

Poster presentation - International Society of Thrombosis and Haemostasis (ISTH), London

Poster presentation – European Platelet Network (EUPLAN), Milan

Poster presentation – Northern Vascular Biology Forum (NVBF), Liverpool

2023

Poster presentation – British Society for Cardiovascular Research (BSCR), Manchester

Poster presentation – Joint Platelet society/EUPLAN meeting, Bristol

Poster presentation – NVBF, Manchester (Second Poster Prize)

Publications

Drysdale, A., Unsworth, A., White, S. and Jones, S. (2023) 'The Contribution of Vascular Proteoglycans to Atherothrombosis: Clinical Implications.' *Int J Mol Sci.* 24(14) p11854.

Drysdale, A., Zaabalawi, A. and Jones, S. (2023) 'Modelling arterial thrombus formation *in vitro*.' *Curr Opin Hematol.* (31)1 p16-23.

Drysdale, A., Blanco-Lopez, M., White, S., Unsworth, A. and Jones, S. (2024) 'Differential proteoglycan expression in atherosclerosis alters platelet adhesion and activation.' *Int J Mol Sci.* 25(2) p.950

List of Tables/Figures

Tables

Figures

Abbreviations

AA – Arachidonic acid

ACD – Acid citrate dextrose

ACS – Acute coronary syndrome

ADAMTS - A disintegrin and metalloproteinase with thrombospondin motifs

ADP - Adenosine diphosphate

AGRN - Agrin

AMP - Adenosine monophosphate

ANOVA – Analysis of variance

ANX - Annexin

APS - Ammonium persulphate

AT – Antithrombin

ATP - Adenosine triphosphate

BSA – Bovine serum albumin

BSP - Bone sialoprotein

C1q – Complement component 1q

cAMP - Cyclic adenosine monophosphate

CDM – Cell-derived extracellular matrix

cGMP - Cyclic guanosine monophosphate

CHAD - Chondroadherin

CHAPS - 3-((3-cholamidopropyl) dimethylammonio)-1-propanesulfonate

COL - Collagen

COX - Cyclooxygenase

CS – Chondroitin sulphate

CSPG2 - Versican

CSE – Cigarette smoke extract

CTI – Corn trypsin inhibitor

DAPT – Dual antiplatelet therapy

DAG – Diacylglycerol

dECM – Decellularised ECM

DIC - Differential interference contrast

DIOC-6 - 3,3′-Dihexyloxacarbocyanine iodide

DMP1 - Dentin matrix acidic phosphoprotein 1

DMSO - Dimethylsulphoxide

DPBS – Dulbecco's phosphate buffered saline

DPP - Decapentaplegic

DS – Dermatan sulphate

DSP - Desmoplakin

DTS – Dense tubular system

ECG - Electrocardiogram

ECM – Extracellular matrix

ECs – Endothelial cells

EDTA - Ethylenediaminetetraacetic acid

EGFR - Epidermal growth factor receptor

EMILIN - Elastin microfibril interfacer

EPCR - Endothelial protein C receptor

ERK - Extracellular signal-related kinase

FACITS - Fibril-associated collagens

FAK – Focal adhesion kinase

FBS – Foetal bovine serum

FCS – Foetal calf serum

FeCl3 – Ferric chloride

FN – Fibronectin

FRAS1 - Fraser extracellular matrix component 1

FREM - FRAS1-related extracellular matrix component

FV – Factor V

GAGs – Glycosaminoglycans

GDP - Guanosine diphosphate

GP – Glycoprotein

GPCR - G protein-coupled receptor

GTP - Guanosine triphosphate

HA – Hyaluronan

HABP – Hyaluronan binding protein

HAS – Hyaluronan synthase

HBSS – Hank's balanced salt solution

HCAEC – Human coronary artery endothelial cell

HCASMC – Human coronary artery smooth muscle cell

HCII – Heparin cofactor II

HETE - Hydroxyeicosatetraenoic acid

HMW – High-molecular weight

HS – Heparin sulphate

HSPG2 - Perlecan

HUVEC – Human umbilical vein endothelial cell

HYAL - Hyaluronidase

Ig – Immunoglobulin

IL – Interleukin

IMS - Industrial methylated spirits

IP3 - Inositol 1,4,5 triphosphate

KS – Keratan sulphate

LAM - Laminin

LDL – Low-density lipoprotein

LGALS - Galectin

LMW – Low-molecular weight

LOX – Lysyl oxidase

MACITS - Membrane-associated collagens

MAPK – Mitogen-activated protein kinase

MATN2 – Matrilin

MFI – Median fluorescence intensity

MI – Myocardial infarction

MMPs – Matrix metalloproteinases

MMU – Manchester Metropolitan University

MPO - Myeloperoxidase

NETs – Neutrophil extracellular traps

NH4OH – Ammonium hydroxide

NO – Nitric oxide

NOS – Nitric oxide synthase

NPNT - Nephronectin

NSAID – Non-steroidal anti-inflammatory drug

OCS - Open canalicular system

OPN - Osteopontin

PAF – Platelet activating factor

PAI-1 – Plasminogen activator inhibitor-1

PAR – Protease-activated receptor

PC – Protein C

PDGF – Platelet-derived growth factor

PDMS - Polydimethylsiloxane

PF4 – Platelet factor 4

PFA - Paraformaldehyde

PGH2 – Prostaglandin H2

PGI2 – Prostacyclin

PGs – Proteoglycans

PIP - Phosphatidylinositol (4,5)-bisphosphate

PKC – Protein kinase C

PLA2 – Phospholipase A2

PLC – Phospholipase C

PLG - Plasminogen

PRELP - Proline and arginine-rich end leucine rich repeat protein

PRP – Platelet-rich plasma

PS – Phosphatidylserine

rH – Recombinant human

RHAMM - Receptor for hyaluronan-mediated motility

ROS – Reactive oxygen species

RT – Room temperature

SDS - Sodium dodecyl sulphate

SEM – Standard error of the mean

SERPINE1 – Plasminogen activator inhibitor 1

SLRP – Small leucine-rich proteoglycan

SMA – Smooth muscle actin

SMCs – Smooth muscle cells

SNAREs - Soluble N-ethylmale-imide-sensitive factor-attachment protein receptors

TGF – Transforming growth factor

THBS - Thrombospondin

TF – Tissue factor

TFPI – Tissue factor pathway inhibitor

TLR – Toll-like receptor

TM – Thrombomodulin

TNC - Tenascin

TNF - Tumour necrosis factor

TP – Thromboxane receptor

tPA – Tissue-type plasminogen activator

TSG – TNF-stimulated gene

TSP – Thrombospondin

TXA2 – Thromboxane A2

uPA – Urokinase plasminogen activator

VEGF - Vascular endothelial growth factor

VEGFR - Vascular endothelial growth factor receptor

VN - Vitronectin

vWF – von Willebrand Factor

WP – Weibel Palade bodies

1. Introduction

1.1 General Introduction

Acute coronary syndrome (ACS) is a term used to describe ischaemic heart conditions, including ST elevated and non-ST elevated myocardial infarction (MI) and unstable angina pectoris (Dai *et al.,* 2016). It occurs primarily as a result of atherosclerotic plaque rupture, erosion or calcified nodules (Jia *et al.,* 2013; Thygesen *et al.,* 2018). In 2019, mortality from ACS reached over 9 million worldwide, a rise of 11% from 1990 (Vos *et al.,* 2020). Plaque rupture occurs on macrophage and lipid-rich plaques with thin fibrous caps, whereas erosion generally occurs on plaques with few resident leukocytes and a thickened fibrous cap comprising an abundance of vascular smooth muscle cells (SMCs) and extracellular matrix (ECM) proteins (Farb *et al.,* 1996; Burke *et al.,* 2003; Kolodgie *et al.,* 2004; Virmani *et al.,* 2006; Pedicino *et al.,* 2018). Both fibrous cap rupture and endothelial erosion can promote formation of an occlusive thrombus, reducing or ablating perfusion and potentially triggering Type I MI. This is diagnosed using a variety of clinical tools, including imaging, electrocardiogram (ECG) and measurement of various biomarkers including troponin (Roffi *et al.,* 2016; Feinberg *et al.,* 2017; Cohen and Visveswaran, 2020)., Current treatments include the use of dual antiplatelet therapy (DAPT) and anticoagulants (Cohen and Visveswaran, 2020; Matsuzawa *et al.,* 2021). There is emerging evidence suggesting that differences between plaque phenotype may be responsible for limited treatment efficacy, and distinguishing between plaque type may help to improve patient therapies. This chapter will therefore begin by discussing normal vascular and platelet function, and how a combination of risk factors and cellular dysfunction can lead to the development of different types of atherosclerotic plaque. The role of the endothelium and ECM proteins will be discussed in detail, in direct relevance to data presented in subsequent results chapters.

1.2 Coronary artery structure and physiology

The coronary arteries provide the cardiac system with oxygen-rich blood to ensure normal function. Rheological dynamics and the vascular environment within coronary arteries are therefore essential factors in maintaining cardiac health. Vessel integrity is maintained by the structure of the vascular wall, of which there are three main components – the tunica intima, media and adventitia. The innermost intimal layer consists of an endothelial monolayer and a sub-endothelial collagen-rich basement membrane and internal elastic lamina, with ECM components and SMCs located deeper in the tunica media (Fatkhullina *et al.,* 2016). The outermost adventitia in large arteries contains the vasa vasorum – a network of small blood vessels which supply the vascular wall with essential nutrients and oxygen.

1.2.1 Vascular endothelial cells

1.2.1.1 Appearance and function

Endothelial cells (ECs) are small vascular cells, measuring around 30-50µm in length and 10-30µm in width (Kruger-Genge *et al.,* 2019). *In vivo,* ECs are elongated, and line up in the direction of blood flow, whereas *in vitro* ECs cultured under static conditions have a cobblestone appearance, although they maintain the ability to alter their phenotype when cultured under flow (Dunzendorfer *et al.,* 2004; Kroon *et al.,* 2017; Vion *et al.,* 2021). ECs have a key role in mediating interactions between the vascular wall and blood components, specifically red blood cells, leukocytes and platelets (Hennigs *et al.,* 2021). The EC glycocalyx mediates endothelial permeability, aiding the passage of cells and other molecules to the sub-endothelial layer (Reitsma *et al.,* 2007; Hamilos *et al.,* 2018). In addition, ECs maintain vessel homeostasis by regulating vascular tone and suppressing SMC proliferation in the tunica media, preventing the invasion of these cells into the intimal layer (Scott-Burden and Vanhoutte, 1994; Li *et al.,* 2018; Kruger-Genge *et al.,* 2019).

1.2.1.2 Regulation of platelet activity and coagulation

In addition to vessel homeostasis, the endothelium also has a key role in regulation of thrombosis, coagulation and thrombolysis. The release of vasodilators such as nitric oxide (NO) and prostacyclin from the healthy endothelium inhibit platelet activation and aggregation, maintaining platelet quiescence, by increasing intracellular cyclic guanosine monophosphate (cGMP) and cyclic adenosine monophosphate (cAMP) levels respectively (Armstrong, 1996; Moro *et al.,* 1996; Chan *et al.,* 2016)**.** In addition, endothelial-derived CD39 hydrolyses circulating adenosine diphosphate (ADP) to adenosine monophosphate (AMP) (Kaczmarek *et al.,* 1996; Hamilos *et al.,* 2018), preventing unwarranted platelet activation. Thrombomodulin (TM) expressed on the surface of ECs prevents aberrant coagulation by binding to thrombin together with the endothelial protein C receptor (EPCR), activating the protein C pathway to inactivate active Factor V (FVa) and FVIIIa. The expression of tissue factor pathway inhibitor (TFPI) inhibits tissue factor (TF)-FVIIa activity (van Hinsbergh, 2012), and soluble antithrombin (AT) binds to proteoglycans on the EC glycocalyx to inhibit thrombin, disrupting the continuation of the coagulation cascade (Catieau *et al.,* 2018). Finally, fibrinolysis is promoted by secretion of tissue-type plasminogen activator (tPA), which converts plasminogen to plasmin via Annexin A2 (Navarro *et al.,* 2011; Kruger-Genge *et al.,* 2019; Lim and Hajjar, 2021)**.** A summary of important endothelial-derived mediators and their regulation of platelet activity is outlined in Figure 1.1.

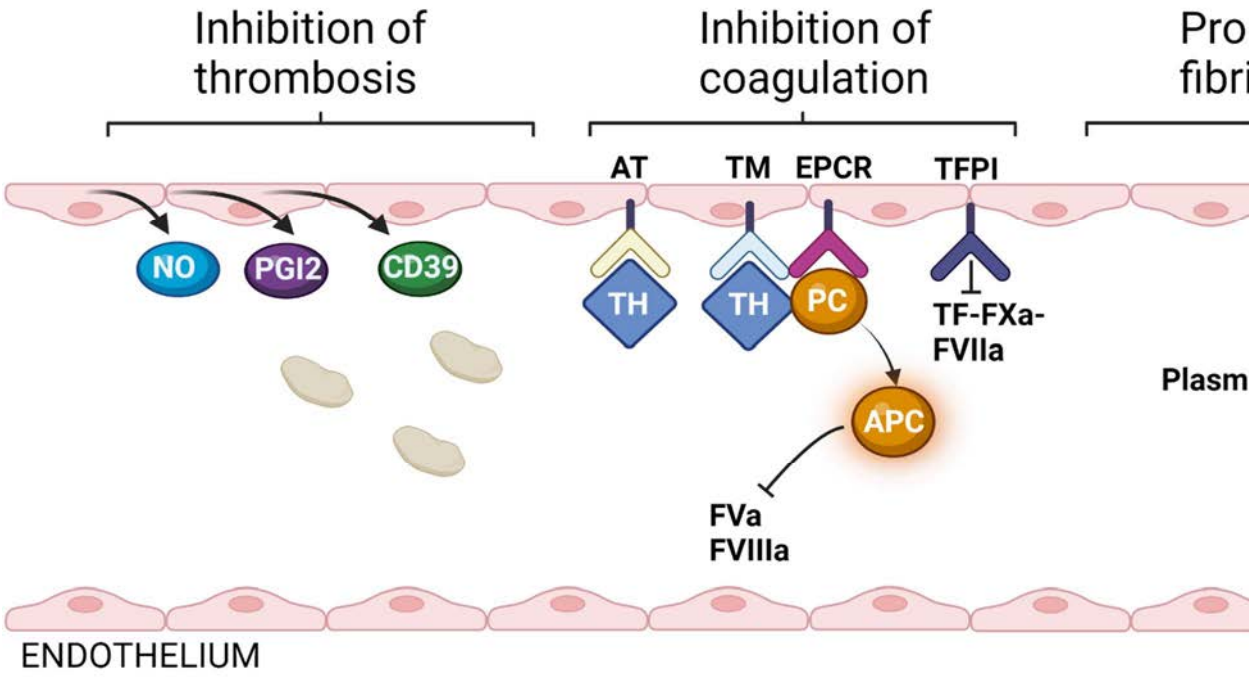

Figure 1.1 – Endothelial regulation of thrombosis and haemostasis. Endothelial release of nitric oxide (NO) and p
AMP, and CD39 hydrolyses adenosine diphosphate to adenosine monophosphate, inhibiting platelet activation
thrombomodulin (TM) expressed on the surface of endothelial cells inhibit coagulation by binding to thrombin (T
endothelial protein C receptor (EPCR), binding protein C (PC) and activating the protein C pathway (APC) to inactiv
inhibitor (TFPI) inhibits TF-FXa-FVIIa activity, and fibrinolysis is promoted by secretion of tissue-type plasminogen ac
to plasmin. Created with BioRender.com.

1.2.2 Vascular smooth muscle cells

SMCs are spindly, non-striated, uninuclear cells measuring around 200µm in length, located in the tunica media of coronary arteries (Wilson, 2011; Durham *et al.,* 2018; Frismantiene *et al.,* 2018). SMCs produce a large portion of the vascular ECM, and have roles in the regulation of vessel tone, blood pressure and contraction (Owens *et al.,* 2004; Gang Wang *et al.,* 2015), the latter of which is made possible by the presence of actin and myosin filaments spanning the length of the cell. SMCs are extremely sensitive to environmental cues, and are rich in cell junctions, which link adjacent cells and control cell synchronisation and membrane potential (Touyz *et al.,* 2018). Under normal function, in a human coronary artery, SMCs exhibit a quiescent phenotype, and express a variety of markers necessary for contraction, such as α smooth muscle actin (α-SMA), smooth muscle myosin heavy chain, calponin and smoothelin, amongst others (Gang Wang *et al.,* 2015; Bennett *et al.,* 2016).

1.2.3 The sub-endothelial extracellular matrix

The ECM consists of a viscoelastic network of fibrillar proteins, surrounded by vascular proteoglycans (PGs), glycoproteins and various matricellular proteins. This network acts as a structural scaffold for cells and comprises two matrices. The pericellular matrix surrounds cells, and consists of laminin, perlecan, collagen IV and integrins, and the outermost interstitial matrix contains elastin, fibronectin, collagens, extracellular proteoglycans and other ECM macromolecules (Figure 1.2) (Theocharis *et al.,* 2016). Vascular proteoglycans are important regulators of the vascular wall, and support cell function by forming a glycocalyx around cells, mediating cell permeability and interaction with growth factors, cytokines and chemokines as well as crosstalk between vascular ECs and SMCs (Iozzo and Schaefer, 2015; Ganesan *et al.,* 2017; Hamilos *et al.,* 2018). The vascular ECM is composed of proteins secreted from both ECs and SMCs. Indeed, previous studies have demonstrated differences in the ECM profiles of ECs and SMCs (Lavigne *et al.,* 2010), albeit without characterisation of specific ECM components.

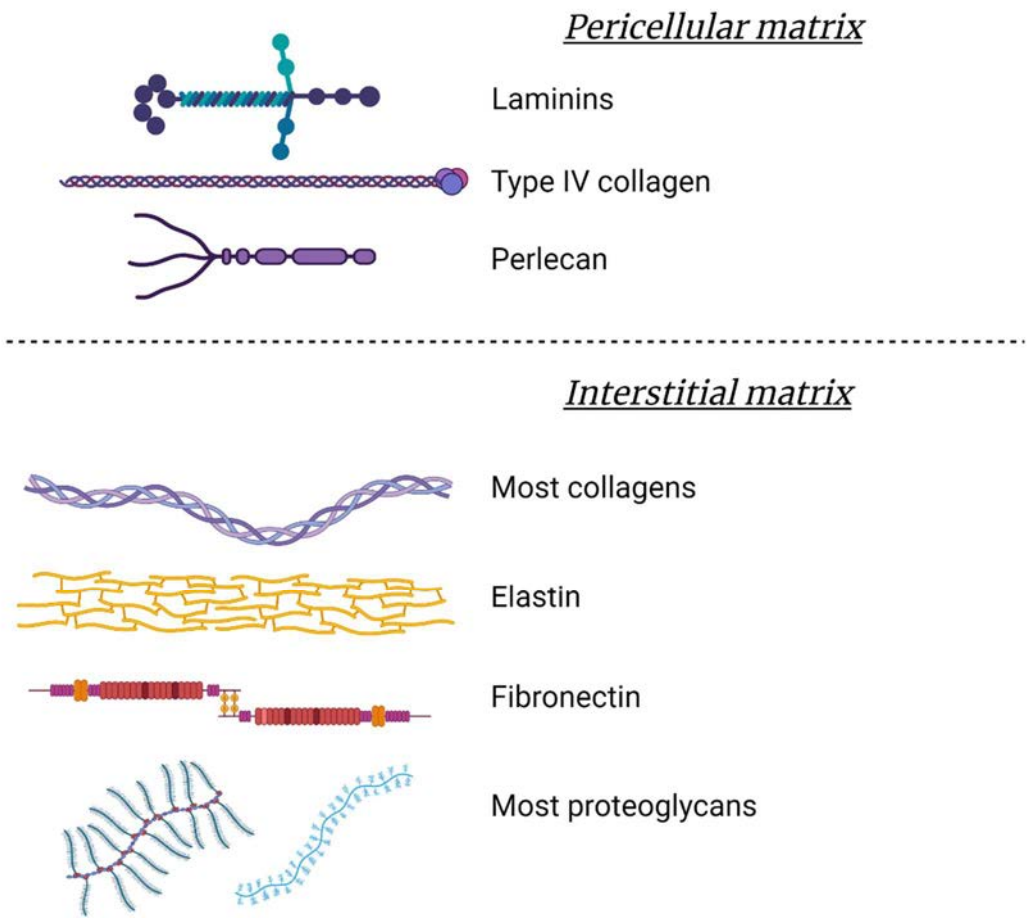

Figure 1.2 – Structural composition of the vascular extracellular matrix. Vascular cells are surrounded by a pericellular extracellular matrix and an outermost interstitial extracellular matrix. The pericellular matrix is composed of basement membrane proteins, including perlecan, Type IV collagen and laminins, and the interstitial matrix contains most collagens and proteoglycans, fibronectin and elastin. The vascular ECM also contains growth factors, cytokines and integrins (not shown). Created with BioRender.com.

1.2.3.1 Fibrillar proteins

The most abundant proteins located in the ECM are the fibrillar proteins, including the collagens, elastin and fibronectin (Yamauchi *et al.,* 2018). Collagen fibres are stiffer than elastin and fibronectin (Sun, 2021), and each protein has a different functional role within the ECM.

Collagens

There are 28 different types of collagen present in the human body, which can be categorised into fibril-forming collagens (Types I, II, III, V, XI, XXIV and XXVII), network-forming collagens (Types IV, VIII and X), fibril-associated collagens (FACITS) (Types IX, XII, XIV, XVI, XIX, XX, XXI and XXII), membrane-associated collagens (MACITS) (Types XIII, XVII, XXIII, XXV), beaded filament-forming collagens (Types VI, XXVI and XXVIII), anchoring fibril collagen (Type VII) and endostatin-producing collagens (Types XV and XVIII) (Gordon and Hahn, 2010; Theocharis *et al.,* 2016; Karamanos *et al.,* 2021). The primary function of collagen is to provide ECM structural support and stability, and various post-translational modifications, including glycosylation and hydroxylation, further add to the versatility of this protein (Yue, 2014).

Type I collagen is the major structural collagen present in tissues, and upon secretion, undergoes cleaving of its propeptides. Crosslinking between lysine residues, catalysed by lysyl oxidase (LOX), facilitates fibril assembly (Palombo *et al.,* 2014; Yue, 2014; Sun, 2021), which then self-assemble to form collagen fibres of different sizes, depending on tissue type, ambient conditions such as pH and temperature, and the presence of vascular PGs such as biglycan and decorin (Theocharis *et al.,* 2016; Holmes *et al.,* 2018; Sun, 2021). Usually, there is an abundance of one type of collagen, which other ECM components and non-fibrillar collagens then interact with to dictate overall ECM architecture and function, influencing aspects of cell behaviour including migration, angiogenesis and tissue repair (Theocharis *et al.,* 2016; Chaudhuri *et al.,* 2020)

Elastin

The primary function of elastin is to provide elasticity to tissues undergoing significant stretching, which includes the vascular wall. Elastin fibres bind to collagen fibrils, aiding tissue recoil after stretching (Sun, 2021). Elastin is secreted as tropoelastin, which, similarly to collagen, crosslinks its lysine residues following LOX activity, giving rise to

desmosine and isodesmosine, amino acids essential to elastic fibre stability (Palombo *et al.,* 2014; Yue, 2014; Ozsvar *et al.,* 2021). The proportion of elastin present has an influence on the mechanical properties of the ECM and is important in physiological function, in addition to diseases such as atherosclerosis (Palombo *et al.,* 2014). The fibres are degraded by proteases such as matrix metalloproteinases (MMPs), and are often improperly repaired, resulting in dysfunction (Van Doren, 2015; Theocharis *et al.,* 2016).

Fibronectin

Fibronectin (FN) is a ubiquitous ECM protein which regulates not only ECM tension, but also interaction with a variety of cells, growth factors and ECM macromolecules (Karamanos *et al.,* 2021). FN is secreted in its soluble form as dimers, able to bind other dimers, fibrin, collagen and various cell surface receptors (Yue, 2014). Fibrillogenesis occurs following cell intervention, converting FN to its functional fibrillar form, which unfolds to expose integrin binding sites (Schwarzbauer and DeSimone, 2011; Theocharis *et al.,* 2016; Sun, 2021). Alternative splicing of FN can give rise to isoforms with roles in cell adhesion, differentiation and signalling, and can aid in wound healing by binding to fibrin and facilitating cell migration to fibrin clots (Makogonenko *et al.,* 2002; Dalton and Lemmon, 2021).

1.2.3.2 Vascular proteoglycans

Proteoglycans and glycosaminoglycans (GAGs) are key components of the vascular ECM and have roles in the regulation of vascular function. The core GAGs found in the vascular wall are chondroitin sulphate (CS), dermatan sulphate (DS), heparan sulphate (HS) and keratan sulphate (KS), which may attach to a core protein to form a proteoglycan (Wight, 2018). The exception is hyaluronan (HA), a GAG which does not attach to a core protein. Vascular proteoglycans and GAGs are important in the development and progression of an atherosclerotic plaque and regulate cell behaviour and platelet function (Fischer *et al.,* 2001; Guidetti *et al.,* 2002; Schaefer *et al.,* 2003; D'Antoni *et al.,* 2012; Grandoch *et al.*, 2016), as well as having roles in lipid retention, elastic fibre assembly and inflammation (O'Brien *et al.,* 2004; Hwang *et al.,* 2008; Poluzzi *et al.,* 2019).

Biglycan

Biglycan is a Class I small leucine-rich proteoglycan (SLRP) located in the vascular wall, comprising a protein core and two GAG chains of CS or DS (Wight, 2018). It is synthesised by a variety of cells, including ECs, fibroblasts and SMCs (Grandoch *et al.,* 2016). GAG elongation is regulated by the mitogen-activated protein kinase (MAPK) pathway, specifically extracellular signal-related kinase (ERK)-1 and -2 (Getachew *et al.,* 2010). Biglycan expression can regulate cell behaviour, SMC migration and inflammation in the vascular wall. It has a pro-angiogenic effect on ECs (Chui *et al.,* 2017), perhaps elucidated by its ability to bind vascular endothelial growth factor (VEGF)-A, increasing availability of the growth factor in the sub-endothelial matrix (Berendsen *et al.,* 2014). Biglycan also supports smooth muscle cell migration by reducing focal adhesion kinase (FAK) levels and vinculin gene expression in cells (D'Antoni *et al.,* 2012), negatively regulating formation of focal adhesions.

Decorin

Decorin is a SLRP structurally similar to biglycan, possessing a protein core but only one GAG chain of CS or DS (Robinson *et al.,* 2017). Decorin binds to collagen I via the protein's C-terminal (Keene *et al.,* 2000; Paderi *et al*., 2011; Wight, 2018) and has a role in collagen crosslinking and structure and connective tissue functionality (Iozzo and Schaefer, 2015; Robinson *et al.,* 2017). Decorin can negatively regulate cell growth by impairing SMC response to transforming growth factor (TGF)-β (Yamaguchi *et al.,* 1990; Fischer *et al.,* 2001), and by activating the epidermal growth factor receptor (EGFR) pathway, resulting in activation of p21 (Iozzo *et al.,* 1999), a suppressor of cell growth. Exposure to decorin reduces cell proliferation and focal adhesion formation in SMCs, inducing a migratory phenotype (D'Antoni *et al.,* 2012). The effects of this proteoglycan, however, appear to be cell specific. Indeed, recent studies have shown decorin increasing endothelial proliferation and angiogenesis (Paderi *et al.,* 2011; Chui *et al.,* 2014; Scott *et al.,* 2017) and evoking autophagy in endothelial cells via vascular endothelial growth factor receptor (VEGFR)2 (Buraschi *et al.,* 2013).

Versican

Versican is a large extracellular hyalectan encoded by the gene CSPG2 (Naso *et al.,* 1994; Iozzo and Schaefer, 2015), and comprises an N-terminal G1 domain which binds HA and

thrombospondin-1 (Naso *et al.,* 1994; Kuznetsova *et al.,* 2006), a GAG attachment region and an adhesive lectin-binding G3 domain (Naso *et al.,* 1994; Wight, 2002; Wu *et al.,* 2002; Zheng *et al.,* 2006). At least five isoforms of versican exist due to alternate exon splicing (Wight, 2018). RNA splicing occurs in Exon 7 and 8, which encode versican GAG attachment sites α and β respectively (Dours-Zimmermann and Zimmermann, 1994; Naso *et al.,* 1994; Bogen *et al.,* 2019). Isoform V0 contains both Exon 7 and 8, V1 contains Exon 8, V2 contains Exon 7 and V3 has no GAG attachment sites (Wight, 2002). The expression of each versican isoform is linked to cell phenotype (Coulson-Thomas *et al.,* 2014; Petrey and de la Motte, 2014), and each isoform holds a different function, which may be dependent on its location in the body (Wu *et al.,* 2002; Wight, 2017). V1 and V3 are the most common isoforms found in SMCs (Lemire *et al.,* 1999; Iozzo and Schaefer, 2015), and have opposing roles in the vasculature. V1 promotes cell proliferation and migration, whereas V3 suppresses cell activity and has an overall anti-inflammatory effect (Wight *et al.,* 2014).

Hyaluronan

Hyaluronan is a large, negatively charged, non-sulphated GAG with unique hydrodynamic properties (Toole, 2004, Liang *et al.,* 2016, Litwiniuk *et al.,* 2016), and is abundant in all tissues, including the vascular ECM. It is synthesised by hyaluronan synthase (HAS)-1, -2 and -3 on the inner surface of the cellular membrane, before being extruded into the extracellular space through a pore (Evanko *et al.,* 2001; Tammi *et al.,* 2002; Toole, 2004; de la Motte *et al.,* 2009; Litwiniuk *et al.,* 2016; Wight, 2017). Hyaluronan binds to receptor for hyaluronan-mediated motility (RHAMM) and CD44, which regulate cell migration and endothelial cell adhesion and proliferation respectively (Turley *et al.,* 2002; Toole, 2004; D'Agostino *et al.,* 2017). CD44 receptor binding to hyaluronan results in CD44 clustering and the activation of signalling pathways such as p38, ERK, Akt and FAK (Wight, 2017), regulating cell proliferation and adhesion, proteoglycan synthesis and inflammation (Zarubin and Han, 2005; Slevin *et al.,* 2007; Osman *et al*., 2014; Manning and Toker, 2017). Hyaluronan inhibits angiogenesis and cell proliferation, coating cells in a glycocalyx with antioxidant and anti-inflammatory properties (Slevin *et al.,* 2007; de la Motte *et al.,* 2009; Litwiniuk *et al.,* 2016; Li *et al.,* 2017; Wight, 2017), maintaining a healthy endothelium. Together with fibrin, it crosslinks and forms a network in the ECM, aiding fibroblast and SMC migration (Weigel *et al.,* 1986; Schultz and Wysocki, 2009; Otsuka *et al.,* 2016; Wight, 2017).

1.3 Platelets

Platelets are small, anucleate cells of around 2-5µm which circulate in the bloodstream with an average lifespan of 7-10 days (Quach *et al.,* 2018). They are formed from megakaryocytes in the bone marrow or lung, which release platelets into the circulation in a resting state (Jurk and Kehrel, 2005; Yadav and Storrie, 2016). Following vascular injury or endothelial dysfunction, platelets can activate to form thrombi and promote wound healing and coagulation. The role of platelets in thrombosis and haemostasis has been well-characterised, but recent evidence demonstrates additional roles for these cells in inflammation, immunity and atherogenesis (Thon and Italiano, 2012; Koupenova *et al.,* 2018).

1.3.1 Structure

The main structural components of a platelet are the plasma membrane, the actin cytoskeleton, the open canalicular system (OCS), the dense tubular system (DTS), and the organelles, including platelet granules (Figure 1.3) (Thon and Italiano, 2012; Gremmel *et al.,* 2016). The platelet plasma membrane consists of a phospholipid bilayer comprising glycoproteins and glycolipids, and regulates platelet function through receptors, which include integrins, transmembrane receptors, C-type lectins and the immunoglobulin (Ig) superfamily (Thon and Italiano, 2012; Gremmel *et al.,* 2016; Kunde and Wairkar, 2021). The sub-membrane space contains actin fibres, required for platelet shape change, structural support, receptor translocation and granule transport prior to secretion (Bearer *et al.,* 2002; Gremmel *et al.,* 2016).

The OCS is connected to the plasma membrane and consists of a network of channels with roles in platelet spreading, granule secretion and transport of plasma components, including fibrinogen and TF, to alpha granules (Thon and Italiano, 2012; Gremmel *et al.,* 2016; Yadav and Storrie, 2016; Selvadurai and Hamilton, 2018). The DTS also consists of membrane-enclosed channels and is a source of calcium sequestration and release. Thrombin-induced platelet activation leads to phosphorylation of protease-activated receptor (PAR)-1, which activates phospholipase C (PLC) to generate inositol 1,4,5 triphosphate (IP3). IP3 binds type II receptors on the DTS membrane to stimulate the release of calcium, regulating granule transport and platelet shape change (Kroll and Schafer, 1989; Ebbeling *et al.,* 1992; Jurk and Kehrel, 2005, Thon and Italiano, 2012).

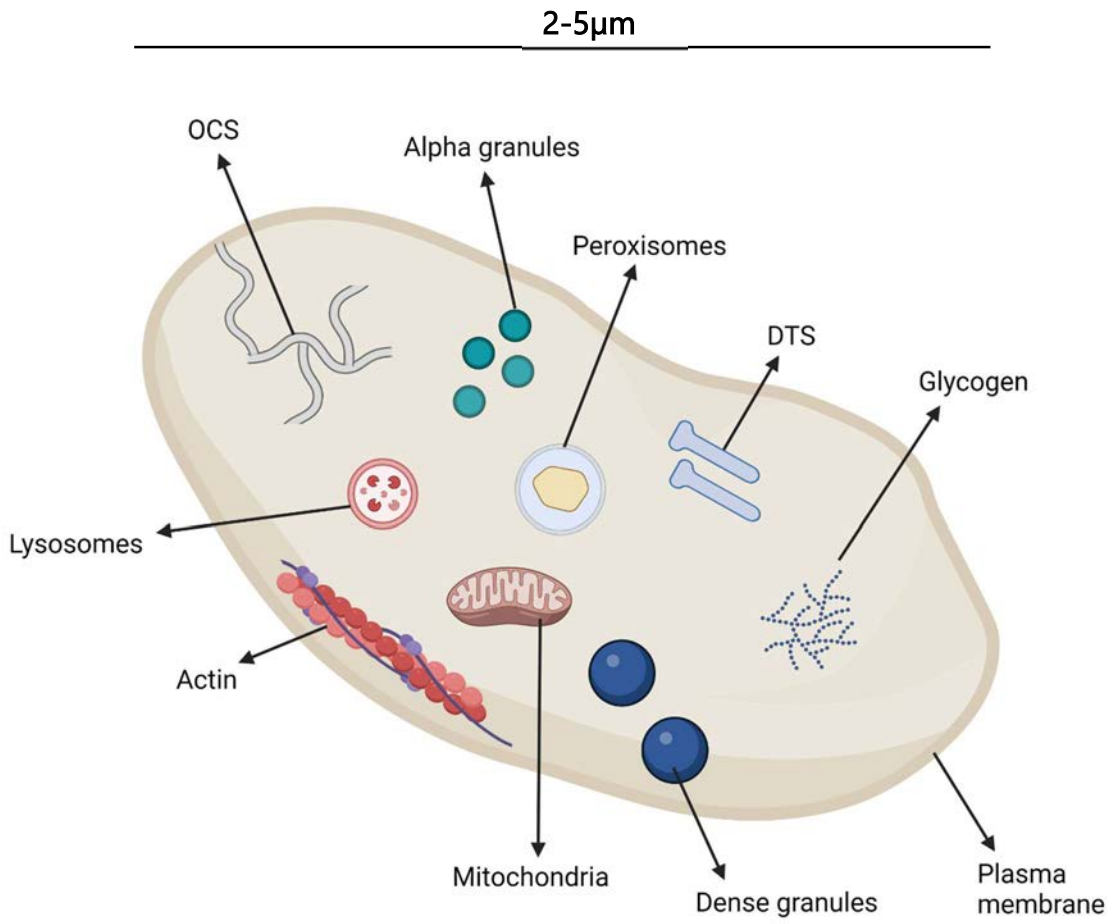

Figure 1.3 – The structure of a platelet. Organelle distribution in a resting platelet, including the open canalicular system (OCS) and dense tubular system (DTS), alpha and dense granules, peroxisomes and lysosomes, mitochondria and the actin cytoskeleton and plasma membrane. Granule secretion is propagated upon fusion with the plasma membrane in the OCS, and calcium is sequestered and released in the DTS. Created with BioRender.com.

The final structural components of a platelet are the organelles, consisting of alpha, dense and T granules, peroxisomes, lysosomes and mitochondria (Thon and Italiano, 2012; Gremmel *et al.,* 2016; Yadav and Storrie, 2016; Chen *et al.,* 2018). Lysosomes and peroxisomes contain enzymes involved in protein degradation, including cathepsins, collagenase and elastase, and mitochondria provide the platelet with the energy required for haemostatic function (Thon and Italiano, 2012; Gremmel *et al.,* 2016; Holinstat, 2017).

The granules are the primary components involved in haemostasis and regulation of surrounding cells. Alpha granules are derived from the trans-golgi network and are the most abundant, with each platelet containing up to 80 granules (Thon and Italiano, 2012; Gremmel *et al.,* 2016; Yadav and Storrie, 2016; Holinstat, 2017). Alpha granules contain over 800 proteins (Zufferey *et al.,* 2014), comprising proteins synthesised from megakaryocytes, including thrombospondin (TSP) and platelet factor 4 (PF4), and proteins endocytosed from plasma, including fibrinogen and vitronectin (Jurk and Kehrel, 2005). Proteins may be soluble (secreted) or membrane-associated, and have roles in the regulation of cell adhesion, migration, angiogenesis, inflammation and immunity (Gremmel *et al.,* 2016; Fernandez-Moure *et al.,* 2017). Endosomal-derived dense granules, in contrast, are smaller and much less abundant, with each platelet containing only up to 8 granules (Thon and Italiano, 2012; Gremmel *et al.,* 2016). Dense granules contain small molecules important in haemostasis and coagulation, including adenosine triphosphate (ATP), ADP, serotonin, calcium and magnesium (Jurk and Kehrel, 2005; Thon and Italiano, 2012; Golebiewska and Poole, 2015; Gremmel *et al.,* 2016; Holinstat, 2017). T-granules are a more recently described granule involved in antimicrobial host defence, releasing toll-like receptors (TLRs) to activate neutrophil extracellular traps (NETs) (Fernandez-Moure *et al.,* 2017).

1.3.2 Function

The primary functional role of platelets is in the regulation of haemostasis. Vascular injury results in exposure of the sub-endothelial ECM, which interacts with platelet surface receptors, including glycoprotein (GP)Ib and GPVI, to induce conformational

change of integrins α2bβ3, α2β1 and αVβ3, allowing ligand binding to fibrinogen, von Willebrand Factor (vWF) and other ECM proteins, and mediating platelet-platelet interactions (Golebiewska and Poole, 2015). Adhesion to vascular wall ECM, and activation of platelet receptors leads to initiation of platelet signalling cascades, which leads to mobilisation of intracellular calcium, driving granule secretion. Platelet granules are transported to the OCS and fuse with the plasma membrane via soluble N-ethylmale-imide-sensitive factor-attachment protein receptors (SNAREs), before their contents are secreted extracellularly or exposed on the platelet surface (Thon and Italiano, 2012; Holinstat, 2017; Selvadurai and Hamilton, 2018). Oxidation of fatty acids, such as arachidonic acid (AA), results in the production of prostaglandins including thromboxane A2 (TXA2), which are also released from platelets (Holinstat, 2017). Secreted ADP and TXA2 recruit nearby platelets to the site of injury, and thrombin binding promotes calcium release from the DTS, further propagating platelet activation and aggregation in the growing thrombus (Golebiewska and Poole, 2015). Phosphatidylserine (PS) exposure on activated platelets facilitates activation of the coagulation pathway and the conversion of fibrinogen to fibrin, forming a stable fibrin-rich clot (Kaminska *et al.,* 2018).

1.3.3 Adhesion receptors

Platelets have many surface receptors, but the most important GPs and integrins involved in platelet adhesion, activation, aggregation and signalling are GPIb-IX-V, GPVI, integrin α2β1 and integrin α2bβ3 (Gremmel *et al.,* 2016; Kunde and Wairkar, 2021).

1.3.3.1 GPIb-IX-V

The GPIb-IX-V complex is composed of GPIbα, GPIbβ, GPIX and GPV, with GPIbα, a type I transmembrane receptor, being responsible for almost all receptor binding in the complex (Canobbio *et al.,* 2004; Quach and Li, 2020). GPIb-IX-V mediates platelet adhesion to cells and ECM proteins via its interaction with a number of ligands, including vWF, P-selectin, Mac-1 and coagulation factors XII, XI and II (thrombin) (Gardiner and Andrews, 2014; Holinstat, 2017). The interaction of this complex with vWF, however, is especially important under high shear conditions in vessels such as arterioles. vWF is a GP stored in Weibel Palade bodies (WP) and alpha granules in ECs and platelets

respectively, and is deposited into the vessel ECM by ECs. Under high shear, GPIb-IX-V-vWF binding is responsible for tethering platelets effectively from the bloodstream to the site of dysfunction or injury, bridging the interaction between platelets and ECM collagen, and promoting platelet adhesion and shape change as well as transmembrane signalling (Canobbio *et al.,* 2004; Randi *et al.,* 2018). Only following this interaction can thrombus growth occur, facilitating activation of integrin αIIbβ3 and platelet interactions with fibrinogen (Gremmel *et al.,* 2016; Quach and Li, 2020).

1.3.3.2 GPVI

GPVI is a receptor from the Ig superfamily, and is the major collagen receptor expressed on the surface of platelets, but also has the ability to bind fibrin, fibronectin, vitronectin and laminin (Andrew and Berndt, 2004; Gremmel *et al.,* 2016; Holinstat, 2017; Rayes *et al.,* 2019; Kunde and Wairkar, 2021). GPVI exists in monomeric and dimeric form, with the dimeric form having a much higher affinity for collagen. Receptor dimerisation occurs upon platelet activation, reinforcing platelet adhesion and activation, and enabling collagen interaction with low affinity GPVI (Gawaz *et al.,* 2014). Activation of GPVI initiates tyrosine phosphorylation, which activates PLC to convert phosphatidylinositol (4,5)-bisphosphate (PIP) into diacylglycerol (DAG) and IP3. DAG activates the protein kinase C (PKC) pathway, leading to activation of integrins αIIβI and αIIbβ3, and IP3 leads to an increase in intracellular calcium, regulating platelet shape change and granule secretion (Gremmel *et al.,* 2016; Huang *et al.,* 2019; Rayes *et al.,* 2019). Following GPVI binding and under high shear rates, the receptor is shed from the platelet to prevent further activation downstream of the vessel injury (Gardiner and Andrews, 2014; Gremmel *et al.,* 2016; Rayes *et al.,* 2019).

1.3.3.3 Integrin αIIβ1

Integrin αIIβ1 is a heterodimeric transmembrane receptor, not exclusive to platelets, which is involved in platelet adhesion to ECM proteins, including collagen, laminin and fibronectin (Andrew and Berndt, 2004). It binds with high affinity to type I and IV collagen and is the main adhesion receptor for these proteins, in contrast to type III collagen, on which adhesion is largely dependent on the GPIb-IX-V-vWF binding tether (Jung *et al.,* 2010; Holinstat, 2017; Kunde and Wairkar, 2021). Integrin α2β1 binding primarily mediates initial platelet adhesion and spreading on ECM proteins; platelet

activation occurs during GPVI binding and activation of integrin αIIbβ3 (Jung and Moroi, 2000; Andrew and Berndt, 2004; Gremmel *et al.,* 2016).

1.3.3.4 Integrin αIIbβ3

Integrin αIIbβ3 is a commonly expressed integrin in platelets and has a key role in platelet aggregation. Upon agonist- or ligand-stimulated platelet activation, inside-out signalling initiates and αIIbβ3 undergoes a conformational change by separation of α and β subunits (Huang, 2019). This converts αIIbβ3 to a high affinity state, enabling ligand binding and promoting platelet-platelet interactions through its interactions with vWF, fibronectin, vitronectin and TSP (Jurk and Kehrel, 2005; Gardiner and Andrews, 2014; Holinstat, 2017). Integrin αIIbβ3 has roles in almost all stages of thrombus formation, including platelet adhesion, spreading, aggregation and thrombus stability and growth, as well as coagulation, including fibrin clot retraction (Kasirer-Friede *et al.,* 2007; Gremmel *et al.,* 2016; Huang *et al.,* 2019; Kunde and Wairkar, 2021). As an established promoter of thrombosis and haemostasis, this integrin is often a prime target in antiplatelet therapy.

1.3.4 Soluble agonists

Soluble agonists, released by adhesion receptor-mediated platelet activation and degranulation, can activate platelets directly through binding to agonist receptors. The main agonists with key roles in haemostasis are thrombin, ADP and TXA2, and their corresponding receptors are PAR-1 and -4, P2Y1 and P2Y12, and the thromboxane receptors (TPs) α and β (Gremmel *et al.,* 2016). These receptors are all G protein-coupled receptors (GPCRs), coupled to different G proteins, which when bound convert guanosine diphosphate (GDP) to guanosine triphosphate (GTP), facilitating interactions with membrane signalling proteins to activate platelets (Gurbel *et al.,* 2015).

1.3.4.1 Thrombin

Thrombin (also known as Factor IIa) is a serine protease released in its zymogen form – prothrombin – from alpha granules in activated platelets (Golebiewska and Poole, 2015). Following coagulation, prothrombin is cleaved by the prothrombinase complex (Factor Xa, Va and phospholipids) into proteolytic thrombin, with the ability to degrade

protein and cellular debris, including growth factors released from platelets (Velez *et al.,* 2015; Al-Amer and Osama, 2022). However, the primary roles of thrombin are in the propagation of coagulation and the activation of blood platelets. During the coagulation cascade, thrombin has two major opposing roles. It can convert plasma fibrinogen to fibrin, stabilising the growing thrombus and propagating coagulation (Gremmel *et al.,* 2016), however it can also bind to thrombomodulin on ECs to activate protein C, having an anticoagulant effect (Al-Amer and Osama, 2022), as well as other negative regulators of coagulation.

Thrombin is also a potent platelet activator. Upon binding, it cleaves PAR-1 and PAR-4 on platelets at the receptor N-terminal exodomain to reveal a new N-terminus, which then initiates transmembrane signalling via activation of G proteins (G_q, G_{13} and G_i) and PLC, generating IP3 and DAG and leading to calcium mobilisation and PKC pathway activation respectively (Shen *et al.,* 2017; Vilahur *et al.,* 2018). To activate this process, PAR-1 cleavage requires low concentrations of thrombin and can be rapidly inactivated, whereas PAR-4 cleavage requires higher concentrations of thrombin and is slower, having a more prolonged effect on platelets (Candia, 2012; Gremmel *et al.,* 2016). The PAR-4 receptor, unlike in humans, is the only thrombin receptor expressed on murine platelets, and has been shown to be essential for venous thrombosis to occur in mice (Lee *et al.,* 2021), demonstrating important differences in platelet physiology between species.

1.3.4.2 ADP

Over 50% of ADP in platelets is contained in dense granules and released upon platelet activation (Jurk and Kehrel, 2005; Packham and Mustard, 2005). ADP is a potent platelet activator, and its main function in primary haemostasis is to amplify platelet response and stabilise aggregates. ADP acts on purinergic P2Y GPCRs, specifically P2Y1 and P2Y12 on platelets, which are G_q and G_i coupled respectively (Cattaneo, 2015). P2Y1 stimulation results in weak PLC activation, generating IP3 and DAG and leading to calcium mobilisation, platelet shape change and reversible aggregation (Packham and Mustard, 2005; Gremmel *et al.,* 2016). P2Y12 stimulation results in inhibition of adenylyl cyclase, amplification of the aggregation response and agonist-induced platelet degranulation (Jurk and Kehrel, 2005; Packham and Mustard, 2005; Cattaneo, 2015). To ensure normal aggregation in response to ADP, both receptors must be co-stimulated

(Guidetti *et al.,* 2008; Cattaneo, 2015; Shen *et al.,* 2017). Another function of both P2Y receptors is in enhancing TF-mediated thrombin generation (van der Meijden *et al.,* 2005; Cattaneo, 2015), further demonstrating the importance of both receptors working in tandem.

1.3.4.3 TXA2

TXA2 is a prostanoid synthesised and secreted from platelets upon activation by ADP, thrombin or collagen. Fatty acids, such as AA, are liberated by phospholipase A2 (PLA2) and oxidised by cyclooxygenase (COX)-1 to form the intermediary prostaglandin H2 (PGH2), before this is metabolised by TXA2 synthase into TXA2 (Ellinsworth *et al.,* 2014; Holinstat, 2017; Lucotti *et al.,* 2019). Platelet prostanoid production by COX-1 or a pro-inflammatory environment can induce production of another COX isoform, COX-2, in ECs (Ornelas *et al.,* 2017; Lucotti *et al.,* 2019).

TXA2 binds to TPα and TPβ thromboxane G_q coupled GPCRs on the surface of platelets, with the β isoform distinguishable by the presence of an extended C-terminal cytoplasmic domain (Huang *et al.,* 2004; Mumford *et al.,* 2010; Ellinsworth *et al.,* 2014; Moscardo *et al.,* 2014). It has a half-life of only 30 seconds and can therefore act in only an autocrine and paracrine manner to activate and recruit platelets from the circulation to the growing thrombus (Nakahata *et al.,* 2008; Nisar *et al.,* 2014). Upon TXA2 stimulation, TPα and TPβ activate PLC signalling, generating IP3 and DAG and initiating calcium mobilisation and PKC pathway activation respectively. Additionally, G protein ($G_{12}/_{13}$) signalling activates downstream kinases and promotes activation of Ras, Rho and Rac pathways (Huang *et al.,* 2004; Mumford *et al.,* 2010; Moscardo *et al.,* 2014). TP binding regulates thrombosis and haemostasis, but also has wider implications in immunity, inflammation, cell migration and apoptosis (Huang *et al.,* 2004; Mumford *et al.,* 2010), and other ligands for this receptor include prostacyclin (PGI2) and hydroxyeicosatetraenoic acids (HETEs) (Ellinsworth *et al.,* 2014).

A visual representation of important platelet signalling events governing platelet function is summarised in Figure 1.4.

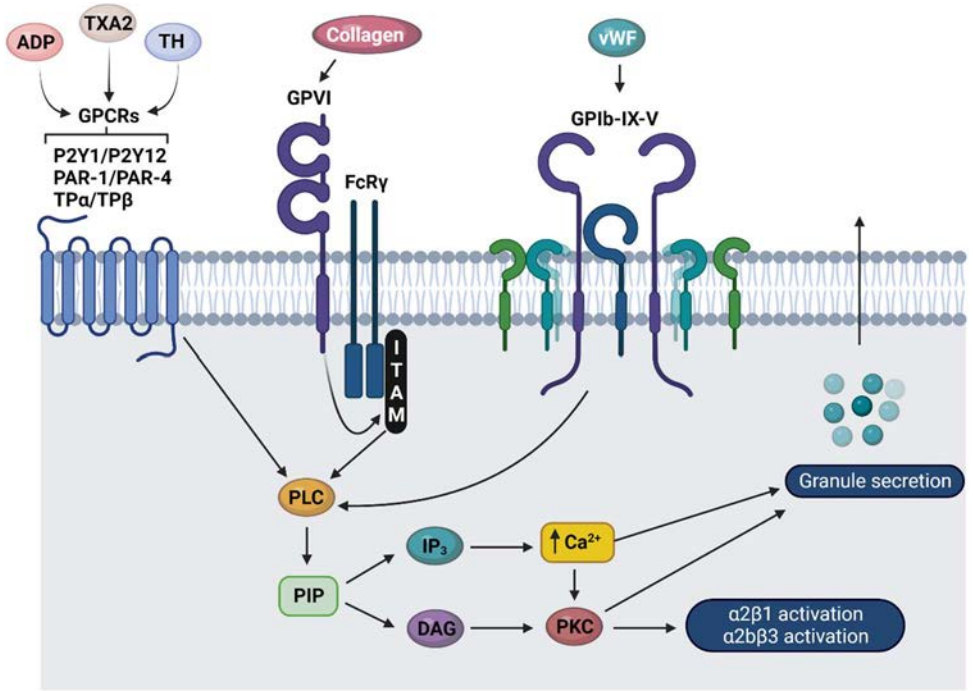

Figure 1.4 – Glycoprotein (GP) and G protein-coupled receptor (GPCR) signalling pathways in platelets. GPVI activation by collagen results in phosphorylation of immunoreceptor tyrosine-based activation motifs (ITAMs) and activation of phospholipase C (PLC) signalling, promoting conversion of phosphatidylinositol (4,5)-bisphosphate (PIP) into diacylglycerol (DAG) and inositol triphosphate (IP_3). DAG activates the protein kinase C (PKC) pathway, resulting in activation of integrins α2β1 and α2bβ3, and IP_3 promotes calcium (Ca^{2+}) mobilisation and platelet granule secretion. Activation of GPIb-IX-V complex by von Willebrand Factor (vWF) and agonist-stimulated GPCR activation also leads to initiation of the PLC signalling pathway. ADP - adenosine diphosphate; TXA2 - thromboxane A2; TH – thrombin; FcR – Fc receptor; P2Y – purinergic receptor; TP – thromboxane receptor; PAR – protease-activated receptor. Created with BioRender.com.

1.3.5 Coagulation

The coagulation cascade is important in secondary and tertiary haemostasis, and regulates thrombin generation, fibrin formation and the recruitment of RBCs and immune cells to the growing thrombus (Chapin and Hajjar, 2015). Two pathways lead to blood coagulation and converge at FX – the intrinsic and extrinsic pathways. The extrinsic pathway is activated upon vessel injury, where exposed TF (also known as FIII) binds to circulating FVII, resulting in autocatalysis to FVIIa (active) which then activates FX (Winter *et al.,* 2017). The resulting TF-FVIIa-FXa complex activates FVIII and FIX, linking the extrinsic and intrinsic pathways (Winter *et al.,* 2017). The intrinsic pathway is particularly important in medical devices and *in vitro* thrombosis models, and begins with the activation of FXII by negatively charged surfaces such as glass and silica (Grover and Mackman, 2019). FXIIa catalyses sequential activation of FXI and FIX, the latter of which forms a complex with activated FVIII to activate FX.

Both pathways meet upon activation of FX. FXa then forms the prothrombinase complex with FVa on the platelet membrane surface, facilitated by PS exposure, to cleave prothrombin (FII) to thrombin (FIIa), which then converts soluble fibrinogen (FI) to fibrin (FIa) – the primary product of the coagulation cascade (Mastenbroek *et al.,* 2015). Thrombin then activates FXIII, promoting crosslinking of the fibrin clot, but also acts in a positive feedback loop to activate FXI, FV and FVIII (Chee, 2014; Winter *et al.,* 2017). The stable, fibrin-rich clot is eventually degraded in a process termed fibrinolysis. tPA and urokinase plasminogen activator (uPA), released from ECs and monocytes, cleaves plasminogen on the surface of the clot into plasmin, resulting in the proteolysis of fibrin into fibrin degradation products (Chapin and Hajjar, 2015; Pant *et al.,* 2018). The coagulation cascade is summarised visually in Figure 1.5.

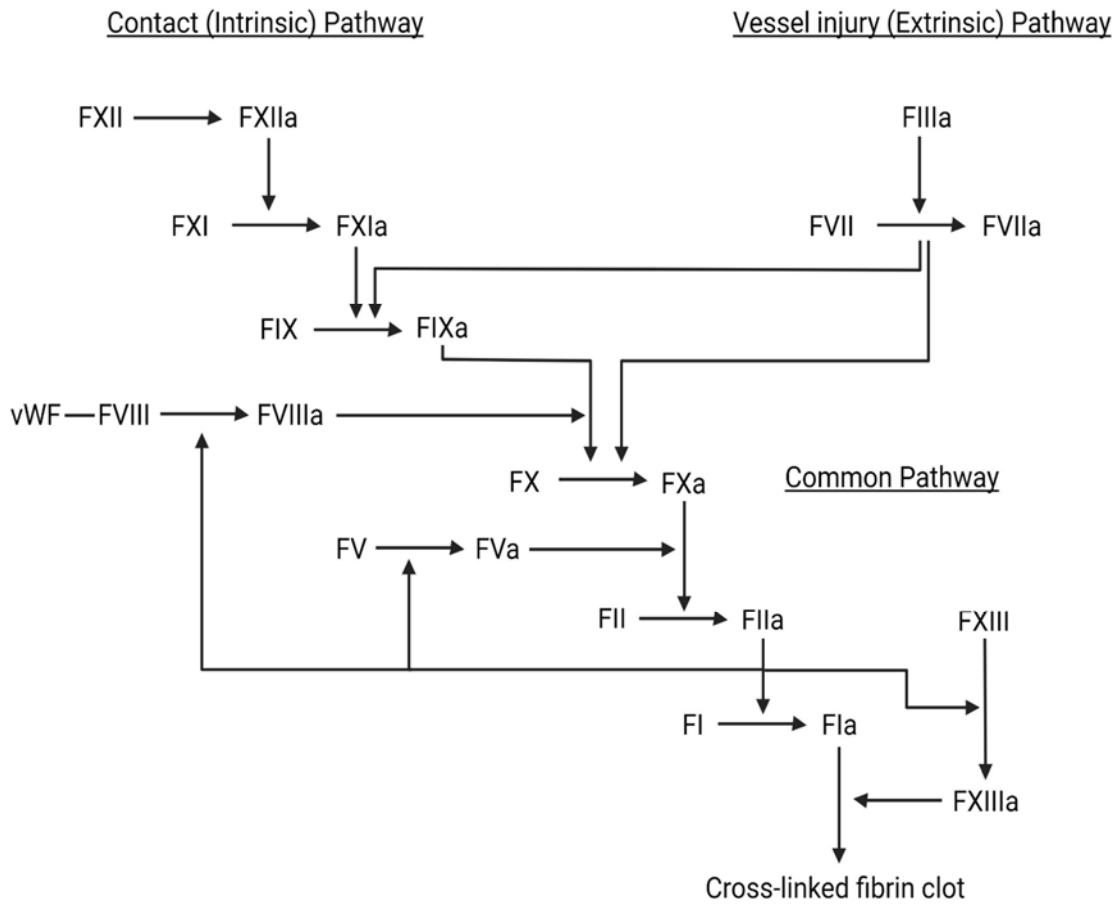

Figure 1.5 – A summary of the coagulation cascade. Vessel injury activates the extrinsic pathway of coagulation, with tissue factor (FIIIa) forming a complex with FVIIa to activate FX in the common pathway. The contact pathway is activated upon FXII activation. FXII activates FXI, which then activates FIX. FIXa forms a complex with FVIIIa, cleaved from von Willebrand Factor (vWF), to activate FX in the common pathway. FXa then forms a complex with FVa to convert prothrombin (FII) to thrombin (FIIa). Thrombin catalyses conversion of fibrinogen (FI) to fibrin (FIa), which then forms a complex with FXIIIa to crosslink the developed fibrin clot. Thrombin also activates FV, FVIII and FXIII in the coagulation cascade to further propagate this process. Created with BioRender.com.

1.4 Atherosclerotic plaque development

Atherosclerosis is a chronic, inflammatory vascular disease caused by the development of an atherosclerotic plaque. Plaque development occurs at arterial bifurcations and curved sections of arteries where the endothelium is exposed to disturbed, multidirectional flow (Zhang and Dou, 2015; Camare *et al.,* 2017; Sloop *et al.,* 2017).

1.4.1 Endothelial dysfunction

Endothelial dysfunction is a key event in the development and progression of atherosclerosis. Risk factors associated with atherosclerosis damage the vascular wall, increasing the permeability of the endothelium (Cahill and Redmond, 2016; Huang *et al.,* 2019). Risk factors associated with plaque development are distinct for the different types of plaque (rupture prone vs erosion prone) (Table 1.1).

Table 1.1 – Risk factors associated with atherosclerotic plaque rupture and erosion.

Plaque rupture	**Plaque erosion**	**References**
Age (increasing)	Age (under 50)	(Burke *et al.,* 1998; Loftus, 2011; Bentzon *et al.,* 2014; Yahagi et al., 2015)
Sex (male)	Sex (female)	
Smoking, Hypertension	Smoking, Hypertension	
Hypercholesterolaemia,		
Diabetes		

The endothelium has roles in regulating thrombosis, coagulation and fibrinolysis (as described in Section 1.2.1.2). However, upon vessel injury and endothelial damage, the endothelium switches to a pro-thrombotic phenotype, activating and promoting aberrant thrombosis and coagulation and inhibiting fibrinolysis (Figure 1.6). To promote thrombosis, vWF, TXA2 and platelet activating factor (PAF) are released from the endothelium, promoting platelet adhesion, activation and thrombus formation. Additionally, the release of TF promotes activation of the coagulation cascade (extrinsic pathway of activation) and vWF propagates this process by its involvement in FVIII stability and fibrin crosslinking. Finally, to support thrombus formation, fibrinolysis is inhibited by release of plasminogen activator inhibitor-1 (PAI-1), which inhibits tPA activity in the vasculature, preventing fibrin degradation (Pearson, 1999; Kaur *et al.,* 2018).

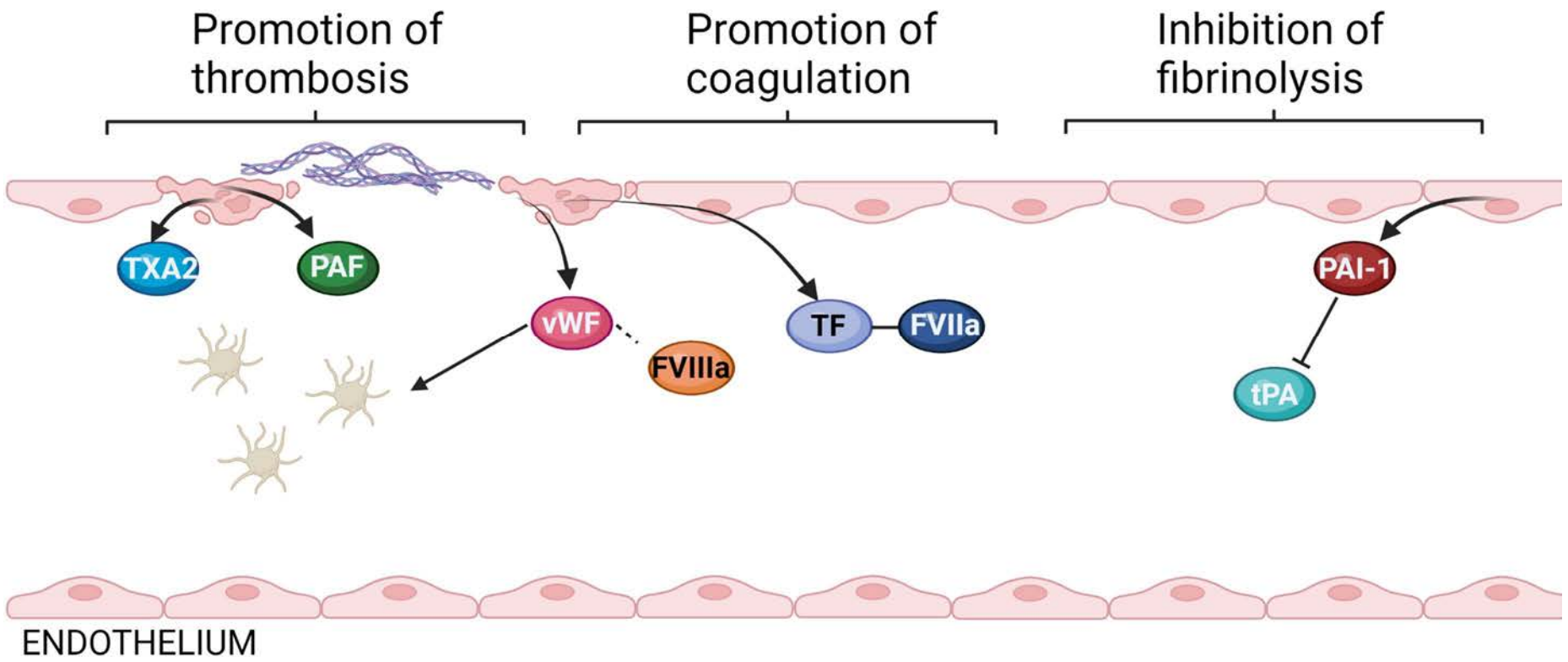

Figure 1.6 – Pro-thrombotic endothelial phenotype in response to vessel injury. Upon vessel injury, von Willebrand Factor (vWF), thromboxane A2 (TXA2) and platelet activating factor (PAF) are released from the endothelium, promoting platelet adhesion, activation and thrombus formation. The release of tissue factor (TF) promotes activation of the coagulation cascade and vWF propagates this process by its involvement in FVIII stability and fibrin crosslinking. The release of plasminogen activator inhibitor-1 (PAI-1) inhibits tissue plasminogen activator (tPA) activity, having an inhibitory effect on fibrinolysis. Created with BioRender.com.

1.4.2 Plaque development

Intimal hyperplasia is characterised by SMC migration, proliferation and ECM production in the vascular intima. Increased permeability of the endothelium increases low-density lipoprotein (LDL) transcytosis (Cahill and Redmond, 2016; Huang *et al.,* 2019) leading to the accumulation of LDL in the sub-endothelial layer (Weber *et al.,* 2017). LDL binds to proteoglycans, leading to oxidation, inflammation and lipid retention (Camare *et al.,* 2017; Wight, 2018). Invading monocyte-derived macrophages and SMCs internalise oxidised LDL and become foam cells, forming an intimal xanthoma (fatty streak) in the first stage of the development of an atherosclerotic plaque (Otsuka *et al.,* 2016; Olie *et al.,* 2018). Oxidant stress created by generation of reactive oxygen species (ROS) promotes inflammation, reducing endothelial NO bioavailability. Additionally, upregulation of adhesion molecule expression on activated ECs increases platelet binding and leukocyte recruitment (Wu *et al.,* 2017), increasing thrombotic risk. Adherent platelets release platelet-derived growth factor (PDGF) which promotes intimal hyperplasia (Hamilos *et al.,* 2018), and an accumulation of neutrophils leads to the formation of NETs, which aggravate endothelial damage, increase thrombotic risk and destabilise growing lesions (Doring *et al.,* 2017; Quillard *et al.,* 2017; Liu *et al.,* 2019). The morphology of a fully developed atherosclerotic plaque varies depending on risk factors and disease progression, but the two plaque phenotypes relevant in ACS are plaques prone to rupture or erosion.

1.4.2.1 Plaque rupture

Plaques prone to rupture have lipid-rich, inflammatory necrotic cores and sparse SMCs (Quillard *et al.,* 2017). The fibrous cap is thin, and consists predominantly of type I collagen, biglycan and decorin (Kolodgie *et al.,* 2002; Otsuka *et al.,* 2016). Plaque rupture is mediated by inflammatory molecules, which increase plaque vulnerability and propensity to rupture. Tumour necrosis factors (TNFs), interleukins (ILs) and MMPs released from leukocytes, ECs and platelets degrade the ECM, promoting platelet activation and upregulating expression of adhesion molecules (Fatkhullina *et al.,* 2016; Hamilos *et al.,* 2018). Over time, MMPs weaken the fibrous cap, leading to plaque rupture and the exposure of thrombogenic TF, vWF, vascular proteoglycans and lipids to circulating platelets (Ten Cate and Hemker, 2016; Otsuka *et al.,* 2016). The presence

of TF propagates coagulation, and the resulting fibrin-rich thrombus traps circulating erythrocytes, which aggregate and promote vessel occlusion. The final thrombus characteristic of plaque rupture has a platelet-rich head and a fibrin- and erythrocyte-rich tail (Otsuka *et al.,* 2016; Olie *et al.,* 2018).

1.4.2.2 Plaque erosion

Plaques prone to erosion have a lower lipid content and a thicker fibrous cap, rich in SMCs and type III collagen, versican and hyaluronan (Kolodgie *et al.,* 2002; Otsuka *et al.,* 2016; Quillard *et al.,* 2017). The vascular environment has few inflammatory cells, with a higher density of myeloperoxidase (MPO) positive cells and NETs (Ferrante *et al.,* 2010; Otsuka *et al.,* 2016; Quillard *et al.,* 2017; Yamamoto *et al.,* 2019). Overexpression of endothelial TLR-2 impairs cell viability and attachment, resulting in NETosis, EC denudation and the exposure of the underlying ECM and SMCs to circulating platelets (Hansson *et al.,* 2015; Quillard *et al.,* 2017). Histones released from NETs activate platelets (Semeraro *et al.,* 2011) and exposed vascular proteoglycans interact with platelets to promote local thrombosis. The final thrombus characteristic of plaque erosion appears platelet-rich and generally causes less vascular occlusion than thrombi formed following plaque rupture (Quillard *et al.,* 2017). A visual representation of atherothrombosis occurring on each plaque type is summarised in Figure 1.7.

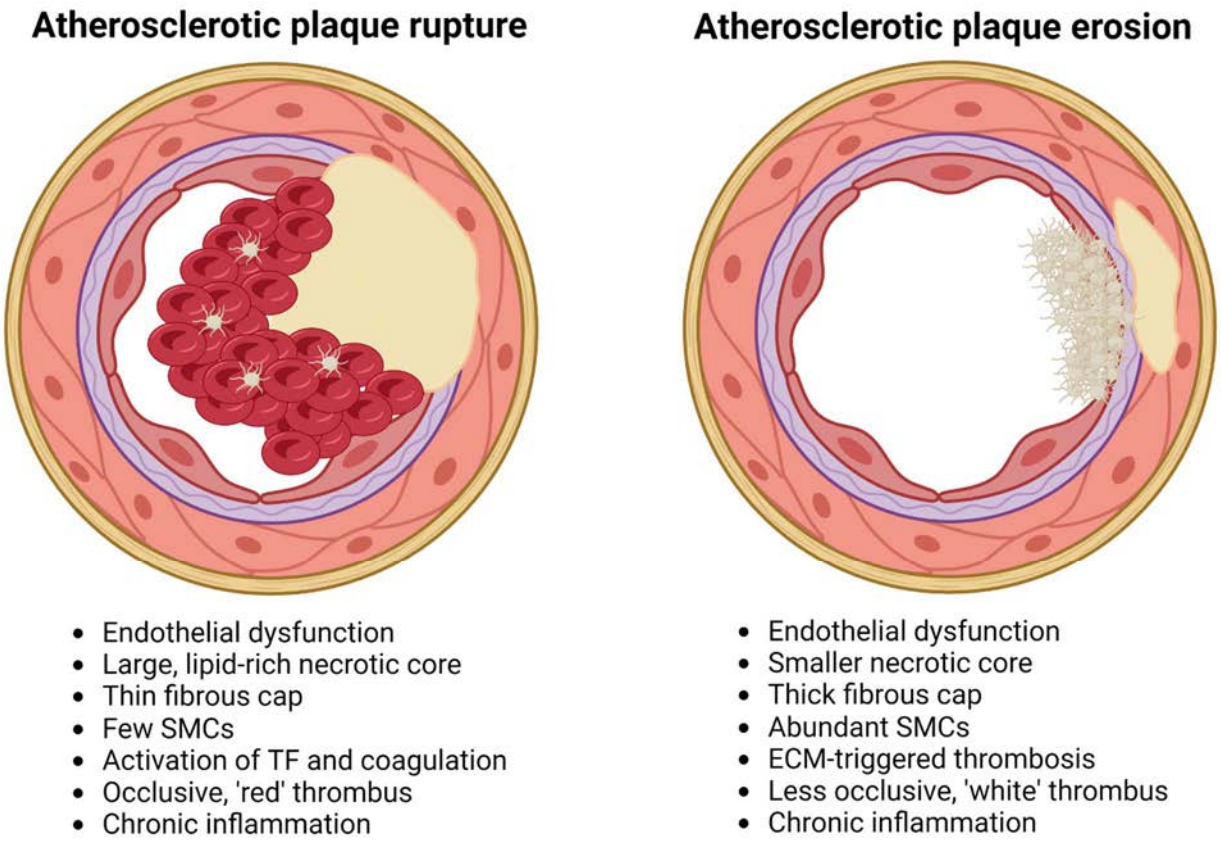

Figure 1.7 – A comparison of the features of ruptured and eroded atherosclerotic plaques. Plaque rupture (left) is different to plaque erosion (right), with plaques having a larger, lipid-rich necrotic core and thinner fibrous cap. Thrombi associated with plaque rupture appear red, in comparison to erosion thrombi which appear more platelet-rich. Chronic inflammation and endothelial dysfunction are features of both. SMC – smooth muscle cell; ECM – extracellular matrix; TF – tissue factor. Created with BioRender.com.

1.5 Antiplatelet therapy

Current treatments for atherothrombosis include antiplatelet therapy, where aspirin and thienopyridines such as clopidogrel have been shown to reduce the risk of major vascular events by over 10% (Patrono *et al.,* 2017). Treatment efficacy is, however, limited by high inter-individual variability and increased risk of bleeding, and the risk of recurrent events/death after 12 months remains at around 20% (Hamilos *et al.,* 2018; Olie *et al.,* 2018). Antiplatelet therapy may also be used in combination with lipid-lowering drugs, such as statins. Statins are the gold standard for treating patients with thin-capped atheromatous plaques, slowing lipid accumulation and delaying plaque progression, however efficacy is limited by variations across patient groups and plaque phenotype (Honda *et al.,* 2018).

1.5.1 Aspirin

Aspirin is a non-steroidal anti-inflammatory drug (NSAID) commonly used to reduce pyrexia, pain and platelet activation. It prevents platelet prostanoid synthesis by inhibiting COX enzymes, preventing oxidation of AA. In low doses COX-1 is irreversibly inhibited, preventing TXA2 synthesis and reducing local platelet activation and aggregation (Nisar *et al.,* 2014). Higher doses of aspirin result in inhibition of both COX-1 and COX-2, and consequently this higher dosage has a more widespread anti-inflammatory effect on local vascular cells (Xu *et al.,* 2018; Tao *et al.,* 2021), however COX-2 inhibition has also been linked to a reduction in prostacyclin biosynthesis and the promotion of a pro-thrombotic state (Hennan *et al.,* 2001). Aspirin is often used in combination with thienopyridines such as clopidogrel in DAPT for prevention of cardiovascular events in ACS (Degrauwe *et al.,* 2017).

1.5.2 P2Y12 antagonists

Drugs such as clopidogrel and ticagrelor are thienopyridines - P2Y12 receptor inhibitors – used in the prevention of thrombosis, and are both recommended in the management of ACS (Koski and Kennedy, 2018). ADP released from activated platelets acts in an autocrine and paracrine manner by binding to P2Y12 receptors on the platelet surface (Jurk and Kehrel, 2005; Packham and Mustard, 2005). Receptor stimulation results in platelet activation and degranulation, propagating platelet activity in a positive feedback

mechanism. P2Y12 activation also results in inhibition of adenylyl cyclase, a process which counteracts the activation of adenylyl cyclase and subsequent inhibition of platelet activity by endothelial PGI2 (Cattaneo, 2015). Thienopyridines act by binding specifically to the P2Y12 receptor, resulting in irreversible inhibition and prevention of ADP-induced platelet activation (Mega and Simon, 2015). Although well established for use in the short term, evidence demonstrating the efficacy of DAPT as a preventative treatment beyond 12 months is conflicting. Mauri *et al.* (2014) reported a significant reduction in myocardial infarction following continued treatment with DAPT compared with aspirin monotherapy, in contrast with findings from Bhatt *et al.* (2006), which reported no significant differences between treatments (Sharma *et al.,* 2020), potentially due to variabilities in effectiveness across different patient groups. Indeed, findings from Valgimigli *et al.* (2021) demonstrated that monotherapy with ticagrelor had similar efficacy to DAPT with a reduction in bleeding risk, an effect which segregated with females. Current therapeutic strategies would therefore benefit from a more targeted approach, testing novel compounds in specific patient groups to improve treatment efficacy.

1.6 Established models of atherothrombosis

Experimental models of thrombosis are crucial to investigate platelet function and the molecular mechanisms involved in thrombus development in arterial thrombosis. These models are also important to enable identification of novel potential drug targets and to test new antithrombotics, addressing limitations associated with current antiplatelet therapies (described in Section 1.5). Currently, there are a variety of *in vivo* and *in vitro* thrombosis models, which are reviewed below.

1.6.1 In vivo

Historically, *in vivo* models of thrombosis have utilised zebrafish, rabbits, pigs and rats, but the most common *in vivo* model of thrombosis is the murine model (Getz and Reardon, 2012). This model has many advantages in research – it is economical, shares physiological similarities to humans, and can be genetically modified with ease (Carminita *et al.,* 2022). Common vessels used to study arterial thrombosis in these models include the carotid artery (a macrovessel) and the cremasteric, mesenteric and dorsal arterioles (microvessels). Often, the aforementioned vessels are exposed,

damaged experimentally and intravital microscopy is used to monitor thrombus development (Mackman, 2006). Methods used to induce vascular damage include ferric chloride ($FeCl_3$), photochemical, laser and mechanical injury models. These methods have historically been used in healthy murine vessels, as mice are generally resistant to atherosclerotic development (Getz and Reardon, 2012). However, genetic deletion of apolipoprotein E (apoE), an apolipoprotein responsible for the catabolism of LDL, along with a high-fat diet, has resulted in successful atherogenesis in mice, enabling the investigation of atherothrombosis. These plaques are, however, morphologically different to human plaques, rarely progressing to vulnerability and often requiring mechanical intervention to rupture (Karel *et al.,* 2020).

1.6.1.1 Ferric chloride

$FeCl_3$ application to the adventitia of vessels is the most commonly used method to induce vascular damage in murine models. A concentration of between 5-50% $FeCl_3$ is soaked in filter paper and applied to the outer vessel in a region of interest for a specified amount of time (usually between 30 seconds and 5 minutes), before time to occlusion is measured (Carminita *et al.,* 2022). The mechanism by which $FeCl_3$ causes thrombosis is an area of speculation, although it has been reported that in the most commonly used concentration of 10% (and above), the endothelium is denuded by oxidative damage (Hisada and Mackman, 2018; Palacios-Acedo *et al.,* 2020). The thrombotic process has been linked to RBCs, with $FeCl_3$ having been shown to promote lipid peroxidation, haemolysis and recruitment of platelets (Bonnard and Hagemeyer, 2015; Grover and Mackman, 2019). Although this model has been invaluable in furthering knowledge of atherothrombosis, variations in vessel type, $FeCl_3$ concentration and exposure time create issues with reproducibility and standardisation, and the damage induced is not physiological to the rupture or erosion of a human atherosclerotic plaque.

1.6.1.2 Photochemical injury

Rose Bengal is a photosensitive dye used to inflict photochemical damage in a focal region of interest. Between 10-50mg/kg Rose Bengal is injected intravenously, before a laser irradiates the region of interest at 543nm for a specified duration (Hisada and Mackman, 2018; Carminita *et al.,* 2022). This results in the generation of free radicals, causing EC damage and denudation, and subsequent thrombosis (Karel *et al.,* 2020).

Time to occlusion is then measured as a thrombotic parameter. Similarly to the $FeCl_3$ method, lack of standardisation in dosage, laser intensity and exposure time creates issues with method standardisation and reproducibility.

1.6.1.3 Laser injury

An additional method of creating a focal injury is using laser ablation. Briefly, a nitrogen laser at 440nm is focally concentrated in a region of interest and pulsed 1-2 times to initiate local thrombosis (Carminita *et al.,* 2022). In contrast to the $FeCl_3$ and Rose Bengal methods, the endothelium is not removed, but is instead activated, and thrombus formation is imaged in real time using intravital microscopy (Palacios-Acedo *et al.,* 2020). An advantage of using this method is that multiple injuries can be inflicted within the same vessel, creating multiple regions of local thrombus formation (Hisada and Mackman, 2018). However, this model is limited to small, transparent vessels and by variations in protocol development and instrument customisation (Bonnard and Hagemeyer, 2015), creating issues with method standardisation and reproducibility.

1.6.1.4 Mechanical injury

Mechanical injury to vessels may be inflicted by ligation, wire or using a needle. Ligation occurs by creating a suture around an externalised vessel and tightening for a specified amount of time (usually 5 minutes), before measurement of non-occlusive thrombus formation (Karel *et al.,* 2020). In a further development of this method, an angioplasty guidewire may be introduced to denude the endothelium, inducing intimal hyperplasia and vascular remodelling but not acute thrombus formation (Roque *et al.,* 2000; Schober *et al.,* 2002). Another method of inflicting mechanical injury is through the use of a needle. This is commonly used to encourage mechanical rupture of a murine atherosclerotic plaque, exposing plaque material to platelets and propagating the formation of an occlusive thrombus (Karel *et al.,* 2020).

1.6.2 In vitro

In vitro models were developed to address limitations associated with *in vivo* models, such as comparability, low throughput, species differences, standardisation and reproducibility (Zhang *et al.,* 2017). *In vitro* models have developed over time, improving

comparability to *in vivo* models whilst maintaining some advantages over these models. The different types of *in vitro* models used and components used in these models are described below.

1.6.2.1 Microfluidics and PDMS-based models

In flow modelling, the system widely used by researchers is the parallel plate flow system. A monolayer of ECs is cultured on the base of the plate, and cell culture medium or whole blood is perfused through an inlet and outlet on either side of the plate. This system is useful to investigate EC behaviour including adhesion, migration and mechano-transduction under flow (Khodabandehlou *et al.,* 2017; Hoseini *et al.,* 2021). These systems in a thrombosis model, however, would use a large volume of blood, and so the microfluidic modelling system was developed. These models are similar to parallel-plate flow systems but are much smaller and more cost efficient – using fewer cells and reagents and enabling more precise control of flow rates (Hoseini *et al.,* 2021). Microfluidic chambers enable investigations demonstrating the influence of whole blood rheology on platelet activity and thrombus formation, as they often use smaller amounts of blood, increasing accessibility (Aelst *et al.,* 2016). Additionally, these models reduce time, cost and ethical issues surrounding current *in vivo* models (Khodabandehlou *et al.,* 2017). Popular custom-made microfluidic devices are biocompatible polydimethylsiloxane (PDMS)-based, and incorporate well plates (Conant *et al.,* 2011) and, more traditionally, chambers (Neeves *et al.,* 2008). These devices have been used to investigate platelet behaviour under different conditions, on various substrates and under varying shear rates, and are inexpensive, however lack of standardisation of these custom-made devices limits widespread uptake (Westein *et al.,* 2012), and it is often not possible to manually access chambers following cell seeding, preventing mechanical injury and limiting comparability with *in vivo* models.

Consideration must be taken, when using *in vitro* models, to use a flow rate representative of human coronary arteries, as under different shear rates, platelet thrombus formation is variable (Pivkin *et al.,* 2006). The shear stress in a human coronary artery is roughly 10-15 dynes/cm^2 (Meng *et al.,* 2022), compared with 40-45

dynes/cm^2 in a murine carotid artery (Castier *et al.,* 2005) and as a model of human atherothrombosis, the shear stress used should be representative of the human coronary artery. Indeed, the flow rate used by some *in vitro* thrombosis models is closer to the cremaster arteriole of mice than to the human coronary artery (Zhang *et al.,* 2017; Hoseini *et al.,* 2021; Panteleev *et al.,* 2021). This can be useful to compare murine platelet responses, however this project aims to enable accurate comparisons to be made between humanised and murine models, and therefore an arterial shear stress of 15 dynes/cm^2 will be used for the in vitro thrombosis model.

1.6.2.2 The development of *in vitro* thrombosis models

Early development of *in vitro* models consisted of whole blood perfused over coatings of Type I Horm collagen (and sometimes TF) to investigate the efficacy of DAPT under different conditions (Hosokawa *et al.,* 2012) as well as pathologies such as von Willebrand Disease, haemophilia and various platelet disorders (Schoeman *et al.,* 2017). These models are, however, non-occlusive. More recently, an occlusive model of thrombosis was developed by Berry *et al.* (2021), using a pressure relief PDMS-based model to generate occlusive clot formation on a coating of Type I Horm collagen and TF, enabling measurement of time to occlusion following treatment with antiplatelet drugs. ECM-based modelling systems have historically been useful in modelling thrombosis *in vitro,* however the endothelium has a key role in the regulation of thrombus formation (Kaczmarek *et al.,* 1996; Hamilos *et al.,* 2018), and advances in model development have focused more on the incorporation of ECs to more accurately measure thrombosis. An early study by Sakariassen *et al.* (1983) developed a chamber to measure thrombus formation on ECM components and ECs under flow, using flow rates ranging from 300-1100 s^{-1}. Here, it was discovered that platelets did not adhere to a healthy, intact endothelium *in vitro*, but activated under sub-confluency conditions in the surrounding ECM. This work was followed by Brouns *et al.* (2019), who created a similar model by culturing endothelial cells on Type I collagen and TF to investigate thrombus formation. However, the lack of a confluent endothelial monolayer and native ECM means this model is unsuitable for investigations in arterial thrombosis.

Flow models have, however, been developed to incorporate a confluent endothelium, and recent advances in the field have favoured the use of bioprinting in these models. Briefly, a pattern representing a vascular network is created and cast by a hydrogel (usually Type I collagen-based), before being removed, leaving behind channels which can be seeded with ECs and perfused with cell culture medium or whole blood (Zhang *et al.,* 2016). These models are reproducible and can be used to investigate cell behaviour, coculture crosstalk and transendothelial migration (Zheng *et al.,* 2012), but rely on the use of custom-made moulds and require expertise to build and operate, discouraging widespread uptake by researchers. Additionally, it is difficult to perform thrombus formation investigations in these models, as there is no method to damage endothelial cells and expose the underlying thrombogenic ECM. Indeed, this is a factor limiting the use of ECs in current modelling systems.

In summary, there are advantages and disadvantages associated with both *in vivo* and *in vitro* models (Table 1.2). A more commercially available, standardised, reproducible in vitro thrombosis model, which incorporates relevant cell types, native ECM and enables focal damage of ECs will enable widespread uptake by researchers, comparability to *in vivo* models and a more standardised approach to antithrombotic therapy.

Table 1.2 - Advantages and disadvantages associated with current *in vivo* and *in vitro* models. R&S – reproducibility and standardisation. EC – endothelial cell. ECM – extracellular matrix.

	Advantages	Disadvantages	References
In vivo			Roque *et al.,* 2000; Schober *et al.,* 2002; Getz and Reardon, 2012; Bonnard and Hagemeyer, 2015; Hisada and Mackman, 2018; Karel *et al.,* 2020; Palacios-Acedo *et al.,* 2020; Carminita *et al.,* 2022
$FeCl_3$ damage	• Occlusive thrombus formation	• Reduced R&S due to variations in concentration and exposure time, thrombotic mechanism unclear	
Photochemical	• Local, targeted thrombosis • Can compare with *in vitro* methods (no direct access to chambers required)	• Reduced R&S due to variations in dosage, laser intensity and exposure time	
Laser injury	• Local, targeted thrombosis • Multiple injuries in same vessel	• ECs activated, not removed. No standardised protocol • Limited to small, transparent vessels	
Mechanical injury	• Guidewire – EC denudation leading to atherosclerotic events • Needle – enables 'rupture' of plaques	• Ligation – non-occlusive thrombus formation • Guidewire – does not result in acute thrombosis • Needle – EC healthy, no dysfunction	
$ApoE^{-/-}$ model	• Successful plaque development in mice • Economical, ease of genetic modification	• Variations in plaque morphology, phenotype compared with humans	
In vitro			Hosokawa *et al.,* 2012; Westein *et al.,* 2012; Zheng *et al.,* 2012; Zhang *et al.,* 2016; Khodabandehlou *et al.,* 2017; Schoeman *et al.,* 2017; Zhang *et al.,* 2017; Berry *et al.,* 2021; Hoseini *et al.,* 2021; Panteleev *et al.,* 2021
Parallel plate	• Can manually alter flow rate • No species differences	• Lack of standardisation of custom-made devices limits uptake • Large volume of blood	
Microfluidics	• High throughput, reproducible • Uses less blood, cost efficient	• Different flow rates may be used – both murine and human • Often cannot manually access chambers to injure cells	
Type I collagen model	• High throughput • Effective platelet function testing	• Singular ECM component – no complete ECM • Non-occlusive models	
Occlusive model	• Occlusive thrombus formation • Time to occlusion can be measured	• No ECs incorporated in model	
EC model	• Can investigate role of ECs in thrombus formation	• No confluent monolayer, or difficult to access confluent ECs in chambers. No representative dysfunctional ECM	
Vascular model	• Includes ECM, ECs and blood in model • Reproducible, enables detailed cell studies	• Rely on custom-made moulds, require expertise to operate • Difficult to access ECs in chambers to damage and perform thrombus formation experiments	

1.7 Aims, objectives and hypothesis

Current research in atherothrombosis is limited by disadvantages associated with both *in vivo* and *in vitro* models. *In vivo* models have historically been useful in furthering our knowledge of thrombosis, but use vessels not associated with cardiovascular disease, and the species difference limits translatability of these models to humans. Current *in vitro* models use human blood, representative of human thrombosis, but do not incorporate key regulators of thrombosis observed in cardiovascular disease, including representative endothelial cells and an ECM associated with cardiovascular disease.

The aim of this project was to help address these limitations by creating a novel, endothelialised *in vitro* model of human atherothrombosis.

The objectives in this project were to:

- Define, develop and evaluate disease-relevant matrices to reflect the distinct platelet-plaque interface in plaque rupture and erosion
- Develop 'endothelialised' flow chambers and establish experimental protocols to induce endothelial dysfunction representative of plaque rupture and erosion
- Establish novel protocols to focally damage endothelial cells, to translate *in vivo* protocols to *in vitro* models

Hypothesis: - Disease-relevant matrices and the presence of the endothelium alter platelet responses and thrombus formation, and should be included in future models of atherothrombosis.

2. Methods

2.1 Human Blood Preparation

2.1.1 Venepuncture

All health and safety, risk assessments and potential ethical issues were considered prior to the start of the project, which was subject to Manchester Metropolitan University (MMU) ethical approval (EthOS reference 12762). All donors signed an informed consent form and had a 48-hour cooling off period prior to donating blood. Peripheral blood was taken from healthy male and female volunteers aged 18-65 into 5mL 3.2% (v/v) sodium citrate BD vacutainers (Bunzl Healthcare, Manchester, UK) before being gently inverted 3-4 times to mix with the anticoagulant. Individuals with anaemia, blood-borne infections, blood clotting disorders, and those using antiplatelet or anticoagulant therapy 10 days or less prior to donating were excluded from the study. Blood samples were kept at RT and used within a maximum of 4 hours following venepuncture.

2.1.2 Preparation of platelet-rich plasma (PRP) and washed platelets

Whole blood in sodium citrate tubes was centrifuged at 100g for 20 minutes at RT, separating it into red blood cells (bottom layer), and platelet rich plasma (PRP) (top layer), separated by a thin buffy coat. PRP was transferred to falcon tubes, before being used for experiments. To prepare ADP-sensitive washed platelets, 150µL acid citrate dextrose (ACD; 29.9mM trisodium citrate, 113.8mM glucose, 2.9 mM citric acid, pH 6.4) was added per 1mL of PRP before being centrifuged at 350g for 20 minutes. The platelet pellet was then resuspended in 1mL Tyrodes-HEPES buffer (134mM sodium chloride, 2.9mM potassium chloride, 0.34mM sodium phosphate dibasic, 12mM sodium bicarbonate, 20mM HEPES, 1mM magnesium chloride, pH 7.3) with added glucose (5mM) before platelets were counted using a Sysmex XP-3000 blood analysis system and diluted to the required density of $2x10^7$ platelets/mL for adhesion and spreading assays.

2.2 Primary mammalian cell culture

Cell culture was performed in class II safety cabinets under sterile conditions. All primary cells were adherent and grown in T25 or T75 cell culture flasks, and 6- or 24-well plates

(Nunc™, Thermo Fisher Scientific, Paisley, UK). Cells were incubated in a 5% CO_2 incubator at 37°C, and the medium replaced every 48 or 72 hours.

2.2.1 Human umbilical vein endothelial cell (HUVEC) and human coronary artery endothelial cell (HCAEC) culture

HUVECs (C-12203) and HCAECs (C-12221) were obtained from Promocell (Heidelberg, Germany) and cultured in Endothelial Cell Growth Medium MV2 (Promocell) supplemented with Growth Medium MV2 SupplementPack (Promocell) containing 5% (v/v) foetal calf serum (FCS), 5ng/mL recombinant human (rH) epidermal growth factor, 10ng/mL rH basic fibroblast growth factor, 20ng/mL rH insulin-like growth factor, 0.5ng/mL VEGF 165, 1µg/mL ascorbic acid and 0.2µg/mL hydrocortisone. ECs were used for experiments between passages 3-7 and were passaged at 80-90% confluency at 1:5.

2.2.2 Human coronary artery smooth muscle cell (HCASMC) culture

HCASMCs (C-12511) were obtained from Promocell and cultured in Smooth Muscle Cell Growth Medium 2 (Promocell) supplemented with Growth Medium 2 SupplementPack (Promocell) containing 5% (v/v) FCS, 0.5ng/mL rH epidermal growth factor, 2ng/mL rH basic fibroblast growth factor and 5µg/mL rH insulin. SMCs were used for experiments between passages 3-7 and were passaged at 80-90% confluency at 1:3.

2.2.3 Cell passage and freezing

Once confluent, cell medium was aspirated and cells were washed with pre-warmed Dulbecco's Phosphate Buffered Saline (DPBS; Lonza, Basel, Switzerland). Cells were then incubated at either 37°C (HUVECs and HCAECs) or room temperature (RT; HCASMCs) for 2-4 minutes with pre-warmed Trypsin-Ethylenediaminetetraacetic acid (EDTA; Lonza; 4mL per T75) until cell detachment from the base of the flask/plate. Trypsin was then neutralised with pre-warmed full EC/SMC medium (8mL per T75) and cell suspension transferred to a 15mL falcon. Cells were centrifuged at either 300g (HUVECs and HCAECs) or 220g (HCASMCs) for 5 minutes at RT, before resuspension of the cell pellet in pre-warmed EC/SMC medium. Cells were seeded at $1.3x10^4/cm^2$ in plates and flasks, and at $3.6x10^4/cm^2$ in ibidi VI 0.1 µ-slides (Thistle Scientific, Glasgow, UK). For cryopreservation, cells were passaged as above and the cell pellet resuspended in 90% (v/v) foetal bovine serum (FBS; Lonza) supplemented with 10% (v/v) dimethylsulphoxide

(DMSO; Sigma Aldrich, Dorset, UK). Cell suspension was then transferred to a 1.2mL cryopreservation vial and placed in a Mr Frosty (Sigma Aldrich) for 48 hours at -80^{o}C, before being transferred to longer term liquid nitrogen storage.

2.2.4 Cell culture on coverslips

22x64mm glass coverslips (Scientific Laboratory Supplies, Nottingham, UK) were dipped in ethanol and sterilised under UVC light in a class II safety cabinet for 45 minutes. Coverslips were placed in sterile 4-well plates (Thermo Fisher Scientific) and washed in DPBS before being incubated at 37^{o}C for 1 hour in sterile 0.2% (v/v) gelatin. Coverslips were washed twice in DPBS before being crosslinked with 1% (v/v) sterile glutaraldehyde for 30 minutes and quenched in 1M sterile glycine for 20 minutes at room temperature (RT). Coverslips were again washed twice with DPBS before being incubated at 37^{o}C for 1 hour in fresh cell medium (Godeau *et al.,* 2019). Cells were then seeded directly on to coverslips as previously described and grown over 10 days to produce sufficient ECM for experimental purposes. During the final 3 days of culture, cells were damaged with 1X cigarette smoke extract (CSE) (using methods described previously by Teasdale *et al.,* 2017) or 5ng/mL TNF-α (Peprotech, London, UK) to produce an ECM representative of dysfunctional ECs and SMCs.

2.2.4.1 Retrieval of decellularised cell-derived ECM (CDM)

HCAECs and HCASMCs grown on coverslips were washed gently with DPBS before being incubated in an extraction buffer (2mL Trypsin-EDTA or 20mM NH4OH, 0.5% (v/v) Triton X-100) for 2 minutes at RT. Following cell removal, the ECM was washed gently using DPBS containing calcium and magnesium chloride (DPBS+; Thermo Fisher Scientific) before being incubated with 10µg/mL DNAse I (Sigma Aldrich) for 30 minutes at 37^{o}C. The resulting decellularised, cell-derived ECM (CDM) was then washed twice gently and kept at 4^{o}C in DPBS+ for a maximum of 24 hours.

2.3 Platelet adhesion/spreading assay

2.3.1 Platelet adhesion to ECM proteins

Washed platelets were prepared as previously described, at a concentration of $2x10^7$ platelets/mL. For blocking experiments, wells of an ibidi angiogenesis µ-slide (Thistle Scientific) were firstly blocked using 10µL 5% (v/v) goat serum, 1% (w/v) bovine serum albumin (BSA; Sigma Aldrich) or left without blocking (ibiTreat surface) for 1 hour at RT. Wells were washed twice with DPBS before adding 10µL washed platelet suspension and incubating for 45 minutes at 37°C. Wells were washed twice gently with DPBS to remove non-adherent platelets and fixed in 4% (w/v) paraformaldehyde (PFA) for 10 minutes. Following a further wash with DPBS, 1µM 3,3'-Dihexyloxacarbocyanine iodide (DIOC-6; Sigma Aldrich) was added to platelets and incubated for 30 minutes at RT. Wells were washed well with DPBS and imaged using a Celena S Logos fluorescent digital imaging system. For coating experiments, wells of a 96-well plate were coated with 10, 20 or 50µg/mL Type I collagen (Equine tendon-derived; Labmedics, Abingdon, UK), Type III collagen (Cambridge Bioscience, Cambridge, UK), Biglycan (Caltag MedSystems, Buckingham, UK), Decorin (Bio-Techne, Abingdon, UK), Versican (Cambridge Bioscience), High-molecular weight (HMW) Hyaluronan (Bio-Techne) or Low-molecular weight (LMW) Hyaluronan (Bio-Techne) and left to incubate for 1 hour at 37°C, prior to blocking with 5% (v/v) goat serum. Then, the protocol above was followed, using 50µL of platelet suspension and reagents.

2.3.2 Platelet spreading on CDM

24-well 13mm coverslips (Scientific Laboratory Supplies) were coated with 100µL Type I collagen or fibrinogen (Sigma Aldrich) at a concentration of 100µg/mL and left to incubate overnight at 4°C. CDM was prepared as previously described in Section 2.2.4, on 13mm coverslips. Washed platelets were prepared and coverslips were washed twice gently with DPBS and blocked using 5% (v/v) goat serum for 1 hour at RT. Wells were washed again with DPBS before adding 300µL washed platelet suspension and incubating for 45 minutes at 37°C. Wells were washed, as before, to remove non-adherent platelets, and fixed and permeabilised in 4% (w/v) PFA containing 0.1% (v/v)

Triton-X 100 for 10 minutes. Following a further wash with DPBS, platelets were stained using AlexaFluor 488 Phalloidin (1:400 dilution, Thermo Fisher Scientific) for 45 minutes at RT, washed well with DPBS and mounted on slides using VectaShield Hard Set Antifade Mounting Medium (Thermo Fisher Scientific). Coverslips were then imaged using a fluorescent Leica Thunder Imaging System and image analysis was performed using ImageJ (Fiji) to analyse the number of adhered platelets, average platelet area and morphological classifications of filopodia and lamellipodia. Values were then analysed using Graphpad Prism 9.3.1 (Graphpad, La Jolla, CA, USA).

2.4 Flow cytometry analysis of platelet activation markers

For measurement of P-Selectin exposure and fibrinogen binding, a final volume of 42uL Tyrodes-HEPES buffer was added to wells of a flat bottom 96-well plate, containing 10µM ADP (Sigma Aldrich), 20µg/mL ECM proteins, PRP (1:10 dilution) and either mouse anti-human PE-Cy5 CD62P (BD Biosciences, Berkshire, UK) or rabbit anti-human FITC fibrinogen (Agilent, London, UK) (1:20 dilution). The plate was incubated in the dark for 30 minutes and 200µL 2% (w/v) PFA was added to plates to stop the reaction and fix. To quantify Annexin V, a final volume of 42uL Tyrodes-HEPES buffer containing 1mM calcium chloride was added to wells of a flat bottom 96-well plate, containing 10µM ADP (Sigma Aldrich), 20µg/mL ECM proteins, PRP (1:10 dilution) and FITC Annexin V antibody (BD Biosciences; 1:20 dilution) as previously described, in 30 second increments per well. Following a 30-minute incubation in the dark, 200µL Tyrodes-HEPES buffer containing 1mM calcium chloride was added to wells to stop the reaction by dilution. Imaging was performed on a Miltenyi Biotec MACSQuant flow cytometer. Platelets were gated based on forward and side scatter profiles, with 10,000 events counted per gate. Median fluorescence intensity of the positive population was then calculated using FlowJo software (version 7.10.1; BD Biosciences, Berkshire, UK) and values analysed using GraphPad Prism 9.3.1.

2.5 Immunofluorescence

Immunofluorescence was performed to quantify tissue factor expression in damaged HCAECs. Cells were firstly fixed in 4% (w/v) PFA for 15 minutes, before being blocked and permeabilised in blocking buffer (5% (v/v) goat serum, 0.1% (w/v) Triton-X 100) for 1 hour at RT. For tissue factor expression, recombinant anti tissue factor antibody (ab228968; Abcam, Cambridge, UK) was added to HCAECs cultured on 24-well 13mm coverslips at a dilution of 1:100 in blocking buffer without Triton-X 100, and plates were incubated overnight at 4^{o}C. Wells were washed with DPBS before cells were counterstained with AlexaFluor 568 goat anti-rabbit (1:500 dilution; Thermo Fisher Scientific), AlexaFluor 488 Phalloidin (1:400 dilution) and DAPI (1:5000 dilution; Thermo Fisher Scientific) for 1 hour at RT. Cells were then washed well and coverslips mounted on slides using VectaShield Hard Set Antifade Mounting Medium before being imaged on a Stellaris 5 confocal microscope. ImageJ (Fiji) was used to quantify fluorescence intensity and values were then analysed using Graphpad Prism 9.3.1.

2.6 Translating *in vivo* injury models to *in vitro* HCAECs

2.6.1 Modelling vessel injury

HCAECs grown on coverslips in 24-well plates were washed gently with DPBS and aspirated before addition of 50µL cell culture medium. A 1mm hole punch was used to create 1mm filter paper patches, which were then soaked in ECM extraction buffer, 10% sodium dodecyl sulphate (SDS) or 0.8%, 5% or 10% (w/v) FeCl3 (Sigma Aldrich). Filter paper was applied to a focal region on the cells for 30 seconds or 2 minutes before being removed, or cells were 'punched' with an 18 or 25 gauge needle, and wells were washed with DPBS. For *in vitro* thrombosis flow model experiments, the above was repeated on HCAECs grown on 22x64mm coverslips.

2.6.2 LIVE/DEAD assay

To quantify HCAEC cell death around the focal region following application of filter paper/needle injury, a LIVE/DEAD Viability/Cytotoxicity kit (Thermo Fisher Scientific) was used. Calcein AM (2µM) and ethidium homodimer (4µM) were added directly to

focally damaged HCAECs and plates were incubated for 40 minutes at RT. Coverslips were then mounted on slides in Hank's balanced salt solution (HBSS; 140mM sodium chloride, 5mM potassium chloride, 1mM calcium chloride, 0.4mM magnesium sulphate heptahydrate, 0.5mM magnesium chloride hexahydrate, 0.3mM sodium phosphate dibasic, 0.4mM potassium phosphate monobasic, 6mM glucose, 4mM sodium bicarbonate) and sealed using a bioinert Valap sealant (2g lanolin, 2g paraffin wax, 2g petroleum jelly, warmed to 20^{o}C) before imaging on a Leica Thunder Imaging System using the tiling feature to visualise the entire region of focal damage. ImageJ (Fiji) was then used to quantify hole size, and the LIVE/DEAD plugin was used to assess HCAEC viability (%).

2.7 RNA Analysis

2.7.1 RNA extraction and purification

HCAECs were grown in 24-well plates and damaged over 24 hours with TNF-α and 10% CSE. RNA extraction and purification was performed using the Norgen BioTek Total RNA Purification Plus Kit (Geneflow, Lichfield, UK). Following a wash step with DPBS, 200µL RT Buffer was added to wells and lysates were stored at -80^{o}C until purification was performed. Lysates were centrifuged through genomic DNA (gDNA) removal columns at 5200g for 1 minute, before addition of 120µL 100% ethanol and a further centrifugation step at 3500g for 1 minute through RNA purification columns. The RNA purification columns then underwent 3 wash steps using 400µL of wash solution A at 3500g for 1 minute, before being eluted in 50µL elution buffer at 200g for 2 minutes, followed by 14000g for 1 minute. The purified RNA was then stored at -80^{o}C until ready for use.

2.7.2 Reverse transcription

Purified RNA was quantified using a Nanodrop One Spectrophotometer (Thermo Fisher Scientific) and diluted in Invitrogen ultrapure DNAse/RNAse-free water (Thermo Fisher Scientific). RNA was reverse transcribed to complementary DNA (cDNA) using a Quantitect Reverse Transcription Kit (Qiagen, Manchester, UK). 12µL of 200ng purified

RNA was added to 2µL gDNA wipeout buffer and samples were heated for 2 minutes at 42°C to remove any residual gDNA. RT, Primer mix and RT buffer were added to samples as instructed in the protocol sheet, and a Blue Ray Turbocycler (Blue-Ray Biotech, Scientific Laboratory Supplies) thermal cycler was used for reverse transcription. Samples were incubated at 25°C for 3 minutes (primer annealing), followed by 45°C for 10 minutes (DNA polymerisation), and finally 85°C for 5 minutes (enzyme inactivation). 20µL DNAse/RNAse-free water was then added to cDNA to yield a final concentration of 5ng/µL, which was then stored at 4°C for use within 48-72 hours.

2.7.3 Real-time quantitative PCR (RT-qPCR)

PCR experiments were performed using the QuantiNova SYBR Green PCR Kit (Qiagen) and in 96-well PCR plates (Scientific Laboratory Supplies) to a total reaction volume of 10µL. Each reaction comprised 1µL cDNA, 5µL SYBR green, 3µL DNAse/RNAse-free water and 1uL primer mix containing 2µM forward and reverse primers. Primers used for PCR reactions are detailed in Table 2.1. NCBI Primer blast was used to design primers, ensuring exons were common to all transcripts. The PCR product size was specified to be 90-250, with specified melting temperature of 65°C. The primers were intron spanning with an intron length range of 100-10,000. PCR was performed using a CFX Connect Real Time PCR Thermocycler (Bio-Rad Laboratories, Watford, UK). Primer efficiencies were calculated and standard curves were generated (Section 7.3) To calculate efficiencies, average Ct value was calculated from replicate wells. Then, the log of each sample dilution was calculated. Using these values, the slope of the regression was then calculated between average Ct and log value using the SLOPE function in Excel. The primer efficiency was then calculated using the following equation:

$$\text{Efficiency (\%)} = \left(10^{\frac{-1}{slope}} - 1\right) x\ 100$$

Samples were incubated at 95°C for 5 minutes, before 40 cycles were performed at 95°C for 20 seconds, 62°C for 20 seconds and 72°C for 25 seconds. Following successful amplification, gene of interest (GOI) Ct values were normalised to housekeepers GAPDH and RPLP0 and analysed using the delta delta Ct method ($2^{-\Delta\Delta Ct}$; Livak and Schmittgen, 2001). Ct values for housekeeper technical replicates were averaged before calculation

of the geometric means. Technical replicates for sample Ct values were then averaged and delta Ct obtained by subtraction of the average housekeeper Ct from the sample Ct. The delta delta Ct value was obtained by subtracting the control delta Ct value from the sample delta Ct value, and the fold gene expression using 2^-(delta delta Ct).

Table 2.1 – A table of primers used for qPCR, including genes and their associated sequences. F – forward, R – reverse.

Gene	Sequence
CD39	**F** - ACACATCCATGTGCCCATCACA
	R - GGTGCCTTCCTCTGGATGCACT
COX2	**F** - CTGGGCCATGGGGTGGACTT
	R - CCTGCCCCACAGCAAACCGT
eNOS	**F** - TCGGCCGGAACAGCACAAGA
	R - AAAGGCGCAGAAGTGGGGGT
TBXAS1	**F** - TGGCAAAGTGGCTCGCCCAT
	R - GGGTGCGGGTATGCTGTGGA
vWF	**F** - TGCCATGGAACGTGGTCCCG
	R - ACCACCGCCTTTGAGGCTCC
RPLP0	**F -** GCAGCAGATCCGCATGTCCC
	R - TCCCCCGGATATGAGGCAGCA
GAPDH	**F -** CGGATTTGGTCGTATTGGGCG
	R - GTCTTCACCACCATGGAGAAGGC

2.8 Proteomic analysis

2.8.1 Generation of protein lysates

HCAECs and HCASMCs were grown in 6-well plates over 10 days and damaged for the final 3 days with 5ng/mL TNF-α and 10% CSE, with treatments refreshed daily. Following CDM retrieval, as previously described in Section 2.2.4, 100µL pre-warmed reducing sample buffer (100mM Tris-HCl [pH 6.8], 10% (v/v) glycerol, 4% (w/v) SDS, 0.004% (w/v) bromophenol blue, 8% (v/v) β-mercaptoethanol) was added to the first well. Protein was collected using a cell scraper (Scientific Laboratory Supplies), before the sample was aspirated and added to the next well, pooling samples from the same treatment to maximise ECM recovery. ECM lysates were then kept at -80^{o}C until ready to use.

2.8.2 Gel pouring and Coomassie staining

A 10% acrylamide gel was poured using a TGX FastCast 10% Acrylamide Kit (Bio-rad). 3mL resolver A and B were combined with 6µL tetramethylethylenediamine (TEMED) and 60µL 10% ammonium persulphate (APS), before vortexing and adding to a plate. The top was sprayed with 70% industrial methylated spirits (IMS) to flatten, and the gel left to set for 30 minutes. Next, residual IMS was removed from the gel top using a pipette, and 1mL stacker A and B were combined with 4µL TEMED and 20uL 10% APS, vortexed and added to the top of the resolver gel. Finally, a standard 1.5mm gel comb with 10 teeth was added to the gel and left to set for 30 minutes.

The gel comb was removed and 40µL ECM protein lysates were added to each well, before the gel was submerged in running buffer (25mM Tris, 192mM glycine, 0.1% (w/v) SDS, pH 8.3) and ran at 180V for 3 minutes. The gel was then removed from the running buffer and plate, and added to a square plate (Sigma Aldrich) before Coomassie staining (3.7µM coomassie blue, 60% (v/v) methanol, 12% (v/v) acetic acid) for 1 hour. The gel was then destained (10% (v/v) methanol, 10% (v/v) acetic acid) regularly and overnight until clear, before submission to the BioMS facility at the University of Manchester for mass spectrometric analysis.

2.8.3 Mass spectrometry

Following destaining, 24 gel bands containing enriched ECM fractions were submitted to the BioMS facility at the University of Manchester. In-gel trypsin digestion was performed by collaborators at the University of Manchester, in a protocol as described by Shevchenko *et al.* (1996). Protein bands were chopped and transferred to wells of a 96-well plate and dehydrated, dried and suspended in reduction buffer (10mM dithiothreitol, 25 mM NH_4HCO_3) before alkylation and digestion at 37°C. Peptides were then centrifuged and extracted in 20mM NH_4HCO_3 before resuspension in 5% (v/v) formic acid in 50% (v/v) acetonitrile. Samples were then processed through S-Trap and Thermo Exploris 480 (Thermo Fisher Scientific) at the BioMS facility. HCAEC and HCASMC CDMs derived from healthy and stimulated cells were compared to quantify abundance of ECM components and analyse ECM composition. Samples were analysed following quantification by the facility at the University of Manchester using the Proteome Discoverer software (Thermo Fisher Scientific). Identified proteins were then filtered in the Excel sheet provided by specifying High protein FDR confidence only, and ≥2 Unique peptides. Following initial analysis, the sample p-values were log transformed and processed through DAVID Functional Annotation Tool (DAVID Bioinformatics, National Institutes of Health, 9000 Rockville Pike, Bethesda, Maryland 20892) for gene ontology and pathway analysis, and GraphPad Prism 9.3.1 was used to generate volcano plots with annotations showing genes of interest. Matrisomal proteins were identified using a matrisome database (MatrisomeDB; Shao *et al.,* 2019).

2.9 Development of the thrombosis model

2.9.1 High throughput thrombosis model

Ibidi VI 0.1 µ-slides (Thistle Scientific) were used in the high throughput model setup to measure thrombus formation on ECM proteins, enabling six chambers to be under flow at one time. Slide chambers were coated with 1.7µL 100µg/mL Type I collagen (Equine tendon-derived; Labmedics), Type III collagen (Cambridge Bioscience), Biglycan (Caltag MedSystems), Decorin (Bio-Techne), Versican (Cambridge Bioscience), HMW Hyaluronan (Bio-Techne) or LMW Hyaluronan (Bio-Techne) for one hour at RT prior to performing experiments. Proteins were also combined to form composites at these concentrations, generating disease-relevant composites. The model was set up using a six-channel programmable syringe pump (ProSense, Chepstow, UK) with 5, 10 and 20mL syringes (Thermo Fisher Scientific) connected to silicone tubing with an internal diameter of 0.8mm (RS Components, UK) and Luer adaptors creating a high throughput flow model (Figure 2.1). Platelets in whole blood were incubated with 1µM DIOC-6 for 15 minutes at RT. In experiments using antiplatelet drugs, 30µM aspirin (Tocris, Bio-Techne) and 10µM clopidogrel (Tocris, Bio-Techne) were added to whole blood for 30 minutes prior to perfusion. Slide chambers were washed under flow with Tyrodes-HEPES buffer (with added glucose) at 46.7µL/min (15 dynes/cm^2), before 330µL DIOC-6 fluorescently tagged whole blood was perfused through chambers. Thrombus formation was imaged at 488nm using a Celena S Logos fluorescent digital imaging system and Stellaris 5 confocal microscope, and average thrombi number, size, area coverage and volume analysed using ImageJ (Fiji) thresholding. To calculate thrombus volume, the Cavalieri principle was used, multiplying the area coverage of each Z-stack image by the change in Z (0.69µm) and totalling the values (Pugh *et al.,* 2010).

2.9.2 Thrombosis model with an accessible chamber

Ibidi sticky slide I Luers (Thistle Scientific) were used to facilitate access to cells and ECM immediately prior to running the model. Cells and decellularised ECM were prepared on coverslips as previously described in Section 2.2. For CDM experiments, DIOC-6-labelled whole blood was perfused through channels, as previously described in Section 2.10.1.

Coverslips were removed from 4-well plates using tweezers and dried around the edges using white roll. The sticky slide film was removed and the coverslip was lined up with the slide and pressed firmly against the edges to seal the chamber. The chamber was then connected to the flow system (as in Figure 2.1) and perfused with Tyrodes-HEPES buffer (with added 5mM glucose) at 550µL/min (15 dynes/cm^2), before being perfused with 3.85mL labelled whole blood. For cellularised coverslips, before whole blood perfusion, cell detachment was firstly monitored over 5 minutes to ensure adhesion to coverslips under an arterial shear rate. Thrombus formation was then imaged on a Celena S Logos digital fluorescent imaging system and a Stellaris 5 confocal microscope, before analysis of average thrombi number, size, area coverage and volume using ImageJ (Fiji) thresholding. To calculate thrombus volume, the Cavalieri principle was used, multiplying the area coverage of each Z-stack image by the change in Z (0.69µm) and totalling the values (Pugh *et al.,* 2010).

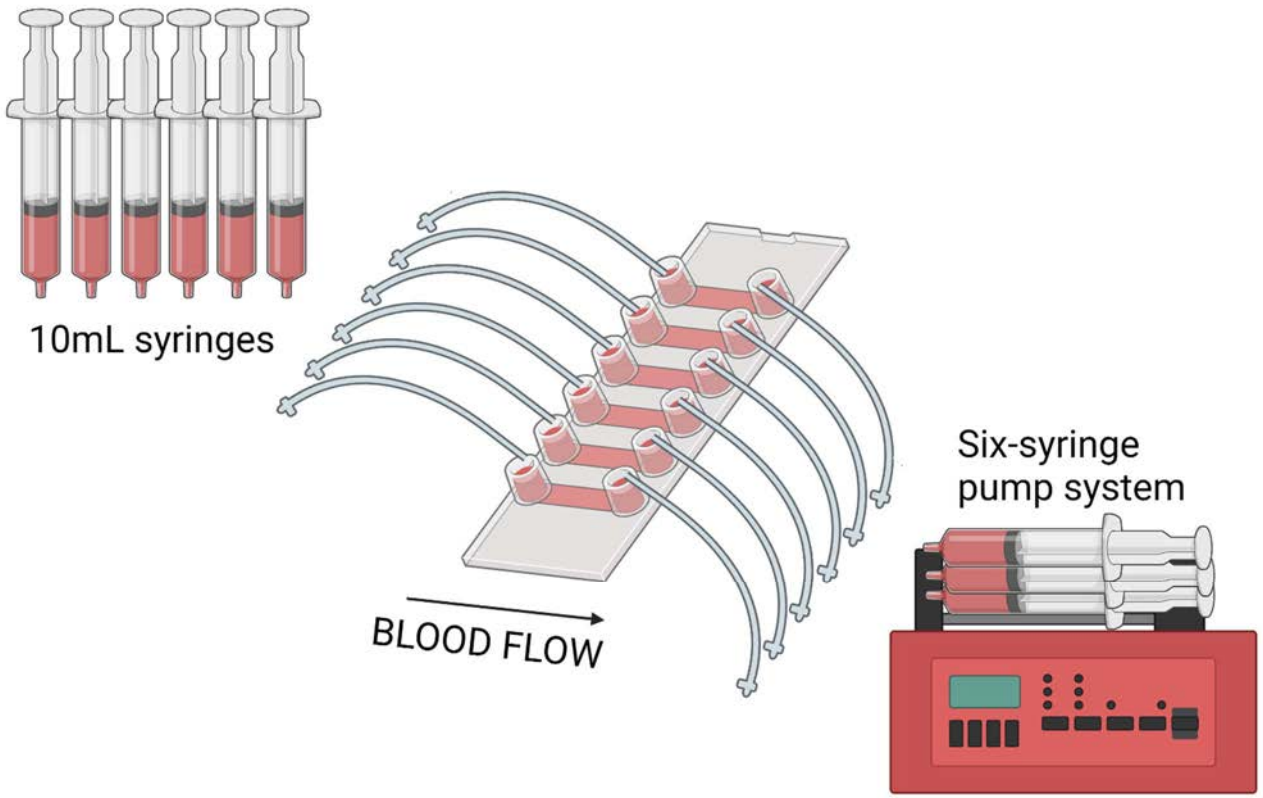

Figure 2.1 – The high-throughput thrombosis model using ibidi µ-slides. DIOC-6 labelled whole blood was added to 10mL syringes before perfusion of blood through ibidi µ-slide chambers at an arterial shear rate on the 'withdraw' setting on the syringe pump. Thrombus formation in chambers was measured using a fluorescent microscope (FITC channel). Created with BioRender.com.

2.10 Statistical analysis

Statistical analysis was executed from a minimum of three biological repeats from different blood donors or batches of cells (different donors), and was performed using GraphPad Prism 9.3.1. Normal distribution of data was confirmed using a Shapiro-Wilk test and statistical significance determined using paired or unpaired one-way analysis of variances (ANOVAs) (with Tukey post hoc correction for multiple comparisons). The ImageJ (Fiji) thresholding feature and the LIVE/DEAD plugin was used for microscopy and image analysis. Data is expressed as ± standard error of the mean (SEM) and P values <0.05 are considered significant.

3. Investigating platelet responses to a recombinant extracellular matrix

3.1 Introduction

As previously discussed in Section 1.4, atherosclerotic plaque development is a complex, multifactorial process involving many mediators of thrombosis and haemostasis. As a primary trigger for the initiation of thrombosis, the exposure of the ECM is a key stage in the development of an occlusive thrombus. Emerging evidence reveals differences in the composition of this underlying ECM in plaque rupture and erosion (Kolodgie *et al.,* 2002; Otsuka *et al.,* 2016), which has the potential to introduce variation in the thrombotic process for each plaque type. Indeed, thrombi associated with ruptured plaques are commonly occlusive and red in appearance, in contrast to erosion thrombi which are generally less occlusive and more platelet-rich in appearance (Quillard *et al.,* 2017). Risk factors associated with each plaque type may account for some ECM variations. The more traditional risk factors of hypertension, hyperlipidaemia and increasing age are associated with plaque rupture, whereas plaque erosion has a propensity to occur in women, smokers and those under the age of 50 (Virmani *et al.,* 2006; Jia *et al.,* 2013; Pedicino *et al.,* 2018). There is evidence to show that dysfunctional endothelial cells may also contribute to ECM variations (Davis and Senger, 2005), as well as signal transduction to SMCs in chronic inflammatory settings (Mendez-Barbero *et al.,* 2021). Despite these complex factors potentially having a significant effect on atherothrombosis, *in vivo* and *in vitro* models fail to acknowledge ECM variations and incorporate these into current models.

Vascular proteoglycans, as described in Section 1.2.3.2, are key components of the ECM with functional roles in modifying the biomechanical properties of fibrillar collagen, as well as regulating cell behaviour, platelet function and the development and progression of atherosclerotic plaques (Iozzo and Schaefer, 2015; Ganesan *et al.,* 2017; Hamilos *et al.,* 2018). Evidence shows that PG abundance at the plaque-thrombus interface differs between ruptured and eroded plaques, with decorin and biglycan present in ruptured plaques, and versican and hyaluronan in eroded plaques. Currently, it is unknown whether these variations will have a role in the initiation and progression of thrombosis

in each plaque type. A summary of current knowledge surrounding platelet responses to vascular proteoglycans relevant in plaque rupture and erosion is summarised below.

3.1.1 Biglycan

Whilst its expression in the vascular endothelium is well established, the role of biglycan in thrombosis has not been investigated in detail, despite a reduction of the proteoglycan being observed to increase thrombotic risk in foetal growth restriction (Murthi *et al.,* 2010) and increase platelet activation in mice (Grandoch *et al.,* 2016). Platelets only weakly adhere to biglycan (Mazzucato *et al.,* 2002) and as such, recent research has focused on interactions between biglycan and growth factors associated with platelets. Biglycan has been shown to regulate thrombin activity (Grandoch *et al.,* 2016) by binding to and activating thrombin inhibitor heparin cofactor II (HCII; McGuire and Tollefson, 1987; He *et al.,* 2008). Indeed, thrombin binds to endothelial PAR-1 and upregulates expression of biglycan (Tiede *et al.,* 2009), potentially as a mechanism of self-regulation to reduce thrombin availability and prevent unwarranted platelet activation. Collectively, these findings suggest an inhibitory role for biglycan, indirectly suppressing platelet activity and the propagation of atherothrombosis. However, the direct effect of biglycan on platelets and its role in various thrombotic pathologies is yet to be determined.

3.1.2 Decorin

Decorin is a Class I SLRP, and consequently has a similar effect on platelets and platelet-derived mediators as biglycan. Like bigylcan, decorin has been shown to have an inhibitory effect on thrombin activity (Chui *et al.,* 2014), perhaps elucidated by its ability to bind to HCII (Whinna *et al.,* 1993) in a DS-dependent mechanism similar to that of biglycan. Resting platelets bind decorin weakly, with adhesion facilitated by DS binding receptors on platelets (Mazzucato *et al.,* 2002), specifically integrin αIIβ1 (De Witt *et al.,* 2014). Interaction of αIIβ1 with decorin results in activation of PLC, mediating shear-dependent platelet activation and aggregation under flow (Speich *et al.,* 2008). However, as both Type I collagen and decorin bind to αIIβ1 on platelets and are

colocalised in the vascular wall, the weak interaction between platelets and decorin may be transient, and occur to prevent excess platelet adhesion and activation on ECM collagens. Indeed, there is also evidence to suggest that decorin has indirect inhibitory effects on platelets. Paderi *et al.* (2011) suggest that decorin binding to Type I collagen covers the platelet binding site, preventing platelet adhesion and activation. Additionally, decorin can bind to complement component 1q (C1q), preventing its binding to endothelial cells (Groeneveld *et al.,* 2005) and subsequent platelet adhesion and activation via the release of vWF (Peershke *et al.,* 1993; Peershke and Ghebrehiwet, 1997; Kolm *et al.,* 2016). Collectively, these findings indicate a potentially inhibitory role for decorin in the propagation of atherothrombosis, however further research is essential to investigate the interactions of this proteoglycan with other matrix proteins in thrombotic pathologies.

3.1.3 Versican

Versican is a prominent proteoglycan found at the plaque-thrombus interface in plaque erosion, yet much is still unknown regarding its interactions with platelets. Platelet binding to V1 and V2 isoforms of versican is P-Selectin dependent, and has been shown to promote platelet adhesion but not aggregation (Kawashima *et al.,* 2000; Kolodgie *et al.,* 2002; Mazzucato *et al.,* 2002), potentially due to the ability of the G1 domain of versican to bind to thrombospondin-1 and regulate platelet activation (Kuznetsova *et al.,* 2006). Thrombus growth is promoted in the presence of collagen, however, suggesting that proteoglycan activity is modified in the presence of fibrillar proteins such as collagen (Mazzucato *et al.,* 2002). It has also been suggested that thrombin generation following platelet activation may promote proteolytic degradation of versican into smaller, pro-inflammatory fragments referred to as versikine (Ivey and Little, 2008), potentially contributing to atherothrombosis. The interaction of versican with platelets in atherothrombosis is complex due to the existence of multiple isoforms with opposing pro- and anti-inflammatory effects (Wight *et al.,* 2014), and requires further investigation to fully elucidate.

3.1.4 Hyaluronan

Hyaluronan, unlike previously described proteoglycans, is a GAG without a protein core, and exists in fragments of differing molecular weight. HMW hyaluronan is found in healthy tissue and has a molecular weight of over 100 kDa (Litwiniuk *et al.,* 2016). Upon tissue injury, growth factors such as PDGF stimulate SMCs to preferentially synthesise both hyaluronan and versican, forming cable-like structures which promote cell migration, cell proliferation and leukocyte adhesion (Evanko *et al.,* 1999; Evanko *et al.,* 2001; Holm *et al.,* 2008; Wight *et al.,* 2014; Wight, 2017). Excessive production of HMW hyaluronan, however, stimulates the release of hyaluronidase from fibroblasts (Li *et al.,* 2017), which degrades hyaluronan into angiogenic, inflammatory LMW fragments (de la Motte *et al.,* 2009; Campo *et al.,* 2010; Petrey and de la Motte, 2014; Litwiniuk *et al.,* 2016). LMW hyaluronan (<20 kDa) binds TLRs and promotes signalling pathways upregulating NFκB, TNF-α, and the propagation of inflammation (Petrey *et al.,* 2016; D'Agostino *et al.,* 2017; Quillard *et al.,* 2017; Wight, 2017). TNF-α, associated with inflammatory vascular environments, also stimulates the formation of TNF-stimulated gene (TSG)-6, which modifies hyaluronan by addition of heavy chains (Kohda *et al.,* 1996; Stober *et al.,* 2017). This process is irreversible in LMW hyaluronan and is associated with chronic inflammatory diseases (Colón *et al.,* 2009; Lauer *et al.,* 2013).

Unlike previously described proteoglycans, the interaction of platelets and HMW hyaluronan has been well-documented. HMW hyaluronan binds to platelets via the CD44 receptor (Koshiishi *et al.,* 1994; Holm *et al.,* 2012), and has been shown to inhibit platelet activation, aggregation and adhesion (Verheye *et al.,* 2000; Mazzucato *et al.,* 2002; Liu *et al.,* 2016; Li *et al.,* 2017). However, upon tissue injury, however, activated platelets can degrade HMW hyaluronan into LMW hyaluronan by releasing hyaluronidase (HYAL)-2, an enzyme located in a population of platelet alpha granules lacking P-Selectin, fibrinogen and vWF (Stern and Jedrzejas, 2006; Harada and Tarakashi, 2007; Albeiroti *et al.,* 2015; Petrey *et al.,* 2016). Although LMW hyaluronan is pro-inflammatory (D'Agostino *et al.,* 2017), research suggests that it has a role in preventing atherogenic cardiovascular events. HMW heavy chain hyaluronan, associated with TNF-α, is pathological and leukocyte adhesive (Wight, 2008; Lauer *et al.,* 2013). Research conducted by Petrey *et al.* (2019) demonstrated that platelet HYAL-2 degradation of HMW heavy chain hyaluronan into LMW hyaluronan significantly reduced leukocyte

migration into the sub-endothelial layer. Additionally, HYAL-2 and CD44 can interact to catalyse the cleavage of HMW hyaluronan to LMW hyaluronan (de la Motte *et al.,* 2009), and are both elevated in patients with plaque erosion (Pedicino *et al.,* 2018). In the absence of HYAL-2, hyaluronan accumulates and remodels the ECM (Chowdhury *et al.,* 2013), a pathological event central to the development of atherosclerosis. There is therefore evidence to suggest that the interaction of platelets and hyaluronan in atherothrombosis is still to be fully elucidated. Currently, the overreliance of Type I collagen in thrombosis models means that any interactions in the vascular ECM between collagens and vascular PGs are not taken into account, and as a result, the effect of this interaction on platelets and thrombosis has not been observed. Additionally, there are currently no models of plaque erosion, so any differences in ECM composition between ruptured and eroded plaques, which may have an effect on arterial thrombosis, have not been taken into account.

3.1.5 Chapter aim, objectives and hypothesis

The aim of this Chapter is to investigate platelet responses to vascular proteoglycans relevant in the development and progression of atherosclerosis, and to elucidate whether these findings could be significant when considering differences in ECM composition in plaque rupture and erosion.

Objectives:

1. Elucidate the regulation of platelet adhesion, activity and thrombus formation by collagens and vascular proteoglycans
2. Explore the interplay and regulation of platelet activity by collagens and vascular proteoglycans
3. Generate disease-relevant composites of plaque rupture and erosion, and use to investigate platelet adhesion and thrombus formation under physiological and pathological shear rates
4. Characterise the efficacy of DAPT on ‘rupture’ and ‘erosion’ ECM composites.

Hypothesis: - Platelet thrombus formation is altered on and regulated by different ECM substrates, which affects the efficacy of DAPT.

3.2 Results

3.2.1 Recombinant vascular proteoglycans can inhibit or promote platelet adhesion

Variations in platelet responses to vascular PGs, or variations in the abundance of different PGs in the vascular ECM may explain differences in thrombus formation *in vivo*. However, studies are lacking where platelet interactions with, and activation by vascular proteoglycans have been directly compared. Platelet adhesion assays were performed to determine ligand binding affinity to ECM proteins and as an indication of initial platelet spreading. Initial experiments were performed to determine the optimum blocking buffer and ECM protein concentrations to use. Washed platelets ($2x10^7$/mL) were allowed to adhere to 20µg/mL Type I and III collagen, recombinant biglycan, decorin, versican and HMW and LMW hyaluronan for 45 minutes at 37^{o}C, before being stained with 1µM DIOC-6 (membrane dye) and imaged using a fluorescent microscope. For each ECM protein, platelets were counted using ImageJ and average area calculated, to reflect platelet adhesion and degree of spreading. HMW and LMW hyaluronan were both used in experiments to reflect anti- and pro-inflammatory isoforms respectively.

Results demonstrated that 5% (v/v) Goat serum for 1h was the optimum blocking buffer, having the least platelet adhesion compared with both 1% (w/v) BSA and ibiTreat ($P<0.05$) (Figure 3.1) under the same conditions. Next, wells were coated with varying concentrations of the different vascular PGs to determine optimum concentrations for platelet adhesion. Results from coating optimisation experiments demonstrated that ECM protein concentration was optimal at 20µg/mL (Figure 3.2), defined as the lowest concentration at which the platelet response to all PGs was consistent. Platelet adhesion assays demonstrated that the number of adhered platelets was significantly higher on Type I collagen than Type III collagen (Figure 3.3; $P<0.05$). The most adhesive vascular proteoglycan under static conditions was versican, with significantly higher platelets adhered than on decorin ($P<0.01$), biglycan ($P<0.01$), HMW hyaluronan ($P<0.01$) and Type III collagen ($P<0.05$) (Figure 3.3). The least adhesive proteins were decorin and HMW hyaluronan. Average platelet area was highest on Type I collagen, compared with decorin ($P<0.01$) and versican ($P<0.01$). In summary, platelet adhesion and spreading to individual ECM components varies significantly amongst collagens and vascular PGs, with Type I collagen being one of the most adhesive proteins in the sample set.

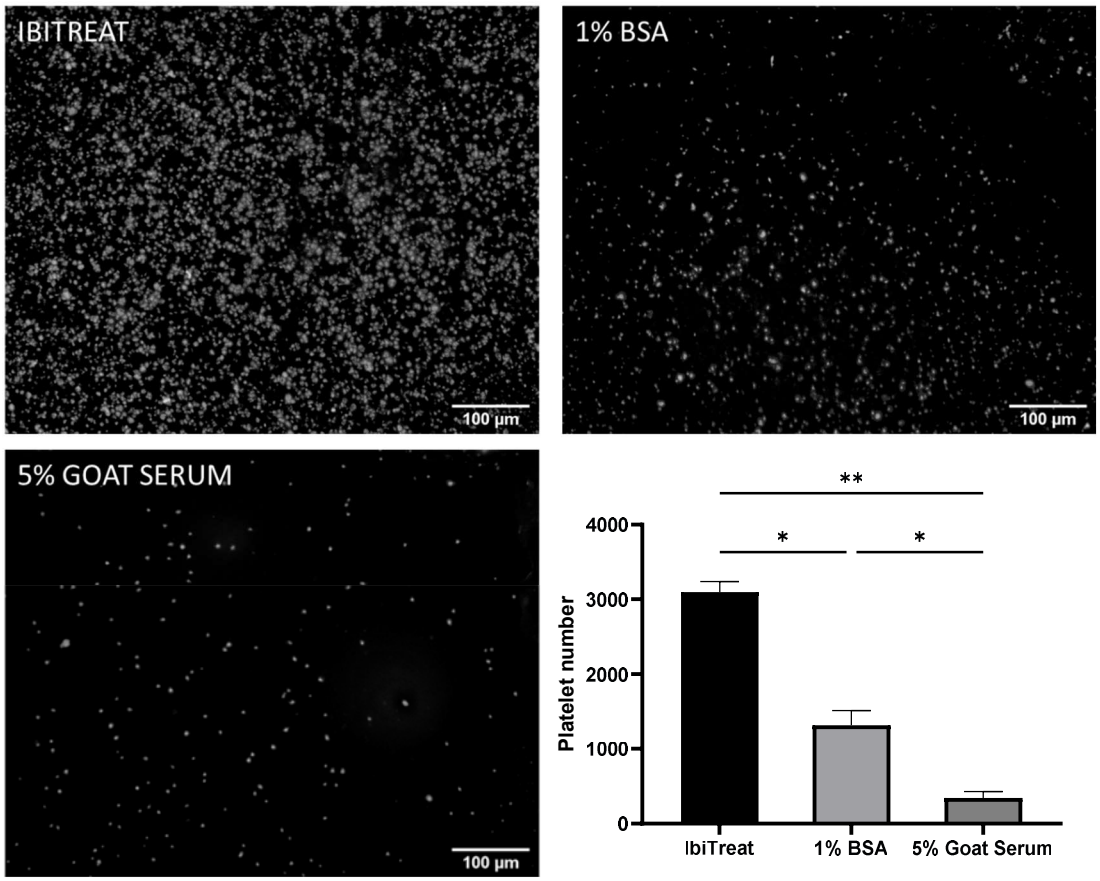

Figure 3.1 – Optimisation of blocking buffer for platelet adhesion on disease-relevant extracellular matrix proteins. Initial experiments were performed to optimise blocking buffer by incubating ibiTreat, 1% (w/v) BSA and 5% (v/v) Goat serum on ibidi µ-slides, before addition of washed platelets ($2x10^7$/mL). Fixed platelets were stained with 1µM DIOC-6 and visualised on a Celena S Logos fluorescent microscope. A one-way ANOVA with Tukey correction was used for statistical analysis. Error bars represent ± SEM. n=3; *P<0.05; **P<0.01.

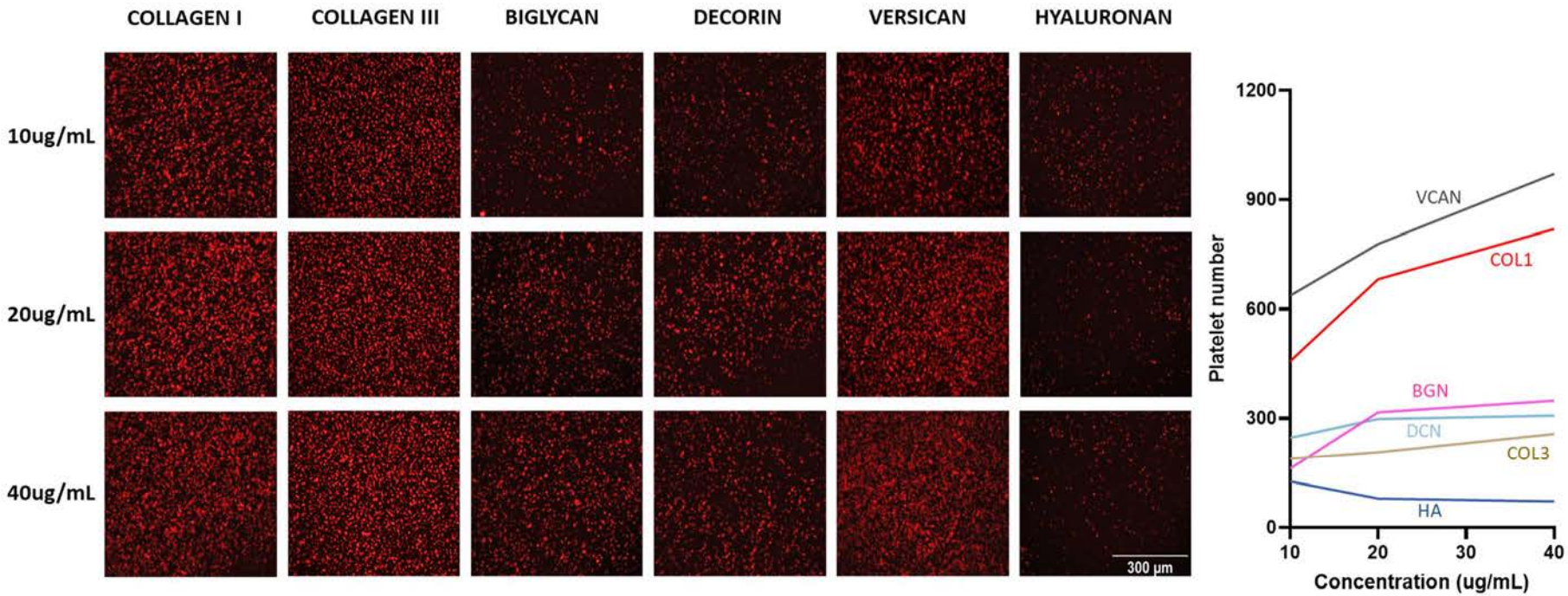

Figure 3.2 – Optimisation of platelet adhesion on different concentrations of extracellular matrix (ECM) proteins. ECM proteins were coated in wells at concentrations of 10, 20 and 40µg/mL for 1 hour at RT before addition of washed platelets ($2x10^7$/mL). Fixed platelets were stained with 1µM DIOC-6 and platelet number at different ECM protein concentrations was visualised on a Celena S Logos fluorescent microscope. n=2. COL1 – Type I Collagen; COL3 – Type III Collagen; VCAN – Versican; BGN – Biglycan; DCN – Decorin; HA – Hyaluronan.

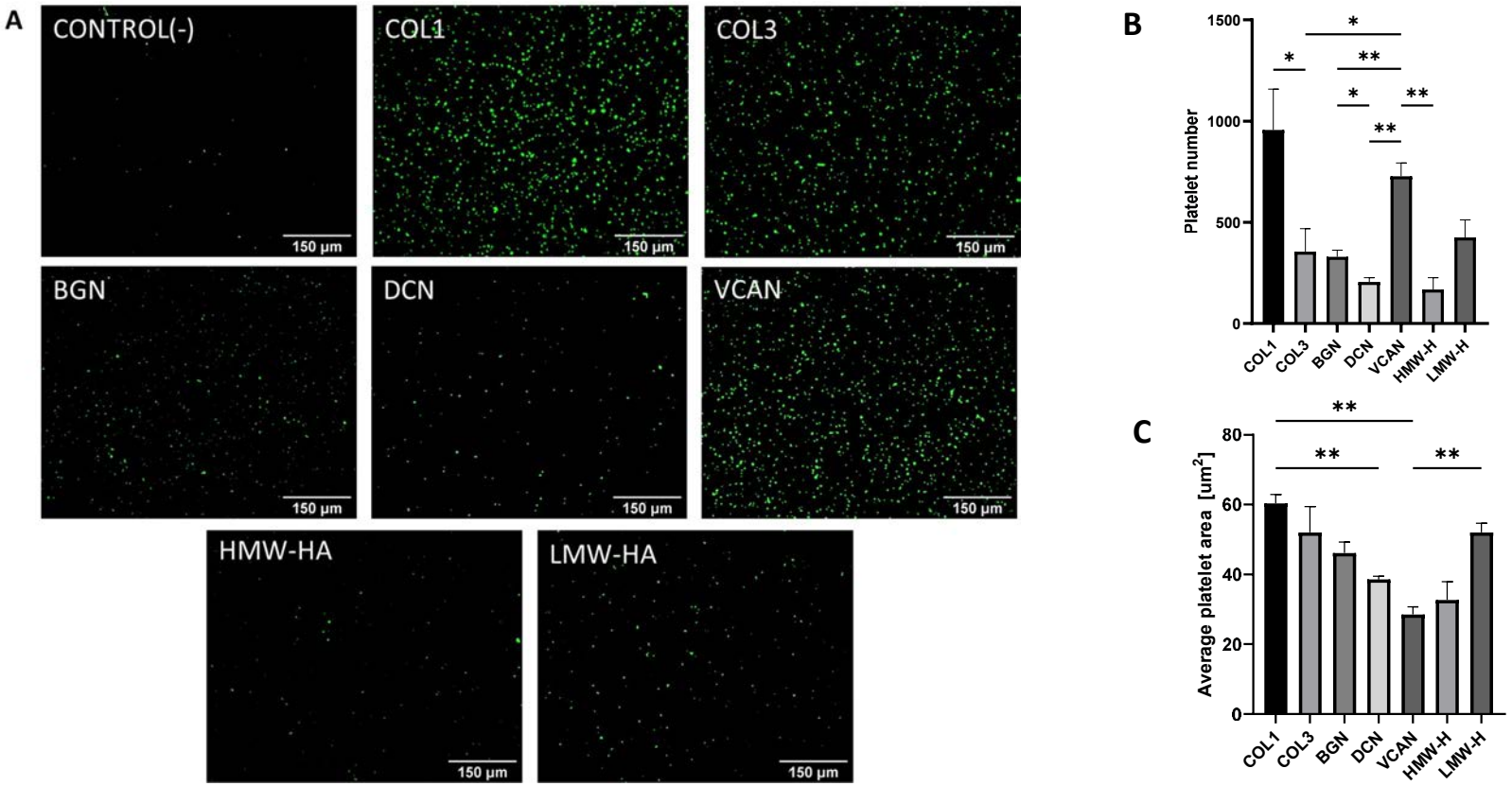

Figure 3.3 – Platelet adhesion to individual disease-relevant extracellular matrix proteins. 20ug/mL ECM proteins were coated in wells for 1 hour at room temperature, before washed platelets were added at $2x10^7$/mL. Platelets were incubated for 45 minutes at 37°C before being fixed, permeabilised and stained with 1µM DIOC-6. Platelet adhesion (A) was visualised on a Celena S Logos microscope and platelet number (B) and average area (C) analysed using ImageJ. A one-way ANOVA with Tukey correction was used for statistical analysis. Error bars represent ± SEM. n=5; *P<0.05; **P<0.01. COL1 – Type I Collagen; COL3 – Type III Collagen; VCAN – Versican; BGN – Biglycan; DCN – Decorin; H – Hyaluronan; HMW – High molecular weight; LMW – Low molecular weight.

3.2.2 A composite 'rupture' matrix has higher platelet binding affinity under static conditions than a composite 'erosion' matrix

To further investigate the interaction between platelets and the vascular ECM, disease-relevant composites (plaque rupture and erosion matrices) were generated (Table 3.1), incorporating collagens and vascular PGs using findings from Kolodgie *et al.* (2002). Platelet adhesion on these composites was then compared with the commonly used *in vitro* standard of Type I collagen.

Table 3.1 – Components in plaque 'rupture' and 'erosion' composites, adapted from Kolodgie *et al.* (2002).

'Rupture' composite	'Erosion' composite
Type I collagen – 20µg/mL	Type III collagen– 20µg/mL
Biglycan– 20µg/mL	Versican– 20µg/mL
Decorin– 20µg/mL	HMW/LMW hyaluronan – 20µg/mL

The final composites reflect the ECM composition described in Section 1.4. The composites were gently mixed with a pipette and coated, in addition to Type I collagen (20µg/mL). After 1 hour, washed platelets ($2x10^7$/mL) were allowed to adhere to composites for 45 minutes at 37°C, before being fixed in 4% (w/v) PFA for 10 minutes, stained with 1µM DIOC-6 for 30 minutes and imaged using a fluorescent microscope. For each sample, platelets were counted using ImageJ and average area calculated, to reflect platelet adhesion and degree of spreading respectively.

Results from the adhesion assay demonstrated that the highest platelet binding affinity occurred on the 'rupture' composite (Figure 3.4). Significantly more platelets adhered to the rupture matrix than both 'erosion' matrices ($P<0.05$; $P<0.05$) and Type I collagen ($P<0.05$). However, platelet spreading was significantly greater on Type I collagen compared with both 'rupture' ($P<0.01$) and 'erosion' ($P<0.01$; $P<0.001$) matrices. There were no significant differences observed on the measured parameters of platelet number and average platelet area between 'erosion' composites containing HMW and LMW hyaluronan.

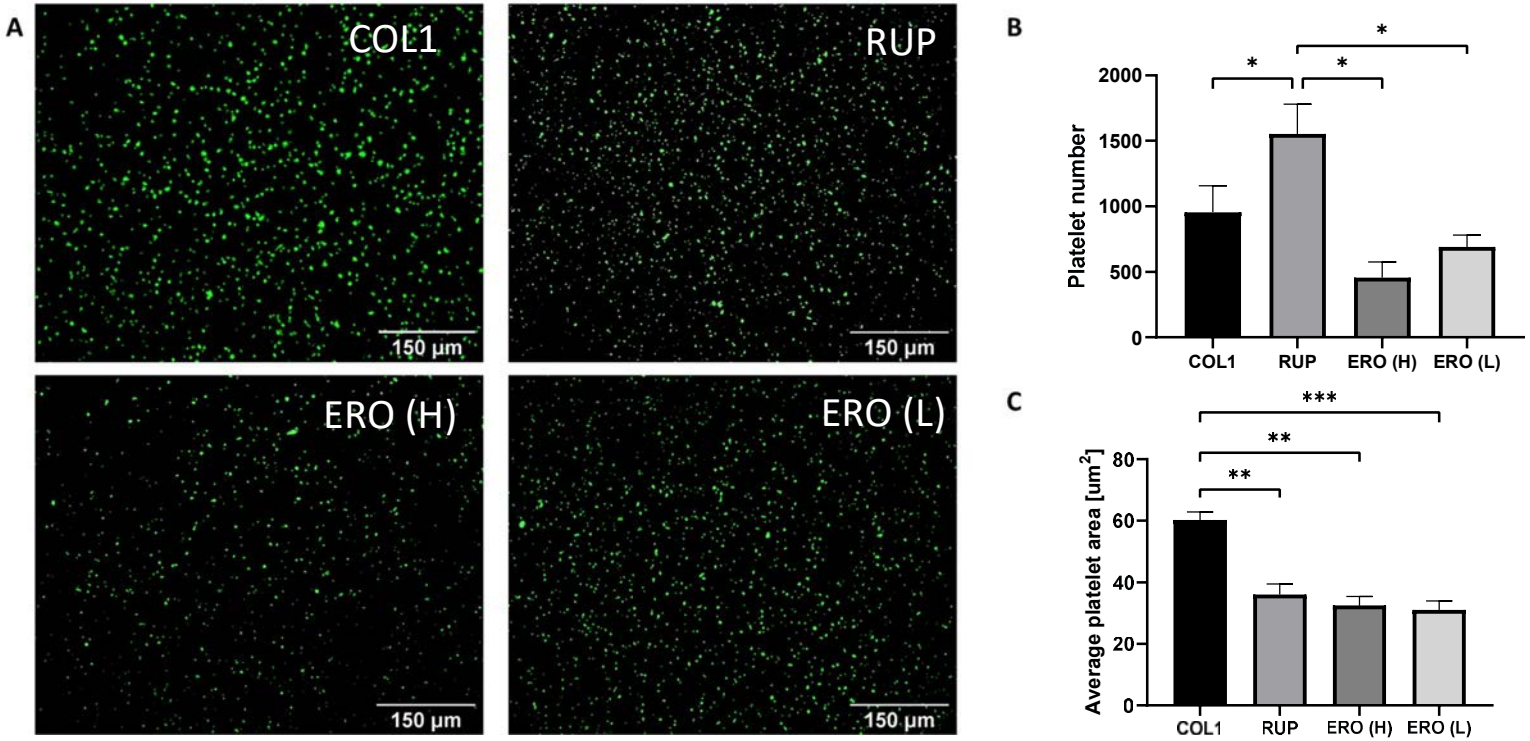

Figure 3.4 – Platelet adhesion to Type I collagen compared to disease-relevant 'rupture' and 'erosion' matrices. Type I collagen (COL1), biglycan and decorin were combined to form the rupture (RUP) matrix, and Type III collagen, versican and either HMW or LMW hyaluronan to form the erosion (ERO (H) and ERO (L)) matrices respectively. Type I collagen and disease-relevant composites were coated in wells for 1 hour, before washed platelets were added and incubated for 45 minutes at 37°C before being fixed, permeabilised and stained with 1µM DIOC-6. Platelet adhesion (A) was visualised on a Celena S Logos microscope and platelet number (B) and average area (C) analysed using ImageJ. A one-way ANOVA with Tukey correction was used for statistical analysis. Error bars represent ± SEM. n=5; *P<0.05; **P<0.01; ***P<0.001

3.2.3 Resting platelets do not activate in response to different vascular proteoglycans

To account for variations in platelet adhesion, flow cytometry was performed to investigate platelet alpha granule secretion (P-Selectin exposure) and conformational change of integrin αIIbβ3 (Fibrinogen binding), measures of platelet activation, in response to ECM proteins. Types I and III collagen, versican, HMW and LMW hyaluronan, biglycan and decorin (20µg/mL) were added to PRP and Tyrodes-HEPES buffer alongside either mouse anti-human PE-Cy5 CD62P or rabbit anti-human FITC fibrinogen. Following a 30-minute incubation in the dark, 2% (w/v) PFA was added to wells to stop the reaction, before flow cytometry analysis. Platelets were gated on size and 10,000 events were counted, and platelet marker expression (median fluorescence intensity (MFI)) calculated using FlowJo software (version 7.10.1).

Results from flow cytometry analysis demonstrated that most of the ECM proteins investigated, both collagens included, do not appear to promote P-selectin exposure and alpha granule secretion in resting platelets, except LMW hyaluronan ($P<0.05$) (Figure 3.5). Indeed, there are some differences in platelet responses between LMW hyaluronan and other vascular PGs such as biglycan and decorin ($P<0.05$). Vascular PGs also do not appear to promote fibrinogen binding in platelets, in contrast to Type I ($P<0.05$) and III ($P<0.01$) collagens. Versican does appear to be having some effect on blocking platelet activity, but this was not a significant effect in the experiments performed. In summary, vascular PGs, in contrast to Types I and III collagen, do not appear to have roles in the initiation of platelet activation, when using P-selectin exposure and fibrinogen binding as markers of activation.

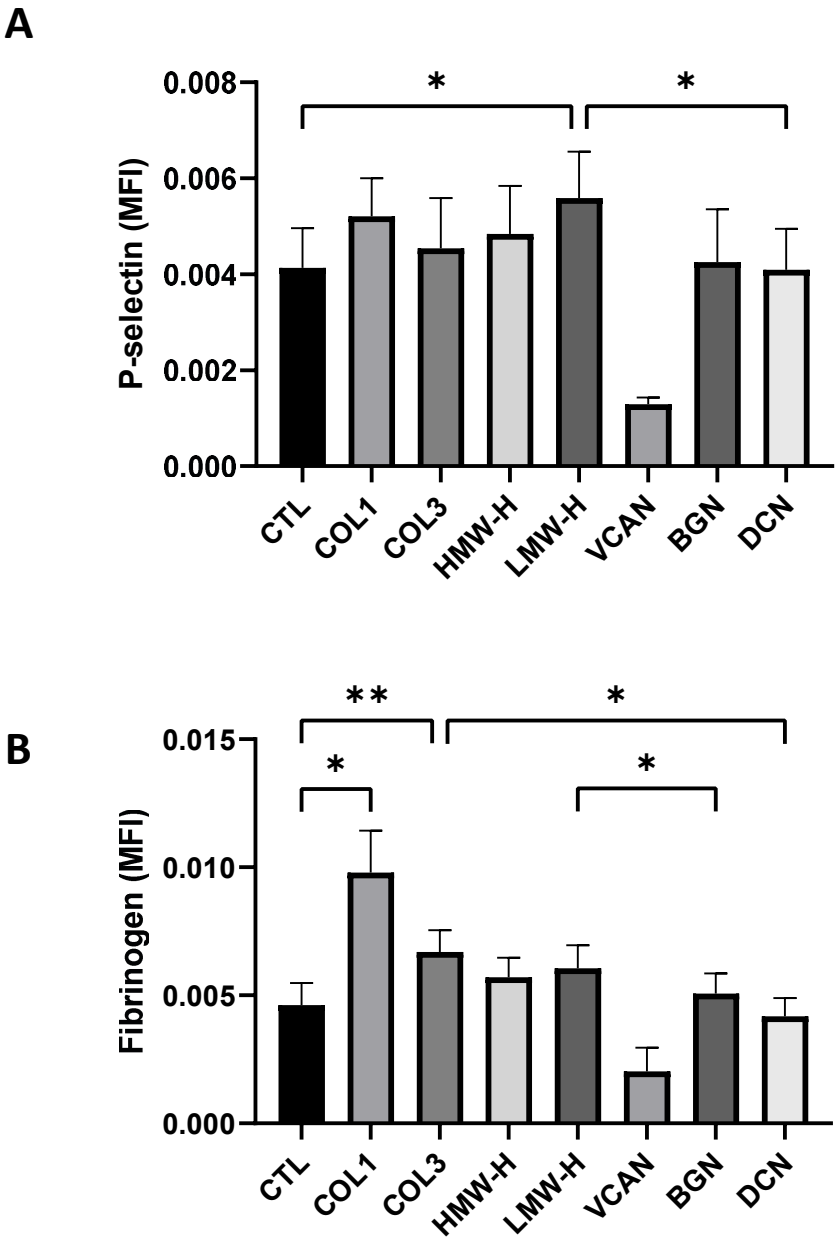

Figure 3.5 – Platelet activation marker expression in response to Type I and III collagen and vascular proteoglycans. 20µg/mL ECM proteins were added to resting platelets to measure P-selectin exposure (A) and fibrinogen binding (B). Platelets were stained for 30 minutes in the dark, gated on size and passed through a flow cytometer for analysis. A one-way ANOVA with Tukey correction was used for statistical analysis. Error bars represent ± SEM. n=4; *P<0.05; **P<0.01. CTL – Control; COL1 – Type I Collagen; COL3 – Type III Collagen; VCAN – Versican; BGN – Biglycan; DCN – Decorin; H – Hyaluronan; HMW – High molecular weight; LMW – Low molecular weight.

3.2.4 Vascular proteoglycans do not potentiate ADP mediated platelet activation, but alter PS exposure

Following vascular injury, components of the vascular ECM may also encounter activated platelets and may therefore have the ability to potentiate platelet activation. Figure 3.5 demonstrates that the collagens are platelet agonists, but does not elucidate the potential role of vascular PGs following platelet activation. To investigate this concept in more detail, flow cytometry was performed to investigate platelet alpha granule secretion (P-Selectin exposure), conformational change of integrin αIIbβ3 (Fibrinogen binding) and PS exposure (procoagulant activity) as measures of platelet activation, in response to ECM proteins and 10μM ADP. Types I and III collagen, versican, HMW and LMW hyaluronan, biglycan and decorin (20μg/mL) were added to PRP and Tyrodes-HEPES buffer (with or without 1mM calcium chloride) alongside either mouse anti-human PE-Cy5 CD62P, rabbit anti-human FITC fibrinogen or FITC Annexin V. Following a 30-minute incubation in the dark, 2% (w/v) PFA or Tyrodes-HEPES buffer (with 1mM calcium chloride) was added to wells to stop the reaction, before flow cytometry analysis. Platelets were gated on size and 10,000 events were counted, and platelet marker expression calculated using FlowJo software (version 7.10.1).

Results from flow cytometry analysis demonstrated that, following platelet stimulation with 10μM ADP, platelet activation (measured by P-selectin exposure and fibrinogen binding) is not potentiated in the presence of the investigated ECM components, including both collagens (Figure 3.6). There is a trend showing a reduction in platelet activation upon platelet exposure to versican, similar to Figure 3.5, however this was not significant in the experiments performed. Results from experiments measuring PS exposure, platelet procoagulant activity, demonstrated significant increases in PS exposure upon platelet exposure to LMW hyaluronan ($P<0.05$) and reductions in PS exposure upon platelet exposure to versican ($P<0.05$) (Figure 3.6). In summary, vascular PGs do not appear to have a role in the potentiation of platelet activation, following stimulation with 10μM ADP, but may have a role in promoting or inhibiting PS exposure and platelet procoagulant activity.

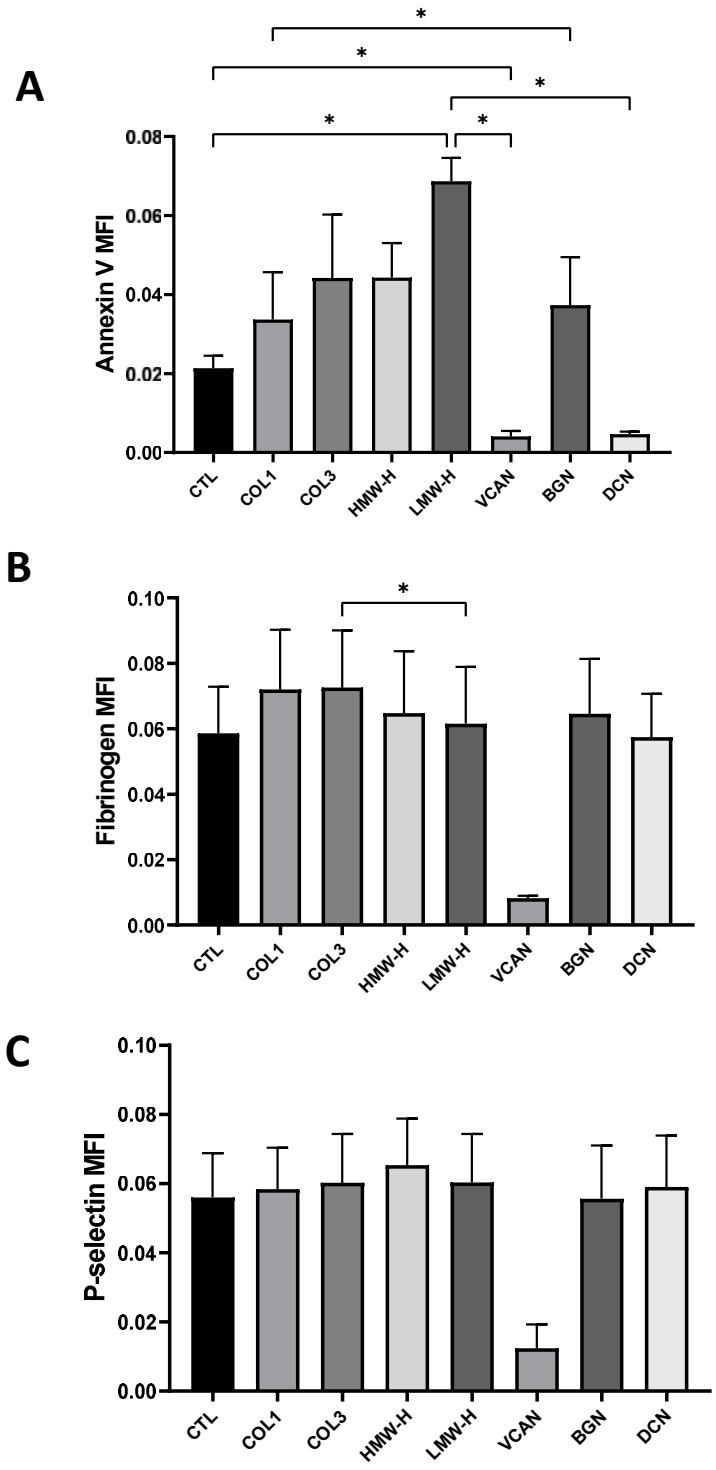

Figure 3.6 – Platelet phosphatidylserine exposure and measurement of potentiation of platelet activation by vascular proteoglycans and Type I and III collagen in the presence of 10µM ADP. 20µg/mL ECM proteins were added to ADP-stimulated platelets to measure phosphatidylserine exposure (A), fibrinogen binding (B) and P-selectin exposure (C). A one-way ANOVA with Tukey correction was used for statistical analysis. Error bars represent ± SEM. n=4; *P<0.05; **P<0.01. CTL – Control; COL1 – Type I Collagen; COL3 – Type III Collagen; VCAN – Versican; BGN – Biglycan; DCN – Decorin; H – Hyaluronan; HMW – High molecular weight; LMW – Low molecular weight.

3.2.5 Types I and III collagen are significantly more thrombogenic under an arterial shear stress than vascular PGs

Static plate-based assays are useful as measures of platelet adhesion and activation marker expression, however the binding affinity of various platelet receptors are altered under different haemodynamic conditions, for example the interaction between GPIb and vWF (Casa *et al.,* 2015). To investigate further the interactions between platelets and different proteoglycans under more physiological conditions, thrombus formation experiments were performed at an arterial shear stress (15 dynes/cm^2) to mimic the vascular environment in the coronary arteries *in vivo*. Ibidi slide chambers were coated with Type I collagen, Type III collagen, biglycan, decorin, versican and HMW and LMW hyaluronan at a concentration of 100µg/mL, the most commonly used concentration of Type I collagen in *in vitro* thrombosis models (Heemskerk *et al.,* 2011; Neeves *et al.,* 2013; Liu *et al.,* 2022) to enable comparability with current models. ECM proteins were left to coat at RT for 1 hour, before slides were perfused with whole blood labelled with 1µM DIOC-6. Thrombus parameters including thrombi number, size and area coverage were measured using fluorescent microscopy.

Under an arterial shear stress, there were no significant differences in thrombus formation between Types I and III collagen, or between vascular PGs. There were, however, differences in thrombus formation between Types I and III collagen and vascular PGs. Thrombi formed on the collagens were generally larger, covered a larger surface area and were more abundant than thrombi formed on vascular PGs ($P<0.05$) (Figure 3.7). In summary, these findings support previous findings from Figure 3.5, indicating that vascular PGs have a significantly smaller effect on platelet activity than vascular collagens. Additionally, the differences observed in platelet adhesion between vascular PGs (Figure 3.3) appear to be lost under an arterial shear stress (Figure 3.7).

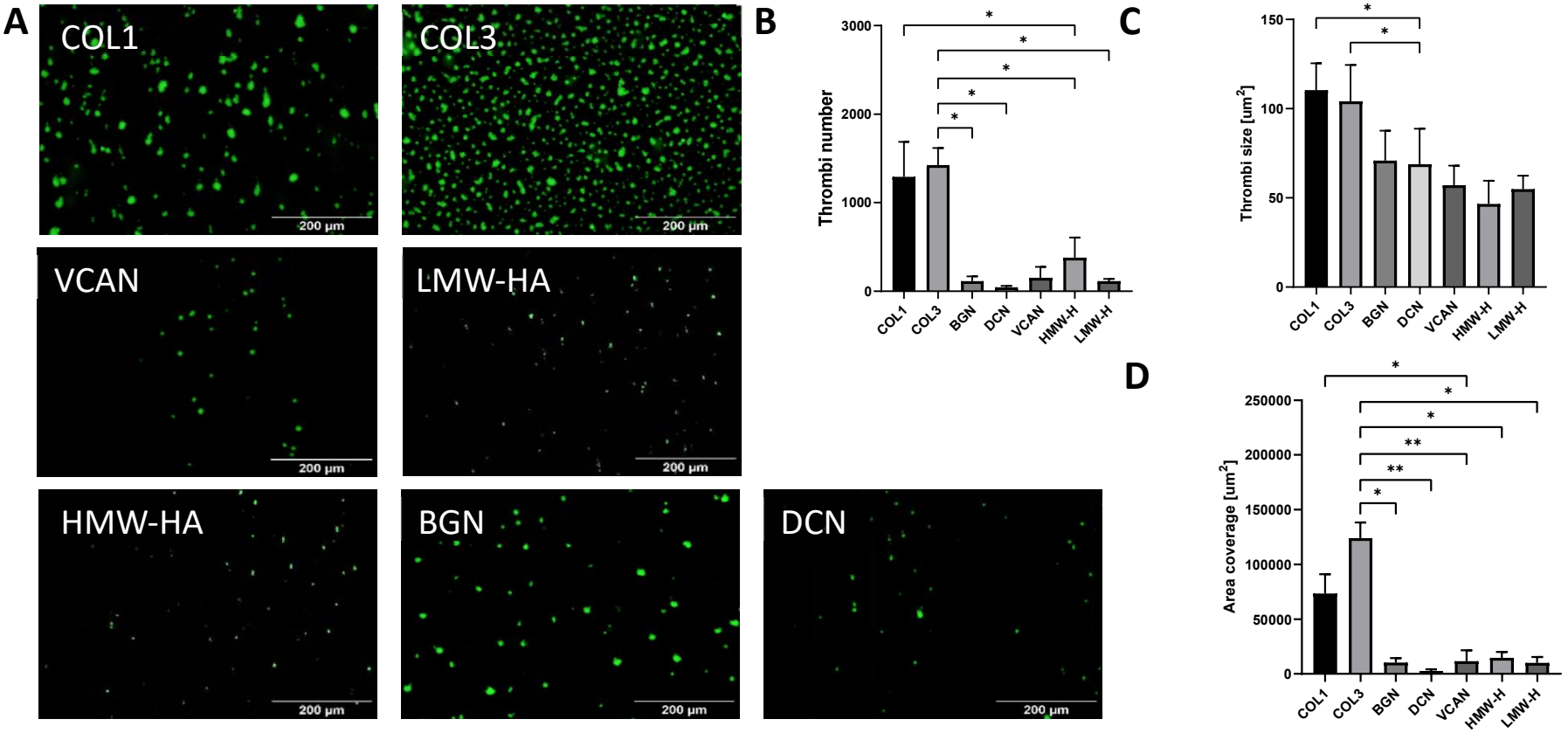

Figure 3.7 – Thrombus formation on disease-relevant extracellular matrix proteins using an arterial shear stress. 100µg/mL ECM proteins were coated in ibidi µ-slides before DIOC-6 labelled whole blood was perfused through channels at 15 dynes/cm^2. Chambers were imaged (A) on a fluorescent microscope and thrombi number (B), size (C) and area coverage (D) analysed using ImageJ. A one-way ANOVA with Tukey correction was used for statistical analysis. Error bars represent ± SEM. n=5; *P<0.05; **P<0.01. COL1 – Type I Collagen; COL3 – Type III Collagen; VCAN – Versican; BGN – Biglycan; DCN – Decorin; H – Hyaluronan; HMW – High molecular weight; LMW – Low molecular weight.

3.2.6 Type I collagen is more thrombogenic than composite 'rupture' and 'erosion' matrices under an arterial shear stress

To explore the relevance of ECM composition in arterial thrombosis, thrombus formation on 'rupture' and 'erosion' matrices, combinations of vascular proteoglycans and collagens generated in Section 3.2.2, were compared with the commonly used *in vitro* standard of Type I collagen (100µg/mL) under an arterial shear stress. Ibidi slide chambers were coated with Type I collagen (100µg/mL) and 'rupture' (Type I collagen, biglycan and decorin, 100µg/mL final each) and 'erosion' (Type III collagen, versican, and HMW or LMW hyaluronan, 100µg/mL final each) matrices. ECM proteins were left to coat at room temperature for 1 hour, before slides were perfused with whole blood labelled with 1µM DIOC-6 at an arterial shear stress (15 dynes/cm^2). Thrombus parameters including thrombi number, size and area coverage were measured using fluorescent microscopy.

Significant differences in thrombus formation were observed between Type I collagen and the 'erosion' matrices, with the latter supporting the development of smaller thrombi covering a significantly lower surface area compared with Type I collagen ($P<0.05$; Figure 3.8). There was a similar trend in the 'rupture' matrix compared with Type I collagen, but this was not significant. Variations were also observed between both 'erosion' matrices, with matrices containing LMW hyaluronan forming more thrombi covering an increased surface area than matrices containing HMW hyaluronan ($P<0.05$) (Figure 3.8). In summary, thrombus formation on composites representing plaque rupture and erosion was reduced compared with Type I collagen, demonstrating that a combination of different collagens and vascular PGs significantly alters thrombus formation on an ECM *in vitro.*

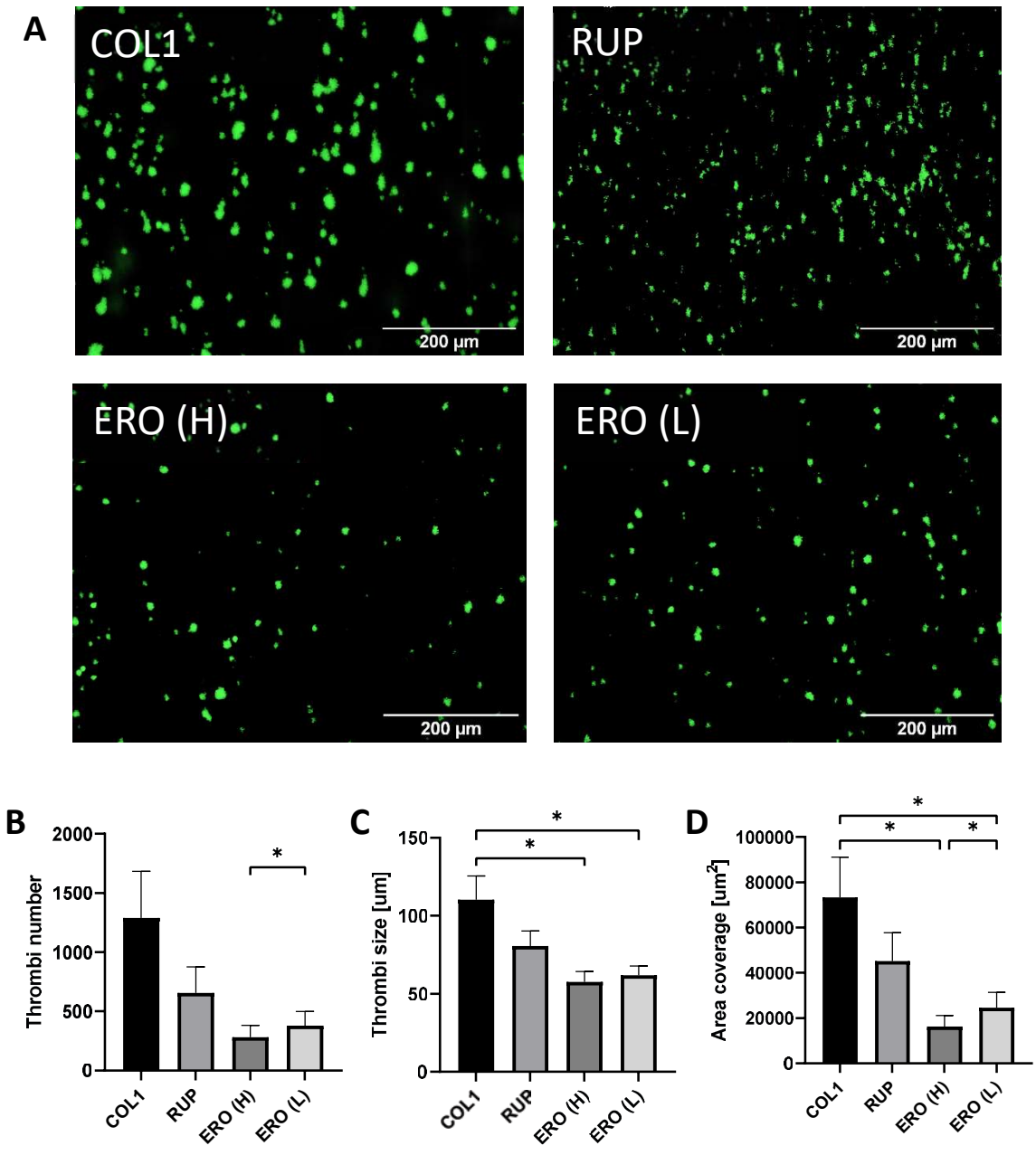

Figure 3.8 – Thrombus formation on disease-relevant matrix composites using an arterial shear stress. Type I collagen (COL1), biglycan and decorin were combined to form the rupture (RUP) matrix, and Type III collagen, versican and either HMW or LMW hyaluronan to form the erosion (ERO (H) and ERO (L)) matrices respectively. Type I collagen (100µg/mL) and disease-relevant composites were coated in ibidi µ-slides for 1 hour at RT, before DIOC-6 labelled whole blood was perfused through channels at 15 dynes/cm^2. Chambers were imaged (A) on a fluorescent microscope and thrombi number (B), size (C) and area coverage (D) analysed using ImageJ. Error bars represent ± SEM. n=5; *P<0.05.

3.2.7 Combining vascular proteoglycans relevant in plaque rupture with Type I collagen significantly alters thrombus formation under an arterial shear stress

In vitro thrombosis models often use coatings of Type I collagen, as one of the most prominent structural proteins in the ECM. However, altering the abundance of vascular proteoglycans in the native ECM may also affect the interaction of platelets with collagen and explain observed differences in thrombus composition following plaque rupture or erosion. Following on from previous results, which demonstrated differences in thrombus formation in composites compared with Type I collagen (Figure 3.8), thrombus formation assays were performed under flow, to investigate the regulation of platelet activity by vascular PGs. Combinations of Type I collagen, biglycan and decorin (100µg/mL each final) were used to represent an ECM reflecting plaque rupture. ECM proteins were left to coat in ibidi slides at RT for 1 hour, before slides were perfused with whole blood labelled with 1µM DIOC-6 at an arterial shear stress (15 dynes/cm^2). Thrombus parameters including thrombi number, size and area coverage were measured using fluorescent microscopy.

Thrombi formed on Type I collagen were larger and more abundant than thrombi formed on biglycan and decorin ($P<0.05$) (Figure 3.9). Adding Type I collagen to biglycan or decorin significantly increased thrombi size ($P<0.05$), increasing the thrombogenicity of the ECM. In contrast, adding biglycan or decorin to Type I collagen reduced the area coverage of thrombi ($P<0.05$) compared with Type I collagen alone, indicating that the presence of either PG may reduce the thrombogenicity of Type I collagen. Combining both biglycan and decorin without the influence of collagen also increased platelet adhesion to the ECM ($P<0.05$). In summary, Type I collagen is the main platelet agonist in the 'rupture' ECM, and proteoglycans associated with plaque rupture can alter the thrombogenicity of Type I collagen, indicating that the interplay between proteins is important in the regulation of thrombus formation in the ECM.

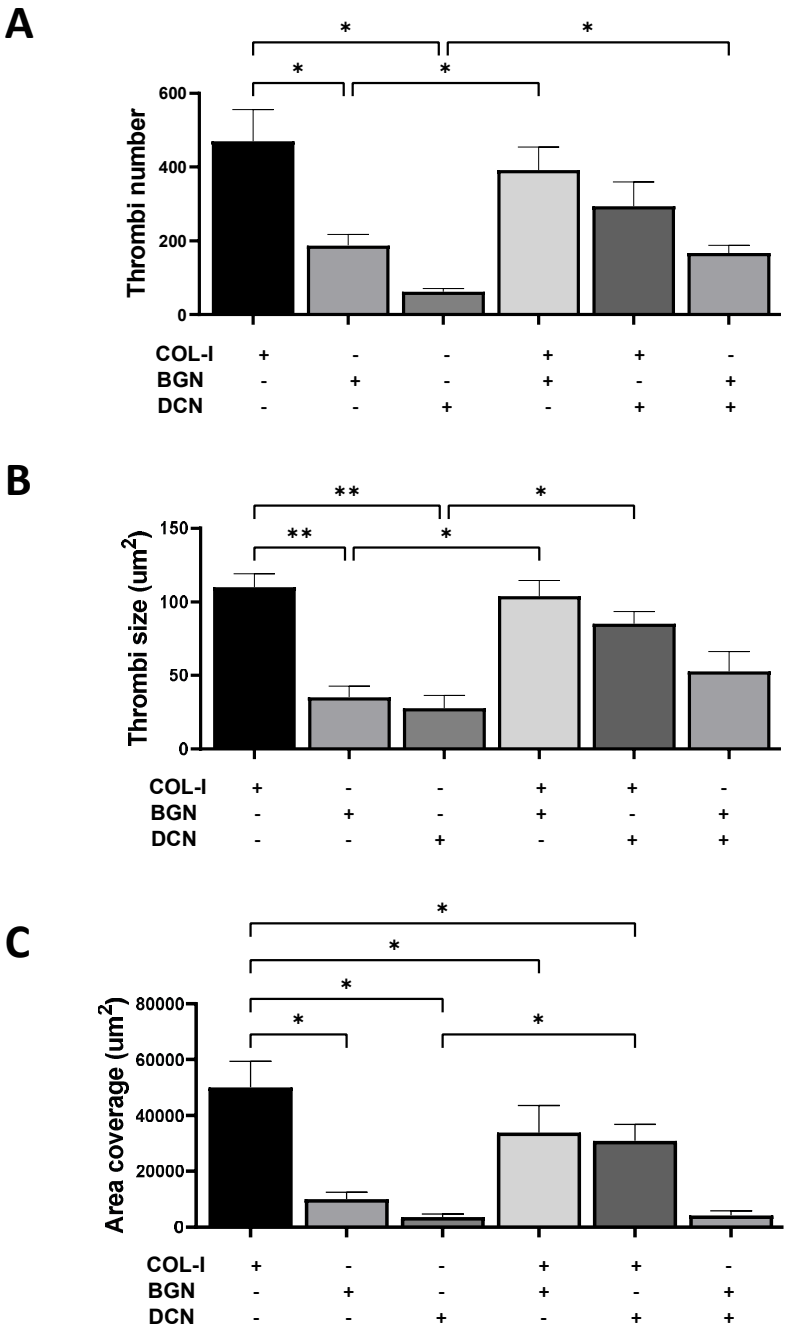

Figure 3.9 – Regulation of platelet activity by vascular proteoglycans associated with plaque rupture. Vascular proteoglycans were coated in ibidi µ-slides both individually and combined with Type I collagen before DIOC-6 labelled whole blood was perfused through channels at 15 dyne/cm^2. Thrombus formation on rupture-relevant ECM combinations was imaged on a fluorescent microscope and thrombi number (A), size (B) and area coverage (C) analysed using ImageJ. Error bars represent ± SEM. n=5; *P<0.05; **P<0.01. COL-I – Type I Collagen; BGN – Biglycan; DCN – Decorin.

3.2.8 Combining vascular proteoglycans relevant in plaque erosion with Type III collagen significantly alters thrombus formation under an arterial shear stress

Previous results demonstrated differences in the regulation of platelet activity by vascular proteoglycans relevant in plaque rupture (Figure 3.9). It is important to also consider plaque erosion and the potential regulation of platelet activity on an erosion ECM, as the thrombi associated with this plaque type is different from rupture thrombi, having a smaller, much more platelet-rich appearance (Otsuka *et al.,* 2016). Thrombus formation assays were therefore performed under flow, to investigate the regulation of platelet activity by vascular PGs relevant in plaque erosion. Combinations of Type III collagen, versican, and either HMW or LMW hyaluronan (100µg/mL each final) were used to represent an ECM reflecting plaque erosion. ECM proteins were left to coat in ibidi slides at RT for 1 hour, before slides were perfused with whole blood labelled with 1µM DIOC-6 at an arterial shear stress (15 dynes/cm^2). Thrombus parameters including thrombi number, size and area coverage were measured using fluorescent microscopy.

Similar to results from Section 3.2.7, thrombi formed on Type III collagen were larger and more abundant than thrombi formed on versican ($P<0.05$) and both hyaluronans ($P<0.01$) (Figure 3.10). Additionally, adding Type III collagen to versican or hyaluronan significantly increased thrombi number and area coverage ($P<0.05$), increasing the thrombogenicity of the ECM. In contrast to Section 3.2.7, however, adding versican or hyaluronan to Type III collagen did not alter any measured parameters of thrombus formation. An additional observation was that adding HMW hyaluronan to versican resulted in a reduction in thrombi number and area coverage ($P<0.05$) (Figure 3.10), reducing thrombogenicity and demonstrating that vascular proteoglycans can also regulate platelet activity independently of structural constituents such as collagens. In summary, Type III collagen is the main platelet agonist in the 'erosion' ECM, and proteoglycans associated with plaque erosion can regulate platelet activity independently of collagen, but do not appear to alter platelet interaction with Type III collagen.

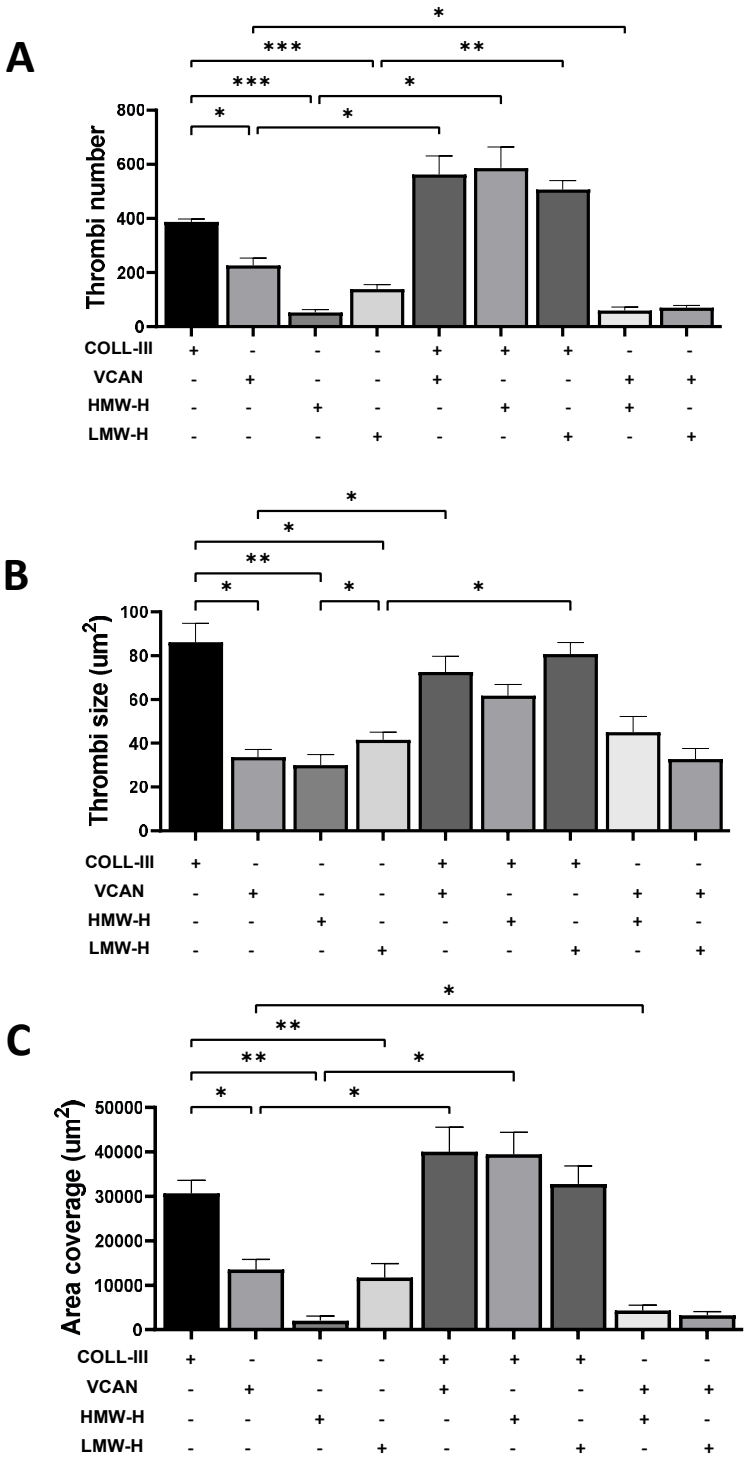

Figure 3.10 – Regulation of platelet activity by vascular proteoglycans associated with plaque erosion. Vascular proteoglycans were coated in ibidi µ-slides both individually and combined with Type III collagen before DIOC-6 labelled whole blood was perfused through channels at 15 dyne/cm^2. Thrombus formation on erosion-relevant ECM combinations was imaged on a fluorescent microscope and thrombi number (A), size (B) and area coverage (C) analysed using ImageJ. Error bars represent ± SEM. n=5; *P<0.05; **P<0.01. COL-III – Type III Collagen; VCAN – Versican; H – Hyaluronan; HMW – high molecular weight; LMW – low molecular weight.

3.2.9 Types I and III collagen are significantly more thrombogenic under an elevated shear stress than vascular PGs

Advanced atherosclerotic lesions, over time, can begin to occlude the artery, causing vessel stenosis. This stenosis may cause elevated shear stress in patients with cardiovascular disease, reaching up to 75 dynes/cm^2 in the vasculature (White *et al.,* 2010). Additionally, the binding affinity of various platelet receptors can be altered under different haemodynamic conditions (Casa *et al.,* 2015). To investigate further the interactions between platelets and different proteoglycans under pathological conditions, thrombus formation experiments were performed at an elevated shear stress (75 dynes/cm^2) to mimic the vascular environment of a stenosed coronary vessel *in vivo*. Ibidi slide chambers were coated with Type I collagen, Type III collagen, biglycan, decorin, versican and HMW and LMW hyaluronan at a concentration of 100µg/mL (Heemskerk *et al.,* 2011; Neeves *et al.,* 2013; Liu *et al.,* 2022) to enable comparability with current models. ECM proteins were left to coat at RT for 1 hour, before slides were perfused with whole blood labelled with 1µM DIOC-6. Thrombus parameters including thrombi number, size and area coverage were measured using fluorescent microscopy.

Under an elevated shear stress, thrombi formed on Type III collagen were significantly more abundant than thrombi formed on Type I collagen ($P<0.05$). The thrombi formed also appeared larger on Type III collagen, but this was not significant in the experiment. Thrombi formed on the collagens were generally larger, covered a larger surface area and were more abundant than thrombi formed on vascular PGs ($P<0.05$) (Figure 3.11), similar to results observed under an arterial shear stress (Figure 3.7). No significant differences were observed in thrombus formation between vascular PGs. In summary, under an elevated shear stress the collagens remain the most thrombogenic proteins, compared with vascular PGs.

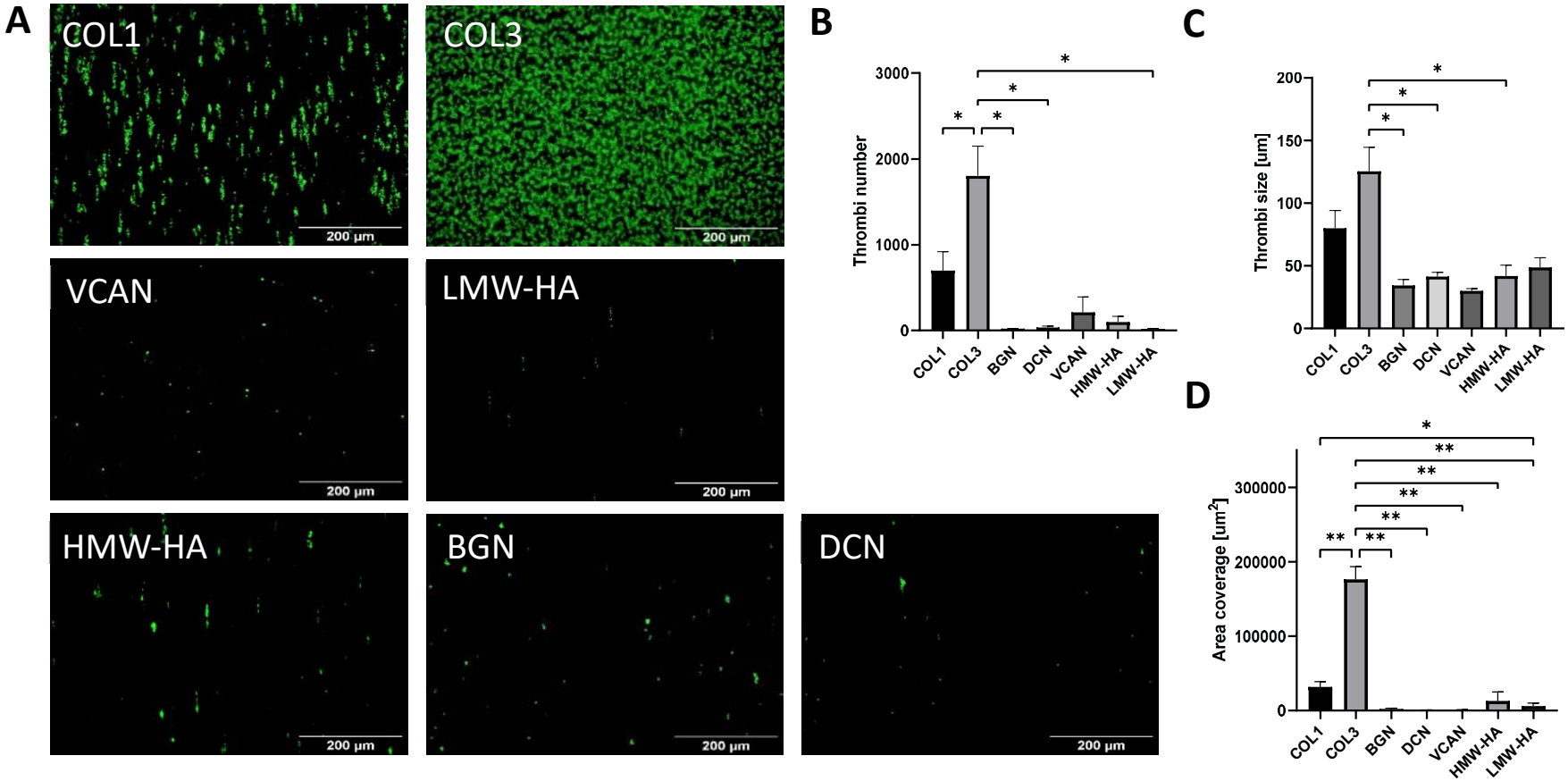

Figure 3.11 – Thrombus formation on disease-relevant extracellular matrix proteins using an elevated flow rate. 100µg/mL ECM proteins were coated in ibidi µ-slides before DIOC-6 labelled whole blood was perfused through channels at 75 dynes/cm^2. Chambers were imaged (A) on a fluorescent microscope and thrombi number (B), size (C) and area coverage (D) analysed using ImageJ. A one-way ANOVA with Tukey correction was used for statistical analysis. Error bars represent ± SEM. n=5; *P<0.05; **P<0.01. COL1 – Type I Collagen; COL3 – Type III Collagen; VCAN – Versican; BGN – Biglycan; DCN – Decorin; HA – Hyaluronan; HMW – High molecular weight; LMW – Low molecular weight.

3.2.10 Types I and III collagen are significantly more thrombogenic under an elevated shear stress than vascular PGs

To explore the relevance of ECM composition in stenosed vessels in cardiovascular disease, thrombus formation on 'rupture' and 'erosion' matrices, combinations of vascular proteoglycans and collagens generated in Section 3.2.2, were compared with the commonly used *in vitro* standard of Type I collagen (100µg/mL) under an elevated shear stress (75 dynes/cm^2) to mimic the vascular environment of a stenosed coronary vessel *in vivo*. Ibidi slide chambers were coated with Type I collagen (100µg/mL) and 'rupture' (Type I collagen, biglycan and decorin, 100µg/mL final each) and 'erosion' (Type III collagen, versican, and HMW or LMW hyaluronan, 100µg/mL final each) matrices. ECM proteins were left to coat at room temperature for 1 hour, before slides were perfused with whole blood labelled with 1µM DIOC-6 at an elevated shear stress. Thrombus parameters including thrombi number, size and area coverage were then measured using fluorescent microscopy.

Under an elevated shear stress, similar to findings from Section 3.2.6, thrombi formed on Type I collagen were significantly larger and covered a larger surface area than thrombi formed on 'erosion' matrices ($P<0.05$; Figure 3.12). Additionally, there was a similar trend in the 'rupture' matrix compared with Type I collagen, but this was not significant. In summary, under an elevated shear stress, thrombus formation on composites representing plaque rupture and erosion was reduced compared with Type I collagen, demonstrating that a combination of different collagens and vascular PGs significantly alters thrombus formation on an ECM under an elevated shear stress *in vitro.* The patterns observed were also similar to those observed under an arterial shear stress.

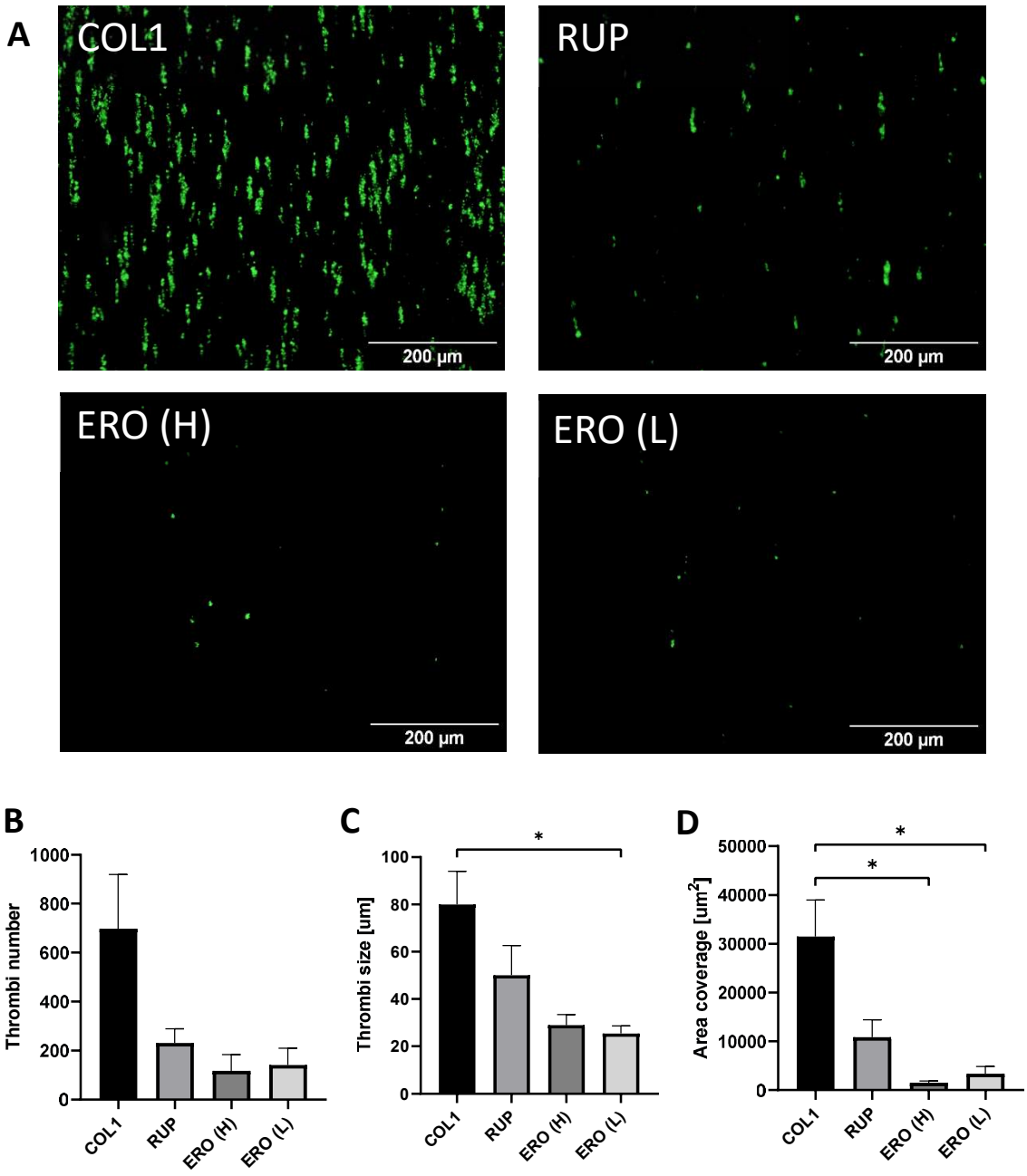

Figure 3.12 – Thrombus formation on disease-relevant matrix composites using an elevated flow rate. Type I collagen (COL1), biglycan and decorin (each 100µg/mL final) were combined to form the rupture (RUP) matrix, and Type III collagen, versican and either HMW or LMW hyaluronan (each 100µg/mL final) to form the erosion (ERO (H) and ERO (L)) matrices respectively. Type I collagen (100µg/mL) and disease-relevant composites were coated in ibidi µ-slides for 1 hour at RT, before DIOC-6 labelled whole blood was perfused through channels at 75 dynes/cm^2. Chambers were imaged (A) on a fluorescent microscope and thrombi number (B), size (C) and area coverage (D) analysed using ImageJ. Error bars represent ± SEM. n=5; *P<0.05.

3.2.11 Antiplatelet efficacy is altered on composite 'rupture' and 'erosion' matrices, compared with Type I collagen

A high-throughput *in vitro* thrombosis model is a useful tool to enable low cost, efficient screening of novel antiplatelet compounds, testing both efficiency and toxicity of drugs. This screening, however, would be limited in accuracy using traditional models (collagen only) if antiplatelet efficacy is altered in response to different ECM compositions. Having identified differences in the thrombogenic capacity of rupture and erosion ECM composites compared to collagen alone, investigations were therefore performed to explore antiplatelet efficacy on composite 'rupture' and 'erosion' matrices, generated in Section 3.2.2, compared with Type I collagen. Ibidi slide chambers were coated with Type I collagen (100µg/mL) and 'rupture' (Type I collagen, biglycan and decorin, 100µg/mL final each) and 'erosion' (Type III collagen, versican, and HMW or LMW hyaluronan, 100µg/mL final each) matrices. 30 minutes prior to perfusion, 30µM aspirin and 10µM clopidogrel (active metabolite) were added to whole blood. ECM proteins were left to coat at RT, before slides were perfused with whole blood labelled with 1µM DIOC-6 at an arterial (15 dynes/cm^2) flow rate. Thrombus size, a measure of secondary recruitment of platelets, was then measured using fluorescent microscopy.

Results comparing antiplatelet efficacy on the composite 'rupture' matrix compared with Type I collagen demonstrated similarities in platelet inhibition following treatment with clopidogrel ($P<0.05$) (Figure 3.13) with around a 40% reduction in average thrombus size. This inhibition was not observed in aspirin-treated platelets, where the reduction in thrombi size on the Type I collagen ECM ($P<0.01$) was not observed on the 'rupture' matrix. Thrombi size was also reduced on all ECM samples following DAPT treatment ($P<0.05$), demonstrating an increase in effectiveness on the 'rupture' matrix. In summary, the effectiveness of aspirin, clopidogrel and a combination of both treatments varied depending on the ECM substrate used in experiments.

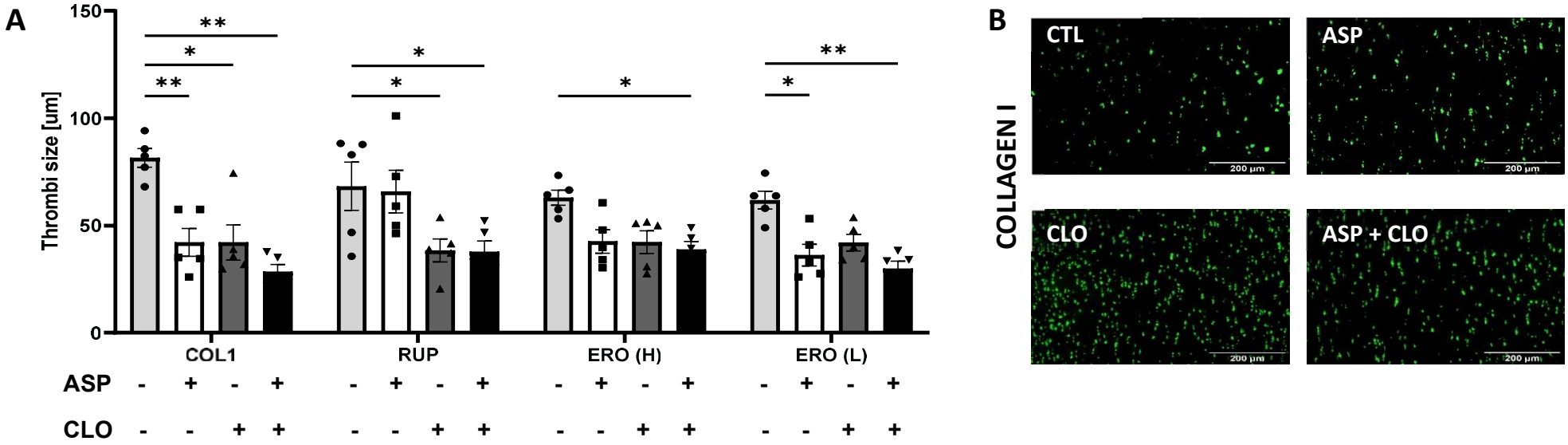

Figure 3.13 – Thrombus formation on ECM composites following treatment with aspirin and clopidogrel. 100µg/mL ECM proteins were combined to generate disease-relevant composites. Type I collagen (COL1), biglycan and decorin were combined to form the rupture (RUP) matrix, and Type III collagen, versican and either high- or low-molecular weight hyaluronan to form the erosion (ERO (H) and ERO (L)) matrices respectively. DIOC-6 labelled whole blood, pre-treated with either aspirin (ASP), clopidogrel (CLO), or both (ASP+CLO), was perfused through ECM-coated channels at 15 dynes/cm^2. Chambers were imaged (B) on a fluorescent microscope and thrombi size (A) analysed using ImageJ. Error bars represent ± SEM. n=5. *P<0.05; **P<0.01. CTL – Control (no pre-treatment).

3.3 Discussion

3.3.1 Platelet responses to collagens are altered by the presence of vascular proteoglycans

The purpose of this chapter was to investigate platelet responses to vascular proteoglycans relevant in the development and progression of atherosclerosis, and to elucidate whether these findings could be significant when considering differences in ECM composition in plaque rupture and erosion. Any differences observed in platelet responses between vascular proteoglycans could have implications in current models of atherothrombosis, and in current antiplatelet therapies for plaque erosion. Indeed, results from the adhesion assay demonstrated significant differences in platelet response on vascular proteoglycans compared with Type I and III collagen, with collagens significantly more thrombogenic. These results were also observed under arterial and elevated shear rates, with thrombi formed on the collagens significantly larger and more abundant. These findings can be attributed to the different receptors involved. Biglycan and decorin both bind to platelets via integrin αIIβ1 (De Witt *et al.,* 2014), with versican and hyaluronan interacting with platelets via surface P-Selectin and CD44 respectively (Koshiishi *et al.,* 1994; Mazzucato et al., 2002; Holm *et al.,* 2012). These receptors primarily regulate platelet adhesion, in contrast to GPVI collagen receptor binding, which initiates platelet activation signalling pathways resulting in the conformational change of integrin αIIbβ3 and platelet aggregation. Indeed, adding biglycan or decorin to Type I collagen significantly reduced the area coverage of thrombi, potentially due to the proteoglycans masking the collagen binding site, as suggested by Paderi *et al.* (2011), by competitively binding integrin αIIβ1, or by inducing inhibitory signalling in platelets. These findings have significant implications for models using Type I collagen in isolation, particularly in assessing the efficacy of novel antithrombotics, where the thrombogenic substrate *in vitro* should represent the vascular ECM *in vivo* as closely as possible.

Findings from adhesion and thrombus formation assays are also supported by results from flow cytometry, assessing expression of platelet activation markers in response to ECM proteins, where in resting platelets, both collagens were the main activators of integrin αIIbβ3 (fibrinogen binding to active conformation). In contrast to Type I and III

collagens, all other proteoglycans had a minimal effect on fibrinogen binding and P-selectin exposure in resting platelets. Similarly, there was no significant enhancement in ADP mediated platelet activation measured by P-selectin exposure and fibrinogen binding. However, this may be due to the concentration of ADP used to stimulate platelets. Similar studies have used concentrations as low as 2µM (Hayes *et al.,* 2014) to investigate potentiation of platelet activation. Indeed, platelet aggregation has been shown to reach as high as 80% using 10µM ADP (Chan *et al.,* 2018), so it may be that platelets were already fully activated, masking any potentiation that may have otherwise been observed in response to ECM proteins. Indeed, variations were observed in platelet PS exposure in response to vascular proteoglycans, indicating a novel role for PGs in modulating PS exposure and platelet procoagulant activity. Results from the adhesion assay demonstrated an increase in platelet spreading on LMW hyaluronan compared with versican, but not HMW hyaluronan. It is important to note, however, that there are multiple factors influencing platelet spreading and cytoskeletal reorganisation outside of receptor binding, including the architecture of ECM and ligand spacing and density (Zarka *et al.,* 2019), factors which may affect platelet adhesion and thrombus formation variations between HMW and LMW hyaluronan. There was a trend in platelet area and number, for example, appearing higher on LMW hyaluronan than HMW hyaluronan in the adhesion assay, and thrombus aggregates formed on LMW hyaluronan were also observed to be larger under flow.

Flow cytometry results indicated that in resting and activated platelets, across all measured parameters, versican appeared to inhibit P-Selectin expression, fibrinogen binding and PS exposure. This was not statistically significant, but an observed trend. Versican is a large proteoglycan, with the core protein having a molecular weight of 360kDa, in addition to 12-15 GAG chains of approximately 45kDa each (Boskey and Robey, 2013), so these results could be explained by the interaction of versican with platelet P-Selectin, whereby initial binding may mask all other binding sites, preventing antibody binding. Versican could therefore have a similar inhibitory effect on platelets *in vivo,* as experimental findings demonstrate adhesion but not spreading, and that this adhesion is weak and reduced under increasing shear rates. Adding HMW hyaluronan to versican further reduces platelet number and area coverage under flow, supporting versican as a regulator of platelet activity alongside HMW hyaluronan in the provisional matrix (Wight, 2017).

Variations in platelet activity were also observed between both collagens. Type I collagen adhered significantly more platelets than Type III collagen under static conditions, however under an arterial shear stress, this effect was abolished, and under an elevated shear stress, Type III collagen became significantly more thrombogenic than Type I collagen, with thrombi formed on the former covering a significantly larger area. Similar findings were observed in a study by Monnet and Fauvel-Laféve (2000), where a novel platelet receptor specific to Type III collagen – Type III collagen binding protein – was identified, and when inhibited, reduced thrombus formation on Type III collagen but not Type I collagen. It is, however, difficult to compare results between flow rates, as the volume of blood used and the time the experiment was running for both varied under arterial and elevated shear stresses. The largest variations in platelet activity on the surface of PGs occurred in the adhesion assays, suggesting that any interactions between these ECM proteins and platelets would potentially occur following platelet binding to more thrombogenic substrates, such as Type I or III collagen. To investigate this concept further, composites were developed to represent a plaque rupture and plaque erosion ECM, and experiments were repeated to investigate variations in platelet response.

3.3.2 Thrombus formation between 'rupture' and 'erosion' ECM composites varies significantly, altering the efficacy of antiplatelet drugs aspirin and clopidogrel

Currently, there are no models of plaque erosion, despite the composition and occlusive potential of thrombi varying between ruptured and eroded plaques (Otsuka *et al.,* 2016). Novel composites were therefore developed to represent the ECM underlying ruptured and eroded plaques, based on work conducted by Kolodgie *et al.* (2002), and platelet responses were compared with Type I collagen, the ECM protein most commonly used in thrombosis models and for antiplatelet drug screening. The 'rupture' composite contained Type I collagen, biglycan and decorin, whilst the 'erosion' composite consisted of Type III collagen, versican and either HMW or LMW hyaluronan. Variations in platelet activity on the 'rupture' matrix compared with Type I collagen included a significant increase in platelet number and reduction in platelet surface area in adhesion assays, demonstrating that the presence of biglycan and decorin had an

influence on platelet interactions with Type I collagen, increasing adhered but not spread platelets. Moreover, under flow, the addition of biglycan and decorin to Type I collagen to form the 'rupture' matrix did not enhance thrombus formation, despite the concentration of collagen remaining the same. Collectively, these results support previous results suggesting that proteoglycan receptor binding predominantly associates with platelet adhesion, and that competitive binding of integrin αIIβ1 may limit Type I collagen activity in the 'rupture' composite (Paderi *et al.,* 2011). Indeed, we observe a trend in reduction of platelet activity on the 'rupture' composite as shear rate increases, compared with Type I collagen, where thrombus parameters remain relatively stable. Platelet adhesion and spreading on 'erosion' matrices was significantly reduced compared with Type I collagen and the 'rupture' matrix, with adhered platelets smaller and more sparse. Results from thrombus formation experiments using type III collagen in isolation demonstrated that thrombus formation increased with shear stress. This is consistent with type III collagen having high affinity for vWF which is shear dependent (Machha *et al.,* 2017). In the 'erosion' matrix composites however, when the same concentration of type III collagen was present in combination with hyaluronan and versican, this this phenomenon was not observed, demonstrating a role for hyaluronan and versican in the regulation of platelet interactions with Type III collagen under flow.

Results indicating that platelet responses are altered when collagens are exposed in the presence of vascular proteoglycans, such as those found in both plaque rupture and plaque erosion, may have implications on antiplatelet efficacy, which is routinely investigated *in vitro* using collagen in isolation. Differences observed between 'rupture' and 'erosion' matrices also indicated that different mechanisms may be involved in the formation of arterial thrombi, therefore the efficacy of antithrombotic drugs may differ depending on plaque type. To investigate this further, blood was pre-treated with aspirin, the active metabolite of clopidogrel or both drugs, before being perfused through chambers over composites at an arterial shear rate. Thrombi formed on Type I collagen, following the addition of clopidogrel, aspirin or both were significantly smaller than the control sample, demonstrating effective inhibition of platelet aggregation. Smaller thrombi were also formed on the 'rupture' matrix with all treatments except aspirin. This could potentially be due to a reduction in collagen-stimulated prostanoid synthesis (Smith and Murphy, 2008), due to the presence of biglycan and decorin in the 'rupture' composite, limiting the effectiveness of COX inhibition. Thrombi number was

observed to increase on matrices following drug treatments with aspirin and clopidogrel, a phenomenon occurring due to the inability of platelets to aggregate following drug treatment. This was particularly pronounced on 'erosion' matrices following aspirin treatment, and on Type I collagen and the 'rupture' matrix following clopidogrel treatment. Aspirin-treated platelets were not more abundant or larger in size on the 'rupture' matrix compared to control, suggesting reduced antiplatelet efficacy on this matrix, potentially due to variations in ECM-platelet binding dynamics following addition of biglycan and decorin. DAPT was the most consistent drug treatment in the reduction of area coverage across all matrices, although aspirin and clopidogrel were individually as effective on 'erosion' matrices. It was observed that there was a high amount of donor variability in response to drug treatment, reflecting current issues in the testing and screening of novel antiplatelet drugs. However, there were significant variations observed in antiplatelet efficacy where donor response was consistent, demonstrating a novel screening technique which may gain context as our understanding of platelet interaction with the ECM improves.

In summary, the aim of this Chapter was to investigate platelet responses to vascular proteoglycans relevant in the development and progression of atherosclerosis, and to elucidate whether these findings could be significant when considering differences in ECM composition in plaque rupture and erosion. The findings from this Chapter demonstrate that Type I and III collagens are the main platelet agonists present in the 'rupture' and 'erosion' matrices, but also that vascular PGs have a role in regulating platelet interactions with collagen, which may have implications in the use of *in vitro* models using Type I collagen in isolation, especially in antiplatelet drug screening. Indeed, findings from this Chapter demonstrated that the effectiveness of antiplatelet therapy varied depending on which matrix the platelets interacted with. Finally, the patterns in thrombus formation observed under an elevated shear stress were similar to those observed under an arterial shear stress, potentially due to the absence of shear-sensitive proteins such as vWF (Machha *et al.,* 2017). Findings from this chapter demonstrate the importance of considering the interplay between ECM components in order to better understand arterial thrombosis resulting from the rupture or erosion of an atherosclerotic plaque. It is in the next Chapter, therefore, where platelet interactions with an entire cell-derived ECM, complete with collagens, proteoglycans and growth factors, is explored in more detail.

4. Incorporating a cell-derived extracellular matrix into an *in vitro* thrombosis model

4.1 Introduction

4.1.1 Cell-derived extracellular matrices

The use of a recombinant ECM is useful to investigate the regulation of platelet activity by collagens and proteoglycans, however the use of recombinant PGs is not without limitations, indeed, a common challenge in the generation of these proteins is the ability to reproduce the attached GAG chains, retaining structural similarity to the relevant cell (Lord and Whitelock, 2013). Additionally, the native ECM also contains a variety of glycoproteins, growth factors and cytokines (Kim *et al.,* 2019), which may also have an effect on platelet activity and the formation of thrombi *in vivo.* The vascular ECM in particular is composed of several layers, which include the basement membrane (pericellular matrix), an underlying elastic lamina and an interstitial matrix, as previously described in Section 1.2.3. Basement membrane components include Type IV collagen, perlecan and laminin, with the elastic lamina composed of collagens, proteoglycans and glycoproteins interwoven between elastic fibres. The underlying interstitial matrix is primarily composed of Type I and III collagen, proteoglycans and fibronectin, with components such as vitronectin, thrombospondin, osteopontin and tenascin present in lower quantities (Farb *et al.,* 2004; Xu and Shi, 2014; Lindsey et al., 2018). Collagens and elastin, beyond the pericellular matrix, are generated by vascular SMCs, which respond to environmental cues to alter ECM expression, regulating ECM stiffness and arterial remodelling (Lu *et al.,* 2011; Yin *et al.,* 2013), important events in the development and progression of atherosclerosis. For example, coronary artery ectasia has been shown to promote degradation of elastin and preferential synthesis of Type I collagen in place of Type III, altering ECM composition and arterial biomechanics (Liu *et al.,* 2016; Cocciolone *et al.,* 2018; Lin *et al.,* 2018).

Advances in tissue engineering have enabled the isolation of native ECM, from both cells and tissue (Flynn, 2010; Xu *et al.,* 2014). Commonly used techniques include plasma fractionation, and natural and glycoprotein enrichment (Lindsey *et al.,* 2018), techniques, which have been useful for isolation and enrichment of ECM proteins in

clinical MI samples, but are not appropriate for isolating a native matrix in situ, which could be incorporated into an *in vitro* thrombosis model. The decellularisation technique, in contrast, removes cellular components to provide an even coating of bioactive ECM on a surface, with native scaffolding and cell adhesion sites preserved (Kim *et al.,* 2019). Decellularisation may be performed on tissue, to generate a decellularised ECM (dECM), or by using *in vitro* cell monolayers to generate a CDM. dECM has many applications and is widely utilised in tissue engineering. Advantages over synthetic materials include the preservation of the natural tissue environment, with dECM promoting cell proliferation and differentiation through biochemical signalling and growth factors, reducing immunogenicity and providing natural scaffolding for cells to robustly adhere to the surface (Beacham *et al.,* 2007; Kim *et al.,* 2019; Chan *et al.,* 2021; Tamayo-Angorrilla *et al.,* 2022). Current uses include incorporation of dECM in bioink 3D printing for adipose, cartilage and cardiac tissue, decellularised vascular grafts and in tumour modelling in cancer research (Gui *et al.,* 2009; Dimitrievska *et al.,* 2014; Pati *et al.,* 2014; Tamayo-Angorrilla *et al.,* 2022).

CDM shares many of the advantages of dECM, having applications in stem cell research, regenerative therapies and *in vitro* disease modelling (He *et al.,* 2009; Pei and He, 2012; Zhou *et al.,* 2018; Chan *et al.,* 2021). CDM can also overcome some of the disadvantages associated with the use of dECM, including limited availability of human tissue, difficulty in isolation of specialised tissue, and inability to alter ECM composition (Assuncao *et al.,* 2020) due to the increased accessibility, reproducibility and versatility offered by commercially available cell lines. The ability to co-culture cells also the ECM from multiple cell types to be investigated, improving the functionality and relevance when used in model systems (Carvalho *et al.,* 2019). This is especially important as ECM composition and structure is tissue-type specific (Pati *et al.,* 2014).

To isolate CDM, a variety of methods may be employed, which include a combination of mechanical, chemical and enzymatic treatments. Mechanical treatments include perfusion, immersion and agitation/sonication, and freeze-thaw cycles (Zhang *et al.,* 2022). Perfusion and immersion are both widely used in the decellularisation of whole organs. Organs may be either perfused or immersed and agitated/sonicated using a detergent to remove cellular components, before being recellularised for therapeutic applications (Ott *et al.,* 2008; Seetapun and Ross, 2016). Freeze-thaw cycles are currently utilised in decellularisation of tissues, which are freeze-thawed multiple times

prior to enzymatic digestion (Flynn, 2010). Chemical methods utilise detergents, acids and bases, and hyper/hypo-tonic solutions (Zhang *et al.,* 2022). Detergents act by solubilising cell membranes and disrupting protein/lipid interactions and can be ionic (SDS), non-ionic (Triton-X 100) or zwitterionic (3-((3-cholamidopropyl) dimethylammonio)-1-propanesulfonate (CHAPS)) (Crapo *et al.,* 2011; Neishabouri *et al.,* 2022). Acids and bases solubilise cell membranes and degrade biomolecules, with peracetic acid and ammonium hydroxide both commonly used acids and bases respectively (Zhang *et al.,* 2022). Hyper- and hypotonic solutions use osmosis to rupture cell membranes, and commonly used solutions include sodium chloride and PBS (Cornelison *et al.,* 2018; Turkson, 2018). Enzymatic treatments incorporate the use of nucleases and trypsin. Nucleases degrade nuclear DNA and RNA to remove residual nucleic acids, and trypsin cleaves the peptide bonds between the carboxyl groups of arginine and lysine, detaching cells from surfaces. Both methods were designed to be used alongside physical and chemical methods to optimise decellularisation (Rahman *et al.,* 2018; Zhang *et al.,* 2022). Farag *et al.* (2018), for example, observed complete removal of DNA following incorporation of DNAse in two decellularisation techniques, using 0.2% (v/v) SDS and a solution containing 0.5% (v/v) Triton-X 100, 20mM ammonium hydroxide (NH4OH). Advantages and limitations of methods used to isolate CDM are summarised in Table 4.1.

Table 4.1 – A summary of advantages and limitations associated with mechanical, chemical and enyzmatic decellularisation techniques. ECM - extracellular matrix; I – Ionic; NI – Non-ionic; ZI – Zwitterionic; GAG – Glycosaminoglycan.

	Technique	Advantages	Limitations	References
Mechanical	Perfusion	Equal distribution of agents, faster than immersion, larger tissues	Complex, non-standardised – differing flow rates, pressure, detergents. Limit access to complex tissue	(Ott *et al.,* 2008; Crapo *et al.,* 2011; Burk *et al.,* 2013; Guyette *et al.,* 2014; White *et al.,* 2017; Hoe-Ng *et al.,* 2019; Neishabouri *et al.,* 2022; Zhang *et al.,* 2022)
	Immersion, agitation/sonication	Access to complex and thin tissue, improves removal of cellular debris	Non-standardised – agitation/sonication intensity, detergents used. Time and complexity - months	
	Freeze-thaw cycles	Reduces immunogenicity, enhances decellularisation of detergents, preserves ECM composition	Residual cell debris when used alone Multiple freeze-thaw cycles modifies ECM ultrastructure	
Chemical	Detergents	I – Enhances decellularisation NI – Preserves ECM composition and ultrastructure ZI – Improves ECM retention compared with I	I – modifies ECM composition and ultrastructure, hard to remove NI – modifies laminin and FN, residual nuclear DNA ZI – modifies collagens, structural modifications	
	Acids/bases	Catalyses reactions, enhances nucleic acid removal. Preserve ECM composition compared with ionic detergents	Acids – can modify ECM ultrastructure and reduce glycosaminoglycan content	
	Hypo/Hypertonic solutions	Preserve ECM composition	Residual cell debris when used alone	
Enzymatic	Trypsin	Enhances decellularisation	Removes collagens, elastin, fibronectin and GAGs	
	Nucleases	Remove residual DNA/RNA	Hard to remove, ineffective when used alone	

4.1.2 The endothelial and smooth muscle ECM

The vascular ECM is composed of ECM proteins generated by both endothelial cells and smooth muscle cells and acts not only as a structural network but also as a source of proteins which regulate cell signalling and behaviour (Li *et al.,* 2018). The endothelial ECM is largely composed of basement membrane proteins, such as Type IV collagen, perlecan and laminins (Witjas *et al.,* 2019), which can regulate cell migration (including leukocyte extravasation), tissue repair and inflammation (Raines, 2000). The smooth muscle ECM, in contrast, is composed of extracellular proteins such as collagens, fibronectin and proteoglycans (Song *et al.,* 2021), and has roles in tissue remodelling and inflammation (Reed *et al.,* 2022). During atherosclerosis and plaque formation in the vasculature, risk factors such as inflammation and elevated levels of LDL stimulate smooth muscle cells to alter ECM composition, contributing to plaque development and progression (Badimon *et al.,* 2012). There are currently a lack of studies which consider differences in ECM composition relating to arterial thrombosis, however. Indeed, collagens are considered the major ECM components responsible for the formation of thrombi in the vasculature (Akther *et al.,* 2022), and TF as the major driver of the formation of occlusive thrombi (Mojca, 2003).

4.1.3 TNF-α and cigarette smoke extract as cardiovascular-associated insults

The pathogenesis of atherosclerosis in both plaque rupture and erosion includes persistent and chronic inflammation (Spagnoli *et al.,* 2007). TNF-α is a potent inflammatory cytokine that has been shown to promote atherosclerotic plaque development and endothelial dysfunction (Branen *et al.,* 2004; Boesten *et al.,* 2005), including the disruption of endothelial regulation of thrombosis (Zhang *et al.,* 2009; Choi *et al*., 2017). TNF-α is therefore a relevant cytokine to use to investigate changes in ECM composition in response to CVD-associated insults. Following the successful use of this cytokine to measure changes in ECM composition, more inflammatory mediators can be incorporated in future research, to enable the most accurate representation of an atherosclerotic ECM *in vivo.*

Smoking, in contrast, is a risk factor segregating with plaque erosion (Dai *et al.,* 2018). CSE, therefore, is relevant in its use to differentiate the rupture and erosion ECMs in cardiovascular disease.

4.1.4 Chapter aim, objectives and hypothesis

The aim of this Chapter is to incorporate an intact, bioactive CDM into an *in vitro* thrombosis model and to characterise the composition and thrombogenicity of the CDM produced by HCAEC and HCASMCS. Furthermore, alterations to the CDM, induced by common cardiovascular damage stimuli, will be identified and the impact of this on platelet function defined.

Objectives:

1. Optimise a protocol to decellularise HCAECs and HCASMCs, cultured under control conditions or in the presence of cardiovascular disease damage stimuli, leaving the remaining ECM intact for biochemical and functional analysis.
2. To investigate platelet spreading and thrombus formation on the HCAEC- and HCASMC-derived matrices
3. To characterise the composition of the HCAECs and HCASMC-derived matrices, defining alterations induced by cardiovascular-associated insults, which may be relevant to thrombosis and vascular pathology

Hypothesis:- Platelet spreading and thrombus formation are altered on extracellular matrices generated by cells damaged with cardiovascular-associated insults

4.2 Results

4.2.1 A combination of detergent and base is more effective in preserving ECM composition and structure than Trypsin-EDTA

To preserve the native ECM and generate a CDM, methods were developed comparing two potential decellularisation agents, Trypsin-EDTA and a solution containing 0.5% (v/v) Triton X-100 and 20mM NH4OH. Trypsin-EDTA is a commercially available, standardised solution, which would improve model replicability and ease of access. The solution containing 0.5% (v/v) Triton X-100 and 20mM NH4OH is a commonly used solution in CDM isolation (Fitzpatrick and McDevitt, 2015), and has been demonstrated to preserve the structure and composition of native CDM. HCASMCs were grown in 6-well plates over 10 days before addition of 2mL Trypsin-EDTA or 0.5% (v/v) Triton X-100, 20mM NH4OH. CDMs were then washed gently with DPBS+ and treated with DNAse I for 30 minutes at 37^{o}C to remove residual DNA, before being stained with DAPI and Alexafluor 488 Phalloidin.

Successful decellularisation was performed using both Trypsin-EDTA and 0.5% (v/v) Triton X-100, 20mM NH4OH (Figure 4.1). Treatment with Trypsin-EDTA appeared to visibly compromise fibrillar protein integrity or remove/degrade proteins and leave more residual cellular debris than samples treated with 0.5% (v/v) Triton X-100 and 20mM NH4OH. The structure and composition of native ECM in samples treated with 0.5% (v/v) Triton X-100 and 20mM NH4OH, in contrast, appeared intact, with fibrillar proteins orientated in the direction of cell growth, organised in a web-like pattern. Once it was established that 0.5% (v/v) Triton X-100, 20mM NH4OH was the optimum extraction buffer, leaving a more intact matrix following the removal of HCASMCs, experiments were performed using HCAECs to ensure that the same method also effectively removed confluent HCAECs leaving an intact matrix (Figure 4.2). Visualisation of the decellularised matrix using fluorescent and differential interference contrast (DIC) microscopy demonstrated full cellular removal and an abundance of CDM with fibrillar proteins arranged in a network-like structure. In contrast to HCASMCs, the orientation of fibres, showed less directionality consistent with the cobblestone arrangement of the HCAECs when cultured under static conditions. Staining with a Type I collagen antibody demonstrated fibrillar collagens conforming to the structural organisation observed in images from both HCAEC and HCASMC CDMs.

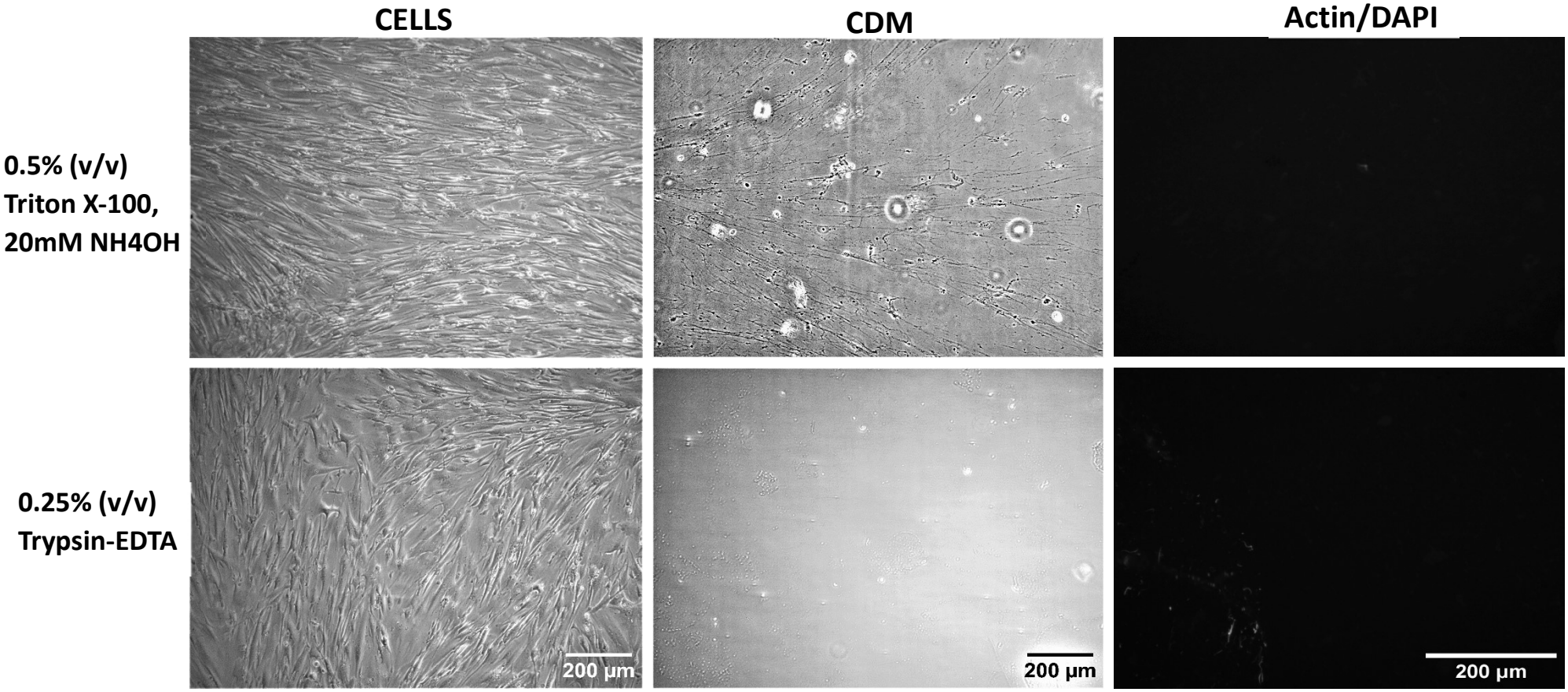

Figure 4.1 – Optimisation of cell-derived matrix (CDM) retrieval in HCASMCs. HCASMCs were grown over 10 days before addition of either 0.25% (v/v) Trypsin-EDTA or 0.5% (v/v) Triton X-100, 20mM NH4OH and DNAse I. Decellularisation efficacy was assessed using brightfield images of CDM and fluorescent visualisation of the presence of cellular and nuclear debris using actin and DAPI staining. N=1. EDTA - Ethylenediaminetetraacetic acid; NH4OH – Ammonium hydroxide. Representative images shown.

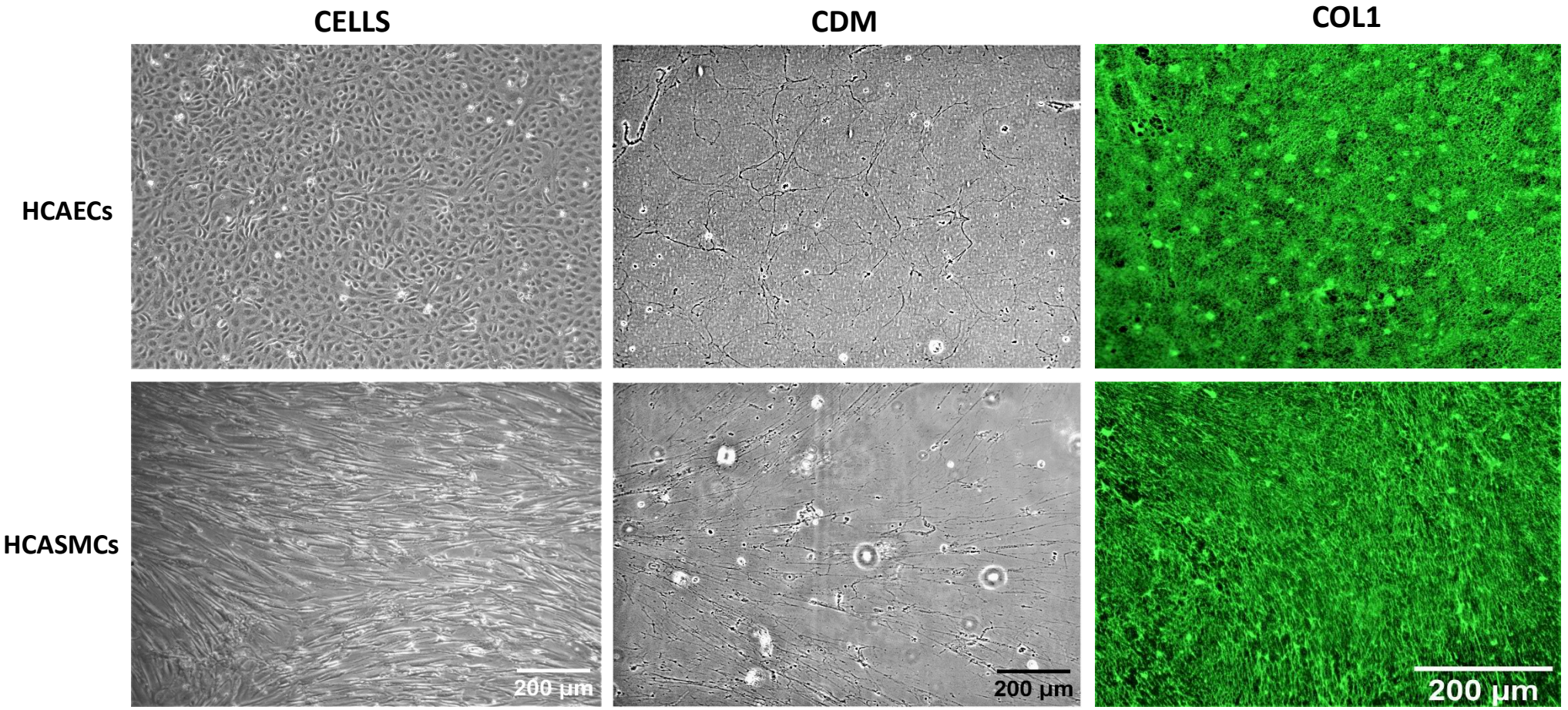

Figure 4.2 – Native cell-derived matrix (CDM) retrieval derived from HCAECs and HCASMCs. HCAECs and HCASMCs were grown over 10 days before addition of 0.5% (v/v) Triton X-100, 20mM NH4OH. Following treatment with DNAse I, decellularisation efficiency was assessed using brightfield images of CDM and fluorescent visualisation of the presence and orientation of Type I collagen fibres. n=1. COL1 – Type I collagen. Representative images shown.

4.2.2 Platelet adhesion and spreading is enhanced on CDMs from control and dysfunctional HCAECs compared with Type I collagen

A functional CDM derived from HCAECs is a useful tool to incorporate in an *in vitro* thrombosis model, as it provides the human vascular ECM exposed following endothelial damage, rather than the Horm collagen derived from equine tendon, routinely used. When developing a thrombosis model, however, it is also important to consider the ECM exposed in CVD. Atherosclerotic plaque development usually occurs following chronic exposure to stimuli associated with risk factors, leading to endothelial dysfunction and altered ECM deposition, which may have an impact on atherothrombosis. Platelet adhesion and spreading assays were performed to investigate platelet responses to CDMs derived from HCAECs and HCASMCs treated with TNF-α, representing inflammation, and CSE, representing smoking, a risk factor for plaque erosion, and samples were compared with platelet adhesion and spreading on Type I Horm collagen and fibrinogen. Type I collagen was used as a comparison to current *in vitro* models, and fibrinogen was used for morphological comparisons of both filopodia and lamellipodia. HCAECs were cultured on coverslips for 7 days to allow generation of 'healthy' ECM before being treated for a further 3 days with 5ng/mL TNF-α, CSE or both to generate an ECM derived from damaged cells. Cells were then removed using the 0.5% (v/v) Triton X-100 and 20mM NH_4OH protocol. Platelets were incubated on coverslips coated with CDM, Type I collagen (100µg/mL) or fibrinogen (100µg/mL) at 37°C for 45 minutes before fixation with 4% (w/v) PFA. Platelet were then stained with AlexaFluor 488 Phalloidin and imaged on a fluorescent microscope.

Platelet adhesion on CDM was greater than that observed on Type I collagen ($P<0.05$). Furthermore, it was demonstrated that platelet adhesion on CDM isolated from TNF-α treated HCAECs was increased compared to CDM from vehicle control treated HCAECs ($P<0.05$; Figure 4.3A). Automated size analysis indicated that there were no differences in average platelet area, however morphological assessment demonstrated that CDM isolated from all conditions enhanced platelet spreading compared to Type I collagen and fibrinogen, with significantly more platelets exhibiting lamellipodia (fully spread) ($P<0.05$).

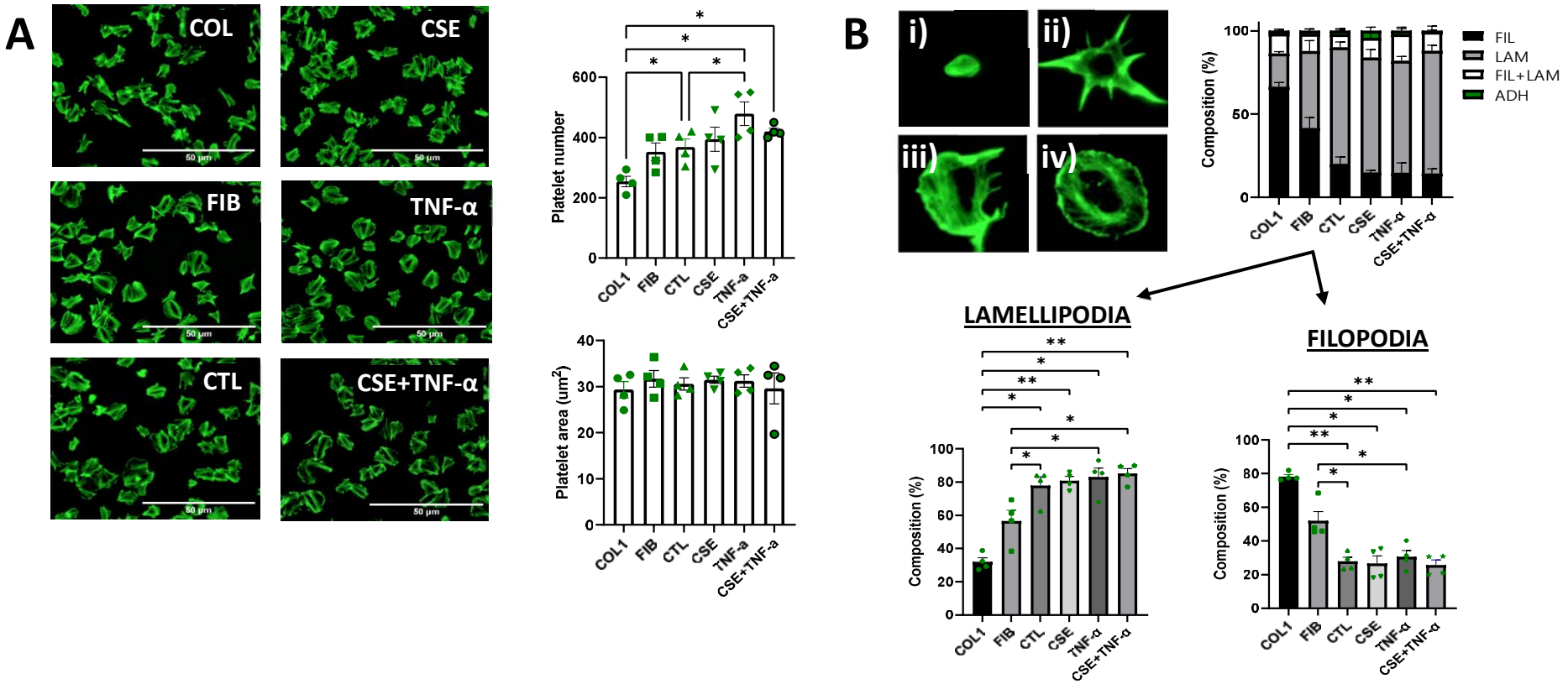

Figure 4.3 – Platelet adhesion and spreading on cell-derived matrices (CDMs) produced by HCAECs. HCAECs were cultured over 7 days and damaged over 3 days with 5ng/mL tumour necrosis factor alpha (TNF-α), 1X cigarette smoke extract (CSE) or both, before decellularisation and addition of washed platelets to CDM or coatings of type 1 collagen (COL1) or fibrinogen (FIB). Platelet adhesion (A) and morphology (B) was assessed using ImageJ. Morphology - ADH - adhered (B(i)), FIL – filopodia (B(ii)), LAM+FIL – features of both lamellipodia and filopodia (B(iii)) and LAM – lamellipodia, fully spread (B(iv)). A one-way ANOVA with Tukey correction was used for statistical analysis. Error bars represent ± SEM. n=4. *P<0.05; **P<0.01; ***P<0.001.

4.2.3 Platelet spreading, but not adhesion, is enhanced on CDMs from control and dysfunctional HCASMCs, compared with Type I collagen

In addition to the ECM from ECs being exposed following plaque rupture or erosions, matrix proteins produced by SMCs are also exposed. Similar to ECs, SMCs are also vulnerable to dysfunction evoked by common CVD risk factors such as inflammation and cigarette smoke. Platelet adhesion and spreading was therefore assessed to compare platelet interactions with HCASMC-derived matrix generated under control conditions, with that deposited following treatment with TNF-α, CSE or both. Adhesion and spreading on the different CDMs were also compared to that observed on Type 1 Horm collagen and fibrinogen (Figure 4.4).

Platelet adhesion to HCASMC-derived matrix was not significantly different to collagen or fibrinogen (Figure 4.4A) and the treatment of HCASMCs with TNF-α or CSE did not alter the adhesive nature of the CDM. Automated measurement of platelet area, as a crude measure of spreading, demonstrated increased platelet area on the CDM isolated from CSE treated HCASMCs ($P<0.05$), suggesting enhanced platelet spreading (Figure 4.4A), although a corresponding reduction in filopodia was not observed during morphological assessment (Figure 4.4B). Indeed, morphological assessment did demonstrate that HCASMC-derived matrices had significantly more lamellipodia ($P<0.05$) – fully spread platelets - than Type I collagen, where filopodia was significantly more abundant ($P<0.05$) (Figure 4.4B). Morphological differences were also observed in the TNF-α and CSE associated HCASMC CDM compared to the control CDM, with significantly more filopodia observed compared to control ($P<0.05$) (Figure 4.4B), although the increase in filopodia did not result in a reduction in lamellipodia (Figure 4.4B). In summary, platelet spreading, but not adhesion, is enhanced on a HCASMC CDM compared with Type I collagen.

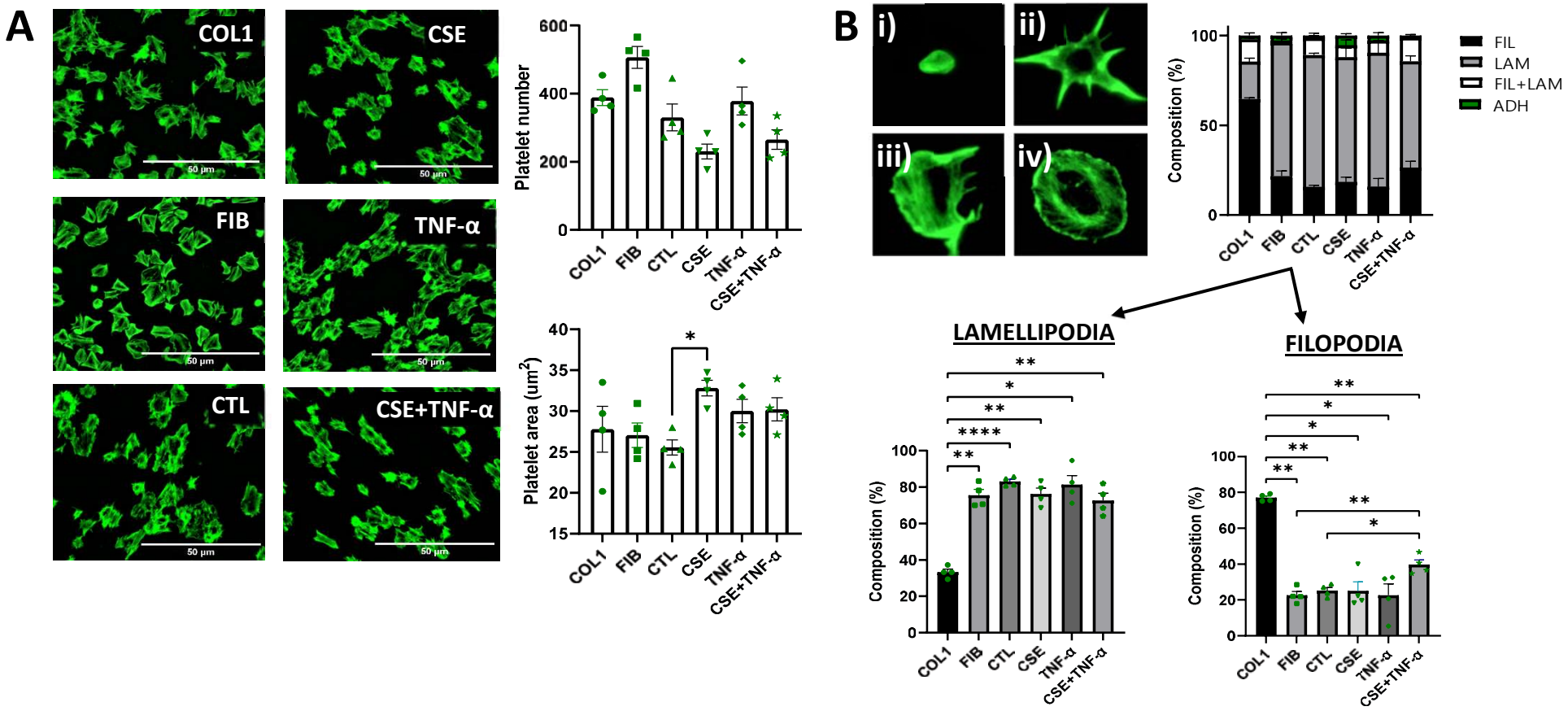

Figure 4.4 – Platelet adhesion and spreading on cell-derived matrices (CDMs) produced by HCASMCs. HCASMCs were cultured over 7 days and damaged over 3 days with 5ng/mL tumour necrosis factor alpha (TNF-α), 1X cigarette smoke extract (CSE) or both, before decellularisation and addition of washed platelets to CDM or coatings of type 1 collagen (COL1) or fibrinogen (FIB). Platelet adhesion (A) and morphology (B) was assessed using ImageJ. Morphology - ADH - adhered (B(i)), FIL – filopodia (B(ii)), LAM+FIL – features of both lamellipodia and filopodia (B(iii)) and LAM – lamellipodia, fully spread (B(iv)). A one-way ANOVA with Tukey correction was used for statistical analysis. Error bars represent ± SEM. n=4. *P<0.05; **P<0.01; ***P<0.001; ****P<0.0001

4.2.4 Cell-derived ECMs can be incorporated in an *in vitro* thrombosis model

Platelet adhesion and spreading assays provide useful information regarding the interaction of platelets with ECM proteins, however they do not inform the process of thrombus formation under flow – a physiological measure of thrombus formation occurring *in vivo.* To measure thrombus formation, CDM derived from vascular cells must be incorporated into an *in vitro* flow model. To achieve this, Ibidi 0.1 sticky slides were used, consisting of open chambers allowing attachment of coverslips prior to thrombus formation. HCASMCs were seeded on coverslips and cultured over 10 days before decellularisation. Ibidi 0.1 sticky slides were assembled and DIOC-6 (1µM) labelled whole blood was perfused over the CDM at an arterial shear rate. Blood was also perfused over coverslips treated with decellularisation agents to ensure platelets were not responding to residual reagents. Immunofluorescence was performed by fixing and staining CDMs with antibodies against human Types I and III collagen and imaging on a fluorescent microscope.

Immunofluorescence staining confirmed the presence of Types I and III collagen in the CDM in a relatively consistent, even coating of the surface following decellularisation (Figure 4.6). Platelets did not adhere to control coverslips treated with extraction buffer and DNAse I, but thrombi were formed on CDMs derived from HCASMCs (Figure 4.6), demonstrating the presence of the CDM in chambers and the ability of the platelets to form thrombi on CDM.

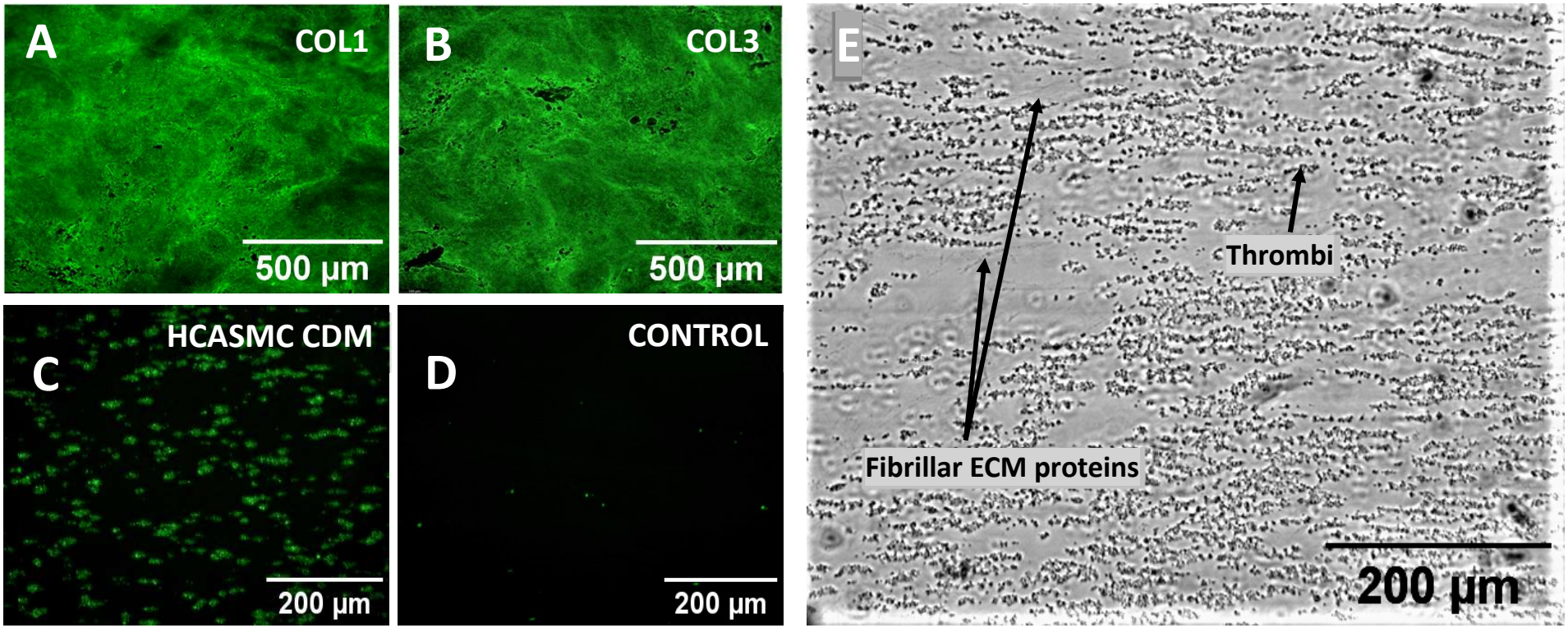

Figure 4.5 – Optimisation and validation of thrombus formation on cell-derived extracellular matrices (CDMs). HCASMCs were seeded on coverslips over 10 days before decellularisation with extraction buffer (0.5% (v/v) Triton X-100, 20mM NH4OH) and removal of residual DNA. Coverslips were fixed and stained with antibodies against Type I (A; COL1) and III (B; COL3) collagen. Control coverslips were treated with extraction buffer and DNAse I, and whole blood was perfused over both CDM (C) and control (D) coverslips at an arterial shear rate, and the presence of fibrillar proteins was validated (E). n=1. ECM – Extracellular matrix.

4.2.5 Type I Horm collagen is significantly more thrombogenic than HCAEC-derived matrices under an arterial shear rate

Following successful incorporation of CDM in the *in vitro* flow model, thrombus formation assays were performed to compare platelet thrombus formation on a HCAEC-derived CDM with Type I collagen, to determine if there were any differences in thrombus formation under an arterial shear stress. HCAECs were seeded on coverslips and cultured over 10 days before decellularisation, and Type I collagen (100µg/mL) was coated on coverslips 1 hour before perfusion. Ibidi 0.1 sticky slides were then assembled and DIOC-6 (1µM) labelled whole blood was perfused over CDMs or Type I collagen at an arterial shear stress (15 dynes/cm^2). Thrombus parameters including thrombi number, size, area coverage and volume were measured using confocal microscopy and ImageJ. Thrombus volume was calculated using Z-stack images, based on the Cavalieri principle.

Results demonstrated successful thrombus formation on both Type I collagen and HCAEC-derived matrices in Ibidi 0.1 sticky slides. Thrombi formed on CDMs were significantly more abundant than thrombi formed on Type I collagen ($P<0.01$) and covered a larger area ($P<0.0001$). Thrombi formed on Type I collagen, however, were significantly larger in volume ($P<0.05$), demonstrating an increase in platelet-platelet interactions resulting in platelet aggregation. These results reflect earlier findings from the adhesion assays, which also demonstrated an increase in platelet number compared with Type I collagen (Figure 4.3). In summary, these findings demonstrate that thrombi formed on a HCAEC-derived matrix are smaller and more abundant than thrombi formed on Type I collagen, demonstrating differences in platelet response to each matrix.

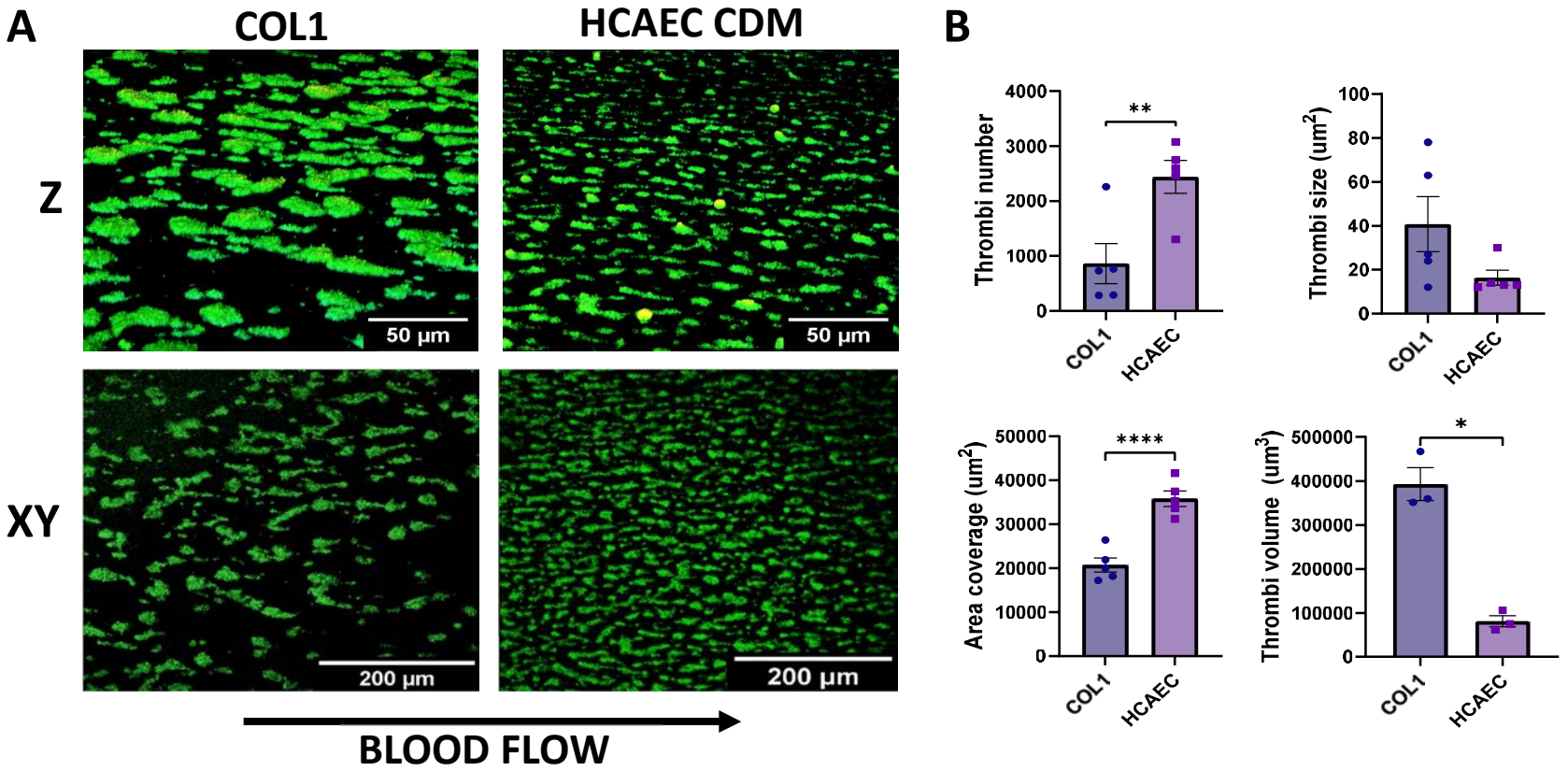

Figure 4.6 – Thrombus formation on Type I collagen compared with a HCAEC-derived extracellular matrix (CDM). HCAECs were cultured on coverslips over 10 days before addition of 0.5% (v/v) Triton X-100, 20mM NH4OH to remove cells. Type I collagen (COL1) was coated on coverslips before assembly of ibidi 0.1 sticky slides and perfusion of DIOC-6 labelled whole blood through channels at an arterial shear rate. Channels were imaged on a confocal microscope (A) and thrombi number, size, area coverage and volume (B) calculated using ImageJ. A one-way ANOVA with Tukey correction was used for statistical analysis. Error bars represent ± SEM. n=5. *P<0.05; **P<0.01; ***P<0.001; ****P<0.0001.

4.2.6 Type I Horm collagen is significantly more thrombogenic than HCASMC-derived matrices under an arterial shear rate

Similarly to an EC-derived matrix, ECM proteins produced by SMCs are also exposed to platelets during atherothrombosis, and platelet responses to SMC-derived matrices must therefore also be measured to assess any differences that may be observed. Thrombus formation assays were therefore performed to compare platelet thrombus formation on a HCASMC-derived matrix with Type I collagen, to determine if there were any differences in thrombus formation under an arterial shear stress. As with HCAECs in Section 4.2.5, HCASMCs were seeded on coverslips before decellularisation, and Type I collagen (100µg/mL) was coated on coverslips 1 hour before perfusion. Ibidi 0.1 sticky slides were then assembled and DIOC-6 labelled whole blood was perfused over CDMs or Type I collagen at an arterial shear stress (15 dynes/cm^2). Thrombus parameters including thrombi number, size, area coverage and volume were measured using confocal microscopy and ImageJ. Thrombus volume was calculated using Z-stack images, based on the Cavalieri principle.

Results demonstrated that thrombi formed on SMC-derived matrices were significantly more abundant than thrombi formed on Type I collagen ($P<0.01$). Thrombi formed on Type I collagen, however, were significantly larger in size ($P<0.05$) but not volume. These results contrast with earlier findings from adhesion assays, which demonstrated no increase in platelet number compared with Type I collagen (Figure 4.4). An increase in platelet abundance on the CDM compared with Type I collagen could indicate the presence of shear-mediated proteins in the HCASMC ECM which maintain/increase platelet adhesion under arterial shear stress. In summary, these findings demonstrate that thrombi formed on a HCASMC-derived matrix are smaller and more abundant than thrombi formed on Type I collagen, demonstrating differences in platelet response to each matrix.

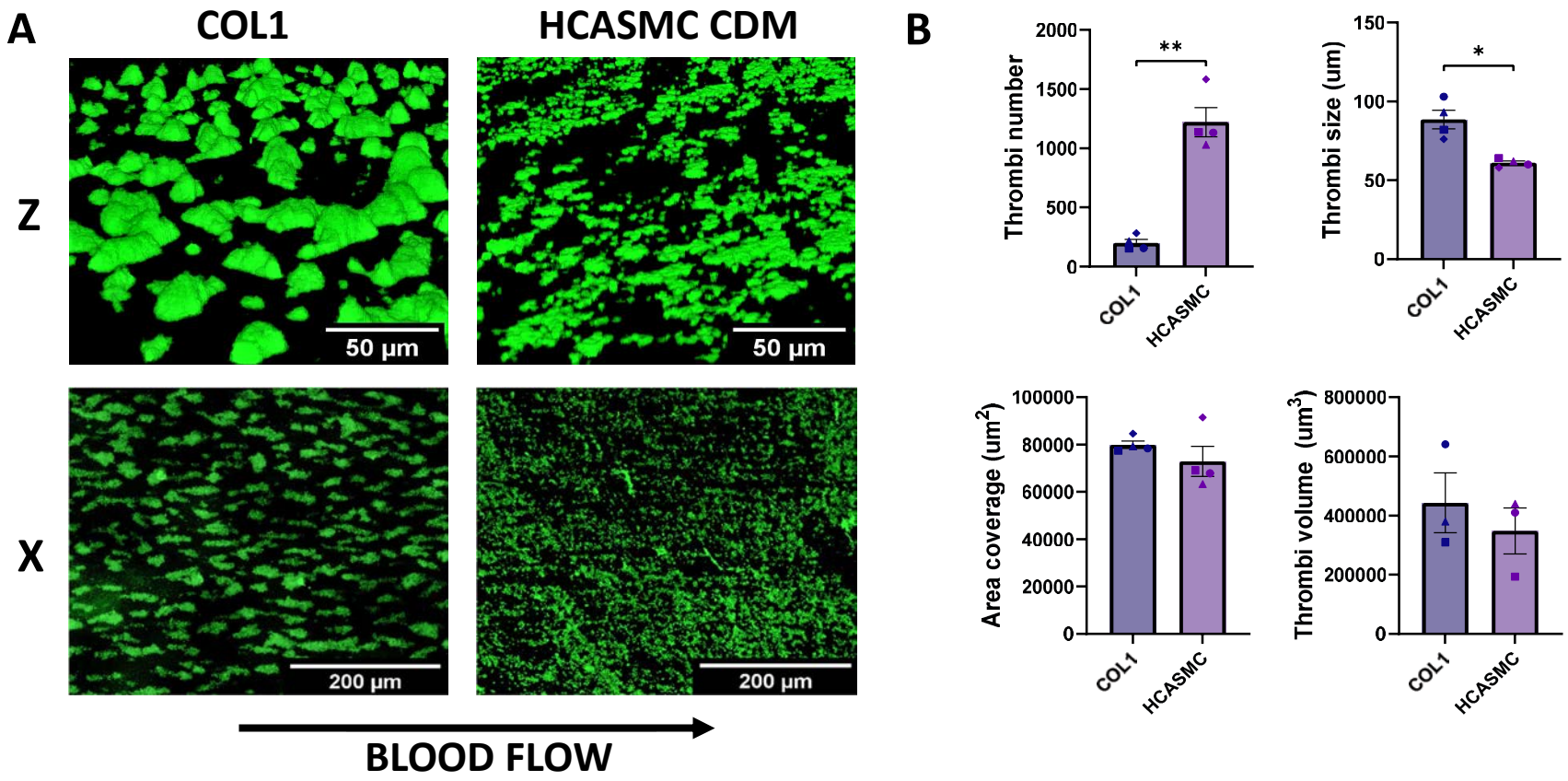

Figure 4.7 – Thrombus formation on Type I collagen compared with a HCASMC-derived extracellular matrix (CDM). HCASMCs were cultured on coverslips over 10 days before addition of 0.5% (v/v) Triton X-100, 20mM NH4OH to remove cells. Type I collagen (COL1) was coated on coverslips before assembly of ibidi 0.1 sticky slides and perfusion of DIOC-6 labelled whole blood through channels at an arterial shear rate. Channels were imaged on a confocal microscope (A) and thrombi number, size, area coverage and volume (B) calculated using ImageJ. A one-way ANOVA with Tukey correction was used for statistical analysis. Error bars represent ± SEM. n=4. *P<0.05; **P<0.01.

4.2.7 Thrombus formation is altered on HCAEC and HCASMC CDMs relative to Type I HORM collagen

Comparing thrombus formation on HCAEC and HCASMC CDMs relative to thrombogenic Type I collagen is useful as it enables differences in the dynamics of thrombus formation to be interrogated between both CDMs. Here, data from Figures 4.6 and Figure 4.7 was transformed to compare the fold change of parameters of end-point thrombus formation, including thrombi number, size, area coverage and volume, between Type I collagen and control HCAEC and HCASMC CDMs.

Results demonstrated that thrombi formed on HCAEC CDMs were significantly smaller in volume ($P<0.01$) and covered a much larger area ($P<0.001$) than thrombi formed on Type I collagen (Figure 4.8). This was in contrast to thrombi formed on HCASMC CDMs, which in contrast to Type I collagen were smaller in size but not volume ($P<0.05$) and more abundant ($P<0.01$). The data suggests that thrombi formed on HCASMC CDMs are comparable to Type I collagen in volume and area coverage, in contrast to thrombi formed on HCAEC CDMs, demonstrating differences in the thrombogenicity of each CDM and consequently platelet responses to each matrix.

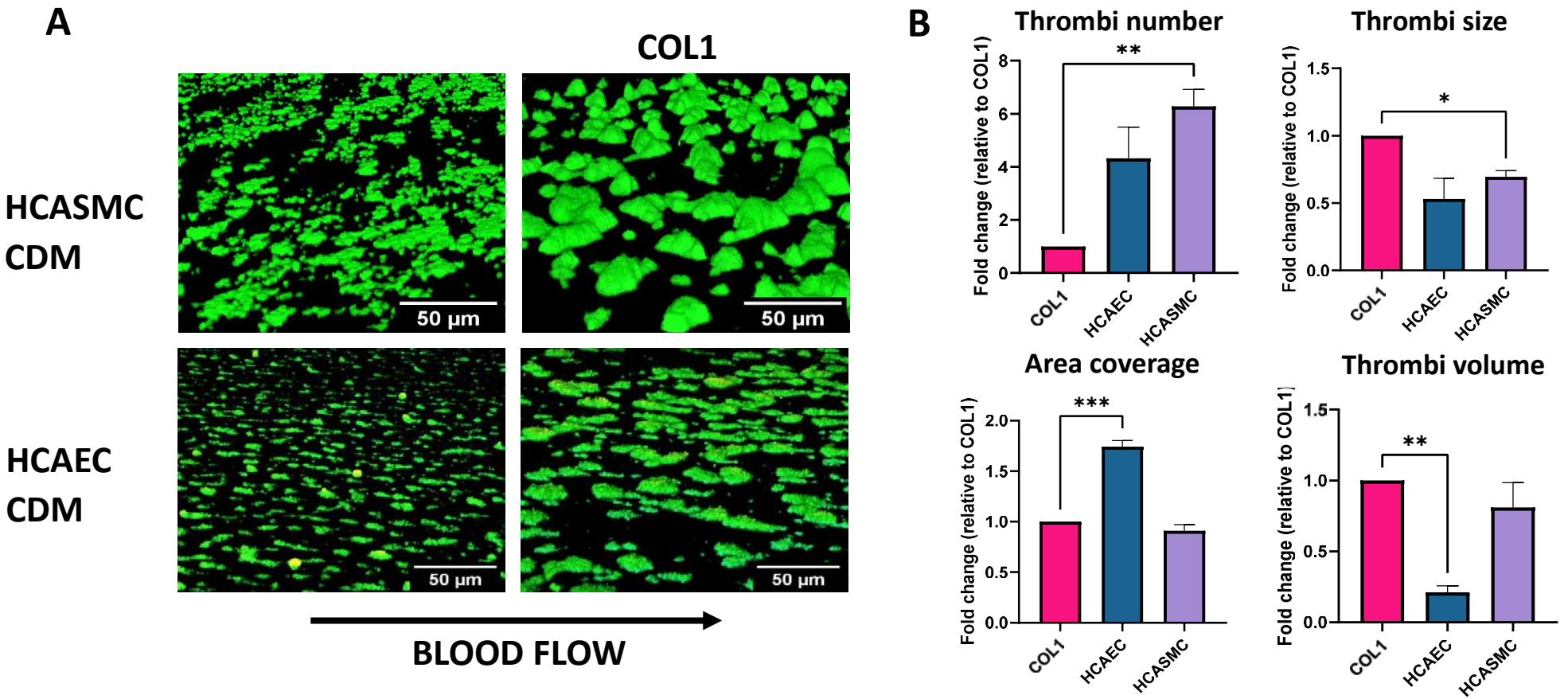

Figure 4.8 – Thrombus formation on Type I collagen compared with HCASMC- and HCAEC-derived extracellular matrices (CDM). Thrombus formation on HCAEC- and HCASMC-derived CDMs was imaged on a confocal microscope (A) and thrombi number, size, area coverage and volume measured using ImageJ. Data was transformed to represent fold change compared with Type I collagen (B; COL1). A one-way ANOVA with Tukey correction for comparisons against COL1 was used for statistical analysis. Error bars represent ± SEM. n=4. *P<0.05; **P<0.01.

4.2.8 HCAECs treated with pro-inflammatory TNF-α produce a more thrombogenic extracellular matrix

Comparing thrombus formation on Type I collagen with native CDM provides a useful assessment of how platelet response varies in current *in vitro* thrombosis models compared with the proposed model of atherothrombosis. However, this does not provide any insight of how platelet responses vary on CDMs with varying compositions, representing cellular dysfunction in atherosclerosis. Thrombus formation assays were therefore performed to investigate platelet responses to CDMs derived from HCAECs treated with TNF-α, representing inflammation, and CSE, representing smoking, a risk factor for plaque erosion. HCAECs were seeded on coverslips and cultured over 7 days, before undergoing treatment over a further 3 days with 5ng/mL TNF-α and CSE. CDMs were decellularized, ibidi 0.1 sticky slides were assembled and DIOC-6 labelled whole blood was perfused over CDMs at an arterial shear rate. Thrombus parameters including thrombi number, size, area coverage and volume were measured using confocal microscopy and ImageJ. Thrombus volume was calculated using Z-stack images, based on the Cavalieri principle.

Differences in thrombus formation were observed between the control CDMs and those derived from cells treated with cardiovascular-associated insults. CDMs retrieved from TNF-α treated HCAECs, both individually and in combination with CSE, appeared more thrombogenic, with larger ($P<0.01$), less abundant ($P<0.05$) thrombi formed compared to control. Indeed, all matrices derived from TNF-α treatment in the HCAEC samples demonstrated increased thrombogenicity. In summary, HCAEC treatment with pro-inflammatory TNF-α resulted in the generation of a CDM with increased thrombogenicity.

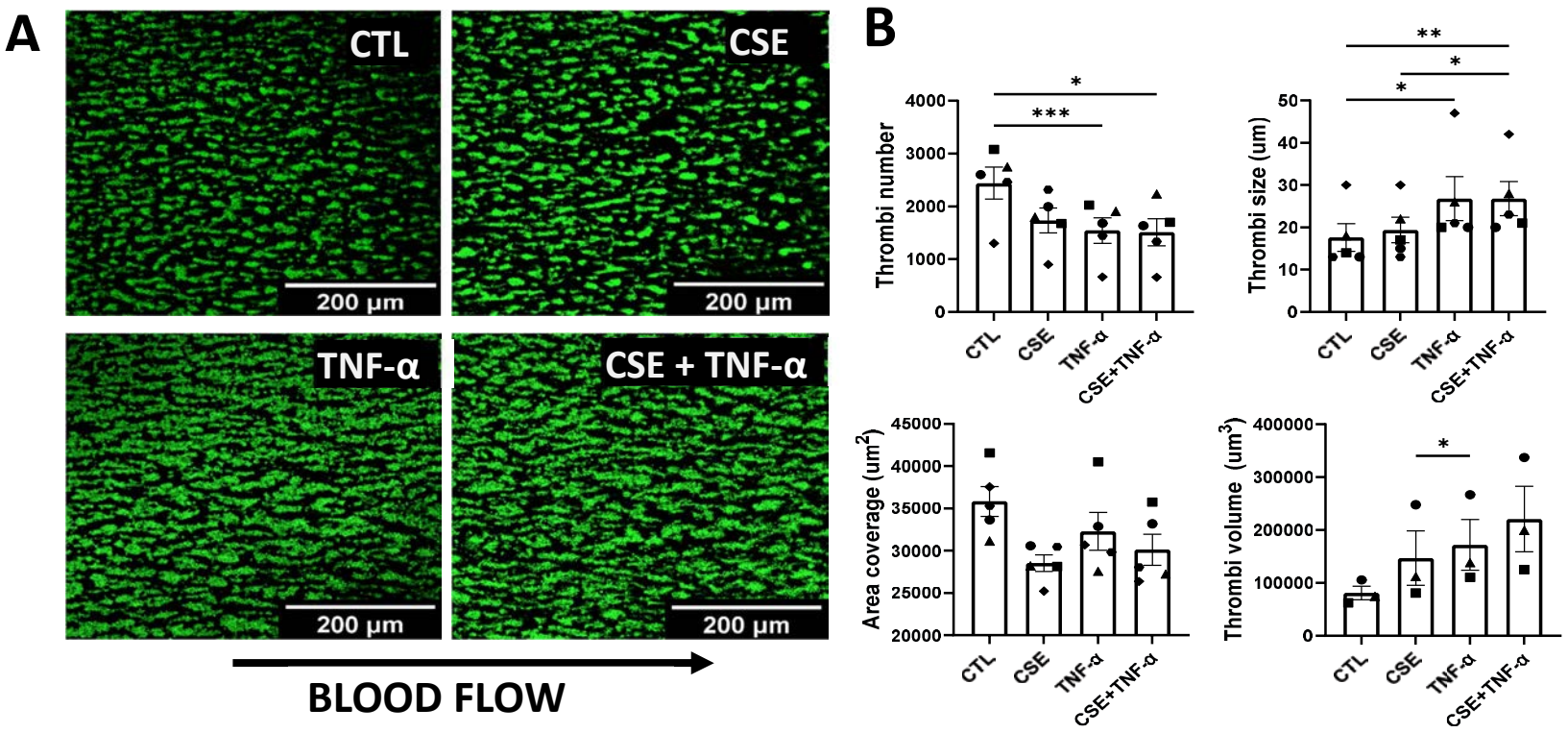

Figure 4.9 - Thrombus formation on healthy and dysfunctional HCAEC-derived matrices. HCAECs were cultured in wells over 7 days and damaged for a further 3 days with 5ng/mL tumour necrosis factor alpha (TNF-α), 1X cigarette smoke extract (CSE) or both, before addition of 0.5% (v/v) Triton X-100, 20mM NH4OH to remove cells. Ibidi 0.1 sticky slides were assembled and DIOC-6 labelled whole blood was perfused through channels at an arterial shear rate. Channels were imaged (A) on a confocal microscope and thrombi number, size, area coverage and volume (B) calculated using ImageJ. A one-way ANOVA with Tukey correction was used for statistical analysis. Error bars represent ± SEM. n=5. *P<0.05, **P<0.01, ***P<0.001.

4.2.9 HCASMCs treated with pro-inflammatory TNF-α produce a more thrombogenic extracellular matrix

Similar to ECs, SMCs are also vulnerable to dysfunction evoked by common CVD risk factors such as inflammation and cigarette smoke. As ECM proteins derived from SMCs are exposed during an atherothrombotic event, platelet responses to SMC-derived matrices must also be measured to assess any differences that may be observed on CDMs with varying compositions, representing cellular dysfunction. Thrombus formation assays were therefore performed to investigate platelet responses to CDMs derived from HCASMCs treated with TNF-α and CSE. As with HCAECs in Section 4.2.8, HCASMCs were cultured and treated with 5ng/mL TNF-α and CSE, before decellularization and perfusion of DIOC-6 labelled blood over CDMs at an arterial shear rate. Thrombus parameters including thrombi number, size, area coverage and volume were measured using confocal microscopy and ImageJ. Thrombus volume was calculated using Z-stack images, based on the Cavalieri principle.

Differences in thrombus formation were observed between the control CDMs and those derived from cells treated with cardiovascular-associated insults. Similarly to findings from Section 4.2.8, CDMs retrieved from TNF-α damaged HCASMCs formed significantly larger thrombi on the matrix surface compared with control and individual CSE-associated matrices ($P<0.05$; Figure 4.10). In summary, treating HCASMCs with TNF-α produced a more thrombogenic CDM, and these results were consistent with previous results demonstrating a similar trend with the TNF-α associated HCAEC CDM.

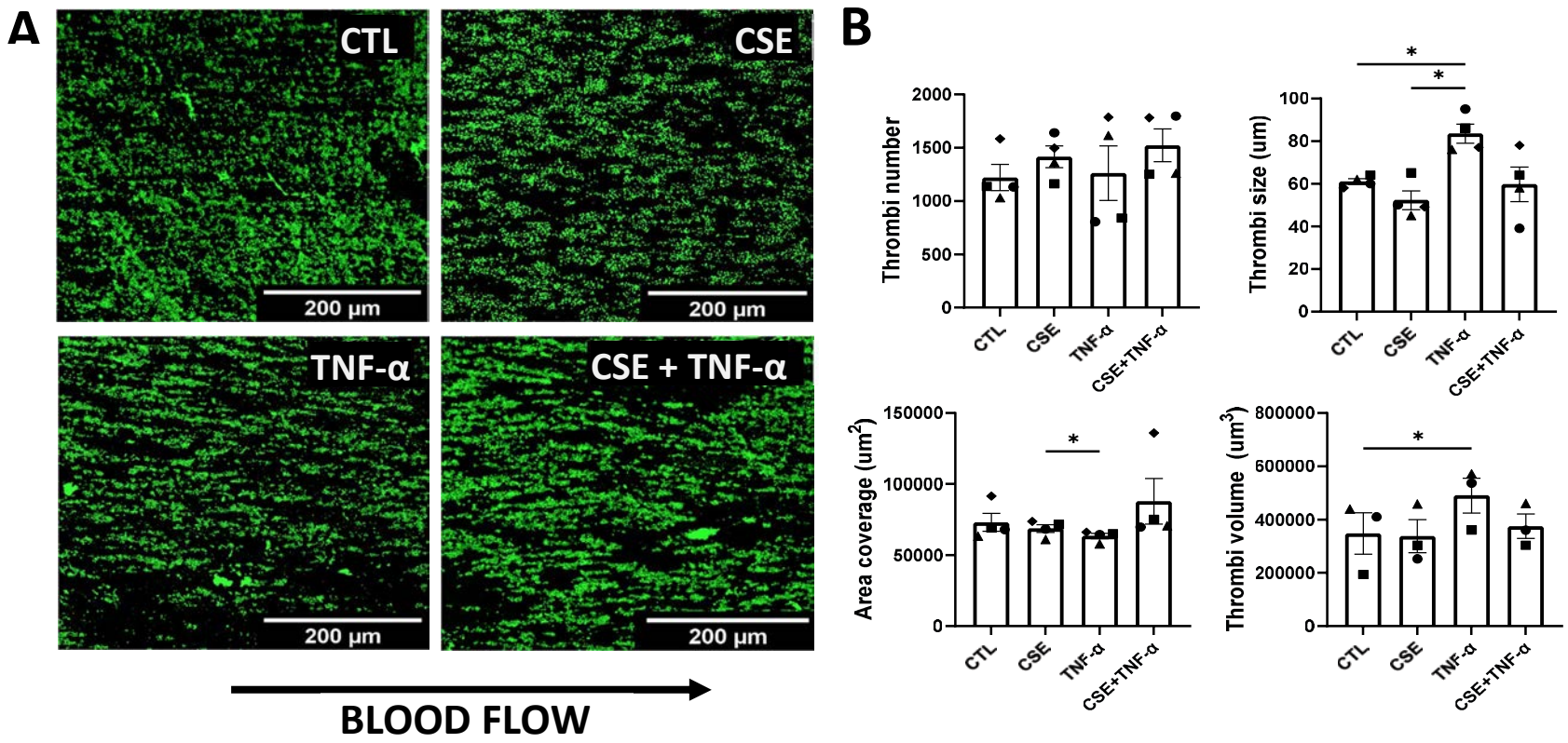

Figure 4.10 - Thrombus formation on healthy and dysfunctional HCASMC-derived matrices. HCASMCs were cultured in wells over 7 days and damaged for a further 3 days with 5ng/mL tumour necrosis factor alpha (TNF-α), 1X cigarette smoke extract (CSE) or both, before addition of 0.5% (v/v) Triton X-100, 20mM NH4OH to remove cells. Ibidi 0.1 sticky slides were assembled and DIOC-6 labelled whole blood was perfused through channels at an arterial shear rate. Channels were imaged (A) on a confocal microscope and thrombi number, size, area coverage and volume (B) calculated using ImageJ. A one-way ANOVA with Tukey correction was used for statistical analysis. Error bars represent ± SEM. n=4. *P<0.05.

4.2.10 HCAEC- and HCASMC-derived matrices are enriched with ECM proteins relevant in platelet adhesion, activation and aggregation

The coronary artery ECM *in vivo* contains ECM proteins not from only one cell type, but instead is synthesised by both HCAECs and HCASMCs. Determining which cells produce certain ECM proteins would provide a novel insight into ECM synthesis and inform the importance of each cell type in contributing to arterial thrombosis.

Mass spectrometry was therefore performed to characterise the proteomics of the underlying ECM in both HCAECs and HCASMCs, to investigate differences in the ECM of both cell types and their contribution to thrombosis. Cells were cultured in 6-well plates over 10 days before undergoing decellularisation and DNAse treatment. 100uL reducing sample buffer (100 mM Tris-HCl, pH 6.8, 20% glycerol, 8% SDS, 0.008% bromophenol blue, 16% β-mercaptoethanol) was added to samples, and a cell scraper was then used to detach the ECM from wells. Samples were pooled over multiple wells to maximise ECM recovery. A 10% TGX Acrylamide kit was used to generate a 10% polyacrylamide gel, and 40uL of sample was loaded into wells before running at 150V for 3 minutes in a running buffer to generate gel-tops. A Coomassie blue stain (3mM Coomassie blue, 50% methanol, 10% acetic acid) was then added to gels and left for 30 minutes at room temperature on a rocker, before subsequent destaining using a destain solution (10% methanol, 10% acetic acid) until the gel was clear with prominent protein bands. Samples were then submitted to the University of Manchester BioMS facility for mass spectrometric analysis, where samples were prepared using an in-gel trypsin digestion and processed using S-TRAP mass spectrometry. Proteome Discoverer software (Thermo Fisher) was used for sample analysis, and DAVID Gene ontology (Open access functional annotation clustering) was used to analyse sample enrichment.

Proteome Discoverer identified over 3000 proteins in the comparison of the HCAEC and HCASMC control samples. DAVID Gene ontology analysis, used for protein grouping and functional analysis, confirmed enrichment of ECM proteins in all samples and both cell types analysed (Figure 4.11). The predominant cellular components identified were extracellular exosomes (Figure 4.11A), which included matrix proteins including collagens, laminins and galectins, as well as S100 calcium binding proteins and thrombospondin. Samples were also enriched with focal adhesion proteins (Figure

4.11A), which included MMPs and Annexins. Analysis also identified that the samples were enriched with proteins important in RNA and protein binding (Figure 4.11B). For the purposes of assessing platelet activity, the most relevant molecular functionalities include protein binding and ECM architecture, which included proteins such as collagens, laminins, thrombospondins and coagulation factors.

KEGG Pathway identification analysis, which identifies/predicts molecular interactions, identified the ECM-receptor pathway as significant in the ECM samples ($P<0.0006$), with many identified proteins present in the sample (Figure 4.11C – proteins present acknowledged with stars). This pathway is particularly relevant in thrombosis, with many integrins present on the platelet surface. Other relevant pathways identified as significant were the complement and coagulation cascade pathways ($P<0.005$).

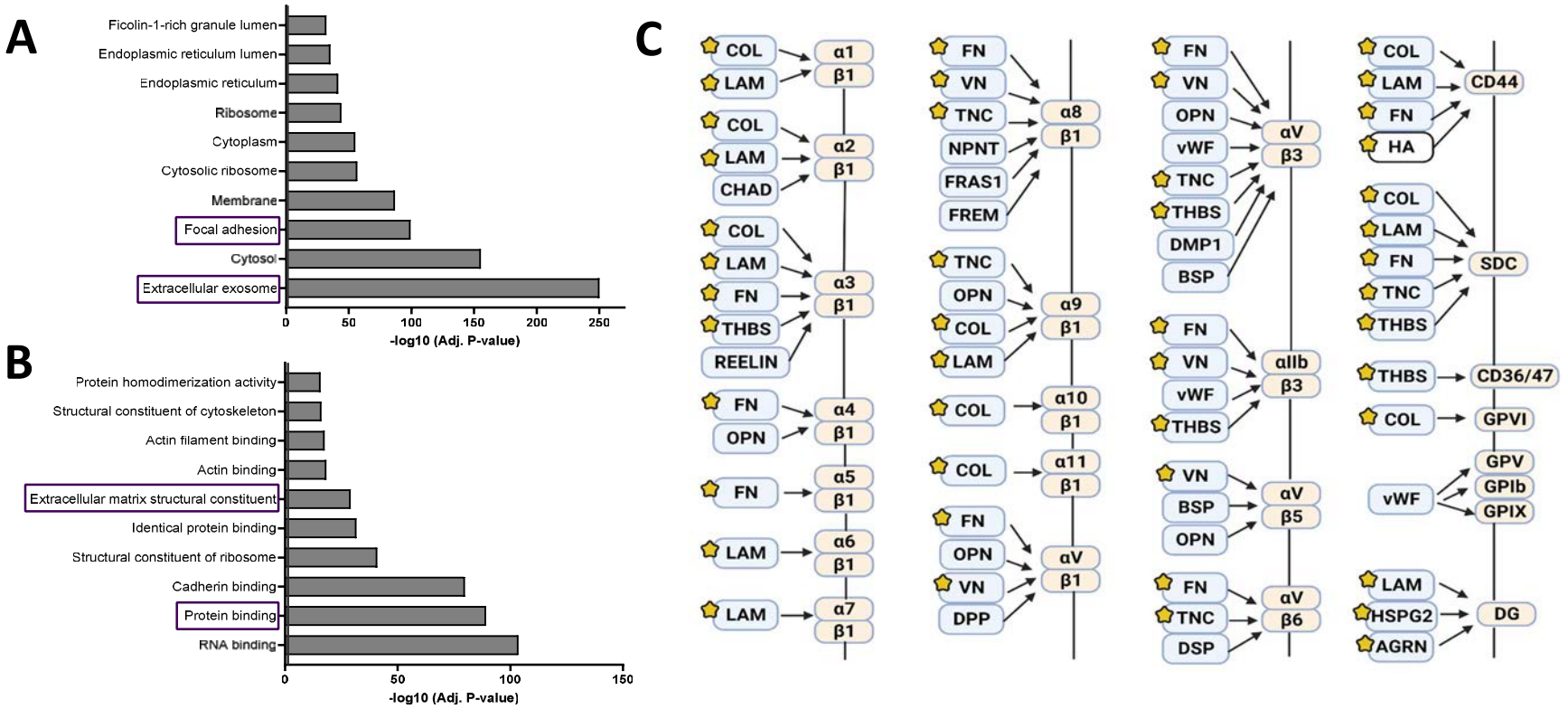

Figure 4.11 – DAVID analysis of the HCAEC and HCASMC ECMs. The entire protein set of proteins retrieved from ECM samples was processed through DAVID gene ontology analysis. Cellular component analysis (A) and molecular function analysis (B) was performed to analyse sample enrichment of each, and KEGG pathway analysis was performed, which identified the ECM-receptor pathway (C; Created with BioRender) as significant. COL- Collagen; LAM – Laminin; CHAD – Chondroadherin; FN – Fibronectin; THBS – Thrombospondin; OPN – Osteopontin; VN – Vitronectin; TNC – Tenascin; NPNT – Nephronectin; FRAS1 – Fraser extracellular matrix component 1; FREM – FRAS1-related extracellular matrix component; DPP – Decapentaplegic; vWF – von Willebrand Factor; DMP1 – Dentin matrix acidic phosphoprotein 1; BSP – Bone sialoprotein; DSP – Desmoplakin; HA – Hyaluronan; HSPG2 – Perlecan; AGRN – Agrin.

4.2.11 Native ECM samples from HCAECs contain more basement membrane- associated and pericellular matrix proteins compared with HCASMCs, which contain more extracellular matrix proteins

Gene ontology analysis from Section 4.2.5 enabled novel functional analysis of proteins present in the HCAEC and HCASMC CDMs. To compare both CDMs, however, the proteins present in each must be analysed and quantified. Volcano plots were therefore used as a measure to compare protein abundance in each CDM. CDMs were prepared for mass spectrometry, as previously described in Section 4.2.10, and submitted to the University of Manchester BioMS facility for mass spectrometric analysis. Proteome Discoverer software (Thermo Fisher) was used for sample analysis, to identify and quantify proteins, and Microsoft Excel was used to log transform P-values and fold changes. A Volcano plot was then generated using Graphpad Prism 9.3.1. Matrisomal proteins were isolated from the dataset using MatrisomeDB (Shao *et al.,* 2019) and proteins relevant in thrombosis and haemostasis were also identified manually and annotated on plots.

Results demonstrated that HCAEC-derived matrices contained a larger amount of basement membrane proteins, such as laminins and basement membrane-associated collagens, than HCASMC-derived matrices (Figure 4.12). Proteins such as S100A7 and Galectin-7 were more common in the HCAEC samples, as well as proteins important in matrix degradation such as hyaluronidase-2 and ADAMTS4. The HCASMC ECM, in contrast, contained more ECM proteins not localised to cells, such as EMILIN1, EMILIN2 and collagen 6, a major component of microfibrils in elastic fibres (Figure 4.12). Proteins such as TIMP3, S100A16 and coagulation factor 13 were also more abundant in HCASMC-derived matrices, as were ECM-associated collagens 22 and 11. The proteoglycan versican was also found in the HCASMC samples and was not detected in any of the HCAEC samples.

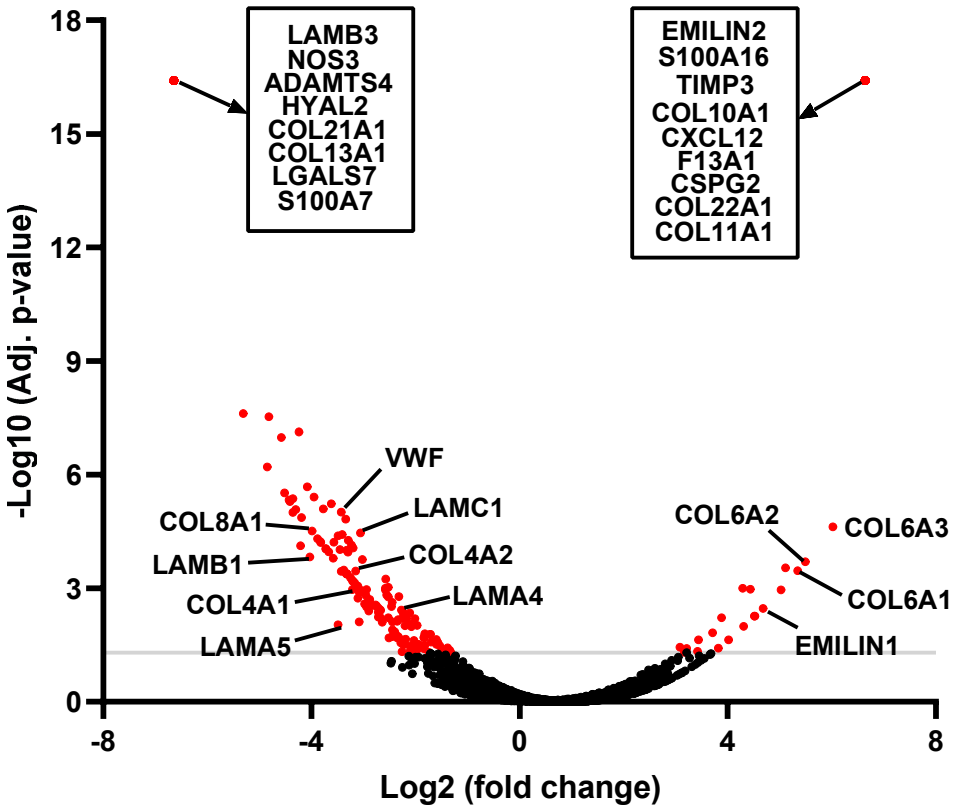

Figure 4.12 – Volcano plot analysis comparing HCAEC and HCASMC ECMs. The native CDM from healthy HCAECs and HCASMCs were compared to identify differences in ECM protein expression. Data retrieved from Proteome Discoverer was transferred to Excel and P-values and fold changes were log transformed. A volcano plot was then created using GraphPad Prism 9.3.1, and matrisomal proteins and proteins relevant in thrombosis and haemostasis were then annotated on the plot. Data is respective to HCASMCs; $P<0.05$. n=3. LAMB – Laminin B, NOS – Nitric oxide synthase; ADAMTS - a disintegrin and metalloproteinase with thrombospondin motifs; HYAL – Hyaluronidase; COL – Collagen, LGALS – Galectin; LAMC – Laminin C; LAMA – Laminin A; VWF – von Willebrand Factor; TIMP – Tissue inhibitor of metalloproteinase; EMILIN – elastin microfibril interfacer; F13 – Factor 13; CSPG2 – Versican.

4.2.12 HCAEC-derived matrices, following stimulation with TNF-α or CSE, are enriched with ECM proteins relevant in platelet adhesion, activation and aggregation

Differences in thrombus formation and platelet spreading on native CDMs compared with Type I collagen suggest that the presence of the different components in the ECM significantly alter platelet activity. Cell stimulation with cardiovascular-associated insults may result in an altered ECM composition, therefore mass spectrometry was performed to characterise the proteomics of the underlying ECM in HCAECs, to investigate differences in ECM composition following stimulation with TNF-α or CSE, and identify any differences that may contribute to thrombosis. CDMs were prepared for mass spectrometry, as previously described in Section 4.2.9, and submitted to the University of Manchester BioMS facility for mass spectrometric analysis. Proteome Discoverer software (Thermo Fisher) was used for sample analysis, to identify and quantify proteins, and DAVID Gene ontology was used to analyse sample enrichment.

Proteome Discoverer identified over 3000 proteins in the comparison of the different HCAEC-derived ECMs. DAVID Gene ontology analysis confirmed enrichment of ECM proteins in all samples analysed (Figure 4.13). The predominant cellular components identified were extracellular exosomes (Figure 4.13A), which included matrix proteins including collagens, laminins and thrombospondins. Samples were also enriched with focal adhesion proteins (Figure 4.13A), which included MMPs and the proteoglycan perlecan. Analysis also identified that the samples were enriched with proteins important in RNA, cadherin and protein binding (Figure 4.13B). For the purposes of assessing platelet activity, the most relevant molecular functionalities include protein binding and ECM architecture, which included proteins such as collagens, laminins, ADAMTS proteins and coagulation factors. KEGG Pathway identification analysis, which identifies/predicts molecular interactions, identified the ECM-receptor pathway as significant in the ECM samples ($P<0.000002$), with many identified proteins present in the sample (Figure 4.13C). This pathway is particularly relevant in thrombosis, with many integrins present on the platelet surface. Another relevant pathway identified as significant was the platelet activation pathway ($P<0.0003$), partly due to the presence of collagen and fibrinogen, but also due to the presence of actin, talin and other cell-associated proteins.

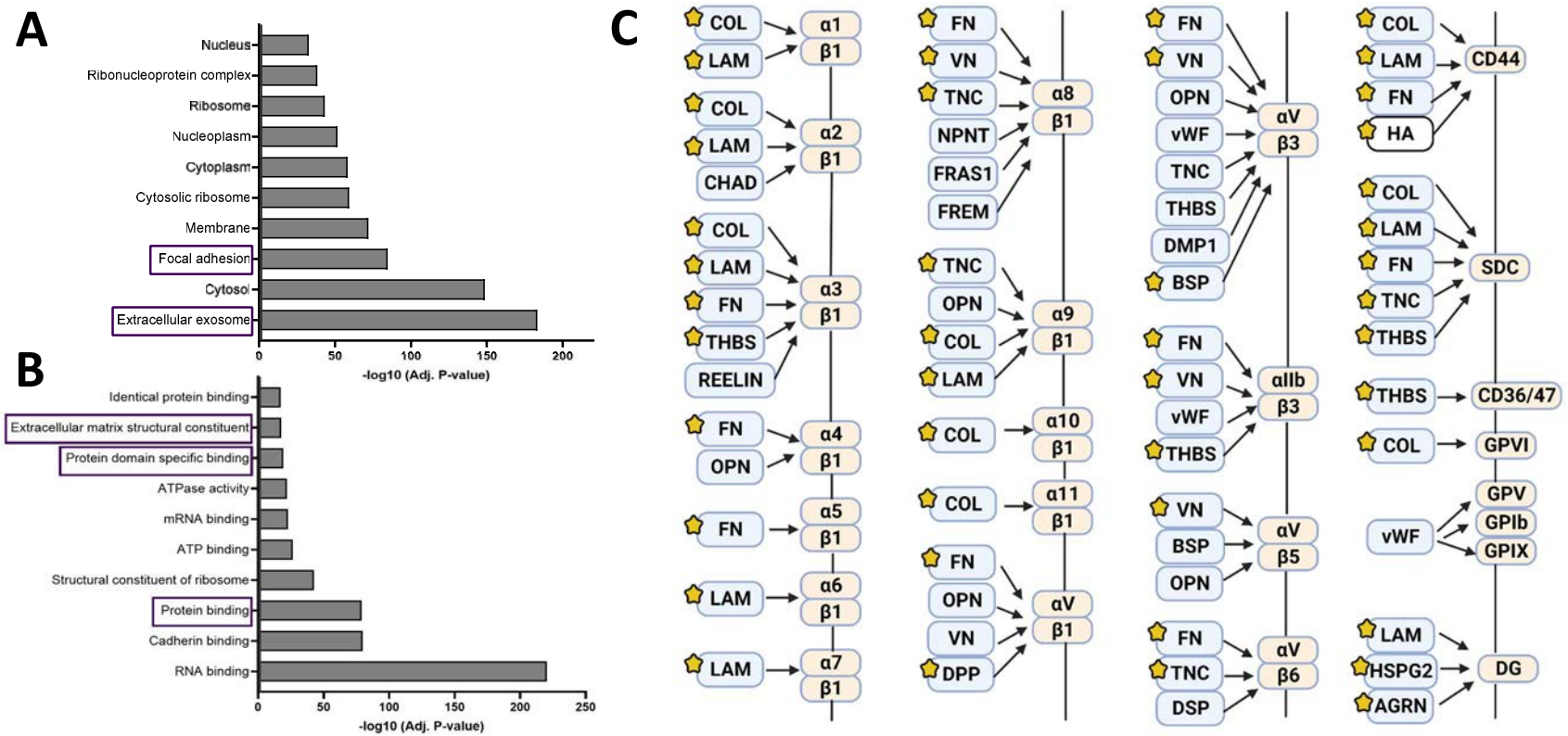

Figure 4.13 – DAVID analysis of HCAEC ECMs generated following cell stimulation with TNF-α and CSE. The entire protein set of proteins retrieved from ECM samples was processed through DAVID gene ontology analysis. Cellular component analysis (A) and molecular function analysis (B) was performed to analyse sample enrichment of each, and KEGG pathway analysis was performed, which identified the ECM-receptor pathway (C; Created with BioRender) as significant. COL- Collagen; LAM – Laminin; CHAD – Chondroadherin; FN – Fibronectin; THBS – Thrombospondin; OPN – Osteopontin; VN – Vitronectin; TNC – Tenascin; NPNT – Nephronectin; FRAS1 – Fraser extracellular matrix component 1; FREM – FRAS1-related extracellular matrix component; DPP – Decapentaplegic; vWF – von Willebrand Factor; DMP1 – Dentin matrix acidic phosphoprotein 1; BSP – Bone sialoprotein; DSP – Desmoplakin; HA – Hyaluronan; HSPG2 – Perlecan; AGRN – Agrin.

4.2.13 Native ECM samples from healthy and dysfunctional HCAECs differentially up- and downregulate expression of proteins relevant in thrombosis and coagulation

Gene ontology analysis from Section 4.2.11 enabled novel functional analysis of proteins present in CDMs derived from dysfunctional HCAECs. To compare the effect of chronic cell stimulation with CVD damage stimuli TNF-α and CSE, however, the proteins present in each matrix must be compared to healthy controls. Volcano plots were therefore used as a measure to compare protein abundance in each CDM. CDMs were prepared for mass spectrometry, as previously described in Section 4.2.9, and submitted to the University of Manchester BioMS facility for mass spectrometric analysis. Proteome Discoverer software (Thermo Fisher) was used for sample analysis, and Microsoft Excel was used to log transform P-values and fold changes. A Volcano plot was then generated using Graphpad Prism 9.3.1. Matrisomal proteins were isolated from the dataset using MatrisomeDB (Shao *et al.,* 2019) and proteins relevant in thrombosis and haemostasis were also identified manually and annotated on plots. Fold change is relative to control CDMs.

Treatment with TNF-α resulted in a significantly reduced collagen content of multiple collagens in HCAEC ECMs compared to the healthy control ($P<0.05$) (Figure 4.14). Indeed, other structural ECM components, including fibrillar matrilin (MATN2) and PRELP- (proline and arginine-rich end leucine rich repeat protein) were also reduced in response to damage stimuli, compared to control. Common across samples was the upregulation of coagulation proteins such as plasminogen (PLG) and Factor XIII (F13), with TF and TFPI also upregulated and found associated with the ECM in response to a combination of TNF-α and CSE, as well as the GAG hyaluronan, compared to control (Figure 4.14). Upregulation of platelet agonists Galectins -9 and -1 as well as C1q was also observed in samples.

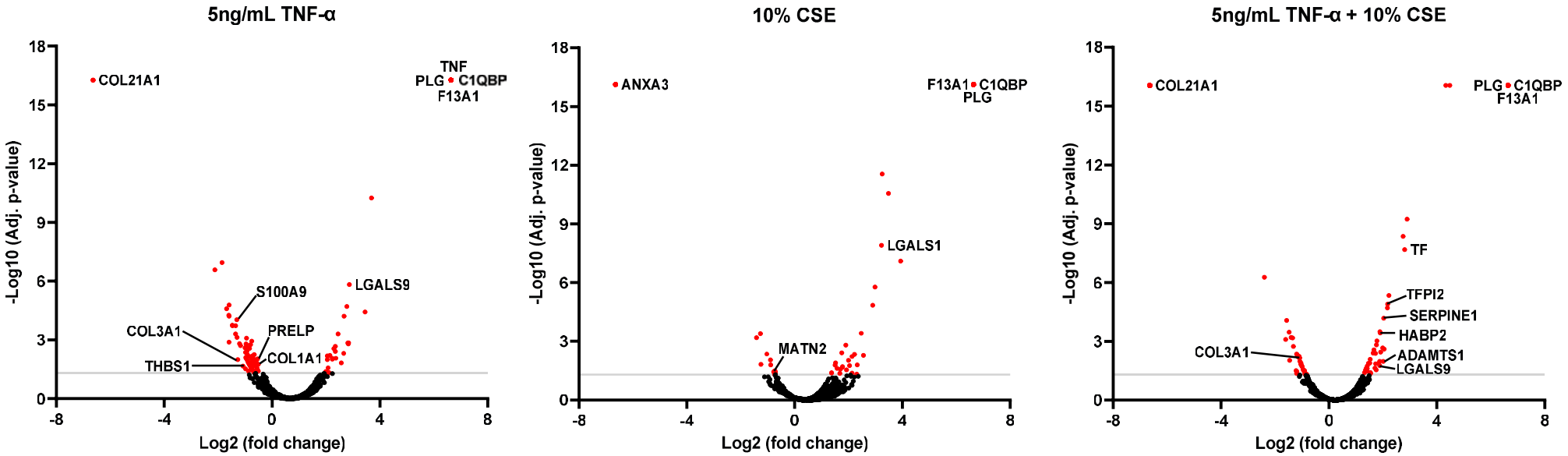

Figure 4.14 – Volcano plot analysis comparing healthy and dysfunctional HCAEC ECMs. Native CDM from healthy (untreated) HCAECs and HCAECs damaged with tumour necrosis factor (TNF)-α and cigarette smoke extract (CSE) were compared to identify differences in ECM protein expression. Data retrieved from Proteome Discoverer was transferred to Excel and P-values and fold changes were log transformed. Volcano plots were then created using GraphPad Prism 9.3.1, and matrisomal proteins and proteins relevant in thrombosis and haemostasis were annotated on the plot. Fold change is relative to control CDMs; $P<0.05$. n=3. COL – Collagen; THBS – thrombospondin; PRELP - proline and arginine-rich end leucine rich repeat protein; LGALS – Galectin; PLG – Plasminogen; C1QBP – C1q binding protein; F13 – Factor 13; ANX – Annexin; MATN2 – Matrilin; ADAMTS – A disintegrin and metalloproteinase with thrombospondin motifs; HABP – Hyaluronan binding protein; SERPINE1 – Plasminogen activator inhibitor 1.

4.2.14 HCASMC-derived matrices, following stimulation with TNF-α or CSE, are enriched with ECM proteins relevant in platelet adhesion, activation and aggregation

Results from Section 4.2.12 indicated that stimulating HCAECs with TNF-α and CSE significantly alters the underlying ECM. To gain a deeper insight into arterial thrombosis, the contribution from the HCASMC-derived ECM must also be considered, as CVD risk factors also affect the SMCs in the vasculature. Mass spectrometry was therefore performed to characterise the proteomics of the underlying ECM in HCASMCs, to investigate differences in ECM composition following stimulation with TNF-α or CSE, and identify any differences that may contribute to thrombosis. CDMs were prepared for mass spectrometry, as previously described in Section 4.2.9, and submitted to the University of Manchester BioMS facility for mass spectrometric analysis. Proteome Discoverer software (Thermo Fisher) was used for sample analysis, to identify and quantify proteins, and DAVID Gene ontology was used to analyse sample enrichment.

Proteome Discoverer identified over 3000 proteins in the comparison of the different HCASMC-derived ECMs. DAVID Gene ontology analysis confirmed enrichment of ECM proteins in all samples analysed (Figure 4.15). The predominant cellular components identified were extracellular exosomes (Figure 4.15A), which included matrix proteins including collagens, fibrinogen and thrombospondins. Samples were also enriched with focal adhesion proteins (Figure 4.15A), which included MMPs and the proteoglycan perlecan. Analysis also identified that the samples were enriched with proteins important in RNA, cadherin and protein binding (Figure 4.15B). For the purposes of assessing platelet activity, the most relevant molecular functionalities include protein binding and ECM architecture, which included proteins such as collagens, elastins, ADAMTS proteins and tissue inhibitor of metalloproteinase (TIMP)s. KEGG Pathway identification analysis, which identifies/predicts molecular interactions, identified the ECM-receptor pathway as significant in the ECM samples ($P<0.01$), with many identified proteins present in the sample (Figure 4.15C). This pathway is particularly relevant in thrombosis, with many integrins present on the platelet surface. Another relevant pathway identified as significant was the platelet activation pathway ($P<0.04$), partly due to the presence of collagen and fibrinogen, but also due to the presence of actin, talin and other cell-associated proteins.

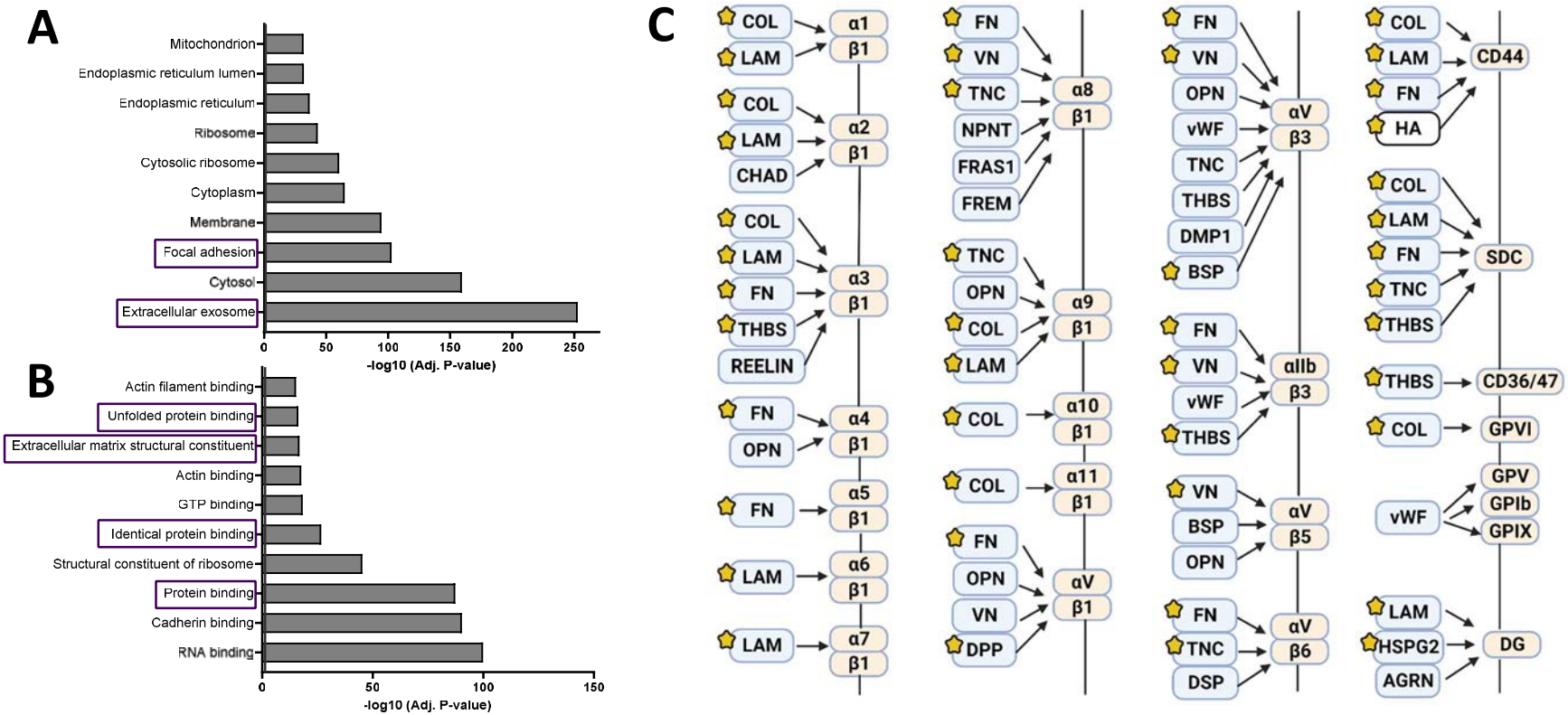

Figure 4.15 – DAVID analysis of HCASMC ECMs generated following cell stimulation with TNF-α and CSE. The entire protein set of proteins retrieved from ECM samples was processed through DAVID gene ontology analysis. Cellular component analysis (A) and molecular function analysis (B) was performed to analyse sample enrichment of each, and KEGG pathway analysis was performed, which identified the ECM-receptor pathway (C; Created with BioRender) as significant. COL- Collagen; LAM – Laminin; CHAD – Chondroadherin; FN – Fibronectin; THBS – Thrombospondin; OPN – Osteopontin; VN – Vitronectin; TNC – Tenascin; NPNT – Nephronectin; FRAS1 – Fraser extracellular matrix component 1; FREM – FRAS1-related extracellular matrix component; DPP – Decapentaplegic; vWF – von Willebrand Factor; DMP1 – Dentin matrix acidic phosphoprotein 1; BSP – Bone sialoprotein; DSP – Desmoplakin; HA – Hyaluronan; HSPG2 – Perlecan; AGRN – Agrin.

4.2.15 Native ECM samples from healthy and dysfunctional HCASMCs differentially up- and downregulate expression of proteins relevant in thrombosis and coagulation

Differences in thrombus formation and platelet spreading on healthy HCAEC CDMs compared with disease-relevant CDMs may be attributable to different proteins than the differences observed on HCASMC CDMs. It is therefore important to determine if thrombotic differences are a consequence of the same proteins, or if the expression of HCASMC-derived ECM proteins is differential. Gene ontology analysis from Section 4.2.13 enabled novel functional analysis of proteins present in CDMs derived from dysfunctional HCASMCs. To compare the effect of chronic cell stimulation with CVD damage stimuli TNF-α and CSE, however, the proteins present in each matrix must be compared to healthy controls. Volcano plots were therefore used as a measure to compare protein abundance in each CDM. CDMs were prepared for mass spectrometry, as previously described in Section 4.2.9, and submitted to the University of Manchester BioMS facility for mass spectrometric analysis. Proteome Discoverer software (Thermo Fisher) was used for sample analysis, and Microsoft Excel was used to log transform P-values and fold changes. A Volcano plot was then generated using Graphpad Prism 9.3.1. Matrisomal proteins were isolated from the dataset using MatrisomeDB (Shao *et al.,* 2019) and proteins relevant in thrombosis and haemostasis were also identified manually and annotated on plots. Fold change is relative to control CDMs.

Results demonstrated that, similarly to in HCAECs, treatment with TNF-α reduced collagen content, and the abundance of structural proteins such as laminin (LAMA3) and PRELP (Figure 4.16). Hyaluronan was more abundant in the healthy ECM than in any dysfunctional ECMs, whereas versican was reduced in the TNF-α treated sample, but interestingly increased in the sample treated with CSE+TNF-α. Platelet agonist Galectin-7 was also increased in the sample treated with CSE+TNF-α. The agonist S100A7 and pro-inflammatory interleukin-1β was upregulated in all dysfunctional ECM samples, compared to control (Figure 4.16). CXCL12, a platelet activator, was reduced in response to samples containing CSE. CSE treatment also appeared to increase expression of some collagens, although collagens were also reduced in these samples in addition to other ECM structural components such as EMILIN2. Unlike responses observed in HCAECs, the coagulation protein F13A1 was downregulated in response to TNF-a.

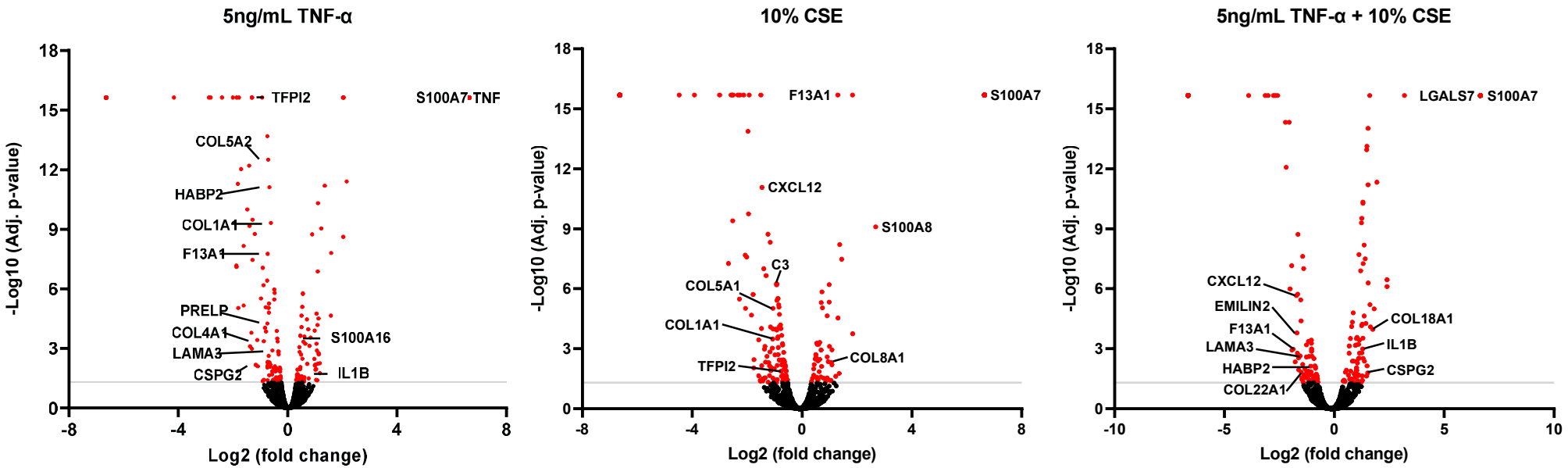

Figure 4.16 – Volcano plot analysis comparing healthy and dysfunctional HCASMC ECMs. Native CDM from healthy HCASMCs and HCASMCs damaged with tumour necrosis factor (TNF)-α and cigarette smoke extract (CSE) were compared to identify differences in ECM protein expression. Data retrieved from Proteome Discoverer was transferred to Excel and P-values and fold changes were log transformed. Volcano plots were then created using GraphPad Prism 9.3.1, and matrisomal proteins and proteins relevant in thrombosis and haemostasis were annotated on the plot. Fold change is relative to control CDMs; $P<0.05$. n=3. COL – Collagen; LAMA – Laminin A; TFPI – Tissue factor plasminogen activator; CSPG2 – Versican; IL1 – Interleukin-1; EMILIN – Elastin microfibril interfacer; PRELP - proline and arginine-rich end leucine rich repeat protein; LGALS – Galectin; F13 – Factor 13; HABP – Hyaluronan binding protein.

4.2.16 Platelet receptor interactions are altered in dysfunctional CDMs

Functional differences observed in thrombus formation and platelet spreading on healthy and dysfunctional CDMs may be in response to differences in platelet receptor interactions, owing to the up- and down-regulation of different proteins in each CDM (Figure 4.14, Figure 4.16). It is therefore important to evaluate differences in platelet receptor interactions occurring as a result of differences in the up- and down-regulation of proteins relevant in thrombosis and haemostasis. Matrisomal proteins and proteins relevant in thrombosis and haemostasis were isolated from the dataset using volcano plots from Figures 4.14 and 4.16. Venn diagrams, generated using BioRender, were then used to compare the up- and down-regulation of proteins in CDMs from HCAECs and HCASMCs damaged with CSE and TNF-α. Colour codes were then added to proteins, depending on which platelet receptors the proteins interacted with. Finally, a table was created to compare the functional effects of each protein on platelet function, coagulation and inflammation.

Results demonstrated the upregulation of coagulation-relevant proteins in both HCAEC and HCASMC samples (Figure 4.17), however the prevalence and variety of these proteins was more pronounced in HCAEC CDMs. Differences were also observed in platelet GPVI interactions, with reductions in the expression of collagens observed in dysfunctional CDMs for both cell types, and overall increases in the expression of galectins. Additionally, proteins binding the platelet adhesion receptor GPIbα were generally reduced in dyfunctional HCAEC CDMs, but in dysfunctional HCASMC CDMs this trend was specific to different proteins. Proteins involved in platelet activation, such as laminin, were observed to reduce, whereas proteins such as S100A8, involved in procoagulant platelet formation, were observed to increase. Engagement of other less prominent platelet receptors, such as CD44 (HABP2), P-selectin (CSPG2) and CXCR4 (CXCL12) was observed mainly in HCASMC samples, and alterations in the expression of these proteins appeared to be dependent on specific damage stimuli, with some proteins observed to increase or reduce depending on the stimuli applied. In contrast, alterations in proteins having an indirect effect on platelet function were observed only in HCAEC samples.

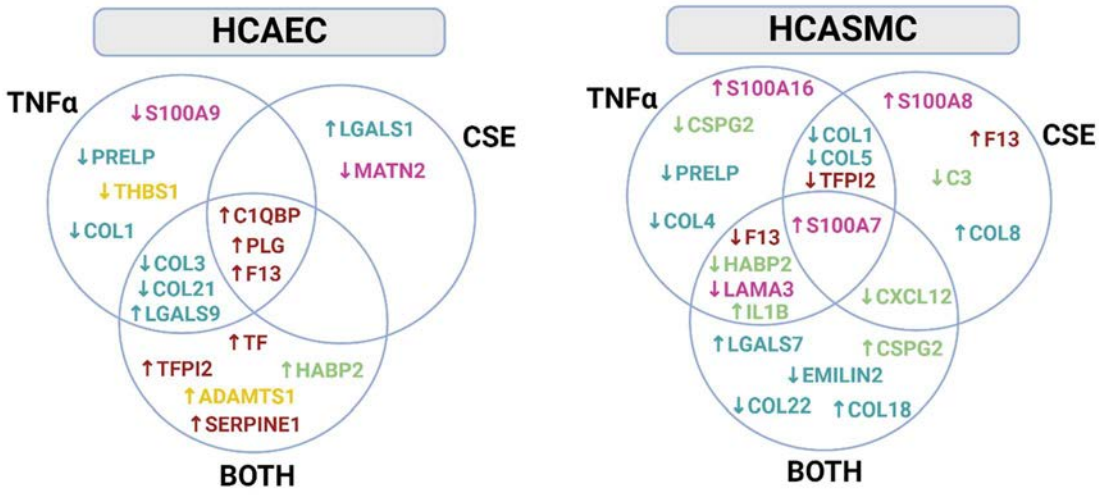

Associated receptors/processes:

- Coagulation
- Platelet GPVI
- Platelet GPIbα
- Other platelet receptor
- Indirect effector

Protein/s	Function/s	References
Coagulation a) C1QBP, F13, TF, SERPINE1 b) TFPI2, PLG	a) Coagulation, clot stability b) Regulation of coagulation	Perrschke and Ghebrehiwet, 1998; Wang *et al.*, 1998; Muratoglu *et al.*, 2000; Inoue *et al.*, 2008; Mosher *et al.*, 2008; Albeiroti *et al.*, 2015; Dong *et al.*, 2018; Brouns *et al.*, 2020; Kaira *et al.*, 2020; Colicchia *et al.*, 2022; Mansour *et al.*, 2022; Freda *et al.*, 2023; Provenzale *et al.*, 2023
GPIbα a) S100 proteins b) Laminins, matrilin	a) Pro-coagulant platelet formation b) Platelet adhesion, activation	
GPVI a) Collagens, galectins. PRELP	a) Platelet aggregation, ECM assembly, inflammation	
Other a) HABP2, CSPG2 b) CXCL12, IL1B, C3	a) Platelet adhesion and regulation b) Inflammation, platelet aggregation	
Indirect effectors a) THBS1 b) ADAMTS1	a) Opposes effect of NO on platelets b) Degrades ECM to pro-inflammatory isoforms	

Figure 4.17 – A summary of changes in platelet receptor interactions within dysfunctional cell-derived matrices of both human coronary artery endothelial cells (HCAECs) and smooth muscle cells (HCASMCs). Platelet receptor interactions on matrices were evaluated using differences in the expression of matrisomal proteins and proteins relevant in thrombosis and haemostasis in native CDM from HCAECs and HCASMCs damaged with tumour necrosis factor (TNF)-α and cigarette smoke extract (CSE). Venn diagrams were created using Biorender to visualise up- and down-regulation of proteins colour coded with the relevant platelet receptor. COL – Collagen; LAMA – Laminin A; SERPINE1 – plasminogen activator inhibitor 1; PLG – plasminogen; TF – Tissue factor; TFPI – Tissue factor pathway inhibitor; CSPG2 – Versican; IL1 – Interleukin-1; EMILIN – Elastin microfibril interfacer; PRELP - proline and arginine-rich end leucine rich repeat protein; LGALS – Galectin; F13 – Factor 13; HABP – Hyaluronan binding protein; MATN – matrilin.

4.3 Discussion

In this chapter, experiments were performed to investigate whether the native matrices produced by coronary artery ECs and SMCs were distinct from one another and whether the thrombogenicity was different between the two. Results were also compared with Type I Horm collagen, the current gold standard matrix protein used the field. In addition to defining the ECM produced by healthy cells, the impact of common CVD damage stimuli on ECM composition and thrombogenicity was also explored.

4.3.1 HCAECs and HCASMCs contribute different ECM proteins to the vascular wall, which appear morphologically distinct

Early experimental results demonstrated distinct differences in the morphology and architecture of CDM derived from HCAECs and HCASMCs (Figure 4.2). The HCAEC CDM demonstrates less directionality, with less fibrillar organisation. The HCASMC CDM in contrast demonstrated fibrillar organisation, with ECM fibres appearing to line up in the direction of the cells. These findings are consistent with Guo *et al.* (2017) and Jalilian *et al.* (2023), where the endothelial CDM appears visually similar to the HCAEC CDM observed in Figure 4.2. The disorganisation in the endothelial CDM may be due to several factors. Firstly, ECs were cultured under static conditions. *In vivo,* mechanosensitive endothelial cells in the coronary artery are exposed to an arterial shear rate of around 15dynes/cm^2, and cells orientate in the direction of flow, as observed in a study by Kroon *et al.* (2017), unlike under static culture, where endothelial cells have a cobblestone appearance (Figure 4.2). In the same way the HCASMC CDM is oriented in the direction of cells, the HCAEC CDM may also do so following cell culture under flow. Another potential reason for observed morphological differences is the content of each CDM. The HCAEC CDM contained more basement membrane-associated proteins, such as laminins and Type 4 collagen, than the HCASMC CDM, which contained ECM proteins found deeper in the vascular wall, such as versican and elastin (Figure 4.12). Indeed, laminin deposition on CDM derived from human dermal fibroblasts appears to have similar disorganisation (Malakpour-Permlid *et al.,* 2021). It may therefore be the content of CDMs that help to inform the resulting architecture, which may involve both fibrillar and non-fibrillar ECM proteins. The HCAEC CDM, for example, contained enzymatic proteins able to degrade ECM, such as hyaluronidase-2

and ADAMTS proteins (Figure 4.12). The presence of these proteins are important in ECM remodelling, an event important in vascular homeostasis, but also occurring as part of the development and progression of atherosclerosis.

4.3.2 Type I collagen is significantly more thrombogenic than cell-derived extracellular matrices derived from HCAECs and HCASMCs

Platelet spreading assays and thrombus formation assays were performed to compare platelet responses to CDMs derived from HCAECs and HCASMCs to the *in vitro* standard of Type I collagen. These experiments were performed to assess if Type I collagen should be used in the model, or if the model should instead incorporate an entire cell-derived ECM to best represent arterial thrombosis. Platelet spreading assays demonstrated a significant enhancement in platelet adhesion to HCAEC CDM compared with Type I collagen (Figure 4.3), but not HCASMC CDM (Figure 4.4). This may be due to the presence of more extracellular collagens in the HCASMC CDM than the HCAEC CDM, such as Type VI collagen. Additionally, the HCAEC CDM contains an abundance of adhesive proteins, such as galectins, laminins and vWF, compared to the HCASMC CDM (Figure 4.12). Indeed, the presence of vWF enhances platelet adhesion to collagen (Tomokiyo *et al.,* 2005) and may play a large part in the enhanced platelet adhesion observed on the HCAEC CDMs. Morphological assessment of platelet spreading on Type I collagen compared with the CDMs demonstrated a significant increase in lamellipodia on both HCAEC and HCASMC-derived matrices. This may be due to an increased platelet response to ECM proteins contained in the CDM, such as vWF, galectins and laminins in the HCAEC CDM, and versican, elastin and CXCL12 in the HCASMC CDM. However, platelet spreading can alter depending on the architecture of the substrate, with a fibrillar structure favouring the formation of filopodia (Sandmann and Koster, 2016). It is therefore possible that differences in platelet spreading on CDMs compared with Type I collagen may be attributed to substrate smoothness. Additionally, morphological classification was conducted manually, and this type of analysis may be subjective. Indeed, despite an increase in lamellipodia observed on HCAEC and HCASMC CDMs, there was no accompanying increase in platelet area compared with Type I collagen (Figure 4.3, Figure 4.4). It is therefore important to carefully consider this factor when drawing any conclusions from the classification.

To investigate platelet responses further, thrombus formation assays under flow were performed, comparing thrombus formation on Type I collagen to HCAEC and HCASMC-derived matrices. Thrombi formed on the HCAEC CDMs were significantly more abundant and smaller in volume than thrombi formed on Type I collagen (Figure 4.6), validating earlier results demonstrating enhanced platelet adhesion to HCAEC CDMs (Figure 4.3). The presence of different mediators of platelet activity in the HCAEC CDM, as previously mentioned, may contribute to enhanced adhesion but not aggregation, as many of the components are basement membrane associated. Indeed, a study by White-Adams *et al.* (2010) showed that thrombi formed on laminin, a basement membrane protein, appeared smaller than on Type I collagen. In contrast, thrombi formed on the HCASMC CDM were more abundant and smaller in size compared with Type I collagen, but not volume (Figure 4.7). These results suggest an increase in platelet-platelet interactions compared with the HCAEC CDM (Figure 4.8), which may be due to an increase in the presence of extracellular collagens and proteoglycans (Figure 4.14).

Overall, despite both HCAECs and HCASMCs depositing abundant Type I collagen (observed in Figure 4.2, following decellularisation), both CDMs are less thrombogenic than Type I Horm collagen. This indicates that other proteins in the CDM negatively regulate platelet responses to Type I collagen, or that Horm collagen, isolated from equine tendons, is artificially more thrombogenic than human vascular Type I collagen. This finding may have implications in the screening of novel antithrombotics, as the resulting recommended dosage may be too high, a hypothesis reflected in the resulting increased risk of bleeding following the use of common antithrombotics (Tsai *et al.,* 2010; Huang *et al.,* 2011). Conversely, the absence of coagulation may have a profound effect on thrombus formation on the CDMs. Many of the proteins identified as significantly up/downregulated in the CDMs were coagulation proteins (Figure 4.12, Figure 4.14, Figure 4.16), therefore in recalcified conditions, the CDM would likely be more thrombogenic. In summary, Type I collagen is useful as a low cost, convenient fibrillary flow model. However, the absence of elastin and other proteins means that the matrix confers little elasticity, and regulation of platelet activity by other ECM components is not observed. The developing model should therefore move forward using a CDM when incorporating focal damage and assessing thrombus formation, in order to more accurately model *in vivo* thrombus formation.

4.3.3 Chronic stimulation of HCAECs and HCASMCs with pro-inflammatory TNF-α and cigarette smoke extract alters ECM composition, enhancing thrombogenicity

Differences observed in platelet activity on CDMs compared with Type I collagen suggested that the presence of different ECM components affected platelet spreading and thrombus formation. In atherosclerotic vascular disease, changes in the vascular ECM are a hallmark of disease development and progression (Chrysostomi *et al.,* 2021). Despite this, relatively little is known about platelet responses to these alterations in the ECM. Experiments were therefore performed to model atherosclerotic disease in both plaque rupture and erosion, with damage stimuli such as inflammation (TNF-α) and smoking (CSE) inflicted upon cells over 3 days, to generate representative ECMs. Platelet function experiments were then performed to inform any differences observed in platelet activity. Indeed, results from platelet adhesion assays demonstrated that the TNF-α associated HCAEC CDM was significantly more adhesive to platelets than the control CDM (Figure 4.3), and under flow, both individually and in combination with CSE, produced larger, less abundant thrombi than the healthy CDM (Figure 4.9). Mass spectrometry proteomic results suggest that the healthy CDM has more structural constituents, such as Type I and III collagen (Figure 4.14). The TNF-α associated CDM, in contrast, has an upregulation in Galectin-9 and C1q binding protein. Both C1q and galectin-9 are potent platelet agonists and are associated with poor outcomes in atherosclerosis (Peerschke *et al.,* 1993; Chen *et al.,* 2022; Krautter *et al.,* 2022; Sasaki *et al.,* 2022). Although the presence of other ECM components means that differences in platelet activity cannot be attributed to one specific protein, it is interesting that galectin-9 is present in both TNF-α matrices exhibiting an increase in thrombogenicity, and absent from the CSE-associated matrix, which displayed no increase in thrombogenicity compared to control (Figure 4.14).

Results from thrombus formation assays performed comparing a healthy HCASMC CDM to damage-associated matrices again demonstrated that a TNF-α associated HCASMC CDM is more thrombogenic than a healthy CDM, promoting the formation of larger thrombi (Figure 4.10). This may be due to a reduction in less potent platelet aggregators, such as laminin, in these samples (Figure 4.16), allowing platelets to interact with more

potent aggregators such as collagens. Alternatively, a reduction in proteoglycans such as versican, able to bind collagens and regulate their activity (Chen *et al.,* 2022), in the TNF-α associated samples may contribute to a more thrombogenic ECM. Another interesting observation was the sizeable upregulation of coagulation proteins such as plasminogen and Factor 13, as well as TF and TFPI in response to both TNF-α and CSE (Figure 4.14). Experiments on HCAEC- and HCASMC-derived CDMs were not performed in the presence of recalcified blood, therefore it was not possible to assess coagulation and due to time constraints, these experiments were not performed. However, it would be useful to determine the importance of coagulation following changes in the ECM, and this is a potential future direction of the project. Indeed, it would be useful to compare differences in coagulation between CDMs from both cell types, as coagulation proteins were more prevalent in HCAEC CDMs than HCASMC CDMs (Figure 4.17).

Overall, proteins relevant in coagulation, inflammation and platelet adhesion and aggregation were all present, and either up- or down-regulated in dysfunctional HCAEC and HCASMC CDMs. There was an overall reduction in structural collagens in both cell types in response to damage stimuli, but an increase in galectins (Figure 4.17), demonstrating continued platelet GPVI engagement and platelet aggregation. Proteins binding to platelet GPIbα, were generally reduced in HCAEC samples but upregulated in dysfunctional HCASMC samples, indicating a potential increase in platelet adhesion between thrombus formation on both cell types (Figure 4.17). Indeed, Figure 4.8 demonstrates an increase in the number of thrombi formed on a HCASMC CDM compared with Type I collagen, but not on a HCAEC CDM. Proteins having an indirect effect on platelet function were generally found on the HCAEC CDM samples (Figure 4.17) and had more of a role in the development of atherothrombosis. THBS1, for example, can reduce platelet sensitivity to NO, contributing to aberrant thrombosis (Mosher *et al.,* 2008). Although singular proteins cannot be verified as causes of alterations in thrombus formation on an entire CDM, in a model of atherothrombosis, a CDM is useful to better represent an *in vivo* vascular ECM, altering in response to cellular damage stimuli. The next Chapter will focus on incorporating endothelial cells into the model, comparing HUVECs and HCAECs, and inflicting focal damage on cells to expose the underlying ECM using ferric chloride-soaked filter paper and a needle, similar to *in vivo* protocols using murine models. This will help to bridge the gap between current *in vivo* and *in vitro* thrombosis models and make both more comparable.

5. An endothelialised, *in vitro* model of human atherothrombosis

5.1 Introduction

5.1.1 Microfluidic models in thrombosis

An *in vitro* model of thrombosis, complete with dysfunctional CDMs, enables simple assessment of antiplatelet efficacy, similar to *in vitro* models using Type I collagen coatings. However, as previously described in Section 1.2, endothelial and smooth muscle cells have key roles in the regulation of platelet activity and vascular function and should be incorporated into models to more accurately reflect thrombosis in ruptured and eroded plaques. Current *in vitro* thrombosis models can take many forms, but often utilise microfluidic devices, for ease of use, versatility, replicability and affordability (Herbig *et al.,* 2018). These microfluidic devices may be commercially available, 3D printed or designed using soft lithography, where channels are designed to run through 3D hydrogels often composed of Type I collagen. From an ECM perspective, a major advantage of hydrogel-based models is the culture duration, often a minimum of 7 days (Weinberg *et al.,* 1985; Hajal *et al.,* 2022), which would enable ECs to create a representative ECM (Hielscher et al., 2012). These models have been adapted for venous systems (Zheng et al., 2012) and could potentially be translated to models of arterial thrombosis, however they can be complex and time-consuming, and focal damage, representing atherosclerotic plaque rupture or erosion, would be challenging to adapt in these models. Akther *et al.* (2022), for example, created a hydrogel-based design to model atherothrombosis incorporating varying degrees of vessel stenosis, and although focal exposure of the hydrogel was achieved, the device did not incorporate dysfunctional ECs or the corresponding ECM to model atherothrombotic pathology.

Commercially available microfluidic models can be simpler in design and more attractive as a reproducible model. ECs can be seeded directly into chambers before inducing dysfunction and monitoring thrombus formation (Riley, 2022). However, it is difficult to introduce focal endothelial damage to these closed chambers to allow discreet exposure of sub-endothelial matrix proteins. Moreover, it is important to optimise EC culture time in simplified models to allow ECs to produce their own ECM. ECs cultured on Type I

collagen alone have been shown to exhibit altered behaviour compared to ECs *in vivo* (Ziegler *et al.,* 1995; Whelan and Senger, 2003; Colombo *et al.,* 2013; Zavala *et al.,* 2018). Results from flow experiments culturing ECs on fibronectin, for example (Greineder *et al.,* 2017), would therefore be difficult to compare to flow experiments culturing ECs on Type I collagen, and even more so to ECs *in vivo,* without adequate culture time. The native ECM produced by ECs would be more physiologically relevant, without artificially increased levels of Type I collagen and fibronectin.

5.1.2 Endothelial cell heterogeneity

Endothelial cells from different locations in the vasculature exhibit heterogeneity, as a result of differences in biochemical signalling responses and mechanosensing in their respective tissues (Yau *et al.,* 2015; Mathur *et al.,* 2021; Gifre-Renom *et al.,* 2022). ECs derived from arteries and veins differ in structure, tight junction architecture and response to inflammatory and atherogenic stimuli (Simionescu *et al.,* 1976; Deng *et al.,* 2005; Eriksson *et al.,* 2005; Aird, 2007). Indeed, the vascular environment in the artery vastly differs from the vein, with arteries having a thicker wall, no valves and carrying highly oxygenated blood. Additionally, the differing shear rates have significant effects on cell behaviour, with increased arterial shear rates inducing endothelial protective Krüppel-like Factor (KLF)-2 and -4 and reduced venous shear rates inducing hypoxia and release of vWF from ECs (Yau *et al.,* 2015; Xu *et al.,* 2021). There is also evidence to demonstrate differences in gene expression between arterial and venous ECs. Arterial ECs express more tPA, and venous ECs more vWF (Yamamoto *et al.,* 1998; Aird, 2007). Heterogeneity derived from the tissue environment, however, is largely lost during *in vitro* culture, although ECs do retain functional differences derived from maturation (Lang *et al.,* 2003; Burridge and Friedman, 2010), which may influence variations in EC behaviour *in vitro.* HUVECs are often used in place of HCAECs to model arterial vascular disease (Shao *et al.,* 2009; Wang *et al.,* 2015; Costa *et al.,* 2017; Hao *et al.,* 2019), due to cost efficiency and ease of access. However, HUVECs may not be representative or comparable to HCAECs. It is therefore important to compare both cell types to determine the optimum endothelial cell type to use in the *in vitro* flow model.

5.1.3 *In vivo* methodology and coagulation

To enable comparability of the model with *in vivo* models, methodologies used *in vivo* should be translated *in vitro*. Comparison is important as there are key differences between human atherosclerosis and murine models, the most notable being the absence of fibrin in murine models (Rosenfeld *et al.,* 2000), but also differences in the vascular bed, plaque morphology and propensity to rupture (Getz and Reardon, 2012; Veseli *et al.,* 2017). A widely used methodology of inducing arterial thrombosis in mice is through the application of $FeCl_3$ (as described in Section 1.6). Filter paper soaked in $FeCl_3$ is applied to the vessel adventitia, initiating thrombosis and vessel occlusion. Tseng *et al.* (2006) report endothelial detachment in response to $FeCl_3$ injury, but Barr *et al.* (2013) propose that instead, thrombosis occurring as a result of $FeCl_3$ treatment is mediated by RBC haemolysis, and not EC detachment. This contrasts with findings from Eckley *et al.* (2011), where $FeCl_3$ was shown to detach ECs and promote the formation of platelet-rich thrombi. Successful translation of the $FeCl_3$ method to an *in vitro* setting would enable comparisons to be made between *in vivo* and *in vitro* modelling of arterial thrombosis, and enable replacement of current *in vivo* models to a more representative human-based model. To investigate $FeCl_3$-mediated EC damage further, Ciciliano *et al.* (2015) used a diffusion co-efficient to translate *in vivo* $FeCl_3$ methodology to an *in vitro* setting, calculating a final concentration of 50mM at the endothelial monolayer. This was used in an endothelialised microfluidic model by perfusing $FeCl_3$ directly through the channel, and the resulting thrombus was RBC-rich with no endothelial detachment. Although this study provides a novel insight into $FeCl_3$-induced thrombosis, the damage is not focal as *in vivo,* and thus the contribution of the surrounding healthy endothelium can not be taken into consideration.

Another important consideration is the recalcification of blood *in vitro* to assess coagulation, to investigate contrasting findings on the role of $FeCl_3$ in thrombosis in multiple studies. Challenges associated with recalcification of blood in *in vitro* model development include inappropriate clotting before the blood reaches the reservoir due to contact-induced coagulation from model tubing and blood tubes, and non-standardisation of the concentration of calcium chloride due to variations in model design (Vogler and Siedlecki, 2009). To resolve the issues surrounding contact-induced coagulation, corn trypsin inhibitor (CTI) may be used to inhibit FXIIa, however the

concentration used across studies is non-standardised (Hosokawa *et al.,* 2011; Sakurai *et al.,* 2018). Additionally, Hansson *et al.* (2014) proposed a link between the use of CTI and inhibition of FXIa and the thrombin feedback loop, advising that CTI should only be used at concentrations below 20mg/L to avoid this effect. Moreover, Nielsen (2009) demonstrated a reduction in tPA-mediated fibrinolysis following the use of CTI, although the concentration of CTI used was 49.6mg/L, higher than the concentration of 20mg/L recommended by Hansson *et al.* (2014). The use of CTI is therefore not without its disadvantages, having effects on multiple components relevant in coagulation and fibrinolysis. Successful models of coagulation have used final concentrations of calcium chloride between 6.3-10mM and infused the blood with the mixture immediately prior to perfusion through channels, to avoid inappropriate clotting (Brouns *et al.,* 2019; Berry *et al.,* 2021; Ciciliano *et al.,* 2015).

5.1.4 Chapter aim, objectives and hypothesis

The aim of this Chapter is to incorporate biologically relevant endothelial cells into an *in vitro* model and to optimise a protocol to inflict focal damage on cells, exposing the underlying ECM. Furthermore, focal damage will be investigated and blood will be recalcified, to enable coagulation to be explored in the model.

Objectives:

1. Compare the thrombotic potential of HUVECs and HCAECs, to elucidate the optimum cell type to use in the model
2. Develop and optimise protocols to inflict focal damage on ECs using $FeCl_3$, needle stick injury and decellularisation buffer
3. Investigate thrombus formation on focally damaged ECs
4. Recalcify blood and investigate coagulation in response to $FeCl_3$-induced EC damage

Hypothesis:- HUVECs and HCAECs vary in their thrombotic potential, and in *vivo* experimental protocols can be optimised for use and comparison *in vitro*

5.2 Results

5.2.1 The thrombotic and haemostatic potential of HCAECs is significantly different to HUVECs

Findings from the previous Chapter demonstrated key differences in the ECM composition of HCAECs in response to chronic inflammatory stimuli (TNF-α) and CSE. However, ECs are key regulators of circulating platelets, and under physiological conditions release mediators which inhibit platelet activity, described in Section 1.2. Following endothelial dysfunction, endothelial cells switch to a pro-thrombotic phenotype, described in Section 1.4. It is therefore important to incorporate the endothelium in the *in vitro* thrombosis model, to represent the cellular contribution to atherothrombosis. HUVECs are often used in these models, as described in Section 5.1, however this cell type is from a venous tissue and, due to heterogeneity of endothelial cells, may not be the optimum cell type to use in the model. To investigate this further, RT-qPCR was performed to compare resting gene expression of markers of platelet function and inflammation. The following genes and their roles in thrombosis and haemostasis have been described in detail in Chapter One but will be summarised here for reference. eNOS is an enzyme produced by endothelial cells which generates atheroprotective NO to maintain platelet quiescence in the vasculature. Changes in eNOS can be used to measure NO production as a measure of physiological platelet inhibition. CD39 is a protein released from endothelial cells which hydrolyses ADP to AMP to prevent ADP-stimulated platelet activation. Endothelial-derived COX-2 promotes synthesis of pro-inflammatory prostaglandins by oxidation of AA. Also having a role in the AA pathway, TXA2 synthase (gene TBXAS1) converts prostaglandins into pro-thrombotic TXA2. Finally, vWF is an important mediator of platelet adhesion to sites of injury in the vasculature, but also has a role as a carrier and stabiliser of coagulation FVIII, enhancing fibrin crosslinking in coagulation. Expression of these markers was quantified to compare the thrombotic and haemostatic potential of HUVECs and HCAECs. The resting levels of eNOS ($P<0.0001$), COX-2 ($P<0.01$) and TBXAS1 ($P<0.05$) were significantly higher in HCAECs than in HUVECs (Figure 5.3), demonstrating variation in regulation of platelet function and inflammatory potential. HUVECs, in contrast, had significantly higher levels of CD39 ($P<0.05$) and vWF ($P<0.05$), demonstrating variation in platelet function and potentially coagulation.

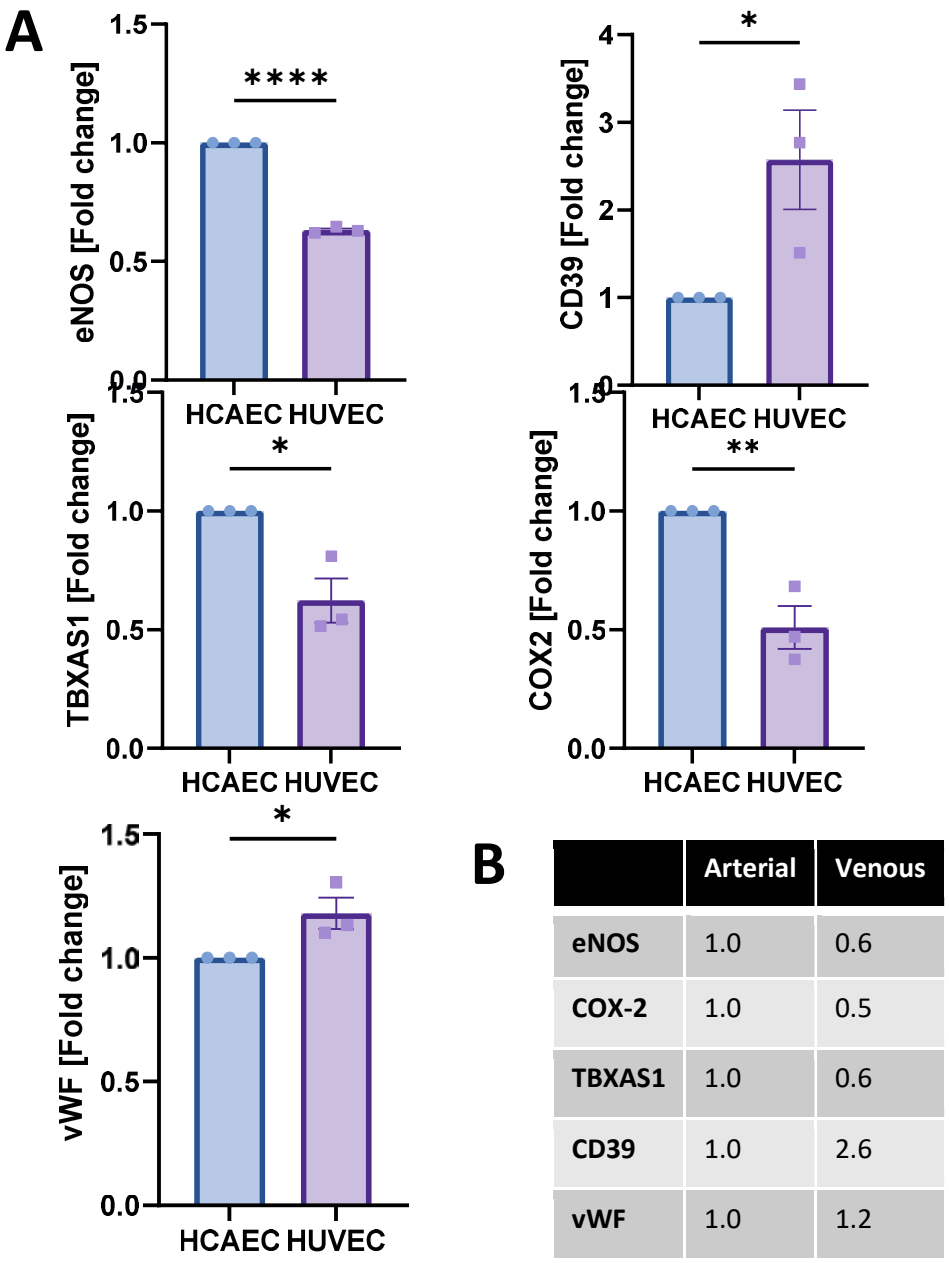

B

	Arterial	Venous
eNOS	1.0	0.6
COX-2	1.0	0.5
TBXAS1	1.0	0.6
CD39	1.0	2.6
vWF	1.0	1.2

Figure 5.1 – Comparison of resting gene expression levels of endothelial-derived markers of thrombosis and haemostasis. RNA from HCAECs (Arterial) and HUVECs (Venous) in culture was extracted and purified before cDNA synthesis and qPCR analysis. Resting gene expression levels were quantified in log fold change from HCAEC control (B) and represented graphically (A) using GraphPad Prism 9.3.1. An unpaired T-test was used for statistical analysis. Error bars represent ± SEM. n=3. *P<0.05; **P<0.01; ***P<0.001; ****P<0.0001. eNOS – Endothelial nitric oxide synthase; COX – cyclooxygenase; TBXAS1 – Thromboxane A synthase 1; vWF – Von Willebrand Factor.

5.2.2 Stimulation of HCAECs with TNF-α and CSE alters gene expression of key mediators of thrombosis

Variations observed in resting gene expression levels in HUVECs and HCAECs indicate the potential for variation in response to damage stimuli. Throughout the development of the model, TNF-α and CSE have been used to represent inflammation and smoking respectively. To enable consistency and comparability, HCAECs were stimulated with these insults and gene expression levels of key mediators of thrombosis, previously described in Section 5.2.3, were measured. HCAECs were cultured in 24-well plates and stimulated with TNF-α, CSE or both. RNA was extracted and purified from cells and synthesised into cDNA, before qPCR was performed to quantify fold-change expression of eNOS, CD39, TBXAS1, COX-2 and vWF.

Results demonstrated significant upregulation of COX-2 expression ($P<0.05$) and downregulation of CD39 ($P<0.05$) following stimulation with CSE, TNF-α and both (Figure 5.2). Additionally, vWF and eNOS were both significantly downregulated in response to TNF-α stimulation, however interestingly, this was abolished with the addition of CSE to samples. There were no significant differences in gene expression of TBXAS1 in any samples. In summary, stimulating HCAECs with TNF-α and CSE altered the gene expression of some mediators of thrombosis, demonstrating that endothelial regulation of thrombosis is altered following the inducement of EC dysfunction.

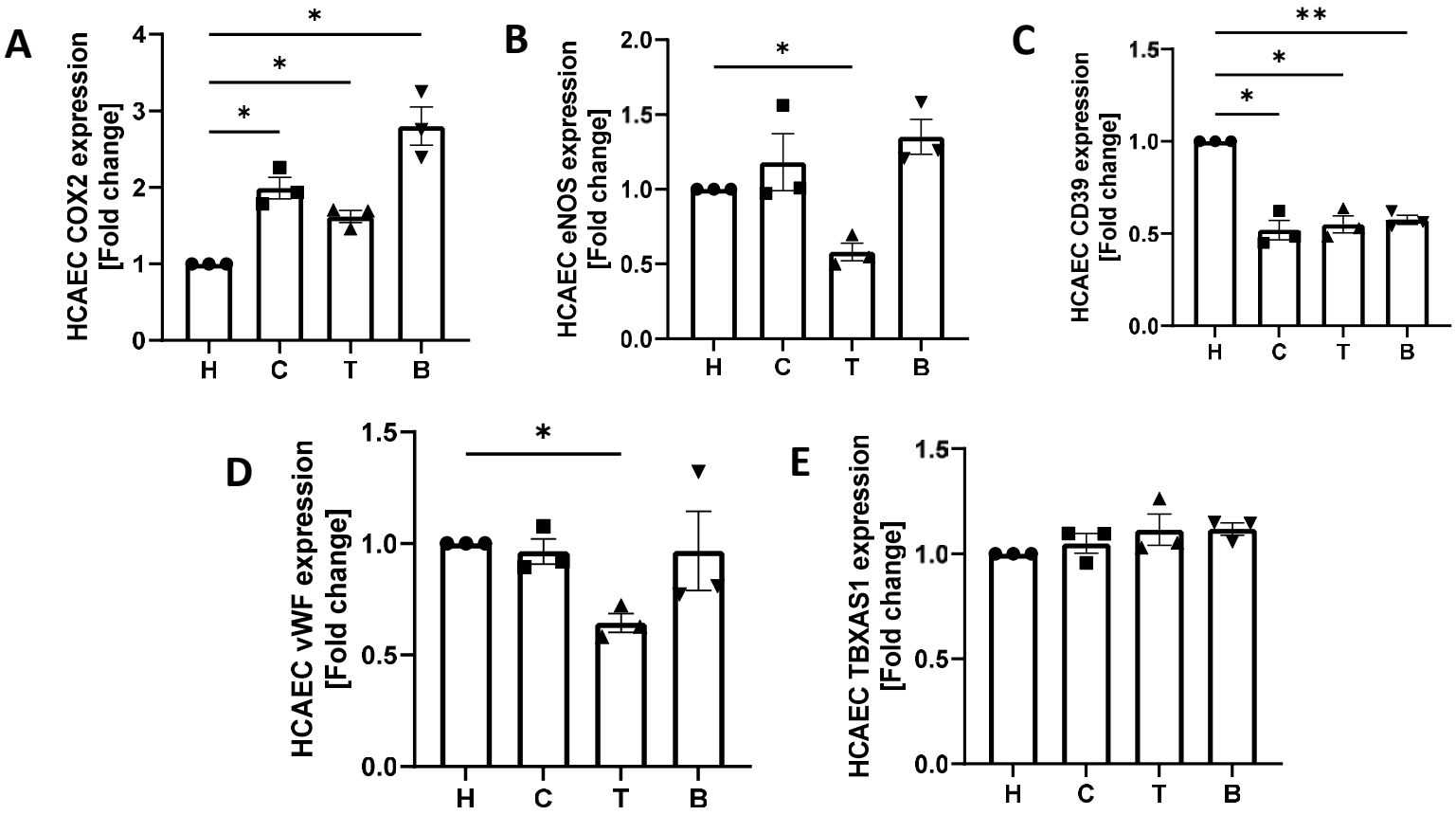

Figure 5.2 – Alterations in HCAEC gene expression levels following stimulation with TNF-α and CSE. Healthy HCAECs in culture were damaged with TNF-α (T), cigarette smoke extract (C) or both (B). RNA was extracted and purified before cDNA synthesis and qPCR analysis. Gene expression levels were quantified in log fold change from HCAEC control (H) and represented graphically using GraphPad Prism 9.3.1 (A-E). A one-way ANOVA was used for statistical analysis. Error bars represent ± SEM. n=3. *P<0.05; **P<0.01. eNOS – Endothelial nitric oxide synthase; COX – cyclooxygenase; TBXAS1 – Thromboxane A synthase 1; vWF – Von Willebrand Factor.

5.2.3 Stimulation of HUVECs with TNF-α and CSE alters gene expression of key mediators of thrombosis

Variations observed in the gene expression levels of key mediators of thrombosis and haemostasis following HCAEC stimulation with TNF-α and CSE indicate dysregulation of thrombosis following EC dysfunction. As previously discussed in Section 5.1.2, HUVECs are often used in thrombosis models due to their ease of access and affordability. However, as venous cells, they may not best represent arterial thrombosis. qPCR was therefore performed to investigate gene expression levels of key mediators of thrombosis following HUVEC stimulation with TNF-α and CSE. HUVECs were cultured in 24-well plates and stimulated with TNF-α, CSE or both. RNA was extracted and purified from cells and synthesised into cDNA, before qPCR was performed to quantify fold-change expression of eNOS, CD39, TBXAS1, COX-2 and vWF.

Similarly to HCAECs, HUVECs also significantly upregulated COX-2 expression ($P<0.05$) following stimulation with CSE, TNF-α and both (Figure 5.3).

Additionally, vWF, eNOS and CD39 were all significantly downregulated in response to TNF-α stimulation ($P<0.05$) (Figure 5.3), however interestingly, this downregulation was abolished in both vWF and eNOS with the addition of CSE to samples. Similarly to HCAECs, there were also no significant differences in gene expression of TBXAS1 in any samples. In summary, stimulating HUVECs with TNF-α and CSE altered the gene expression of some mediators of thrombosis, in a remarkably similar pattern to that of HCAECs, demonstrating that under flow, endothelial regulation of thrombosis is altered following the inducement of EC dysfunction.

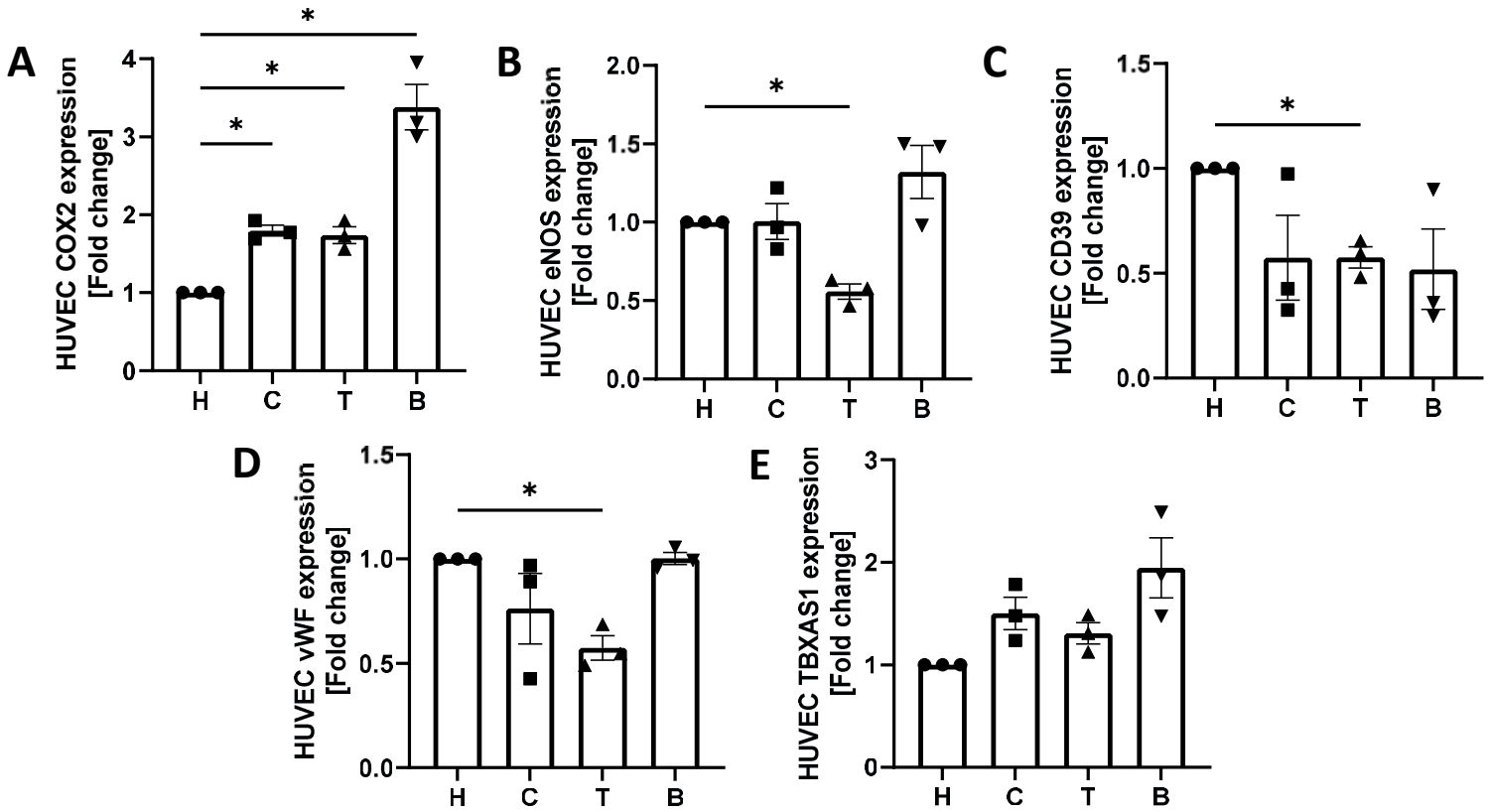

Figure 5.3 – Alterations in HUVEC gene expression levels following stimulation with TNF-α and CSE. Healthy HUVECs in culture were damaged with TNF-α (T), cigarette smoke extract (C) or both (B). RNA was extracted and purified before cDNA synthesis and qPCR analysis. Gene expression levels were quantified in log fold change from HUVEC control (H) and represented graphically using GraphPad Prism 9.3.1 (A-E). A one-way ANOVA was used for statistical analysis. Error bars represent ± SEM. n=3. *P<0.05. eNOS – Endothelial nitric oxide synthase; COX – cyclooxygenase; TBXAS1 – Thromboxane A synthase 1; vWF – Von Willebrand Factor.

5.2.4 HUVECs and HCAECs respond similarly to cardiovascular-associated damage stimuli

Variations observed in resting gene expression levels in HUVECs and HCAECs indicate the potential for variation in response to damage stimuli. Results from Sections 5.2.2 and 5.2.3, however, demonstrate similar patterns in cellular response to CV damage stimuli. It is only by comparing this magnitude of change directly that the two cell types can be compared in their up- and downregulation of mediators of thrombosis. Any variations in response would provide an insight into differences in thrombotic potential, but also inform the optimum cell type to use in the model. HUVECs and HCAECs were cultured in 24-well plates and stimulated with TNF-α, CSE or both. RNA was extracted and purified from cells and synthesised into cDNA, before qPCR was performed to quantify fold-change expression of eNOS, CD39, TBXAS1, COX-2 and vWF.

Results demonstrated that both endothelial cell types responded similarly to CVD damage stimuli in measured gene expression. There were no significant differences observed in HCAEC response to TNF-α, CSE or both, compared with HUVEC responses, except in the measurement of TBXAS1 gene expression, where upregulation of this gene was significantly higher in HUVECs than HCAECs ($P<0.05$) (Figure 5.4). In summary, HUVECs and HCAECs both up- and downregulate gene expression levels of markers of thrombosis in a similar manner, when exposed to CVD-associated insults.

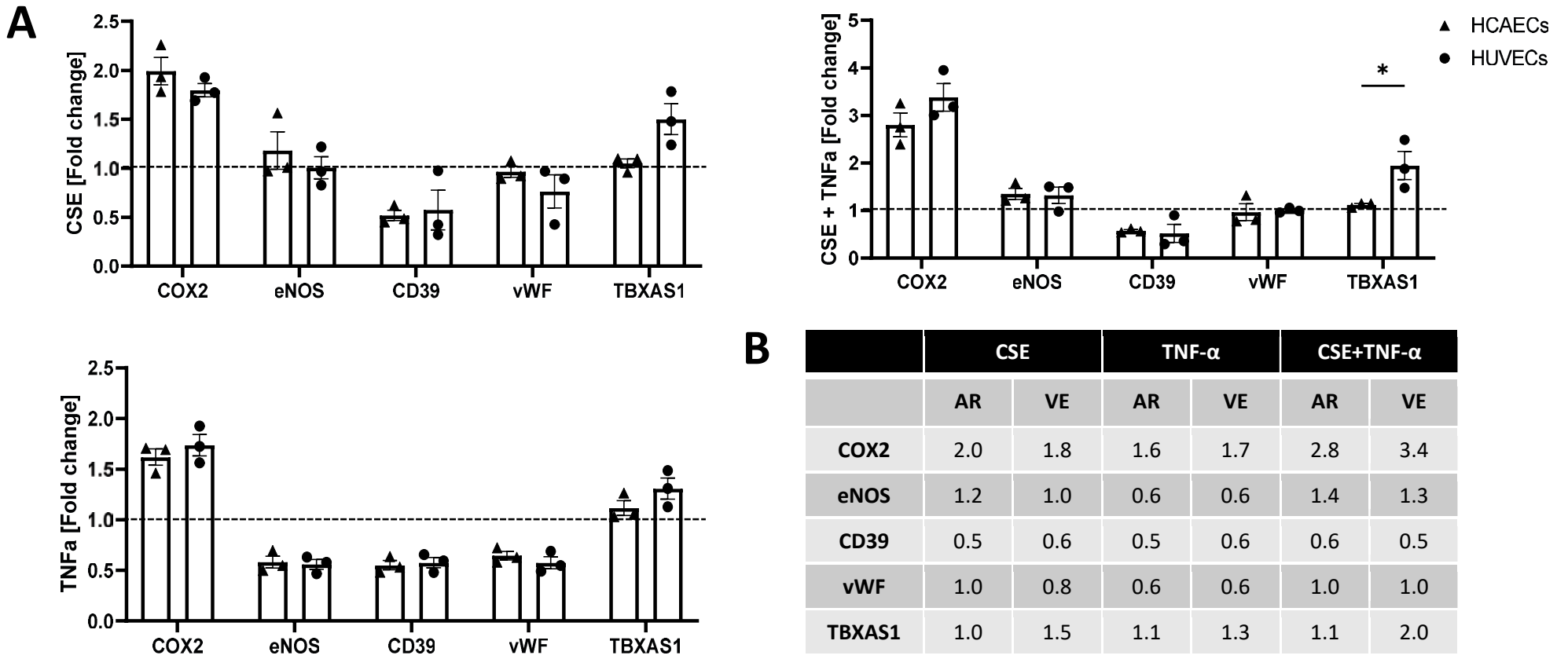

B

	CSE		TNF-α		CSE+TNF-α	
	AR	VE	AR	VE	AR	VE
COX2	2.0	1.8	1.6	1.7	2.8	3.4
eNOS	1.2	1.0	0.6	0.6	1.4	1.3
CD39	0.5	0.6	0.5	0.6	0.6	0.5
vWF	1.0	0.8	0.6	0.6	1.0	1.0
TBXAS1	1.0	1.5	1.1	1.3	1.1	2.0

Figure 5.4 – Comparison of HUVEC and HCAEC responses to cardiovascular-associated damage stimuli. HCAECs (AR) and HUVECs (VE) were cultured and damaged with tumour necrosis factor alpha (TNF-α), 1X cigarette smoke extract (CSE) or both for 24 hours, before RNA extraction, purification and cDNA synthesis was performed. Cell expression of thrombotic and haemostatic markers was quantified in log fold change (B) and represented graphically (A) using GraphPad Prism 9.3.1. Dashed line represents vehicle control. A two-way ANOVA was used for statistical analysis. Error bars represent ± SEM. n=3. *P<0.05. eNOS – Endothelial nitric oxide synthase; COX – cyclooxygenase; TBXAS1 – Thromboxane A synthase 1; vWF – Von Willebrand Factor.

5.2.5 Focal cell damage can be induced using filter paper saturated in $FeCl_3$

Models of thrombosis are continually evolving, with model cellularisation pivotal in our understanding of endothelial regulation of thrombosis. However, these *in vitro* models must be comparable with *in vivo* models, to enable translation of previously reported data and to encourage researchers to move away from animal models by adopting like for like *in vitro* replacements. The aim of this experiment was to optimise a protocol to induce focal cell damage using $FeCl_3$, a reagent commonly used in *in vivo* murine models to promote occlusive thrombus formation. Following successful focal damage, focally damaged ECs will be incorporated into a thrombosis flow model using ibidi sticky slides, which allow access to ECs before the fluidic chamber is assembled. To investigate and characterise $FeCl_3$ damage, 24-well coverslips will be used. Following results from previous experiments indicating differences in the thrombotic and haemostatic potential of HCAECs and HUVECs, HCAECs were determined as the optimum cell type to use in this model of arterial thrombosis and were used in all subsequent experiments. Briefly, hole punchers were used to create circles of filter paper of 1mm and 6mm diameter and soaked in 0.8% (50mM) $FeCl_3$, consistent with the concentration calculated by Ciciliano *et al.* (2015) of the final concentration of $FeCl_3$ present at the endothelial monolayer following diffusion across the vessel. HCAECs were cultured in 24-well plates before careful application of $FeCl_3$-soaked filter paper of both diameters for 2 minutes. Cells were washed with DPBS and fixed with 4% PFA, before staining with Phalloidin, imaging and analysing using ImageJ.

The area was visualised to determine whether the application of $FeCl_3$ initiated localised decellularisation (Figure 5.5A, Figure 5.5B) and the diameter of the decellularised area quantified (Figure 5.5C) to determine the optimum hole punch to use for experimental development. The coverslips used for experiments are 22x64mm, so the focal area of damage should sit comfortably within that region to visualise using ibidi sticky slides, which allow access to ECs and enable focal damage prior to closure of the chamber. The diameter of the largest decellularised area, generated using the 6mm hole punch, was measured at 7.6mm. The smaller decellularised area, in comparison, had a diameter of 1.9mm. For the purposes of microscopy analysis and eventual downscaling of the model, the smaller 1mm hole punch was determined as optimal for future experiments.

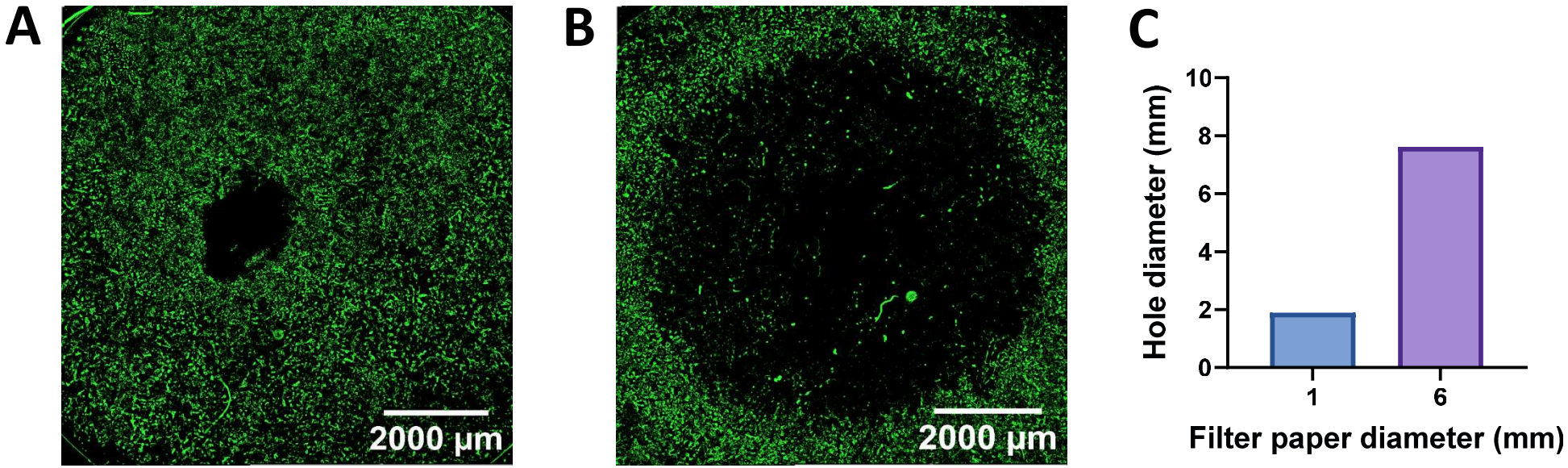

Figure 5.5 – Comparison of focal damage size on the endothelial monolayer following application of $FeCl_3$ soaked filter paper. Hole punches were used to create circular filter paper of 1mm and 6mm diameter, before being soaked in 0.8% $FeCl_3$ and applied to a healthy endothelial monolayer for 2 minutes. Filter paper was removed, and cells were washed with DPBS and fixed in 4% PFA for 15 minutes before staining with Phalloidin and imaging using the tile scan feature (merged) on a fluorescent microscope. (A) and (B) represent the focal damage created by the 1mm and 6mm diameter filter paper respectively. Images were analysed using ImageJ and visualised graphically (C) using GraphPad Prism 9.3.1. n=1. Representative images shown.

5.2.6 The viability of HCAECs treated with $FeCl_3$ is time- and concentration-dependent

Focal damage of endothelial cells in an *in vitro* flow model enables measurement of thrombus formation, considering the contribution of surrounding cells to thrombosis. Additionally, this methodology allows measurement of a variety of different disease scenarios, including simulation of the rupture or erosion of an atherosclerotic plaque and wound healing, for example. To further investigate the effect of $FeCl_3$ on the focal damage to endothelial cells, a LIVE/DEAD stain was used to determine whether cell death extended beyond the area in contact with the $FeCl_3$ soaked filter paper. Furthermore, the effects of different concentrations of $FeCl_3$ and different exposure times was assessed. Briefly, 1mm filter paper was soaked in 0.8%, 5% or 10% $FeCl_3$ and applied directly to HCAECs for either 30 seconds or 120 seconds. Following application of damage stimuli, HCAECs were washed, stained for 30 minutes using a LIVE/DEAD stain and imaged on a fluorescent microscope to measure cell viability (Figure 5.6A).

Cell viability reduced as the time of application increased (Figure 5.6C). Overall, the largest drops in viability were observed at the first time point (Figure 5.6C), following application of $FeCl_3$. Cell viability was significantly reduced following application of 10% $FeCl_3$ compared with 0.8% ($P<0.05$). Reduction in viability was not significant following application of any concentration of $FeCl_3$ compared with control, potentially due to the mechanical force of the filter paper removing cells, as observed in the control sample (Figure 5.6B). For samples treated with 0.8% $FeCl_3$, the reduction in cell viability appeared to slow between 30-120s, but this was not the case for samples treated with higher concentrations. In summary, the viability of HCAECs treated with $FeCl_3$ is reduced and is both time- and concentration-dependent.

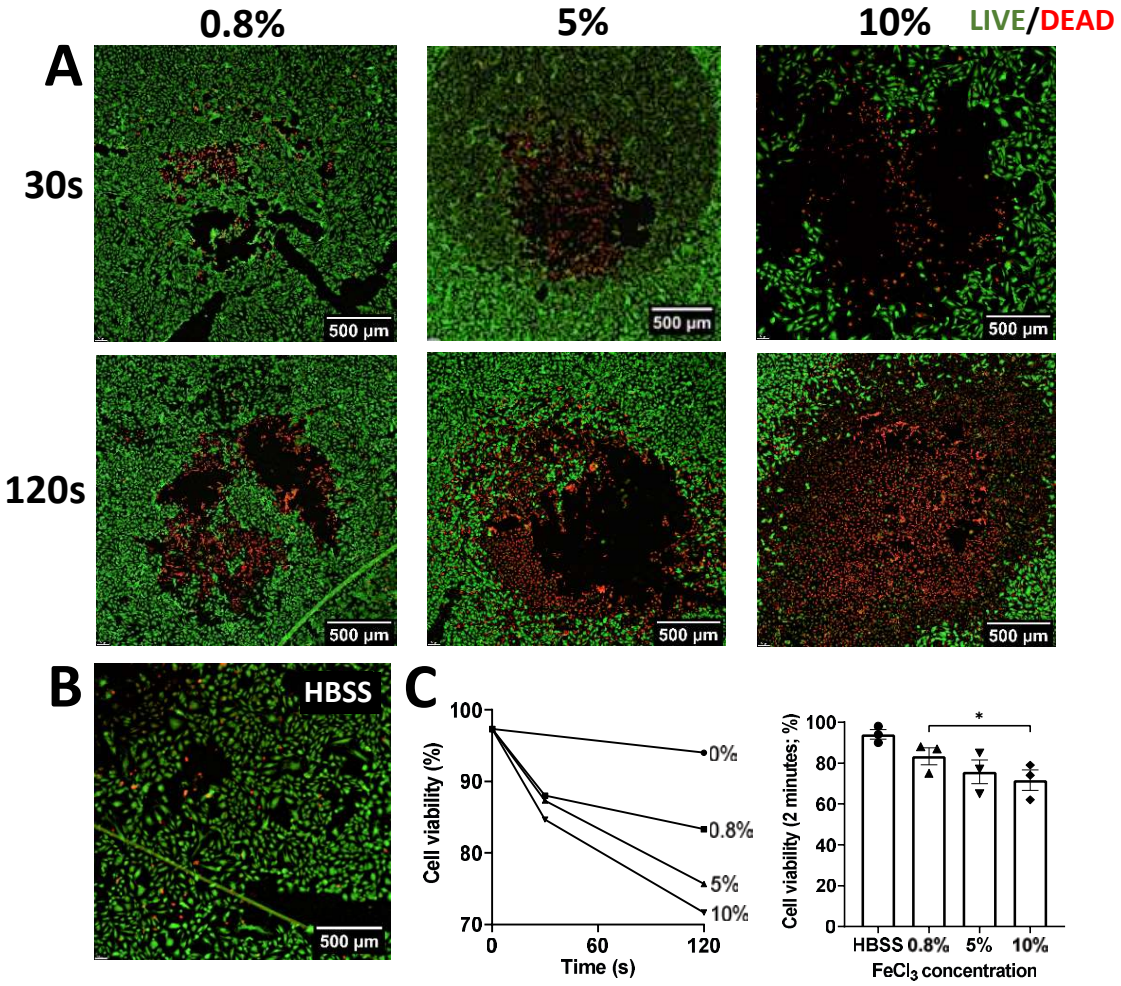

Figure 5.6 - LIVE/DEAD staining of HCAECs following damage with ferric chloride ($FeCl_3$). HCAECs were cultured in 24-well plates before application of filter paper soaked in Hank's balanced salt solution (HBSS) (B), 0.8%, 5% or 10% $FeCl_3$ for either 30 or 120 seconds (A). A LIVE/DEAD stain (Green/Red) was added and cells were imaged on a fluorescent microscope. Cell viability was assessed over time (C) and quantified using ImageJ and GraphPad Prism 9.3.1. A one-way ANOVA was used for statistical analysis. Error bars represent ± SEM. n=3. *P<0.05. Representative images shown.

5.2.7 The size of HCAEC focal damage induced by $FeCl_3$ is concentration- dependent

Using filter paper to damage HCAECs with $FeCl_3$ results in a focal area of damage, however a limitation of measuring cell viability is the removal of cells due to the mechanical force of applying the filter paper. Another measurement that may be used to determine the effect of damage stimuli on focal removal of HCAECs is the size of the decellularised lesion. As previously described in Section 5.2.6, filter paper soaked in $FeCl_3$ was applied to HCAECs for either 30 seconds or 120 seconds. HCAECs were washed, fixed, permeabilised and stained with phalloidin to visualise the presence or absence of actin/cells. Samples were imaged using a fluorescent microscope and the resulting area of focal damage measured using ImageJ.

The average area of the decellularised lesion was increased over time following application of the *in vivo* concentrations of 5% and 10%, but the highest variations were observed between 30s-120s in the lesion area of the HCAECs treated with 10% $FeCl_3$ (Figure 5.7C). The higher concentrations of $FeCl_3$ were also observed to diffuse to surrounding cells, detected by a reduction (but not absence) of phalloidin staining over a greater area over time, particularly after 2 minutes (120s) of treatment (Figure 5.7A). Indeed, after 2 minutes of treatment, the hole area was significantly increased following application of both 5% and 10% $FeCl_3$ (Figure 5.7C; $P<0.05$) compared to the HBSS control. The hole area following treatment with the lowest concentration of 0.8% $FeCl_3$, in contrast, was significantly smaller than the hole area following treatment with 5% $FeCl_3$ ($P<0.05$). Additionally, the hole area generated by the lowest concentration did not appear to change over time (Figure 5.7C).

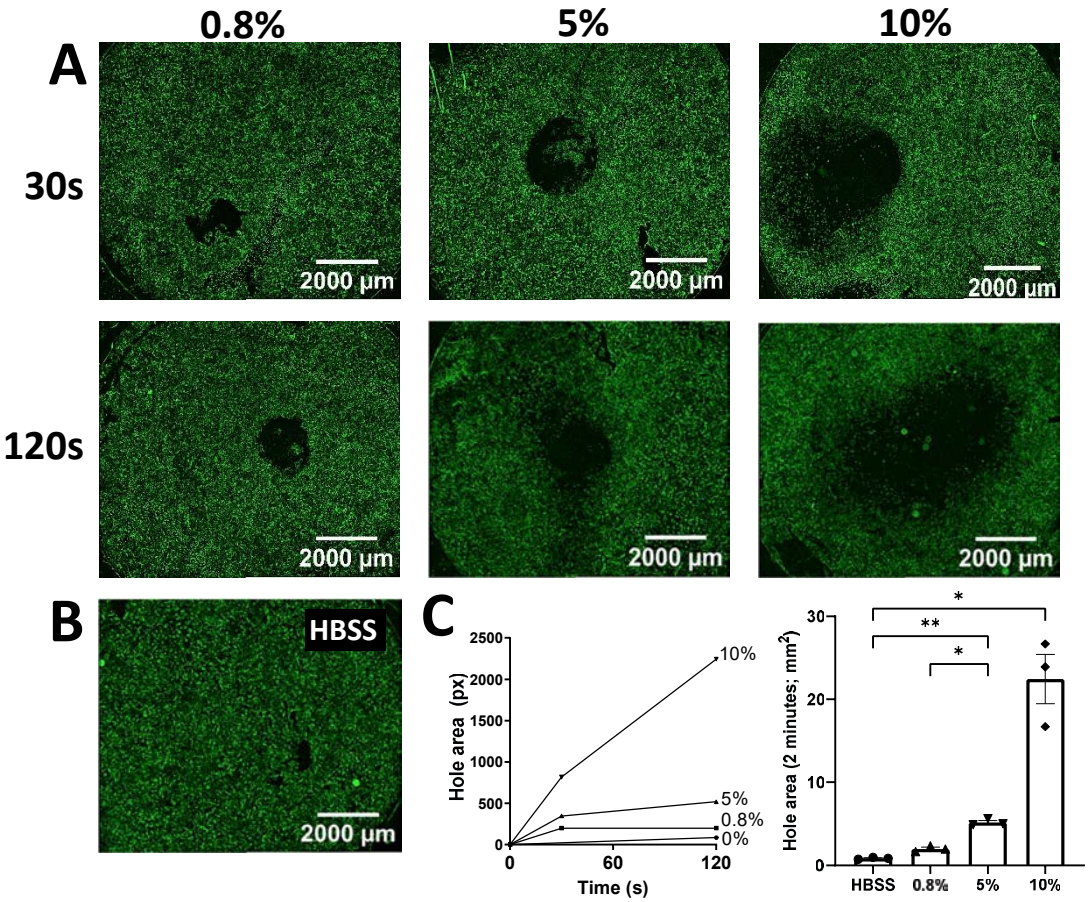

Figure 5.7 – Measurement of hole area following focal damage of HCAECs with ferric chloride ($FeCl_3$). HCAECs were cultured in 24-well plates before application of filter paper soaked in Hank's balanced salt solution (HBSS) (B), 0.8%, 5% or 10% $FeCl_3$ for either 30 or 120 seconds (A). Cells were fixed, stained with Phalloidin and imaged on a fluorescent microscope. Cell viability was assessed over time (C) and quantified using ImageJ and GraphPad Prism 9.3.1. A one-way ANOVA was used for statistical analysis. Error bars represent ± SEM. n=3. *P<0.05; **P<0.01. Representative images shown.

5.2.8 Focal damage of HCAECs with ECM isolation buffer reduces cell viability and increases hole area, but needle injury does not

To further explore alternative mechanisms to initiate focal damage in our *in vitro* flow model, 18G and 25G needles were also used to focally damage endothelial cells directly, to replicate *in vivo* protocols (as described in Section 1.6.1.4). Additionally, to model plaque erosion and endothelial denudation, the ECM isolation buffer used to remove cells leaving an intact ECM (0.5% (v/v) Triton X-100, 20mM NH4OH) was applied to induce focal damage, as a novel *in vitro* protocol. Following application of damage stimuli, the resulting area of focal damage was assessed using a LIVE/DEAD stain to determine cell viability, or cells were fixed in 4% PFA and stained with Phalloidin to measure the damaged lesion. The HBSS- and ECM isolation buffer-soaked filter papers were applied for 2 minutes in this experiment.

Application of ECM isolation buffer-soaked filter paper resulted in a significant increase in hole area (Figure 5.8B; $P<0.0001$) and reduction in cell viability (Figure 5.8C; $P<0.05$) compared to the HBSS control. Focal damage caused by needle injury generated a small focal area of damage in both samples (Figure 5.8A), with no significant reduction in cell viability, potentially due to direct removal of cells in the mechanism of application. Indeed, the hole area generated by the 25G needle was significantly smaller than the hole area generated by application of HBSS-soaked filter paper (Figure 5.8B; $P<0.05$).

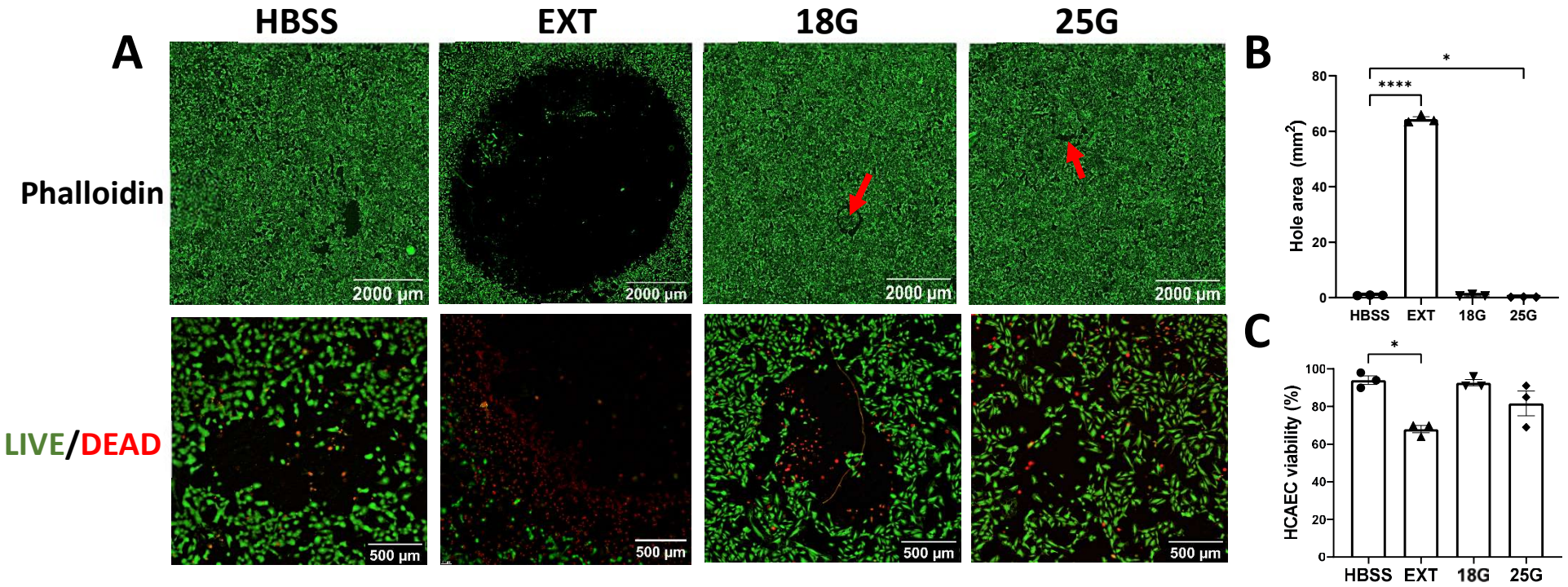

Figure 5.8 – LIVE/DEAD staining of HCAECs and measurement of hole area following focal damage of HCAECs with ECM isolation buffer (EXT) and needles. HCAECs were cultured in 24-well plates before application of filter paper soaked in ECM isolation buffer (0.5% (v/v) Triton X-100, 20mM NH4OH) or direct application of blunt 18 and 25G needles. Cells were either stained with a LIVE/DEAD stain or fixed and stained with Phalloidin before being imaged on a fluorescent microscope (A). Hole area (B) and cell viability (C) were assessed and quantified using ImageJ and GraphPad Prism 9.3.1. A one-way ANOVA was used for statistical analysis. Error bars represent ± SEM. n=3. *P<0.05; **P<0.01; ***P<0.001; ****P<0.0001. Representative images shown.

5.2.9 HCAEC generation of tissue factor following application of $FeCl_3$ is concentration- and not time-dependent

Measuring thrombus formation is useful tool to assess platelet responses to a focal area of damage and would enable some comparisons with *in vivo* protocols. However, there is evidence to demonstrate that occlusive thrombus formation following $FeCl_3$ application is driven by TF release from disrupted endothelial cells (Eckly *et al.,* 2011), and it is therefore important to assess the pro-coagulant potential of HCAECs following application of $FeCl_3$, to inform the importance of incorporating coagulation when measuring thrombus formation under flow. HCAEC generation of TF, an initiator of the coagulation cascade, was measured following application of $FeCl_3$. 1mm filter paper was soaked in 0.8%, 5% or 10% $FeCl_3$ and applied to HCAECs for either 30 or 120 seconds. Cells were washed with DPBS, fixed in 4% PFA and stained with DAPI, Phalloidin and an antibody against human TF before being imaged on a confocal microscope.

TF generation appears to increase with increasing concentrations of $FeCl_3$, but this is not significant between time points (Figure 5.9A). Additionally, the amount of actin appears to reduce between time points in the higher concentrations of $FeCl_3$, but this is not significant in the experiment, potentially due to the variability between samples. After 2 minutes (120 seconds), TF generation was increased in all $FeCl_3$-treated samples compared to the HBSS control (Figure 5.9D), but this was significant only in 5% and 10%-treated samples ($P<0.05$). Additionally, TF generation was significantly increased in samples treated with 10% $FeCl_3$ compared to treatments with 0.8% $FeCl_3$ ($P<0.05$), demonstrating a concentration-dependent response. The amount of cell actin was also significantly reduced in the 5% and 10% $FeCl_3$-treated samples after 120 seconds of treatment (Figure 5.9E; $P<0.05$), potentially due to a reduction in cell membrane integrity.

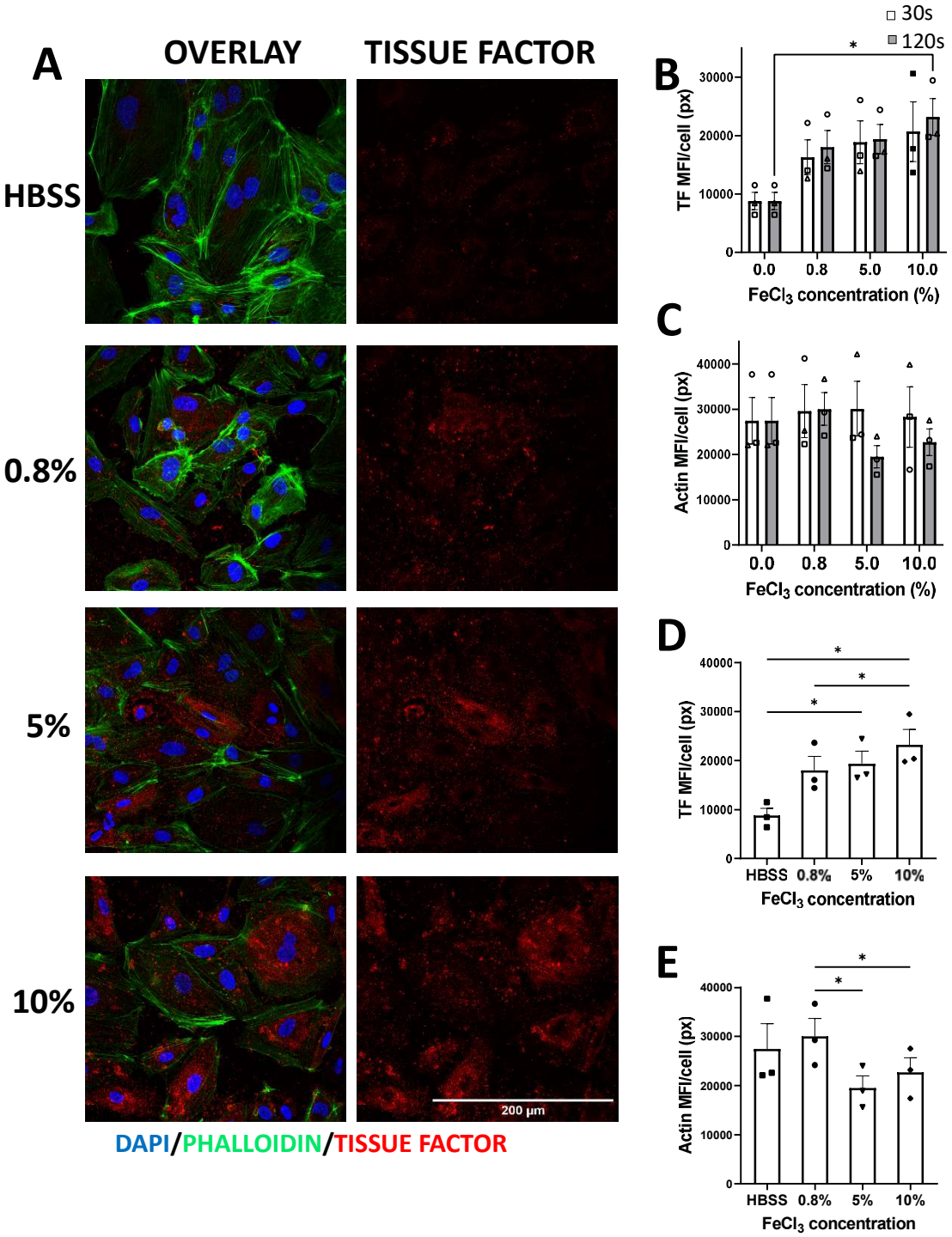

Figure 5.9 - Tissue factor (TF) and Actin staining of HCAECs following focal damage of HCAECs with ferric chloride ($FeCl_3$). HCAECs were cultured in 24-well plates before application of filter paper soaked in Hank's balanced salt solution (HBSS), 0.8%, 5% or 10% $FeCl_3$ for either 30 or 120 seconds. Cells were fixed and stained with DAPI, Phalloidin and antibody against human TF before being imaged on a confocal microscope (A). TF and Actin MFI was measured over time (B; C) and at 120 seconds (D; E) using ImageJ and GraphPad Prism 9.3.1. One-way and two-way ANOVAs were used for statistical analysis. Error bars represent ± SEM. n=3. *P<0.05. Representative images shown.

5.2.10 TF generation in HCAECs is significantly increased following application of ECM isolation buffer, but not 18G and 25G needles

In addition to $FeCl_3$ protocols, the translation of other adapted methodologies must also consider the role of coagulation. Developed methodologies include focal damage with ECM isolation buffer and 18G and 25G needles. HCAECs were cultured in 24-well plates before application of filter paper soaked in HBSS or ECM isolation buffer (EXT; 0.5% (v/v) Triton X-100, 20mM NH4OH) for 2 minutes, or direct application of blunt 18 and 25G needles. Cells were fixed and stained with DAPI, Phalloidin and antibody against human TF before being imaged on a confocal microscope.

Overall, there were no significant differences in TF generation or actin in samples focally damaged with needles (Figure 5.10). Focal damage with ECM isolation buffer resulted in a significant increase in TF generation (Figure 5.10B; $P<0.01$), however the cells surrounding the focal area of damage were not in a confluent monolayer, and cells may therefore have been apoptotic, or the significant ratio may have been an artefact due to a loss of cells (Figure 5.10A). There was a reduction in actin, albeit not significant, which may have been due to the variability between samples.

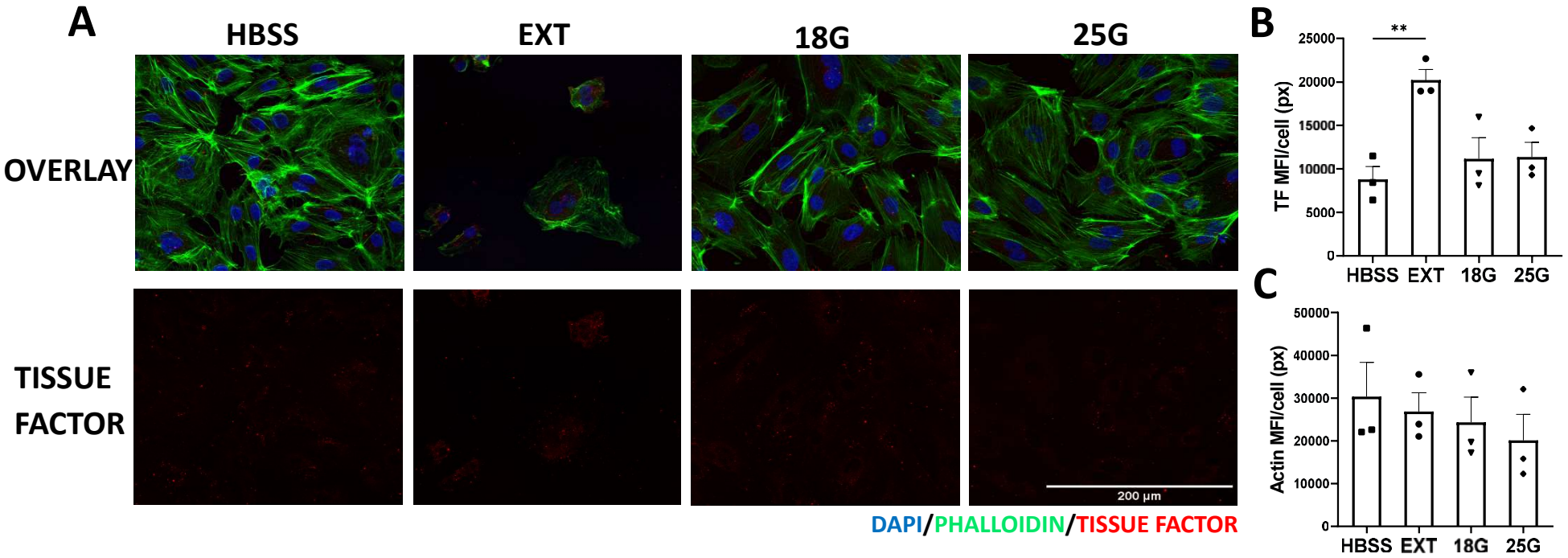

Figure 5.10 - Tissue factor (TF) and Actin staining of HCAECs following focal damage of HCAECs with needles (18G, 25G) and ECM isolation buffer. HCAECs were cultured in 24-well plates before application of filter paper soaked in HBSS or ECM isolation buffer (EXT; 0.5% (v/v) Triton X-100, 20mM NH4OH) for 2 minutes, or direct application of blunt 18 and 25G needles. Cells were fixed and stained with DAPI, Phalloidin and antibody against human TF before being imaged on a confocal microscope (A). TF (B) and Actin (C) MFI was measured using ImageJ and GraphPad Prism 9.3.1. A one-way ANOVA was used for statistical analysis. Error bars represent ± SEM. n=3. *P<0.05; **P<0.01. Representative images shown.

5.2.11 Focal damage may be incorporated into an *in vitro* thrombosis model using ibidi 0.1 sticky slides

Currently, to our knowledge, there are no *in vitro* models of atherothrombosis with the ability to focally damage cells and assess the resulting thrombus formation. Incorporating focal damage in a thrombosis model will enable the contribution of adjacent endothelial cells to thrombosis to then be assessed. The ibidi 0.1 sticky slide is an open, adhesive chamber which attaches to a coverslip to allow perfusion of liquid over the coverslip (Figure 5.11). This slide was piloted to investigate whether focal damage of cells on coverslips could be incorporated into the model under an arterial shear rate. HCAECs were cultured on coverslips before application of filter paper soaked in 0.8% $FeCl_3$ for 2 minutes. Cells were washed with DPBS and coverslips were attached to ibidi sticky slide chambers, before perfusion of DIOC-6 labelled blood through chambers at an arterial shear rate. Imaging was performed using a fluorescent microscope.

HCAECs were successfully cultured and focally damaged on coverslips, demonstrated in brightfield imaging performed following removal of filter paper (Figure 5.12B). Perfusion of citrated blood over coverslips at an arterial shear rate resulted in non-occlusive thrombus formation within the focally damaged area (Figure 5.12C), demonstrating increased platelet activity upon HCAEC damage with filter paper soaked in 0.8% $FeCl_3$.

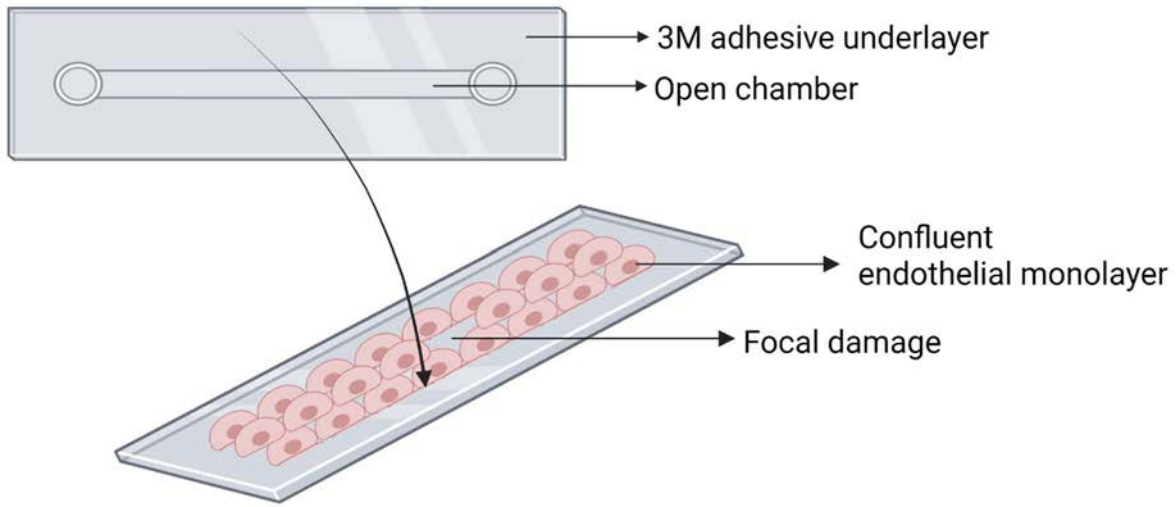

Figure 5.11 – Microfluidic design of the thrombosis model using ibidi 0.1 sticky slides. A representative design of the capabilities of the thrombosis model to focally damage HCAECs. HCAECs are cultured on coverslips and focally damaged using either filter paper soaked in $FeCl_3$, or mechanically using an 18G or 25G needle. Open chambers are then assembled by placing the 3M adhesive side directly on coverslips and pressing firmly to seal, before perfusion with DIOC-6 labelled whole blood. Created with BioRender.com

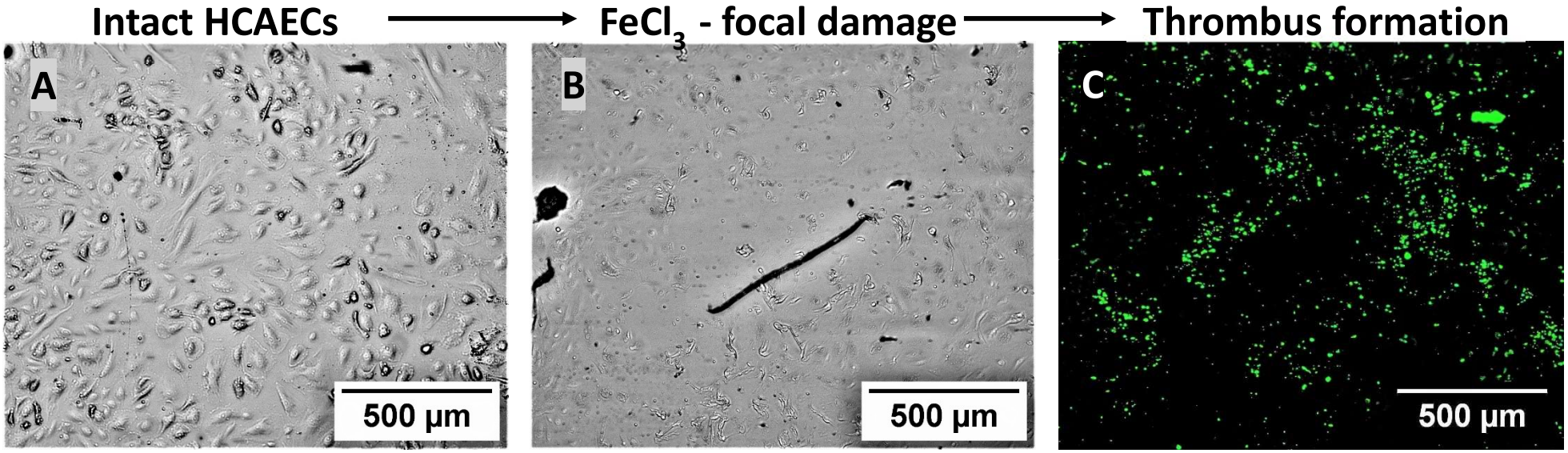

Figure 5.12 – Thrombus formation on HCAECs focally damaged with $FeCl_3$. HCAECs cultured on coverslips (A) were damaged with 0.8% $FeCl_3$ for 2 minutes (B). Coverslips were attached to ibidi sticky slides and DIOC-6 labelled blood was perfused through chambers over coverslips at an arterial shear rate. Imaging was performed at each stage using a fluorescent microscope. n=1. Representative images shown.

5.2.12 Thrombus formation can be measured following focal damage of HCAECs using different methodologies

Following successful incorporation of focal damage in the model, it was then important to assess the ability of the model to incorporate different methodologies of focal damage and assess thrombus formation in response. This would then enable researchers to inflict mechanical damage to cells, bridging the gap between current *in vivo* and *in vitro* methodologies and enabling a more accurate representation of plaque rupture and erosion in atherothrombosis. To investigate this concept further, HCAECs were cultured on coverslips before application of filter paper soaked in 0.8% $FeCl_3$ or ECM isolation buffer (0.5% (v/v) Triton X-100, 20mM NH4OH), or mechanical damage using an 18G needle. Coverslips were washed with DPBS before assembly of ibidi 0.1 sticky slides and perfusion of DIOC-6 labelled blood through chambers at an arterial shear rate over HCAECs and the area of focal damage. Imaging was then performed on a fluorescent microscope.

Results indicated some variability in thrombus formation between methodologies, demonstrating the sensitivity of the model to variations in focal damage. Generally, more platelets adhered to the focal damage following cell removal with the ECM isolation buffer and the 18G needle than the area focally damaged using $FeCl_3$ (Figure 5.13). Thrombus formation in comparison was generally reduced in this sample, although the sample size was too small to perform statistics (n=2).

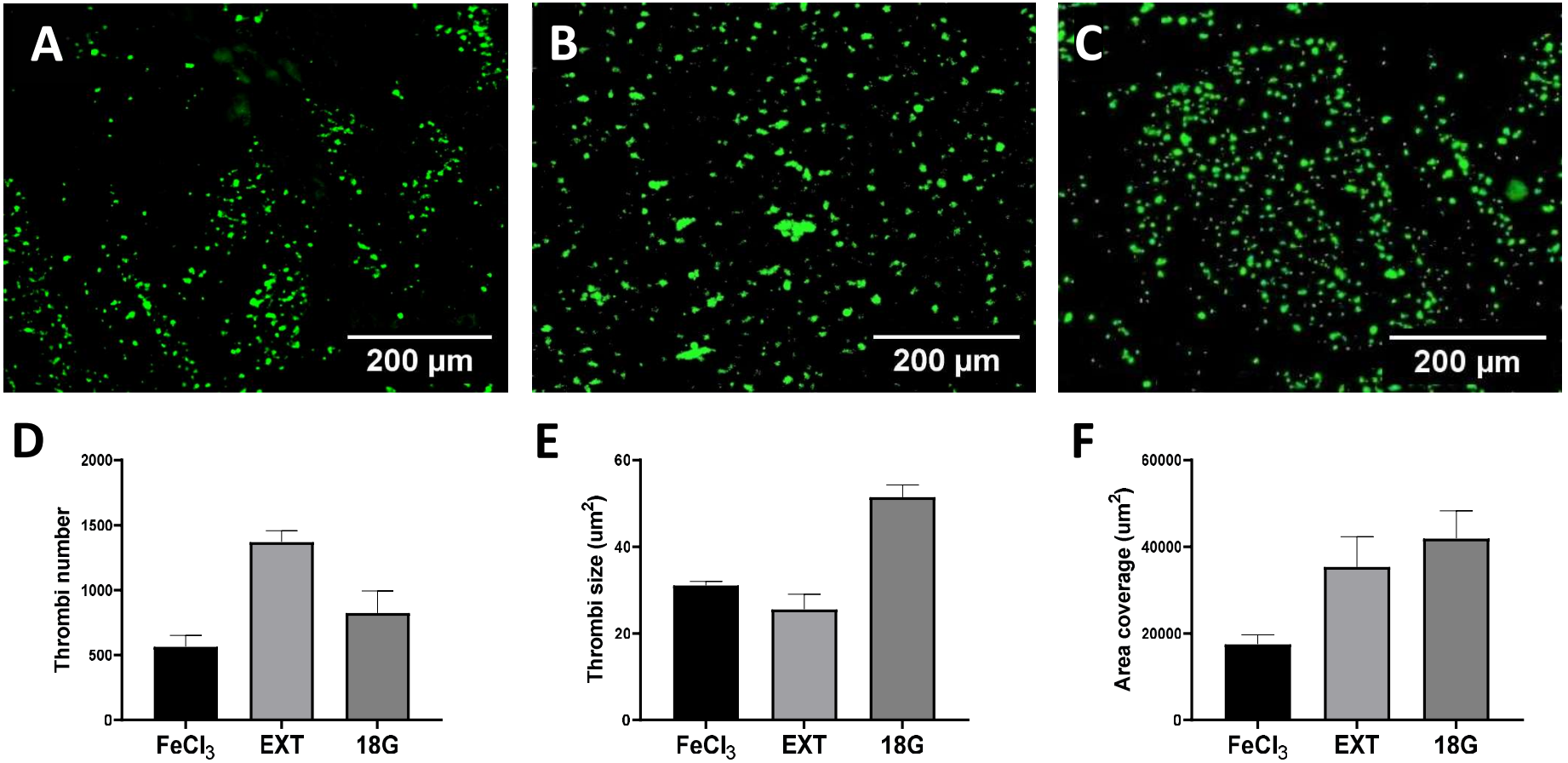

Figure 5.13 – Thrombus formation on HCAECs focally damaged using different methodologies. HCAECs cultured on coverslips were damaged with 0.8% $FeCl_3$ (A), ECM isolation buffer (B) and an 18G needle (C). Coverslips were attached to ibidi sticky slides and DIOC-6 labelled blood was perfused over HCAECs and through chambers at an arterial shear rate. Imaging was performed using a fluorescent microscope and thrombi number (D), size (E) and area coverage (F) quantified using ImageJ and GraphPad Prism 9.3.1. Error bars represent ± SEM. n=2. Representative images shown.

5.2.13 Recalcifying whole blood results in non-occlusive thrombus formation at the area of $FeCl_3$-induced focal damage

Measuring platelet thrombus formation is a useful tool to investigate platelet signalling pathways and test novel antiplatelet approaches. The presence of endothelial cells allows further interrogation into the endothelial regulation of these processes and the contribution of endothelial dysfunction. All experiments thus far in this study have been performed using citrated blood focusing specifically on platelet driven thrombus formation. However, platelet thrombus formation does not occur in isolation *in vivo* and the coagulation pathway, which is calcium dependent, significantly contributes to arterial thrombosis. It is therefore important to take steps to incorporate coagulation in the model, to improve versatility and functionality. Additionally, as described in Section 5.1.3, the propagation of occlusive thrombus formation following $FeCl_3$ damage is thought to be dependent on TF expression and coagulation rather than platelet-ECM interactions. Therefore, to be able to compare *in vitro* methodologies to *in vivo* models, and investigate thrombosis as a whole, recalcification of blood must also take place. Recalcification of blood in *in vitro* models can be notoriously challenging due to spontaneous clotting within the tubing. The presence of endothelial cells within our model could potentially alleviate this issue, due to the natural anticoagulants expressed by this cell type (described in Section 1.2). To determine whether we could recalcify blood in our system and achieve thrombi localised to the $FeCl_3$ induced lesion, without spontaneous clotting within the tubing, HCAECs cultured on coverslips were exposed to 0.8% FeCl3 soaked filter paper for 2 minutes. Coverslips were then washed and assembled with ibidi 0.1 sticky slides prior to perfusion of DIOC-6 labelled blood through chambers at an arterial shear rate. Blood was recalcified immediately before perfusion by addition of 10mM calcium chloride, aligning with protocols used by Brouns *et al.* (2020), Berry *et al.* (2021) and Ciciliano *et al.* (2015). Imaging was then performed on a fluorescent microscope.

Thrombus formation images taken on a fluorescent microscope revealed large thrombi at the area of focal damage (Figure 5.14A). Brightfield images demonstrated inclusion of RBCs in thrombi (Figure 5.14B). It was observed that thrombi formed did not occlude the chamber and flow was continuous throughout the run.

A

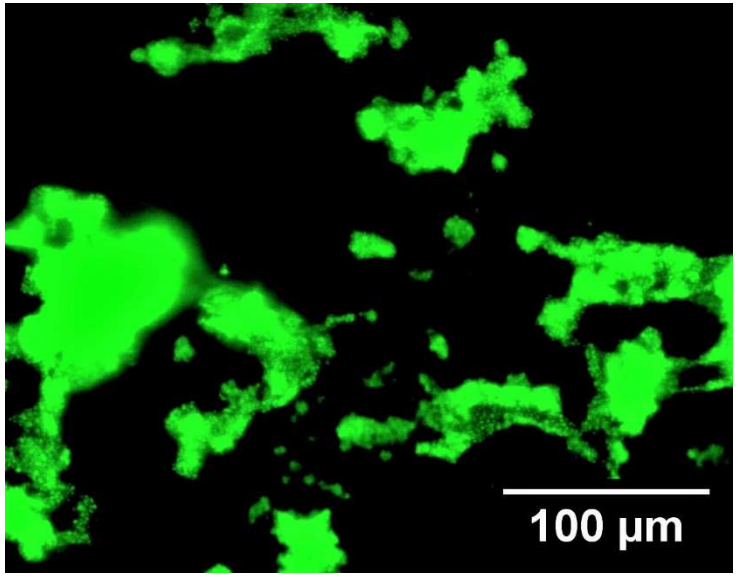

B

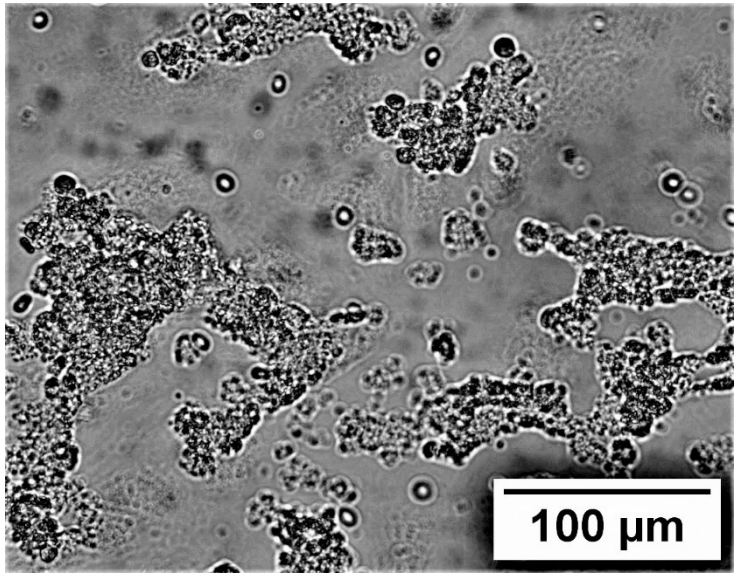

C

Thrombi number	Thrombi size (um^2)	Area coverage (um^2)
222	28686.18	129.217
398	48076.47	120.8

Figure 5.14 – Thrombus formation from recalcified blood on an area of $FeCl_3$-induced focal damage in an endothelialised model of atherothrombosis. HCAECs cultured on coverslips were damaged with 0.8% $FeCl_3$ and washed with DPBS before assembly of coverslips on ibidi 0.1 sticky slides. Recalcified DIOC-6 labelled blood was perfused through chambers at an arterial shear rate and imaging was performed (A;B) on a fluorescent microscope. Thrombi number, size and area coverage were quantified (C) on ImageJ. n=2. Representative images shown.

5.3 Discussion

5.3.1 The thrombotic and haemostatic potential of HCAECs is significantly different to HUVECs

In order to create a representative *in vitro* model of human arterial thrombosis, which has the potential to replace animal experiments if adopted by other researchers, the choice of endothelial cell used is important. It should be relevant to the disease to ensure a valid model, whilst also being readily available and cost effective. HUVECs are most commonly used in models of arterial thrombosis (Shao *et al.,* 2009; Wang *et al.,* 2015; Costa *et al.,* 2017; Hao *et al.,* 2019), as cost-effective alternatives to HCAECs, however ECs have been shown to be heterogeneous in their behaviour, depending on the vascular bed they originate from (Yau *et al.,* 2015; Mathur *et al.,* 2021; Gifre-Renom *et al.,* 2022). The most relevant blood vessels in human arterial thrombosis are the coronary arteries, however HCAECs are roughly four times more expensive than HUVECs to purchase (Promocell, 2023). It was therefore important to compare the antithrombotic capacity of HCAECs and HUVECs, to inform the optimum EC type to use in the model. Key endothelial proteins involved in the regulation of platelet function include eNOS, COX-2, vWF, CD39 and TBXAS1. These markers were quantified in resting HCAECs and HUVECs, and under damage conditions with disease-relevant CSE and TNF-α for 24 hours, using qPCR.

Quantification of resting gene levels demonstrated key differences in gene expression. eNOS levels were significantly higher in HCAECs than in HUVECs, supporting findings from Yang *et al.* (1991) and Fukaya and Ohhashi (1996), who reported higher eNOS and NO levels in arterial cells compared with venous cells, in both humans and canines. The increase in eNOS may be attributed to an increased requirement to maintain platelet quiescence under higher shear rates in arteries, as platelets can be activated at high shear rates (Holme et al., 1997). COX-2 expression was also significantly higher in HCAECs than in HUVECs, potentially due to the differing effect of COX-2 in arteries and the venous system. COX-2 has been shown to have atheroprotective effects in arterial vessels, with the use of COX-2 inhibitors (NSAIDs) associated with adverse cardiovascular events and promotion of a pro-thrombotic phenotype (Kirkby *et al.,* 2014), whereas in the venous system, the release of endogenous prostanoids is

associated with a reduction in the protective effects of NO (Yang et al., 1991). Indeed, TBXAS1 expression is also significantly higher in HCAECs, which correlates with the formation of platelet-rich thrombi in arterial vessels. CD39 expression, in contrast, is significantly higher in HUVECs than in HCAECs, which may be due to the role of the molecule in venous thrombosis, where it has been shown to inhibit venous thrombosis by suppressing inflammatory-procoagulant crosstalk (Yadav *et al.,* 2019). Additionally, blood flow in veins is much lower than in arteries (Klarhofer et al., 2001; Roux et al., 2020), enabling CD39 to be in contact with blood components for longer, potentially increasing the effectiveness of ADP hydrolysis. vWF expression is also significantly higher in HUVECs than HCAECs, supported by findings from Yamamoto *et al.* (1998) and Geenen *et al.* (2012) who demonstrated similar effects in the porcine and murine vasculatures. Indeed, vWF has a role in coagulation and thrombus stability, both important factors in venous thrombosis, acting as a carrier for FVIII and enhancing fibrin crosslinking in coagulation (Yau *et al.,* 2015).

The responses of HUVECs and HCAECs to damage stimuli were remarkably similar, with the only significant difference in response the magnitude of upregulation of TBXAS1 by HUVECs in response to CSE+TNF-α. HUVEC upregulation of TBXAS1 was around 2-fold higher than HCAEC upregulation, however as resting TBXAS1 levels are 2-fold higher in HCAECs, this observation is unlikely to be significant overall. Expression of COX-2, eNOS, CD39, vWF and TBXAS1 were up- and down-regulated in a similar fashion, demonstrating similarities in response to damage stimuli by both EC types. However, as resting levels of these genes are significantly different, platelet response is also likely to be different. eNOS levels, for example, are downregulated in response to TNF-a in both cell types by a similar magnitude. However, as resting eNOS levels are almost 2-fold higher in HCAECs than HUVECs, NO synthesis is still likely to be higher, demonstrating a more atheroprotective phenotype. Additionally, CD39 levels, which are downregulated by a similar magnitude in response to TNF-a in both cell types, are inherently higher in HUVECs and therefore ADP hydrolytic activity is likely to be higher in an *in vitro* thrombosis model.

The 24 hour time point for TNF-α damage, although relevant to represent 'chronic' inflammation, may not be as relevant to measure resting gene levels as a measure of the thrombotic potential of each cell type. Although endothelial cells have been shown to demonstrate a sustained response to TNF-α in the expression of inflammatory

mediators such as VCAM-1 (Lin *et al.,* 2015), it has also been demonstrated in human fibroblasts that the expression of mediators such as COX-2 peak after 4 hours of TNF-α damage, and then start to reduce (Yang *et al.,* 2021), potentially in a compensatory mechanism. A future step to validate resting gene levels could therefore be to incorporate a lower incubation time, such as 4 hours, to measure gene expression of these mediators.

Variations in resting gene level and similarities in response to damage stimuli, when taken together, demonstrate the requirement to use HCAECs to model arterial thrombosis, and HUVECs to model venous thrombosis. It is worth considering, however, that the gene expression levels profiled were platelet regulators, there may also be differences (and similarities) in the expression profiles of regulators of coagulation and fibrinolysis. Further investigation is therefore needed to elucidate the role of HUVECs and HCAECs in coagulation and fibrinolysis.

5.3.2 *In vivo* protocols can be adapted to focally damage ECs

Generally, the primary initiators of atherothrombosis are collagen/ECM driven or ECM and TF driven, representing plaque erosion and rupture respectively. Current *in vivo* models reflect these processes, utilising different damage protocols to simulate arterial thrombosis. It is therefore important to have an *in vitro* thrombosis model able to compare protocols and thrombus formation with *in vivo* models. To create a comparable model, a novel protocol was developed to focally damage ECs, evolving model development to enable investigations involving $FeCl_3$ damage, comparable with murine $FeCl_3$ thrombosis models, and mechanical 'rupture' of a plaque *in vitro*.

The use of a smaller hole punch to produce smaller 1mm diameter filter paper enabled microscopical visualisation of focal damage with intact surrounding cells, with potential to downscale the model, increasing versatility. Focal damage with $FeCl_3$ resulted in removal/lysis of some cells, which may be due to the mechanical force of applying the filter paper, as complete cell removal was not consistent across samples. However, using lower concentrations and in control (HBSS) samples, less cells were removed in focal regions, suggesting the $FeCl_3$ was having this effect, to some extent. The inconsistency in the force used to apply the filter paper to cells and remove it is a limitation in this

experiment, and following further development, efforts should be made to make this process more replicable, potentially via automation. Reductions in cell viability and increases in hole area in response to $FeCl_3$, however, were observed in a concentration-dependent manner. Hole area increased over time in the higher concentrations of $FeCl_3$ but not in the *in vitro* equivalent concentration of 0.8%, where hole area remained relatively stable. Diffusion of $FeCl_3$ is limited at this concentration, and therefore experimental replicability at this concentration is increased. As the mechanical force of applying and removing filter paper has been shown to remove cells, it is not possible to compare these results with previously published findings from Ciciliano *et al.* (2015). In this study, 0.8% $FeCl_3$ was infused into an *in vitro* thrombosis model, with no focal damage, resulting in the formation of an occlusive aggregate with no removal of ECs. A later comparison to this study may be performed following further protocol optimisation. TF generation, however, is increased in all samples in response to $FeCl_3$, and is significant at the 5% and 10% concentrations only, indicating a concentration-dependent response. These results imply a role for coagulation in $FeCl_3$-mediated thrombosis, supporting findings from Barr *et al.* (2013) who state that the process is led by RBCs and from Ciciliano *et al.* (2015) who recovered an erythrocyte-rich thrombus following $FeCl_3$ infusion *in vitro.* The filter paper protocol was also used to investigate cell removal using an ECM isolation buffer, leaving the underlying ECM intact. The ECM isolation buffer used caused widespread cell lysis and death in a focal area, however the buffer diffused into the surrounding area, increasing hole size significantly and making downscaling of this condition more challenging. Additionally, the underlying ECM may not be intact in these samples as it was demonstrated to be in Chapter Four, as the same limitations in applying/removing the filter paper exist and may have resulted in damage of the underlying ECM. This protocol was also adapted to induce focal damage with blunt needles. 18G and 25G needles were applied to cells directly (no filter paper) and cell viability and hole area measured. The hole area generated by the 25G needle was significantly smaller than the hole generated by applying/removing filter paper, increasing downscaling potential. Additionally, the application of the needle is standardised, using one size, and therefore replicable. However, the depth of application is not standardised, therefore this protocol would also benefit from automated application of damage stimuli. Furthermore, the needle had a hole in the middle, leaving intact cells in the middle of the focal area of damage. This hole should

be filled going forward to enable complete damage of the focal area. Interestingly, TF generation was not enhanced in ECs surrounding the focal area of damage following mechanical damage with needles. This may be due to timing, as cells were fixed in 4% PFA soon after damage, but also may offer a potential model of plaque erosion, where the ECM is exposed but TF exposure is not triggered. Further protocol optimisation may incorporate variations in timing, to investigate this further.

5.3.3 Incorporating focal damage and recalcified blood into the thrombosis model using ibidi 0.1 sticky slides

To incorporate focal damage into the model, an accessible chamber was required, to be able to mechanically damage cells, as in *in vivo* thrombosis models. The ibidi sticky slides have an adhesive open chamber, designed to attach to full length (22x64mm) coverslips which do not need to be completely dry. Indeed, Aldrich and Long (2019) used the ibidi perfusion system to perfuse medium through chambers of ibidi sticky slides containing endothelial-coated coverslips, demonstrating the compatibility of this cell type in the slides under flow conditions. HCAECs were cultured on coverslips, focally damaged and attached to the adhesive open chambers before perfusion of blood. Thrombi formed within the focally damaged area, and in some cases, on the damaged cells around the focal area (Figure 5.12C). Indeed, platelets have been shown to adhere to a damaged endothelium (Coenen *et al.*, 2017), potentially due to alteration in endothelial expression of key mediators of thrombosis and haemostasis (Pearson, 1999; Kaur *et al.,* 2018). Varying the focal damage technique resulted in variations in thrombus formation, with more platelets observed to adhere to the area of focal damage following cell removal with the ECM isolation buffer and the 18G needle. This may be in part due to the exposure of an intact underlying ECM, as it was demonstrated in the previous Chapter that the use of the ECM isolation buffer results in the presence of an intact ECM structure. This may also be the case in the needle-damaged sample, or it may be that the surrounding damaged endothelial cells are exhibiting a pro-thrombotic phenotype (Pearson, 1999; Kaur *et al.,* 2018) and promoting thrombosis. However, results from experiments measuring pro-coagulant activity in needle-damaged samples did not reveal any significant increases in TF (Figure 5.10), and cell viability was not significantly reduced in these samples either (Figure 5.8), suggesting the underlying ECM may be

playing a part in thrombus formation on these samples. Thrombus formation on $FeCl_3$ damaged samples appeared less striking, which may be due in part to $FeCl_3$-induced thrombosis being largely coagulation dependent, rather than platelet driven. These findings are consistent with Eckly et al. (2011), who demonstrated that the structure of the underlying ECM is disrupted following application of $FeCl_3$. Indeed, following incorporation of recalcified blood in the model, thrombus formation and platelet activity were observed to increase, however coagulation as a process could not be verified to have taken place, and a future direction of the project should be to investigate this in more detail. Additionally, full chamber occlusion did not occur, which may have been due to increased fluid pressure from the growing thrombi leading to structural components dislodging (Berry *et al.,* 2021). This is a potential limitation of the model, as full occlusion cannot be measured. Introducing a branch-based system may potentially overcome this, maintaining fluid pressure and allowing complete occlusion, as demonstrated by Tsai *et al.* (2012). The design of this would also more accurately represent a blood vessel, but as yet, there is no commercial open chamber with a branching design to overcome this limitation. Additionally, the cost and complexity of the model should be balanced with need. The main output of this model is imaging and thrombus size, therefore full occlusion is not necessary, and would also use a much larger volume of blood. Overall, the protocol developed in our laboratory enables the focal damage of ECs and investigations of this effect on thrombus formation, but the methodologies detailed do require further optimisation to be a comparable tool bridging *in vitro* and *in vivo* methodologies in atherothrombosis.

5.3.4 Summary

In summary, the main findings in this Chapter were that HUVECs and HCAECs have different thrombotic capacity, and this should be considered when modelling arterial thrombosis in order to best represent the process observed *in vivo.* Additionally, *in vitro* protocols can be adapted from *in vivo* methodologies to focally damage ECs, enabling investigations into the resulting disruption of regulators of thrombosis. Furthermore, ibidi 0.1 sticky slides can be used to incorporate focal damage of ECs into an *in vitro* thrombosis model, enabling thrombus formation in the presence of healthy and dysfunctional ECs to be investigated.

6. General discussion

6.1 Introduction

ACS, resulting primarily from thrombosis occurring as a result of the rupture or erosion of an atherosclerotic plaque, has a mortality rate of over 9 million per year, a rise of 11% from 1990 (Vos *et al.,* 2020). Antiplatelet therapy is utilised in the management of ACS; however current treatment strategies are limited by high inter-individual variability, an increased bleeding risk and a residual risk of recurrent events/death within 12 months (Hamilos *et al.,* 2018; Olie *et al.,* 2018). As described in Section 1.4.2, the major culprits in ACS are plaques prone to rupture and plaques prone to erosion (Otsuka *et al.,* 2016), and both phenotypes are quite different in their presentation. Plaques prone to rupture, for example, have a much larger necrotic core, a thinner fibrous cap and cause much more occlusive 'red' thrombus formation compared with plaques prone to erosion (Figure 1.7). Despite these differences, current methods in the screening of antiplatelet drugs adopt a universal approach and do not distinguish between plaque type, with *in vitro* models measuring thrombus formation on Type I Horm collagen (Hosokawa *et al.,* 2012) and most *in vivo* models initiating focal vascular damage in young, healthy mice, devoid of vascular remodelling and endothelial dysfunction. *In vivo* studies which do use atherosclerotic mice frequently use apoE-/- or LDLR -/- genetically modified mice on high fat diets (Karel *et al.,* 2020). These models attempt to mimic plaques vulnerable to rupture, however they are morphologically different to human lesions and are incapable of spontaneous rupture. To date, there are no *in vivo* models available to mimic plaque erosion. Additionally, there is no comparability or standardisation between *in vivo* and *in vitro* models, introducing variability in results from different studies (Zhang *et al.,* 2017). As described in Section 1.6, additional limitations associated with both *in vivo* and *in vitro* models are the lack of an ECM associated with cardiovascular disease, the lack of human vascular ECs and blood, and the lack of a relevant shear stress in murine models (Panteleev *et al.,* 2021).

6.2 Project aim

The aim of this research was to incorporate a disease-relevant ECM, human ECs, human blood and a relevant arterial shear stress in a model of atherothrombosis, to investigate the regulation of thrombosis in cardiovascular disease, to enable both plaque types to be interrogated in more detail, and to bridge the gap between current *in vivo* and *in vitro* models. This thesis describes the development of this model, complete with HCAECs, human blood and a relevant arterial shear stress, and demonstrates sensitivity to treatment with mediators of endothelial dysfunction, chemical injury and mechanical injury.

6.3 Key findings

A key finding from Chapter Three was that PGs associated with plaque rupture or erosion can alter platelet responses to collagen. These results are supported by results from Chapter Four, demonstrating that Type I Horm collagen was significantly more thrombogenic than CDMs derived from HCAECs and HCASMCs, and by findings from Bonacina *et al.* (2016), who demonstrated the ability of an ECM component, pentraxin 3, to limit the pro-thrombotic potential of collagen. The findings in this Chapter have implications in findings from current *in vitro* models of atherothrombosis using Type I Horm collagen (Hosokawa *et al.,* 2012), as the presence of other ECM components can alter thrombus formation on collagen. The use of a multi-component ECM may therefore be more relevant in antiplatelet screening tests.

A key finding from Chapter Four was that HCAECs and HCASMC both produce distinct ECMs with different thrombotic properties. This finding is consistent with published literature describing the main components of each ECM (Figueroa *et al.,* 2003; Chuang *et al.,* 2014), however differences in components relevant in thrombosis and their effect on thrombus formation is a novel finding and has not previously been investigated. An additional finding from this Chapter was that insults associated with the development and progression of atherosclerotic plaques, including TNF-α and CSE (Boesten *et al.,* 2005; Dai *et al.,* 2018), alter ECM composition and thrombogenicity significantly. Ma *et*

al. (2020) describe alterations in ECM composition in response to disease, but there are no studies investigating alterations in the thrombogenicity of the ECM. Overall, the findings from Chapter Four have implications in the use of *in vivo* models using a healthy ECM to investigate atherothrombosis, as results from the Chapter demonstrate differences in the thrombotic potential of the ECM during endothelial and smooth muscle dysfunction.

Key findings from Chapter Five demonstrated differences in the thrombotic potential of HUVECs and HCAECs, with differences observed in resting gene level but not in response to damage stimuli. Lakota *et al.* (2010), in contrast, demonstrated similarities in the responses of HUVECs and HCAECs to inflammatory stimuli, but differences in the magnitude of change. The markers measured, however, were not markers relating to the regulation of thrombosis. The differences in resting gene expression of regulators of thrombosis indicate differences in the thrombotic potential of each EC type, especially considering similarities in their response to damage stimuli. These findings have implications in current *in vitro* models using HUVECs to model arterial thrombosis, as HUVECs may not be the optimum cell type to use for this purpose. Summarising Chapter Five was the incorporation of ECs and focal damage into the model. This section demonstrated successful incorporation of endothelial cells into the model under an arterial shear stress and introduced the concept of focal damage in an *in vitro* thrombosis model. The model developed in this project incorporates a relevant arterial shear stress and human blood, as in current *in vitro* models (Neeves *et al.,* 2008), and also includes cells and an ECM, similar to in vivo models (Mackman, 2006). However, the final model also has a novel ability to generate dysfunctional ECMs which can be used to investigate platelet responses, and incorporates human endothelial cells, which can be focally damaged prior to perfusion of blood. Investigations using this model may help to make current *in vivo* and *in vitro* models more comparable, improving the screening of antiplatelet drugs, but may also help to elucidate inter-individual variability in antiplatelet therapy, providing a more personalised tool in the ability to induce chronic/acute cardiovascular damage stimuli on ECs and explore changes in ECM composition and platelet activity.

6.4 The use of recombinant matrices in a thrombosis model

In Chapter Three, a simplistic approach was undertaken to model the ECM *in vitro*, adding together collagens and vascular PGs implicated in the development and progression of atherosclerosis in plaque rupture and erosion (Kolodgie *et al.,* 2002). Chapter Three concluded that platelet activity and thrombus formation on Types I and III collagen was significantly different than on vascular PGs, with platelet adhesion, thrombus formation and activation marker expression all varying significantly across the PGs compared to collagens (Figure 3.3, Figure 3.5 and Figure 3.8). Based on findings by Bonacina *et al.* (2016) demonstrating the regulation of thrombus formation on collagen by pentraxin 3, a regulatory role is suggested for less thrombogenic PGs, with the presence of some PGs such as versican appearing to have an inhibitory effect on platelet activity (Figure 3.5) and others, when combined, significantly altering platelet activity on collagens and other PGs. Indeed, Figure 3.8 demonstrates key differences in thrombus formation on recombinant 'rupture' (Type I collagen, biglycan and decorin) and 'erosion' (Type III collagen, versican and hyaluronan) matrices. 'Erosion' matrices were significantly less thrombogenic than Type I collagen, which may be elucidated in a number of ways. Firstly, there were no differences observed in thrombus formation between Type I and III collagen under an arterial shear rate (Figure 3.7), therefore any differences observed between Type I collagen and 'erosion' matrices are unlikely to be as a result of differences in thrombus formation between collagens. However, Jooss *et al.* (2019) found Type I collagen to be significantly more thrombogenic than Type III collagen, so it is possible that donor variability or differences in recombinant protein synthesis (Fertala, 2020) may contribute to observed differences in thrombus formation. A reduction in thrombus formation on synthetic 'erosion' matrices compared with Type I collagen is also unlikely to be due to the presence of hyaluronan or versican, as Figure 3.10 demonstrates that adding hyaluronan or versican to Type III collagen does not alter thrombus formation. It is therefore likely that the interaction of Type III collagen, versican and hyaluronan together is responsible for the reduction in thrombus formation, potentially due to the regulation of thrombus formation on collagen by specific ECM components (Bonacina *et al.,* 2016). Indeed, there were no observed differences in thrombus formation on recombinant 'rupture' matrices compared with Type I collagen, despite the presence of biglycan or decorin individually reducing area

coverage of thrombi on Type I collagen (Figure 3.9). Overall, these findings suggest that specific ECM components interact to regulate thrombus formation, and that the presence of multiple ECM components can alter this regulation.

Whilst simplified, using recombinant proteins has been useful to identify variations in platelet responses to individual ECM components, and to investigate their regulation of platelet activity in combination with collagen. However, the vascular ECM is composed of multiple collagens, laminins, PGs, growth factors and cytokines (Theocharis *et al.,* 2016), all of which may alter platelet activity and thrombus formation, and this may have clinical implications for ACS patients. Indeed, results from experiments in Chapter Three, investigating the effect of antiplatelet therapy on thrombus formation in response to different ECM component combinations, demonstrated differences in the efficacy of aspirin and clopidogrel on composite 'rupture' and 'erosion' matrices (Figure 3.13). Aspirin was less effective on 'rupture' matrices compared with Type I collagen, and clopidogrel less effective on 'erosion' matrices than 'rupture' matrices. This finding demonstrates that the presence of different ECM components could have an impact on antiplatelet efficacy, potentially due to their interactions with collagen, as discussed in Section 3.3.2 (Smith and Murphy, 2008; Bonacina *et al.,* 2016).

6.5 The use of an entire, cell-derived ECM in a thrombosis model

To investigate the role of ECM components as a whole, and to determine whether *in vitro* ECM combinations can be representative of an *in vivo* ECM, a complete cell-derived ECM (CDM) was introduced into the model in Chapter Four, using both HCAEC and HCAMSC CDMs to represent the vascular ECM. Similar to Chapter Three, platelet responses to the CDM were compared with Type I collagen, to determine if Type I collagen was representative of vascular thrombosis and sufficient to use in the model, or if a CDM should instead be incorporated. HCAEC and HCASMC-derived matrices were both used, to compare any differences in platelet activity on matrices and investigate the different components comprising the vascular ECM *in vivo.* Indeed, results from Chapter Four demonstrated significant differences in platelet activity on CDMs compared with Type I collagen (Figure 4.6, Figure 4.7), supporting results from Bonacina *et al.* (2016) demonstrating the regulation of the pro-thrombotic potential of collagen

by ECM proteins, and results from Chapter Three demonstrating reductions in platelet activity on Type I collagen following the inclusion of vascular PGs (Figure 3.9). These findings highlight the importance of using a CDM in place of Type I Horm collagen, for studies exploring *in vitro* thrombus formation.

6.5.1 A comparison of recombinant and cell-derived matrices

As previously discussed in Section 4.1.3, TNF-α is a potent inflammatory cytokine that has been shown to promote atherosclerotic plaque development and endothelial dysfunction (Branen *et al.,* 2004; Boesten *et al.,* 2005), and CSE (representing smoking), in contrast, is a risk factor segregating with plaque erosion (Dai *et al.,* 2018). Both are therefore relevant in their use as damage stimuli to differentiate the rupture and erosion ECMs in cardiovascular disease. Further findings from Chapter Four revealed differences in thrombus formation between control CDMs and CDMs generated following cell stimulation with TNF-α and CSE. The 'rupture' CDM (incorporating TNF-α) produced larger thrombi than the healthy 'control' CDM in HCAEC- and HCASMC-derived matrices (Figure 4.9, Figure 4.10 respectively). In contrast, there were no significant differences on synthetic 'rupture' matrices, composed of Type I collagen, biglycan and decorin, compared with the 'control' matrix consisting of Type I collagen (Figure 3.8). This may be due to an absence of more thrombogenic ECM components in the synthetic 'rupture' matrix, as proteomic analysis from Chapter Four demonstrated that one of the most significant upregulations in proteins associated with thrombosis was in Galectin-9, a platelet agonist, in the HCAEC CDM (Figure 4.14). Additionally, the vascular PGs associated with the synthetic 'rupture' matrix, decorin and biglycan, were either detected in very low abundance in some CDM samples, or not at all. This is a common issue when using mass spectrometry to identify proteins of relatively low abundance in CDMs (Hu *et al.,* 2022), with low abundance proteins previously identified *in vivo* and *in vitro* after two weeks of culture (Gocheva *et al.,* 2017; Simunovic *et al.,* 2018), despite the commonly used 5-10 days culture time for CDM generation (Barraza *et al.,* 2016; Carvalho *et al.,* 2019; Rubi-Sans *et al.,* 2021). It is therefore possible that a longer culture time would have resulted in identification of these proteins, and potentially altered matrix thrombogenicity. The increase in thrombogenicity of TNF-α associated matrices may also be due to a reduction in less thrombogenic PGs, such as hyaluronan (Figure

4.16). Indeed, the loss of PGs in the vascular ECM is associated with an increase in thrombosis and coagulation, potentially due to the ability of PGs to regulate mediators such as vWF and TFPI (Kohli *et al.,* 2022), and findings from Chapter Four support this association. Figure 4.14, for example, demonstrates the upregulation of coagulation proteins such as plasminogen and TFPI in response to TNF-α and CSE, and Figure 4.16 demonstrates upregulation of platelet agonists such as S100A7 in HCASMC CDMs, an ECM protein associated with an increase in ADAM10 release in platelets, associated with increased GPVI shedding and thrombotic complications in CVD (Qin *et al.,* 2009; Chatterjee and Gawaz, 2017; Maurer *et al.,* 2020; Montague *et al.,* 2020). Vascular PGs such as PRELP and hyaluronan were observed to be reduced in these matrices (Figure 4.14 and Figure 4.16), however it was not possible to form any association between the reduction in vascular PGs and increase in mediators of thrombosis, due to the vast number of proteins up- and down-regulated in CDMs in response to TNF-α and CSE cell stimulation.

Similarly to the 'rupture' CDM, the 'erosion' CDM (incorporating CSE and TNF-α, representing smoking and inflammation respectively) in HCAECs was significantly more thrombogenic than healthy 'control' CDMs (Figure 4.9), but this was not observed in HCASMCs (Figure 4.10). Synthetic 'erosion' matrices, containing Type III collagen, versican and hyaluronan, in contrast to both HCAEC and HCASMC 'erosion' CDMs, were observed to be significantly less thrombogenic compared to control (Type I collagen; Figure 3.8). This contrast may be accounted for in the regulation of thrombus formation by specific PGs, discussed in Section 6.1.3. Thrombus formation on both hyaluronan and versican is significantly reduced compared with collagen under an arterial shear rate (Figure 3.7). Combining these proteins results in formation of an anti-inflammatory 'provisional matrix' (Wight, 2017) and further reduces ECM thrombogenicity (Figure 3.10). In HCAEC 'erosion' CDMs, an increase in hyaluronan but not versican was observed (Figure 4.14), and in HCASMC CDMs, an increase in versican but not hyaluronan was observed (Figure 4.16). It is therefore possible that versican and hyaluronan together reduce the thrombogenicity of Type III collagen, but not individually, supported by results from Figure 3.10, demonstrating no differences in thrombus formation on Type III collagen with the addition of versican or hyaluronan individually. Another, potentially more likely, cause of the differences in thrombus formation is the inclusion of other ECM proteins significantly up- and down-regulated in

response to TNF-α and CSE, including mediators of coagulation such as TF and TFPI (Figure 4.14) and thrombotic mediators such as S100A7 and Galectin (Figure 4.16). In contrast with findings from Kolodgie *et al.* (2002) which identify Type III collagen as the main collagen in eroded plaques, Type III collagen was downregulated in the 'erosion' CDM in HCAECs (Figure 4.14). This may be due to the effect of cell stimulation with TNF-α, as Type III collagen was also down-regulated in the TNF-α stimulated sample. It may therefore be more relevant to stimulate cells with a different pro-inflammatory cytokine, to improve the relevance of CDMs to plaque erosion.

In summary, differences observed in platelet activity and thrombus formation between CDMs and recombinant matrices were likely a result of the interplay between vascular PGs, growth factors and cytokines regulating thrombus formation on fibrillar proteins such as Types I and III collagen. It should be a consideration that both matrices be used for separate applications. Recombinant matrices are a useful tool to investigate the regulation of thrombus formation by specific ECM components, and CDMs, in contrast, are a more relevant tool to determine overall thrombus formation for clinical applications, such as antiplatelet drug screening. Unfortunately, due to time constraints, antiplatelet efficacy was not assessed on CDMs, but this is a consideration for future work. Additionally, further work is needed to be able to preserve the CDM for coating, similar to the Type I Horm collagen currently used in thrombosis models. This would enable increased uptake of the model by researchers and increase the replicability of results.

6.5.2 Proteomic observations on the CDM

Mass spectrometric analysis of the underlying CDMs revealed significant up- and down-regulation of key mediators of thrombosis and coagulation (Figures 4.11, 4.12), demonstrating that the ECM produced by cells alters in composition in response to stimuli associated with cardiovascular disease, which in turn alters thrombus formation and platelet activity on these substrates. Studies acknowledge that cardiovascular disease is associated with alterations in ECM composition (Ma *et al.*, 2020), however there are no studies investigating the consequent thrombogenicity of the ECM in response. Pro-inflammatory mediators, such as TNF-α, are associated with fibrous cap

degradation and the rupture of atherosclerotic plaques (Luo *et al.,* 2022). The proteomic data of the underlying ECM in TNF-α stimulated samples demonstrated a reduction in multiple collagens compared to control in both HCAEC- and HCASMC-derived samples (Figure 4.14, Figure 4.16), consistent with findings from Greenwel *et al.* (2000) and Zhang *et al.* (2021), who found that TNF-α inhibits the synthesis of structural ECM components and contributes to ECM degradation. Indeed, our findings demonstrated that other proteins downregulated in response to TNF-α included structural matrilin and elastin (Figure 4.16), and overall the data supports the link between TNF-α and fibrous cap degradation. However, there are multiple risk factors associated with atherosclerosis which may significantly alter ECM composition in a CDM. Oxidative stress, for example, is a risk factor associated with the development and progression of atherosclerotic plaques in both plaque rupture and erosion (Kattoor *et al.,* 2017). In contrast with TNF-α, it has been associated with an increase in the expression of structural matrix components, such as collagens (Iglesias-De La Cruz *et al.,* 2001). It is therefore important to consider multiple risk factors when generating cardiovascular disease-relevant CDMs, to best represent the matrices observed *in vivo.* Indeed, the absence of additional risk factors in CDM generation may partially account for differences in CDM 'erosion' composition compared with findings from Kolodgie *et al.* (2002). Findings from the characterisation of CDM in Chapter Four are a useful insight into the potential alterations the ECM adopts in response to cardiovascular disease, and provide novel insights into how this could regulate thrombus formation *in vivo,* but further work should be undertaken to improve the representability of 'erosion' CDMs in particular.

6.6 An endothelialised model of atherothrombosis

Findings from Chapter Four demonstrated that inducing endothelial dysfunction had the potential to increase ECM thrombogenicity. In addition to this, endothelial dysfunction can also alter the regulation of thrombosis in the vasculature. As described in Section 1.4, endothelial dysfunction results in the release of vWF, TXA2 and PAF from the endothelium, promoting platelet adhesion, activation and thrombus formation. Additionally, the release of TF promotes activation of the coagulation cascade and vWF propagates this process by its involvement in FVIII stability and fibrin crosslinking.

Finally, fibrinolysis is inhibited by release of PAI-1, which inhibits tPA activity in the vasculature (Pearson, 1999; Kaur *et al.,* 2018). The final part of the project (Chapter Five) was to incorporate an endothelial monolayer into the model, which could be focally damaged, exposing the underlying CDM to investigate local thrombosis, similar to *in vivo* protocols used with murine models (Tseng *et al.,* 2006; Karel *et al.,* 2020; Carminita *et al.,* 2022).

Results from Chapter Five demonstrated the importance of using a relevant cell type, with key differences observed in the resting gene levels of mediators important in thrombosis between HCAECs and HUVECs, including CD39, vWF and eNOS (Figure 5.1). eNOS gene expression, for example, was observed to be higher in HCAECs than in HUVECs. These findings support literature suggesting eNOS and nitric oxide are important in preventing the development and progression of atherosclerosis (Munzel and Daiber, 2020) and in the regulation of vasodilation in the coronary arteries (Tran *et al*., 2022). CD39, in contrast, is important in venous thrombosis, and has been shown to regulate the inflammatory response following the disturbance of blood flow, resulting in the formation of smaller thrombi (Anyanwu *et al.,* 2019). This supports findings from Chapter Five demonstrating a higher gene expression of CD39 in HUVECs compared with HCAECs. Similarly, results from Figure 5.1 demonstrate higher vWF levels in HUVECs than in HCAECs. This is surprising, as vWF is important in arterial thrombosis and cardiovascular disease, due to its ability to activate under higher stenotic shear stresses and promote thrombus formation (Sonneveld *et al.,* 2014; Okhota *et al.,* 2020). However, there is emerging evidence suggesting vWF has an important role in venous thrombosis (Calabro *et al.,* 2018; Michels *et al.,* 2020), potentially due to its role in coagulation, with the release of tethered FVIII by thrombin promoting coagulation and stable thrombus formation (Chauhan *et al.,* 2007). Findings from Chapter Five demonstrating key differences in gene expression between HUVECs and HCAECs are therefore important, as HUVECs are often used as a cheaper alternative to HCAECs (Promocell, 2023), however, differences observed in thrombotic regulation and protection may alter any resulting thrombus formation following cellular dysfunction which may not be representative of arterial thrombosis. Indeed, Riley (2022) used an endothelialised thrombosis model to investigate the regulation of thrombus formation on Type I Horm collagen by HUVECs and HCAECs by flowing blood over endothelial cells prior to collagen. It was observed that thrombi formed on collagen following perfusion

over HCAECs covered a larger surface area than thrombi formed on collagen following perfusion over HUVECs, and that stimulating HUVECs with TNF-α abolished any thrombotic protection conferred by endothelial cells prior to thrombus formation. These findings support findings from Chapter Five, demonstrating that inducing cellular dysfunction in both HCAECs and HUVECs may result in significant differences in thrombus formation, which would favour the use of HCAECs in models investigating arterial thrombosis.

A novel protocol to focally expose the underlying CDM prior to thrombus formation was also developed in Chapter Five, using filter paper soaked in $FeCl_3$ or ECM isolation buffer, or mechanical needle injury. One purpose of developing these methods was to enable comparison of current *in vivo* and *in vitro* models of atherothrombosis, as commonly used *in vivo* methods include experimental damage of vessels using $FeCl_3$-soaked filter paper and mechanical injury using ligation, wire or a needle (Mackman, 2006; Karel *et al.,* 2020; Carminita *et al.,* 2022). The ECM isolation buffer was used as a model of plaque erosion, as the buffer removes the endothelium, leaving the underlying ECM intact. This is an *in vitro* equivalent of endothelial denudation, a hallmark of plaque erosion (Hansson *et al.,* 2015; Quillard *et al.,* 2017). This developed protocol demonstrated that focal damage could be inflicted on ECs *in vitro* using hole-punched filter paper, and that damaging ECs with $FeCl_3$-soaked filter paper resulted in an increase in TF expression, cell death and EC removal under flow. These findings support findings from Eckley *et al.* (2011), who described the release of TF-rich vesicles from endothelial cells in response to $FeCl_3$-induced damage. Conversely, damaging ECs with needles resulted in no increase in TF expression, demonstrating that needle injury could be a potential model of plaque erosion. However, the developed protocol does require optimisation, as the force of applying the filter paper, for example, appeared to remove cells and was not standardised per sample. This could eventually become an automated process for ease of use and replicability. When fully optimised, this protocol could help to bridge the gap between current *in vivo* and *in vitro* models, allowing researchers to focally damage endothelial cells with a variety of stimuli and investigate the resulting thrombus formation.

The model is comparable to current models of atherothrombosis in its design. Current *in vitro* thrombosis models utilise microfluidic devices which may be 3D printed or designed using soft lithography, where channels are designed to run through 3D

hydrogels often composed of Type I collagen (Akther *et al.,* 2022; Hajal *et al.,* 2022). The major disadvantages of these models are the complexity, lack of replicability and time taken to develop (Herbig *et al.,* 2018). Additionally, focal damage, representing plaque rupture or erosion, would be challenging to adapt in these models. Commercially available microfluidic models are also available and can be simpler in design and more reproducible (Riley, 2022). However, it is difficult to introduce focal endothelial damage to these closed chambers to allow discreet exposure of sub-endothelial matrix proteins. The model developed in this project incorporates a relevant arterial shear stress and human blood, as in current *in vitro* models, but also the ability to focally damage endothelial cells prior to perfusion of blood. *In vivo* models have the advantage of cellularisation and the inclusion of an ECM, but the cells are murine, from healthy mice, and the vessels used are often not standardised or representative of human thrombosis (Westrick et al., 2007). The model developed in this project incorporates endothelial cells and an ECM, similar to *in vivo* models, but the cells are human, and an ECM representative of cellular dysfunction can be generated and used to investigate platelet responses. In summary, the developed model has advantages over existing *in vivo* and *in vitro* models in the incorporation of a disrupted, focally damaged endothelium, disease-relevant ECMs, the use of human blood, a relevant EC type and human arterial shear stress (Figure 6.1).

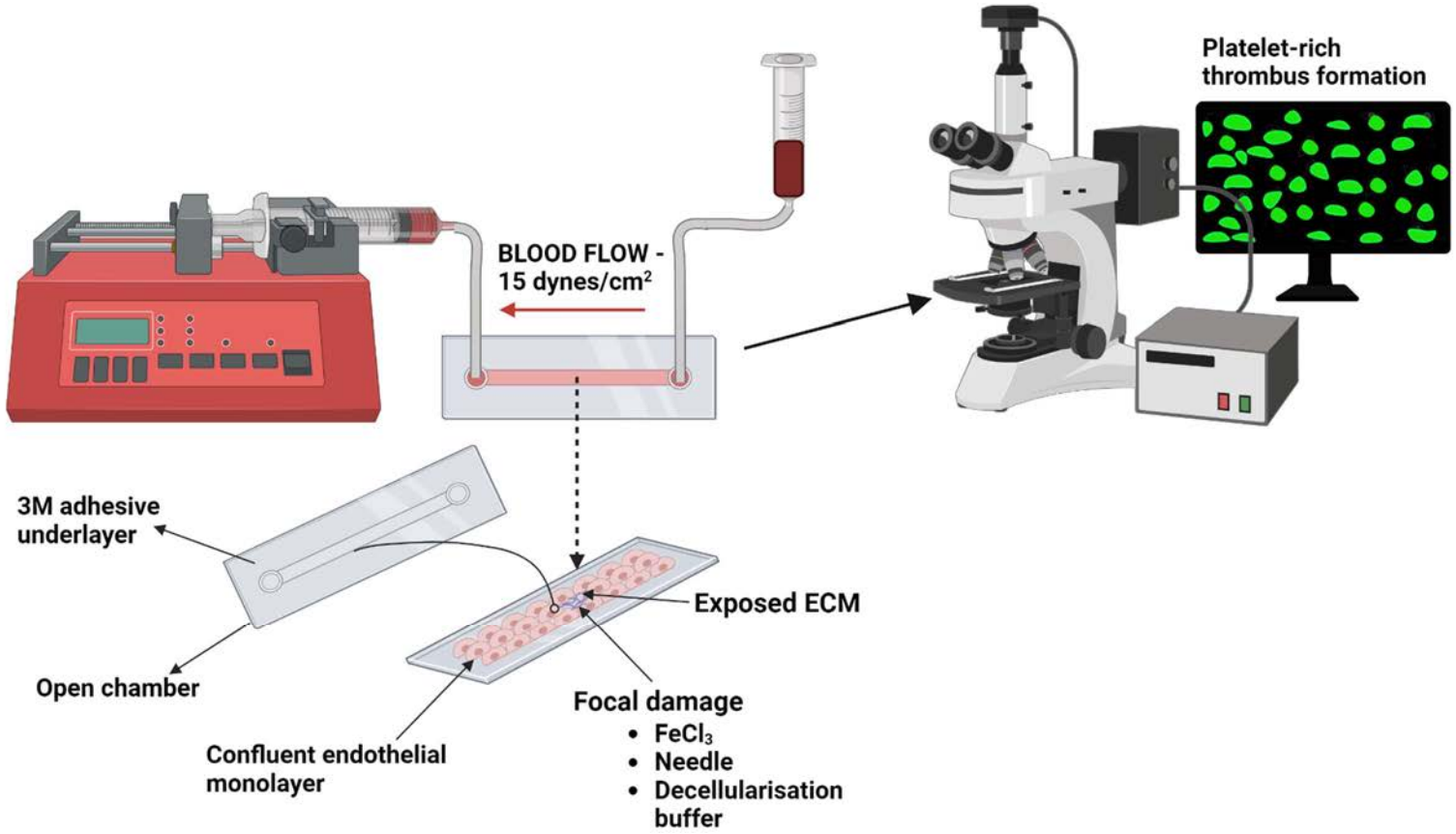

Figure 6.1 - A summary representing the final developed endothelialised model of atherothrombosis. Human coronary artery endothelial cells were grown to confluency on coverslips before undergoing focal damage with ferric chloride ($FeCl_3$), a needle or decellularization buffer to expose the underlying extracellular matrix (ECM). Ibidi sticky slides were used to assemble chambers before perfusion of DIOC-6 labelled whole blood through chambers via a syringe pump at an arterial shear rate (15 dynes/cm^2). The resulting thrombus formation on the focal area was imaged using a fluorescent microscope. Created with Biorender.com.

6.7 Limitations and future work

There were limitations associated with some of the methods used in this project, owing to the novelty of some methods and protocols not yet well established, and avenues for future project development. For ease, these will be addressed in the form of bullet points.

- **Limitation:-** there is no reference point as to the concentrations of individual PGs and collagens in the *in vivo* vascular ECM, indeed the ratios of ECM components is suggested to vary significantly depending on disease stage and due to donor variability (Wittig and Szulcek, 2021), therefore the concentrations used were those used in current thrombosis models using Type I collagen. Indeed, Hoermann *et al*. (2021) combined recombinant biglycan (10µg/mL) with Type I collagen (200µg/mL) and observed enhanced thrombus formation, in contrast with our findings, which determined a reduction in thrombus formation using 100µg/mL of each substrate. The regulation of thrombus formation by proteoglycans may therefore be concentration dependent, which may elucidate cellular response to dysfunction and the resulting changes in ECM composition in atherosclerosis (Ma *et al.*, 2020). **Future work/development:-** Results from the proteomics in Chapter Five, describing changes in ECM composition in response to different stimuli, may be used as a base to optimise the ratios of collagens and proteoglycans.
- **Limitation:-** The analysis was not blinded, but was largely automated in ImageJ, using software-defined limits for thresholding of images. Each image, therefore, went through an automated process of thresholding to determine platelet/thrombi number, size and area coverage, enabling standardisation of results. Morphological classification of platelets (lamellipodia and filopodia), however, was performed manually and was not blinded, therefore the analysis was subject to some bias, despite parameters set for defining filopodia and lamellipodia. **Future work/development:-** The analysis could be adapted and automated using specialist software such as KNIME and ilastik (Pike *et al.*, 2021). However, it is important to consider, as with all automated processes, that specialised software will require training and testing to ensure accurate and replicable results.

- **Limitation:-** The coatings of the composite 'rupture' and 'erosion' matrices in Chapter Three were not visualised, so coating efficacy could not be confirmed. This means that a consistent, even coating could not be verified, and that any resulting thrombus formation may either be on collagen fibres, with platelets not interacting with proteoglycans at all, or the proteoglycans may have localised to the collagen and be regulating thrombus formation on the fibres (Bonacina *et al.,* 2016). **Future work/development:-** Future work should investigate the localisation of platelets on Type I collagen fibres, and if this is altered in the presence of vascular proteoglycans.
- **Limitation:-** Human PGs were combined with equine Type I Horm collagen and not human Type I collagen, to allow for comparison with current thrombosis models. Equine collagen is used as a cheaper alternative, with the highest sequence homology (except bovine) with human collagen (Gallo *et al.,* 2020). However, it is possible that thrombus formation may differ on human vascular Type I collagen compared with equine Horm collagen isolated from tendons.
- **Limitation:-** Variability in donor response to Type I collagen (Lepantalo *et al.,* 2001) may mask variations observed compared with other PGs, due to Type I collagen eliciting such a strong response from platelets. **Future work/development:-** Investigating the role of vascular proteoglycans in platelet activity could focus on comparing intricate differences in platelet responses between vascular proteoglycans without the presence of collagens.
- **Limitation:-** CDM generation was performed over 10 days (Barraza *et al.,* 2016; Carvalho *et al.,* 2019; Rubi-Sans *et al.,* 2021), but this may not have been sufficient for identification of less prominent PGs, such as biglycan, which was not identified in any samples. Indeed, a common disadvantage of the mass spectrometry approach in ECM proteomics is the identification of less abundant ECM components; it may require weeks of cell culture for these components to be identifiable (Hu *et al.,* 2022). Indeed, as previously described in Section 6.1.4.1, Gocheva *et al.,* (2017) and Simunovic *et al.,* (2018) used a culture time of two weeks to enable identification of less prominent ECM components.
- **Limitation:-** Mass spectrometric analysis of the CDM failed to differentiate between the physiological HMW isoform of hyaluronan and the LMW pathological form. **Future work/development:-** This may be addressed by

combining proteomics data with complementary RNA sequencing to enhance isoform characterisation, in a protocol described by Miller *et al.* (2022). The inability to distinguish between these isoforms in the CDM means that it is difficult to draw conclusions from any observed differences in the abundance of hyaluronan in the samples.

- **Limitation:-** The force of applying the filter paper to cells, as discussed in Section 5.3.3, may have unintentionally compromised the structure of the underlying ECM. **Future work/development:-** To address this and improve replicability, application of the filter paper should be automated. This could be achieved by optimising the required distance to the EC monolayer to enable cell damage but not disruption (Schon *et al.,* 2017).
- **Limitation:-** The developed model is not occlusive and time to occlusion cannot be measured. However, as previously described in Section 5.3.3, the main output of this model is imaging and thrombus size, therefore full occlusion is not necessary. **Future work/development:-** Focus on developing the model as an occlusive model and incorporating coagulation, to enable comparisons of occlusive clot formation with *in vivo* counterparts (Westrick *et al.,* 2007)
- **Limitation:-** Although evidence suggests that the ECM is a stable network, with ECM components anchored to the ECM via structural fibres and proteoglycans (Kular et al., 2014; Theocharis *et al.,* 2016), it is possible that the application of an arterial shear stress to the CDM may have removed some ECM components, and this may have contributed to the altered thrombogenicity of the CDM between conditions. **Future work/development:-** Include proteomic analysis of the ECM before and after the application of an arterial shear stress, to ensure ECM components are not lost during flow experiments.
- **Limitation:-** For the purposes of simplicity, ECs were not cultured under flow for experiments. However, it has been shown that ECs alter their behaviour under flow (Kroon *et al.,* 2017), and this may have resulted in different CDM compositions and responses to stimuli such as TNF-α. Indeed, laminar flow has been shown to inhibit the EC inflammatory response to cytokines (Garin *et al.,* 2007). **Future work/development:-** Incorporate ECs cultured under flow, but optimisation experiments should be performed first, to investigate potential

differences between ECM composition and cell responses to cardiovascular-associated insults.

- **Future work/development:-** Unfortunately, due to lab time lost during the pandemic and ongoing construction works at the University, time constraints and issues with the microscopes have meant that some experiments have fewer biological repeats than others.
- **Future work/development:-** Due to time constraints, coagulation was not investigated in developed protocols and on CDMs. This is an important consideration for future work, considering that many up- and down-regulated proteins in the proteomic data were mediators of coagulation.

Figure 6.2 summarises the stages of development taken throughout the project and potential areas for future use and development.

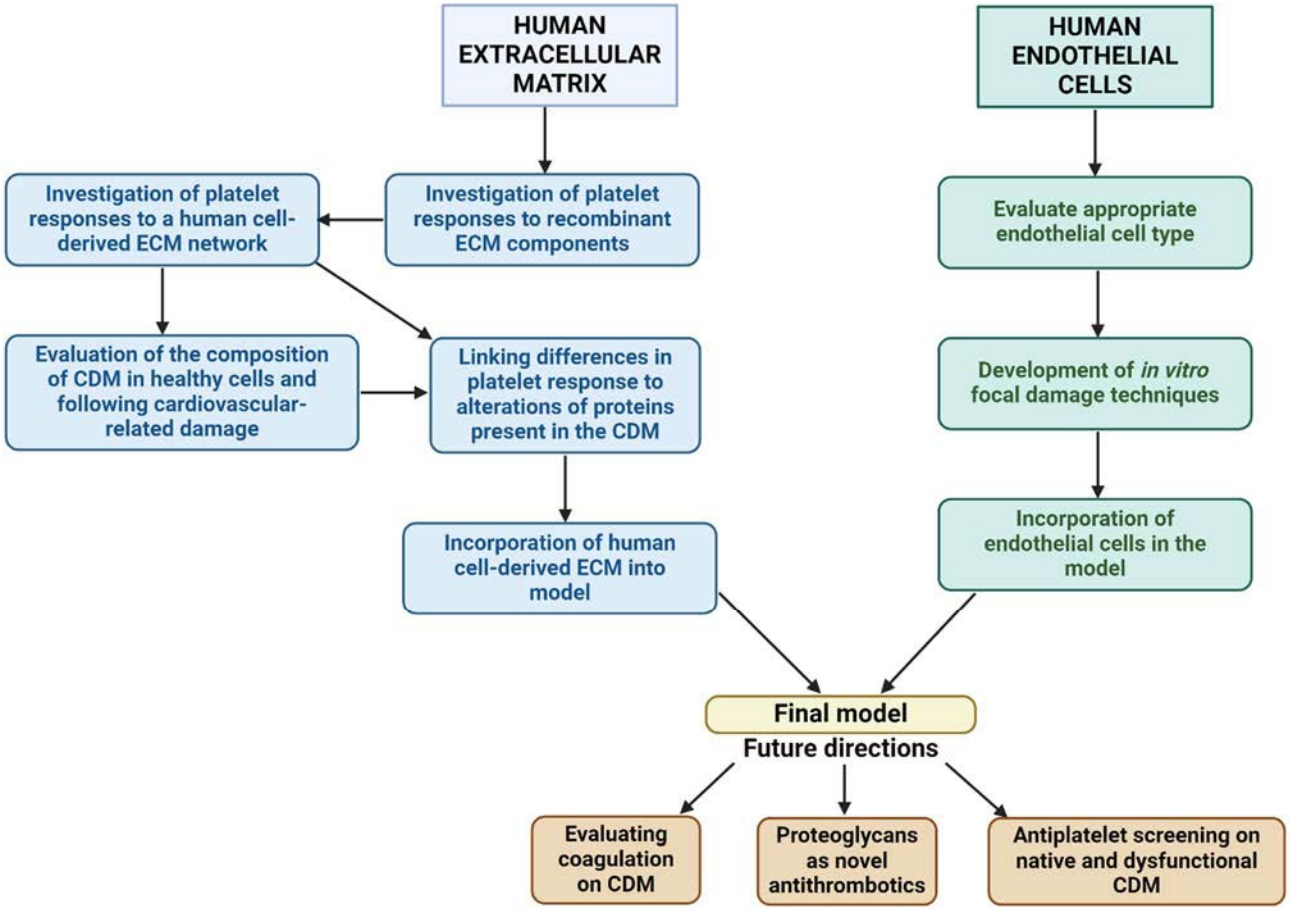

Figure 6.2 – A summary of the stages of development taken throughout the project and potential areas for future use and development. Created with BioRender.com.

6.8 Conclusions

The initial aim of this project was to create a novel, endothelialised *in vitro* model of human atherothrombosis, incorporating vascular ECs and a disease-relevant ECM to investigate the regulation of arterial thrombosis in plaque rupture and plaque erosion and to reduce the number of animals used in current *in vivo* models.

The project has revealed differences in platelet responses on recombinant matrix proteins, enabling further investigation into the use of vascular proteoglycans as potential novel antithrombotics. Additionally, successful development of the model has, for the first time, enabled platelet thrombus formation on an entire human cell-derived extracellular matrix network to be investigated. These experiments have provided a novel insight into the regulation of thrombus formation on Type I collagen by non-fibrillar vascular matrix proteins, which may be key in addressing some current limitations in the use of antiplatelet therapy. Furthermore, the model uses a confluent endothelial monolayer and dysfunctional ECM, in contrast with current models of atherothrombosis, improving representativity to the atherosclerotic vascular ECM. Indeed, the development of the final model has resulted in a multi-component, humanised model with the ability to bridge the gap between current *in vivo* and *in vitro* models by focally damaging a confluent endothelial cell monolayer and exploring the formation of thrombi in this focal area. The final *in vitro* model is both standardised and reproducible, in contrast with many *in vivo* thrombosis models, enabling the replacement of animal models in drug screening for antiplatelet efficacy. This novel tool will help to improve outcomes for patients in cardiovascular disease, both in the improvement of drug screening and in improving our knowledge of cardiovascular disease and atherothrombosis.

7. Appendices

7.1 Participant consent form

Manchester Metropolitan University

Participant Consent Form

Title of Study: Development and Characterisation of a Novel Endothelialised *in vitro* Model of Arterial Thrombosis

	Please initial box
1. I confirm that I have read and understand the information sheet dated 15th October 2019 (Version 2) for the above study.	☐
2. I have had the opportunity to consider the information, ask questions and have had these answered satisfactorily.	☐
3. I understand that my participation is voluntary and that I am free to withdraw at any time without giving any reason, without my medical care or legal rights being affected.	☐
4. I have received sufficient information about this study, including potential risks	☐
5. I have read the exclusion criteria and I am eligible to take part in the study	☐
6. I agree to take part in the above study.	☐

_____ _____ _____

Name of participant Date Signature

_____ _____ _____

Name of witness Date Signature

When completed, 1 copy for participant; 1 (original) for researcher site file

7.2 Ethics approval

Manchester Metropolitan University

10/09/2020
Project Title: Development and Characterisation of a Novel in vitro Model of Atherothrombosis

EthOS Reference Number: 12762

Ethical Opinion

Dear Amelia Drysdale,

The above amendment was reviewed by the Science and Engineering Research Ethics and Governance Committee and, on the 10/09/2020, was given a favourable ethical opinion. The approval is in place until 02/10/2023 .

Conditions of favourable ethical opinion

Application Documents

Document Type	File Name	Date	Version
Additional Documentation	COVID-19 questionnaire AU	23/08/2020	1
Additional Documentation	Participant Information Sheet (Amelia Drysdale)	23/08/2020	3

The Science and Engineering Research Ethics and Governance Committee favourable ethical opinion is granted with the following conditions

Adherence to Manchester Metropolitan University's Policies and procedures

This ethical approval is conditional on adherence to Manchester Metropolitan University's Policies, Procedures, guidance and Standard Operating procedures. These can be found on the Manchester Metropolitan University Research Ethics and Governance webpages.

Amendments

If you wish to make further changes to this approved application, you will be required to submit an amendment. Please visit the Manchester Metropolitan University Research Ethics and Governance webpages or contact your Faculty research officer for advice around how to do this.

We wish you every success with your project.

Science and Engineering Research Ethics and Governance Committee

Science and Engineering Research Ethics and Governance Committee

For help with this application, please first contact your Faculty Research Officer. Their details can be found here

7.3 Primer efficiencies and standard curves

RPLP0 – HCAEC

Tube	Ct 1	Ct 2	Avg Ct	Sample Quantity	Log (sample quantity)
A	19.5	19.42	19.46	1.0000	0.00
B	20.1	20.14	20.12	0.5000	-0.30
C	20.83	21.06	20.945	0.2500	-0.60
D	21.76	22.07	21.915	0.1250	-0.90
E	23.26	23.28	23.27	0.0625	-1.20

Dilution Factor	2
Slope	-3.127595301
R Squared	0.9807
Efficiency (%)	**108.80**
y-intercept	19.259

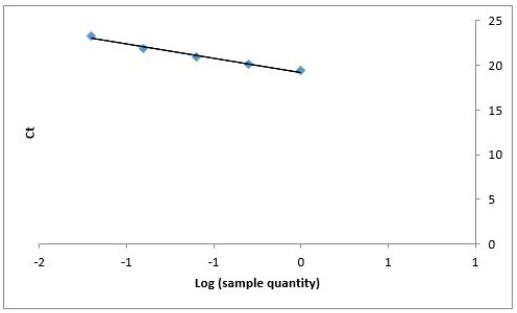

RPLP0 – HUVEC

Tube	Ct 1	Ct 2	Avg Ct	Sample Quantity	Log (sample quantity)
A	19.05	19.01	19.03	1.0000	0.00
B	19.55	19.61	19.58	0.5000	-0.30
C	20.27	20.57	20.42	0.2500	-0.60
D	21.8	21.76	21.78	0.1250	-0.90
E	22.79	22.52	22.655	0.0625	-1.20

Dilution Factor	2
Slope	-3.13922205
R Squared	0.9803
Efficiency (%)	**108.23**
y-intercept	18.803

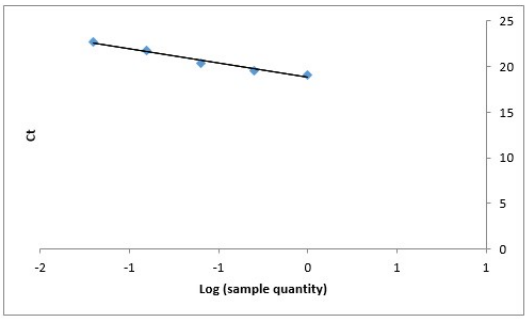

GAPDH – HCAEC

Tube	Ct 1	Ct 2	Avg Ct	Sample Quantity	Log (sample quantity)
A	19.68	19.39	19.535	1.0000	0.00
B	20.44	20.33	20.385	0.5000	-0.30
C	21.2	21.17	21.185	0.2500	-0.60
D	22.21	22.24	22.225	0.1250	-0.90
E	23.63	23.58	23.605	0.0625	-1.20

Dilution Factor	2
Slope	-3.315284239
R Squared	0.9865
Efficiency (%)	**100.28**
y-intercept	19.391

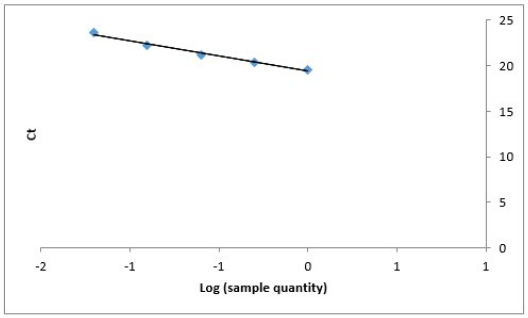

GAPDH – HUVEC

Tube	Ct 1	Ct 2	Avg Ct	Sample Quantity	Log (sample quantity)
A	19.08	19.05	19.065	1.0000	0.00
B	19.79	19.7	19.745	0.5000	-0.30
C	20.39	20.61	20.5	0.2500	-0.60
D	21.63	21.79	21.71	0.1250	-0.90
E	22.92	22.83	22.875	0.0625	-1.20

Dilution Factor	2
Slope	-3.184068079
R Squared	0.9831
Efficiency (%)	**106.09**
y-intercept	18.862

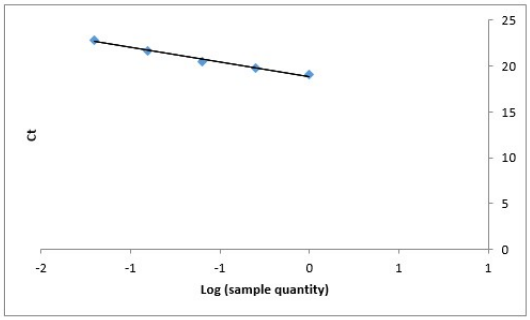

CD39 – HCAEC

Tube	Ct 1	Ct 2	Avg Ct	Sample Quantity	Log (sample quantity)
A	26.92	27.08	27	1.0000	0.00
B	27.63	27.49	27.56	0.5000	-0.30
C	28.75	28.3	28.525	0.2500	-0.60
D	29.74	29.37	29.555	0.1250	-0.90
E	30.59	31.14	30.865	0.0625	-1.20

Dilution Factor	2
Slope	-3.230575072
R Squared	0.9812
Efficiency (%)	**103.96**
y-intercept	26.756

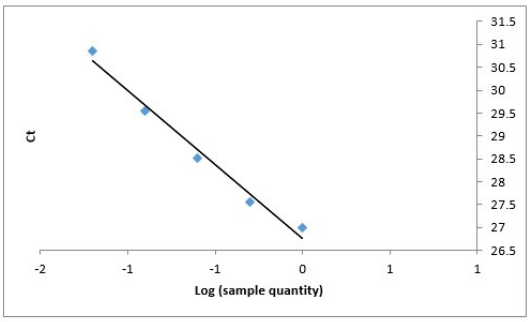

CD39 – HUVEC

Tube	Ct 1	Ct 2	Avg Ct	Sample Quantity	Log (sample quantity)
A	26.83	27.09	26.96	1.0000	0.00
B	27.34	27.77	27.555	0.5000	-0.30
C	28.36	28.75	28.555	0.2500	-0.60
D	29.32	29.86	29.59	0.1250	-0.90
E	30.98	30.77	30.875	0.0625	-1.20

Dilution Factor	2
Slope	-3.277082066
R Squared	0.9848
Efficiency (%)	**101.91**
y-intercept	26.734

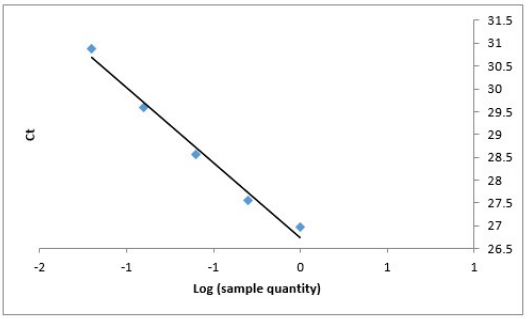

vWF – HCAEC

Tube	Ct 1	Ct 2	Avg Ct	Sample Quantity	Log (sample quantity)
A	23.07	23.17	23.12	1.0000	0.00
B	23.69	23.81	23.75	0.5000	-0.30
C	24.63	24.92	24.775	0.2500	-0.60
D	25.56	26.06	25.81	0.1250	-0.90
E	27.1	27.1	27.1	0.0625	-1.20

Dilution Factor	2
Slope	-3.328571951
R Squared	0.9868
Efficiency (%)	**99.72**
y-intercept	22.907

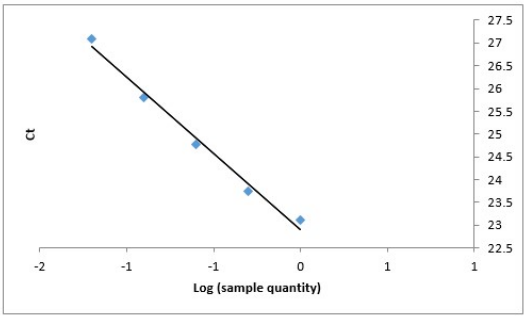

vWF – HUVEC

Tube	Ct 1	Ct 2	Avg Ct	Sample Quantity	Log (sample quantity)
A	22.32	22.17	22.245	1.0000	0.00
B	22.86	23	22.93	0.5000	-0.30
C	23.76	23.85	23.805	0.2500	-0.60
D	25.03	24.82	24.925	0.1250	-0.90
E	26.12	26.24	26.18	0.0625	-1.20

Dilution Factor	2
Slope	-3.277082066
R Squared	0.9860
Efficiency (%)	**101.91**
y-intercept	22.044

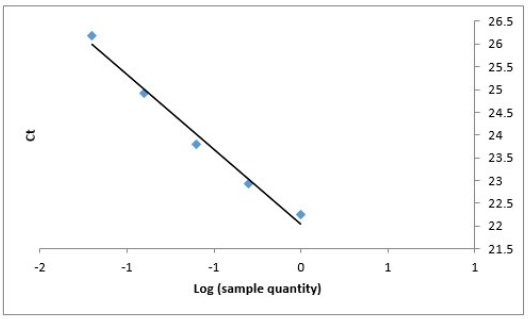

eNOS – HCAEC

Tube	Ct 1	Ct 2	Avg Ct	Sample Quantity	Log (sample quantity)
A	25.29	25.25	25.27	1.0000	0.00
B	26.02	26.02	26.02	0.5000	-0.30
C	27.05	26.78	26.915	0.2500	-0.60
D	28	28.09	28.045	0.1250	-0.90
E	28.86	29.3	29.08	0.0625	-1.20

Dilution Factor	2
Slope	-3.203999648
R Squared	0.9942
Efficiency (%)	**105.17**
y-intercept	25.137

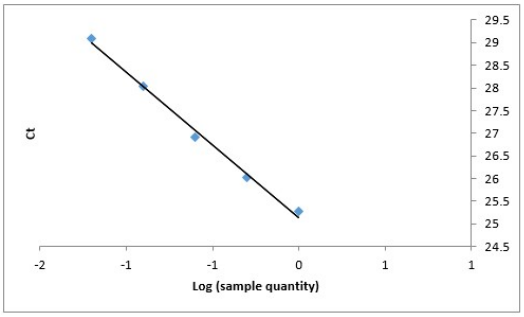

eNOS – HUVEC

Tube	Ct 1	Ct 2	Avg Ct	Sample Quantity	Log (sample quantity)
A	25.08	25.06	25.07	1.0000	0.00
B	26.05	25.79	25.92	0.5000	-0.30
C	26.68	26.73	26.705	0.2500	-0.60
D	27.68	27.54	27.61	0.1250	-0.90
E	29.15	29	29.075	0.0625	-1.20

Dilution Factor	2
Slope	-3.222270252
R Squared	0.9822
Efficiency (%)	**104.33**

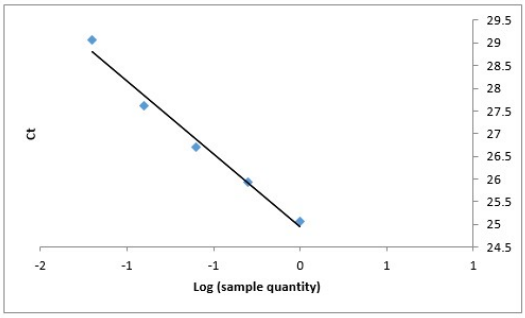

COX2 – HCAEC

Tube	Ct 1	Ct 2	Avg Ct	Sample Quantity	Log (sample quantity)
A	26.5	26.41	26.455	1.0000	0.00
B	27.22	27.22	27.22	0.5000	-0.30
C	28.17	28.42	28.295	0.2500	-0.60
D	29.16	29.21	29.185	0.1250	-0.90
E	30.91	30.31	30.61	0.0625	-1.20

Dilution Factor	2
Slope	-3.413281117
R Squared	0.9889
Efficiency (%)	**96.32**
y-intercept	26.298

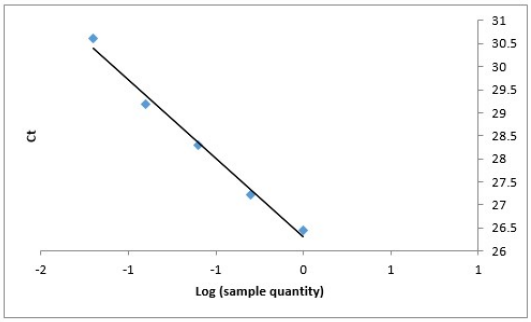

COX2 – HUVEC

Tube	Ct 1	Ct 2	Avg Ct	Sample Quantity	Log (sample quantity)
A	27.19	27.31	27.25	1.0000	0.00
B	27.98	28.15	28.065	0.5000	-0.30
C	29.03	28.75	28.89	0.2500	-0.60
D	29.72	30.17	29.945	0.1250	-0.90
E	31.67	30.82	31.245	0.0625	-1.20

Dilution Factor	2
Slope	-3.27874303
R Squared	0.9889
Efficiency (%)	**101.83**
y-intercept	27.105

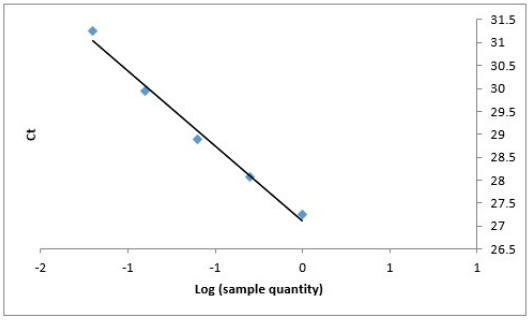

TBXAS1 – HCAEC

Tube	Ct 1	Ct 2	Avg Ct	Sample Quantity	Log (sample quantity)
A	27.28	26.89	27.085	1.0000	0.00
B	27.89	27.92	27.905	0.5000	-0.30
C	28.97	28.2	28.585	0.2500	-0.60
D	29.75	29.61	29.68	0.1250	-0.90
E	30.81	31.25	31.03	0.0625	-1.20

Dilution Factor	2
Slope	-3.210643504
R Squared	0.9813
Efficiency (%)	**104.86**
y-intercept	26.924

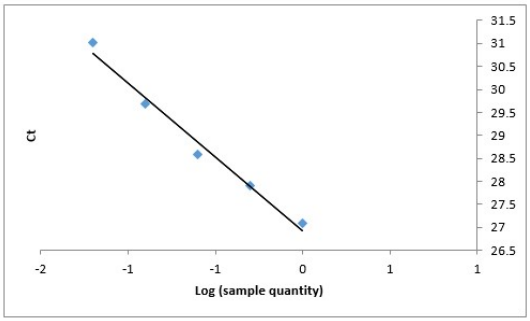

TBXAS1 – HUVEC

Tube	Ct 1	Ct 2	Avg Ct	Sample Quantity	Log (sample quantity)
A	27.24	27.13	27.185	1.0000	0.00
B	27.83	27.65	27.74	0.5000	-0.30
C	28.59	28.86	28.725	0.2500	-0.60
D	29.44	29.98	29.71	0.1250	-0.90
E	30.9	31.13	31.015	0.0625	-1.20

Dilution Factor	2
Slope	-3.199016755
R Squared	0.9820
Efficiency (%)	**105.40**
y-intercept	26.949

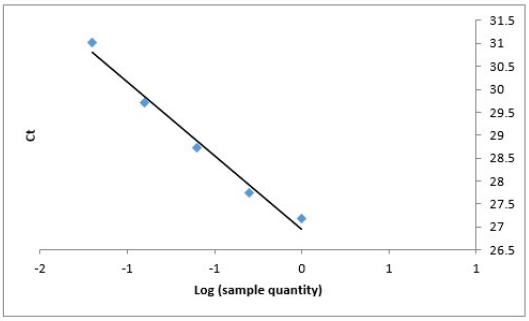

8. References

Aird, W. C. (2007) 'Phenotypic Heterogeneity of the Endothelium.' Circulation Research, 100(2), 2007-02-02, pp. 158-173.

Akther, F., Zhang, J., Tran, H. D. N., Fallahi, H., Adelnia, H., Phan, H. P., Nguyen, N. T. and Ta, H. T. (2022a) 'Atherothrombosis-on-Chip: A Site-Specific Microfluidic Model for Thrombus Formation and Drug Discovery.' Advanced Biology, 6(7), 2022-07-01, p. 2101316.

Akther, F., Zhang, J., Tran, H. D. N., Fallahi, H., Adelnia, H., Phan, H. P., Nguyen, N. T. and Ta, H. T. (2022b) 'Atherothrombosis-on-Chip: A Site-Specific Microfluidic Model for Thrombus Formation and Drug Discovery.' Advanced Biology, 6(7), 2022-07-01, p. 2101316.

Albeiroti, S., Ayasoufi, K., Hill, D. R., Shen, B. and de la Motte, C. A. (2015) 'Platelet hyaluronidase-2: an enzyme that translocates to the surface upon activation to function in extracellular matrix degradation.' Blood, 125(9) 2014/11/19, pp. 1460-1469.

Aldrich, J. L. and Long, D. S. (2019) 'In situ fixation and subsequent collection of cultured endothelial cells in a shear flow.' MethodsX, 6 20190503, pp. 1164-1173.

Alexander, M. R. and Owens, G. K. (2012) 'Epigenetic control of smooth muscle cell differentiation and phenotypic switching in vascular development and disease.' Annu Rev Physiol, 74 20111010, pp. 13-40.

Alqarni, A. A., Brand, O. J., Pasini, A., Alahmari, M., Alghamdi, A. and Pang, L. (2022) 'Imbalanced prostanoid release mediates cigarette smoke-induced human pulmonary artery cell proliferation.' Respiratory Research, 23(1), 2022-12-01,

Anyanwu, A. C., Kanthi, Y., Fukase, K., Liao, H., Mimura, T., Desch, K. C., Gruca, M., Kaskar, S., et al. (2019) 'Tuning the Thromboinflammatory Response to Venous Flow Interruption by the Ectonucleotidase CD39.' Arteriosclerosis, Thrombosis, and Vascular Biology, 39(4), 2019-04-01,

Armstrong, R. A. (1996) 'Platelet prostanoid receptors.' Pharmacology & Therapeutics, 72(3), 1996/01/01/, pp. 171-191.

Assunção, M., Dehghan-Baniani, D., Yiu, C. H. K., Später, T., Beyer, S. and Blocki, A. (2020) 'Cell-Derived Extracellular Matrix for Tissue Engineering and Regenerative Medicine.' Frontiers in Bioengineering and Biotechnology, 8

Badimon, L., Padró, T. and Vilahur, G. (2012) 'Atherosclerosis, platelets and thrombosis in acute ischaemic heart disease.' European Heart Journal: Acute Cardiovascular Care, 1(1), 2012-04-01, pp. 60-74.

Barr, J. D., Chauhan, A. K., Schaeffer, G. V., Hansen, J. K. and Motto, D. G. (2013) 'Red blood cells mediate the onset of thrombosis in the ferric chloride murine model.' Blood, 121(18), May 2, 20130123, pp. 3733-3741.

Beacham, D. A., Amatangelo, M. D. and Cukierman, E. (2006) 'Preparation of Extracellular Matrices Produced by Cultured and Primary Fibroblasts.' Current Protocols in Cell Biology, 33(1), 2006-12-01, pp. 10.19.11-10.19.21.

Bearer, E. L., Prakash, J. M. and Li, Z. (2002) 'Actin dynamics in platelets.' In International Review of Cytology. Elsevier, pp. 137-182. [Accessed on 2023-06-06T12:14:53]

Bentzon, J. F., Otsuka, F., Virmani, R. and Falk, E. (2014) 'Mechanisms of Plaque Formation and Rupture.' Circulation Research, 114(12), 2014-06-06, pp. 1852-1866.

Berendsen, A. D., Pinnow, E. L., Maeda, A., Brown, A. C., McCartney-Francis, N., Kram, V., Owens, R. T., Robey, P. G., et al. (2014) 'Biglycan modulates angiogenesis and bone formation during fracture healing.' Matrix Biology, 35, 2014/04/01/, pp. 223-231.

Berry, J., Peaudecerf, F. J., Masters, N. A., Neeves, K. B., Goldstein, R. E. and Harper, M. T. (2021) 'An “occlusive thrombosis-on-a-chip” microfluidic device for investigating the effect of anti-thrombotic drugs.' Lab on a Chip, 21(21), 2021-01-01, pp. 4104-4117.

Boesten, L. S. M., Zadelaar, A. S. M., van Nieuwkoop, A., Gijbels, M. J. J., de Winther, M. P. J., Havekes, L. M. and van Vlijmen, B. J. M. (2005) 'Tumor necrosis factor-α promotes atherosclerotic lesion progression in APOE*3-leiden transgenic mice.' Cardiovascular Research, 66(1) pp. 179-185.

Bogen, O., Bender, O., Alvarez, P., Kern, M., Tomiuk, S., Hucho, F. and Levine, J. D. (2019) 'Expression of a novel versican variant in dorsal root ganglia from spared nerve injury rats.' Mol Pain, 15, Jan-Dec, 2019/08/21, p. 1744806919874557.

Bonacina, F., Barbieri, S. S., Cutuli, L., Amadio, P., Doni, A., Sironi, M., Tartari, S., Mantovani, A., et al. (2016) 'Vascular pentraxin 3 controls arterial thrombosis by targeting collagen and fibrinogen induced platelets aggregation.' Biochimica et Biophysica Acta (BBA) - Molecular Basis of Disease, 1862(6), 2016/06/01/, pp. 1182-1190.

Bonnard, T. and Hagemeyer, C. E. (2015) 'Ferric Chloride-induced Thrombosis Mouse Model on Carotid Artery and Mesentery Vessel.' Journal of Visualized Experiments, (100), 2015-06-29,

BråNéN, L., Hovgaard, L., Nitulescu, M., Bengtsson, E., Nilsson, J. and Jovinge, S. (2004) 'Inhibition of Tumor Necrosis Factor-α Reduces Atherosclerosis in Apolipoprotein E Knockout Mice.' Arteriosclerosis, Thrombosis, and Vascular Biology, 24(11), 2004-11-01, pp. 2137-2142.

Brouns, S. L. N., van Geffen, J. P. and Heemskerk, J. W. M. 'High-throughput measurement of human platelet aggregation under flow: application in hemostasis and beyond.' (1369-1635 (Electronic))

Brouns, S. L. N., Van Geffen, J. P. and Heemskerk, J. W. M. (2018) 'High-throughput measurement of human platelet aggregation under flow: application in hemostasis and beyond.' Platelets, 29(7), 2018-10-03, pp. 662-669.

Brouns, S. L. N., Van Geffen, J. P., Campello, E., Swieringa, F., Spiezia, L., Van Oerle, R., Provenzale, I., Verdoold, R., et al. (2020) 'Platelet-primed interactions of coagulation and anticoagulation pathways in flow-dependent thrombus formation.' Scientific Reports, 10(1), 2020-07-17,

Buraschi, S., Neill, T., Goyal, A., Poluzzi, C., Smythies, J., Owens, R. T., Schaefer, L., Torres, A., et al. (2013) 'Decorin causes autophagy in endothelial cells via Peg3.' Proc Natl Acad Sci U S A, 110(28), Jul 9, 2013/06/27, pp. E2582-2591.

Burk, J., Erbe, I., Berner, D., Kacza, J., Kasper, C., Pfeiffer, B., Winter, K. and Brehm, W. (2014) 'Freeze-Thaw Cycles Enhance Decellularization of Large Tendons.' Tissue Engineering Part C: Methods, 20(4), 2014-04-01, pp. 276-284.

Burke Allen, P., Virmani, R., Galis, Z., Haudenschild Christian, C. and Muller James, E. (2003) 'Task force #2—what is the pathologic basis for new atherosclerosis imaging techniques?' Journal of the American College of Cardiology, 41(11), 2003/06/04, pp. 1874-1886.

Burke, A. P., Farb, A., Malcom, G. T., Liang, Y.-H., Smialek, J. and Virmani, R. (1998) 'Effect of Risk Factors on the Mechanism of Acute Thrombosis and Sudden Coronary Death in Women.' Circulation, 97(21), 1998-06-02, pp. 2110-2116.

Burridge, K. A. and Friedman, M. H. (2010) 'Environment and vascular bed origin influence differences in endothelial transcriptional profiles of coronary and iliac arteries.' Am J Physiol Heart Circ Physiol, 299(3), Sep, 20100611, pp. H837-846.

Cahill, P. A. and Redmond, E. M. (2016) 'Vascular endothelium – Gatekeeper of vessel health.' Atherosclerosis, 248, 2016-05-01, pp. 97-109.

Calabrò, P., Gragnano, F., Golia, E. and Grove, E. L. (2018) 'von Willebrand Factor and Venous Thromboembolism: Pathogenic Link and Therapeutic Implications.' Semin Thromb Hemost, 44(03), 2018/04/09, 2017/09/12, pp. 249-260.

Camaré, C., Pucelle, M., Nègre-Salvayre, A. and Salvayre, R. (2017) 'Angiogenesis in the atherosclerotic plaque.' Redox Biol, 12, Aug, 20170201, pp. 18-34.

Carminita, E., Crescence, L., Panicot-Dubois, L. and Dubois, C. (2022) 'Role of Neutrophils and NETs in Animal Models of Thrombosis.' International Journal of Molecular Sciences, 23(3), 2022-01-26, p. 1411.

Carvalho, M. S., Silva, J. C., Cabral, J. M. S., Silva, C. L. and Vashishth, D. (2019a) 'Cultured cell-derived extracellular matrices to enhance the osteogenic differentiation and angiogenic properties of human mesenchymal stem/stromal cells.' Journal of Tissue Engineering and Regenerative Medicine, 13(9), 2019-09-01, pp. 1544-1558.

Carvalho, M. S., Silva, J. C., Udangawa, R. N., Cabral, J. M. S., Ferreira, F. C., Da Silva, C. L., Linhardt, R. J. and Vashishth, D. (2019b) 'Co-culture cell-derived extracellular matrix loaded electrospun microfibrous scaffolds for bone tissue engineering.' Materials Science and Engineering: C, 99, 2019-06-01, pp. 479-490.

Casa, L. D. C., Deaton, D. H. and Ku, D. N. (2015) 'Role of high shear rate in thrombosis.' Journal of Vascular Surgery, 61(4), 2015-04-01, pp. 1068-1080.

Castier, Y., Brandes, R. P., Leseche, G., Tedgui, A. and Lehoux, S. P. (2005) 'p47phox-Dependent NADPH Oxidase Regulates Flow-Induced Vascular Remodeling.' Circulation Research, 97(6), 2005-09-16, pp. 533-540.

Cattaneo, M. (2015) 'P2Y12 receptors: structure and function.' Journal of Thrombosis and Haemostasis, 13, 2015-06-01, pp. S10-S16.

Chamley-Campbell, J., Campbell, G. R. and Ross, R. (1979) 'The smooth muscle cell in culture.' Physiological Reviews, 59(1), 1979/01/01, pp. 1-61.

Chan, M. V., Armstrong, P. C. and Warner, T. D. (2018) '96-well plate-based aggregometry.' Platelets, 29(7), 2018-10-03, pp. 650-655.

Chan, M. V., Knowles, R. B., Lundberg, M. H., Tucker, A. T., Mohamed, N. A., Kirkby, N. S., Armstrong, P. C., Mitchell, J. A., et al. (2016) 'P2Y12 receptor blockade synergizes strongly with nitric oxide and prostacyclin to inhibit platelet activation.' Br J Clin Pharmacol, 81(4), Apr, 2015/11/13, pp. 621-633.

Chan, W. W., Yu, F., Le, Q. B., Chen, S., Yee, M. and Choudhury, D. (2021) 'Towards Biomanufacturing of Cell-Derived Matrices.' International Journal of Molecular Sciences, 22(21), 2021-11-03, p. 11929.

Chatterjee, M. and Gawaz, M. (2017) 'Clinical significance of receptor shedding-platelet GPVI as an emerging diagnostic and therapeutic tool.' Platelets, 28(4), 2017-05-19, pp. 362-371.

Chauhan, A. K., Kisucka, J., Lamb, C. B., Bergmeier, W. and Wagner, D. D. (2006) 'von Willebrand factor and factor VIII are independently required to form stable occlusive thrombi in injured veins.' Blood, 109(6) pp. 2424-2429.

Chen, D., Du, Y., Llewellyn, J., Bonna, A., Zuo, B., Janmey, P. A., Farndale, R. W. and Wells, R. G. (2022) 'Versican binds collagen via its G3 domain and regulates the organization and mechanics of collagenous matrices.' Presentation at Cold Spring Harbor Laboratory, 2022-03-27.

Chen, Y., Yuan, Y. and Li, W. (2018) 'Sorting machineries: how platelet-dense granules differ from α-granules.' Bioscience Reports, 38(5) p. BSR20180458.

Choi, S., Kim, J., Kim, J.-H., Lee, D.-K., Park, W., Park, M., Kim, S., Hwang, J. Y., et al. (2017) 'Carbon monoxide prevents TNF-α-induced eNOS downregulation by inhibiting NF-κB-responsive miR-155-5p biogenesis.' Experimental & Molecular Medicine, 49(11), 2017-11-01, pp. e403-e403.

Chuang, C. Y., Degendorfer, G., Hammer, A., Whitelock, J. M., Malle, E. and Davies, M. J. (2014) 'Oxidation modifies the structure and function of the extracellular matrix generated by human coronary artery endothelial cells.' Biochem J, 459(2), Apr 15, pp. 313-322.

Chui, A., Murthi, P., Gunatillake, T., Brennecke, S. P., Ignjatovic, V., Monagle, P. T., Whitelock, J. M. and Said, J. M. (2014) 'Altered decorin leads to disrupted endothelial cell function: A possible mechanism in the pathogenesis of fetal growth restriction?' Placenta, 35(8), 2014/08/01/, pp. 596-605.

Chui, A., Gunatillake, T., Brennecke, S. P., Ignjatovic, V., Monagle, P. T., Whitelock, J. M., van Zanten, D. E., Eijsink, J., et al. (2017) 'Expression of Biglycan in First Trimester Chorionic Villous Sampling Placental Samples and Altered Function in Telomerase-Immortalized Microvascular Endothelial Cells.' Arterioscler Thromb Vasc Biol, 37(6), Jun, 2017/04/15, pp. 1168-1179.

Ciciliano, J. C., Sakurai, Y., Myers, D. R., Fay, M. E., Hechler, B., Meeks, S., Li, R., Dixon, J. B., et al. (2015) 'Resolving the multifaceted mechanisms of the ferric chloride thrombosis model using an interdisciplinary microfluidic approach.' Blood, 126(6), Aug 6, 20150430, pp. 817-824.

Cocciolone, A. J., Hawes, J. Z., Staiculescu, M. C., Johnson, E. O., Murshed, M. and Wagenseil, J. E. (2018) 'Elastin, arterial mechanics, and cardiovascular disease.' American Journal of Physiology-Heart and Circulatory Physiology, 315(2), 2018-08-01, pp. H189-H205.

Coenen, D. M., Mastenbroek, T. G. and Cosemans, J. M. E. M. (2017) 'Platelet interaction with activated endothelium: mechanistic insights from microfluidics.' Blood, 130(26) pp. 2819-2828.

Cohen, M. and Visveswaran, G. (2020) 'Defining and managing patients with non-ST-elevation myocardial infarction: Sorting through type 1 vs other types.' Clinical Cardiology, 43(3), 2020-03-01, pp. 242-250.

Colicchia, M., Schrottmaier, W., Perrella, G., Reyat, J., Begum, J., Slater, A., Price, J., Clark, J., Zhi, Z., Simpson, M., Bourne, J., Poulter, N., Khan, A., Nicolson, P., Pugh, M., Harrison, P., Iqbal,A., Rainger, G., Watson, S., Thomas, M., Mutch, N., Assinger, A. and Rayes, J. (2022) 'S100A8/A9 drives the formation of procoagulant platelets through GPIbα.' Blood, 140(24) pp.2626-2643

Colombo, E., Calcaterra, F., Cappelletti, M., Mavilio, D. and Della Bella, S. (2013) 'Comparison of Fibronectin and Collagen in Supporting the Isolation and Expansion of Endothelial Progenitor Cells from Human Adult Peripheral Blood.' PLoS ONE, 8(6), 2013-06-18, p. e66734.

Colón, E., Shytuhina, A., Cowman, M. K., Band, P. A., Sanggaard, K. W., Enghild, J. J. and Wisniewski, H. G. (2009) 'Transfer of inter-alpha-inhibitor heavy chains to hyaluronan by surface-linked hyaluronan-TSG-6 complexes.' J Biol Chem, 284(4), Jan 23, 2008/11/27, pp. 2320-2331.

Conant, C. G., Schwartz, M. A., Beecher, J. E., Rudoff, R. C., Ionescu-Zanetti, C. and Nevill, J. T. (2011) 'Well plate microfluidic system for investigation of dynamic platelet behavior under variable shear loads.' Biotechnology and Bioengineering, 108(12), 2011-12-01, pp. 2978-2987.

Cornelison, R. C., Wellman, S. M., Park, J. H., Porvasnik, S. L., Song, Y. H., Wachs, R. A. and Schmidt, C. E. (2018) 'Development of an apoptosis-assisted decellularization method for maximal preservation of nerve tissue structure.' Acta Biomaterialia, 77, 2018-09-01, pp. 116-126.

Costa, P. F., Albers, H. J., Linssen, J. E. A., Middelkamp, H. H. T., Van Der Hout, L., Passier, R., Van Den Berg, A., Malda, J., et al. (2017) 'Mimicking arterial thrombosis in a 3D-printed microfluidic in vitro vascular model based on computed tomography angiography data.' Lab on a Chip, 17(16), 2017-01-01, pp. 2785-2792.

Coulson-Thomas, V. J., Gesteira, T. F., Hascall, V. and Kao, W. (2014) 'Umbilical cord mesenchymal stem cells suppress host rejection: the role of the glycocalyx.' J Biol Chem, 289(34), Aug 22, 2014/07/06, pp. 23465-23481.

Crapo, P. M., Gilbert, T. W. and Badylak, S. F. (2011) 'An overview of tissue and whole organ decellularization processes.' Biomaterials, 32(12), 2011-04-01, pp. 3233-3243.

D'Antoni, M. L., Risse, P.-A., Ferraro, P., Martin, J. G. and Ludwig, M. S. (2012) 'Effects of decorin and biglycan on human airway smooth muscle cell adhesion.' Matrix Biology, 31(2), 2012/03/01/, pp. 101-112.

Dai, J., Xing, L., Jia, H., Zhu, Y., Zhang, S., Hu, S., Lin, L., Ma, L., et al. (2018) 'In vivo predictors of plaque erosion in patients with ST-segment elevation myocardial infarction: a clinical, angiographical, and intravascular optical coherence tomography study.' Eur Heart J, 39(22), Jun 7, pp. 2077-2085.

Dai, J., Xing, L., Jia, H., Zhu, Y., Zhang, S., Hu, S., Lin, L., Ma, L., et al. (2018) 'In vivo predictors of plaque erosion in patients with ST-segment elevation myocardial infarction: a clinical, angiographical, and intravascular optical coherence tomography study.' European Heart Journal, 39(22) pp. 2077-2085.

Davis, G. E. and Senger, D. R. (2005) 'Endothelial Extracellular Matrix.' Circulation Research, 97(11), 2005-11-25, pp. 1093-1107.

de la Motte, C., Nigro, J., Vasanji, A., Rho, H., Kessler, S., Bandyopadhyay, S., Danese, S., Fiocchi, C., et al. (2009) 'Platelet-derived hyaluronidase 2 cleaves hyaluronan into fragments that trigger monocyte-mediated production of proinflammatory cytokines.' Am J Pathol, 174(6), Jun, 2009/05/16, pp. 2254-2264.

de Witt, S. M., Swieringa, F., Cavill, R., Lamers, M. M. E., van Kruchten, R., Mastenbroek, T., Baaten, C., Coort, S., et al. (2014) 'Identification of platelet function defects by multi-parameter assessment of thrombus formation.' Nature communications, 5 pp. 4257-4257.

Degrauwe, S., Pilgrim, T., Aminian, A., Noble, S., Meier, P. and Iglesias, J. F. (2017) 'Dual antiplatelet therapy for secondary prevention of coronary artery disease.' Open Heart, 4(2), 2017-10-01, p. e000651.

Deng, D. X.-F., Tsalenko, A., Vailaya, A., Ben-Dor, A., Kundu, R., Estay, I., Tabibiazar, R., Kincaid, R., et al. (2006) 'Differences in Vascular Bed Disease Susceptibility Reflect Differences in Gene Expression Response to Atherogenic Stimuli.' Circulation Research, 98(2), 2006-02-03, pp. 200-208.

Dimitrievska, S., Cai, C., Weyers, A., Balestrini, J. L., Lin, T., Sundaram, S., Hatachi, G., Spiegel, D. A., et al. (2015) 'Click-coated, heparinized, decellularized vascular grafts.' Acta Biomaterialia, 13, 2015-02-01, pp. 177-187.

Dours-Zimmermann, M. T. and Zimmermann, D. R. (1994) 'A novel glycosaminoglycan attachment domain identified in two alternative splice variants of human versican.' Journal of Biological Chemistry, 269(52) pp. 32992-32998.

Döring, Y., Soehnlein, O. and Weber, C. (2017) 'Neutrophil Extracellular Traps in Atherosclerosis and Atherothrombosis.' Circulation Research, 120(4), 2017-02-17, pp. 736-743.

D'Agostino, A., Stellavato, A., Corsuto, L., Diana, P., Filosa, R., La Gatta, A., De Rosa, M. and Schiraldi, C. (2017) 'Is molecular size a discriminating factor in hyaluronan interaction with human cells?' Carbohydrate Polymers, 157, 2017/02/10/, pp. 21-30.

Ebbeling, L., Robertson, C., McNicol, A. and Gerrard, J. M. (1992) 'Rapid ultrastructural changes in the dense tubular system following platelet activation.' Blood, 80(3), Aug 1, pp. 718-723.

Eckly, A., Hechler, B., Freund, M., Zerr, M., Cazenave, J. P., Lanza, F., Mangin, P. H. and Gachet, C. (2011) 'Mechanisms underlying FeCl3-induced arterial thrombosis.' Journal of Thrombosis and Haemostasis, 9(4), 2011-04-01, pp. 779-789.

Emini Veseli, B., Perrotta, P., De Meyer, G. R. A., Roth, L., Van der Donckt, C., Martinet, W. and De Meyer, G. R. Y. (2017) 'Animal models of atherosclerosis.' European Journal of Pharmacology, 816, 2017/12/05/, pp. 3-13.

Eriksson, E. E., Karlof, E., Lundmark, K., Rotzius, P., Hedin, U. and Xie, X. (2005) 'Powerful Inflammatory Properties of Large Vein Endothelium In Vivo.' Arteriosclerosis, Thrombosis, and Vascular Biology, 25(4), 2005-04-01, pp. 723-728.

Evanko, S. P., Angello, J. C. and Wight, T. N. (1999) 'Formation of hyaluronan- and versican-rich pericellular matrix is required for proliferation and migration of vascular smooth muscle cells.' Arterioscler Thromb Vasc Biol, 19(4), Apr, 1999/04/09, pp. 1004-1013.

Evanko, S. P., Johnson, P. Y., Braun, K. R., Underhill, C. B., Dudhia, J. and Wight, T. N. (2001) 'Platelet-derived growth factor stimulates the formation of versican-hyaluronan aggregates and

pericellular matrix expansion in arterial smooth muscle cells.' Arch Biochem Biophys, 394(1), Oct 1, 2001/09/22, pp. 29-38.

Farag, A., Hashimi, S. M., Vaquette, C., Volpato, F. Z., Hutmacher, D. W. and Ivanovski, S. (2018) 'Assessment of static and perfusion methods for decellularization of PCL membrane-supported periodontal ligament cell sheet constructs.' Archives of Oral Biology, 88, 2018-04-01, pp. 67-76.

Farb, A., Burke Allen, P., Tang Anita, L., Liang, Y., Mannan, P., Smialek, J. and Virmani, R. (1996) 'Coronary Plaque Erosion Without Rupture Into a Lipid Core.' Circulation, 93(7), 1996/04/01, pp. 1354-1363.

Farb, A., Kolodgie, F. D., Hwang, J.-Y., Burke, A. P., Tefera, K., Weber, D. K., Wight, T. N. and Virmani, R. (2004) 'Extracellular Matrix Changes in Stented Human Coronary Arteries.' Circulation, 110(8), 2004-08-24, pp. 940-947.

Fatkhullina, A. R., Peshkova, I. O. and Koltsova, E. K. (2016) 'The role of cytokines in the development of atherosclerosis.' Biochemistry (Moscow), 81(11), 2016/11/01, pp. 1358-1370.

Feinberg, J., Nielsen, E. E., Greenhalgh, J., Hounsome, J., Sethi, N. J., Safi, S., Gluud, C. and Jakobsen, J. C. (2017) 'Drug-eluting stents versus bare-metal stents for acute coronary syndrome.' Cochrane Database of Systematic Reviews, 2021(6), 2017-08-23,

Ferrante, G., Nakano, M., Prati, F., Niccoli, G., Mallus Maria, T., Ramazzotti, V., Montone Rocco, A., Kolodgie Frank, D., et al. (2010) 'High Levels of Systemic Myeloperoxidase Are Associated With Coronary Plaque Erosion in Patients With Acute Coronary Syndromes.' Circulation, 122(24), 2010/12/14, pp. 2505-2513.

Fertala, A. (2020) 'Three Decades of Research on Recombinant Collagens: Reinventing the Wheel or Developing New Biomedical Products?' Bioengineering, 7(4), 2020-12-02, p. 155.

Figueroa, J. E., Oubre, J. and Vijayagopal, P. (2004) 'Modulation of vascular smooth muscle cells proteoglycan synthesis by the extracellular matrix.' Journal of Cellular Physiology, 198(2), 2004-02-01, pp. 302-309.

Fischer Jens, W., Kinsella Michael, G., Levkau, B., Clowes Alexander, W. and Wight Thomas, N. (2001) 'Retroviral Overexpression of Decorin Differentially Affects the Response of Arterial

Smooth Muscle Cells to Growth Factors.' Arteriosclerosis, Thrombosis, and Vascular Biology, 21(5), 2001/05/01, pp. 777-784.

Flynn, L. E. (2010) 'The use of decellularized adipose tissue to provide an inductive microenvironment for the adipogenic differentiation of human adipose-derived stem cells.' Biomaterials, 31(17), 2010/06/01/, pp. 4715-4724.

Franco-Barraza, J., Beacham, D. A., Amatangelo, M. D. and Cukierman, E. (2016) 'Preparation of Extracellular Matrices Produced by Cultured and Primary Fibroblasts.' Current Protocols in Cell Biology, 71(1)

Freda, C., Yin, W., Ghebrehiwet, B. and Rubenstein, D. (2023) 'Complement component C1q initiates extrinsic coagulation via the receptor for the globular head of C1q in adventitial fibroblasts and vascular smooth muscle cells.' Immunity, inflammation and disease, 11(1) pp. 769-770.

Frelinger, A., Michelson, A. and Gremmel, T. (2016) 'Platelet Physiology.' Seminars in Thrombosis and Hemostasis, 42(03), pp. 191-204.

Fukaya, Y. and Ohhashi, T. (1996) 'Acetylcholine- and flow-induced production and release of nitric oxide in arterial and venous endothelial cells.' American Journal of Physiology-Heart and Circulatory Physiology, 270(1), pp. H99-H106.

Gallo, N., Natali, M. L., Sannino, A. and Salvatore, L. (2020) 'An Overview of the Use of Equine Collagen as Emerging Material for Biomedical Applications.' Journal of Functional Biomaterials, 11(4) pp. 79.

Ganesan, M. K., Finsterwalder, R., Leb, H., Resch, U., Neumüller, K., de Martin, R. and Petzelbauer, P. (2017) 'Three-Dimensional Coculture Model to Analyze the Cross Talk Between Endothelial and Smooth Muscle Cells.' Tissue Eng Part C Methods, 23(1) pp. 38-49.

Gardiner, E. E. and Andrews, R. K. (2014) 'Platelet Receptor Expression and Shedding: Glycoprotein Ib-IX-V and Glycoprotein VI.' Transfusion Medicine Reviews, 28(2) pp. 56-60.

Garin, G., Abe, J.-I., Mohan, A., Lu, W., Yan, C., Newby, A. C., Rhaman, A. and Berk, B. C. (2007) 'Flow Antagonizes TNF-α Signaling in Endothelial Cells by Inhibiting Caspase-Dependent PKCζ Processing.' Circulation Research, 101(1) pp. 97-105.

Geenen, I. L. A., Molin, D. G. M., Van Den Akker, N. M. S., Jeukens, F., Spronk, H. M., Schurink, G. W. H. and Post, M. J. (2015) 'Endothelial cells (ECs) for vascular tissue engineering: venous ECs are less thrombogenic than arterial ECs.' Journal of Tissue Engineering and Regenerative Medicine, 9(5) pp. 564-576.

Getachew, R., Ballinger, M. L., Burch, M. L., Reid, J. J., Khachigian, L. M., Wight, T. N., Little, P. J. and Osman, N. (2010) 'PDGF β-Receptor Kinase Activity and ERK1/2 Mediate Glycosaminoglycan Elongation on Biglycan and Increases Binding to LDL.' Endocrinology, 151(9) pp. 4356-4367.

Getz, G. S. and Reardon, C. A. (2012) 'Animal Models of Atherosclerosis.' Arteriosclerosis, Thrombosis, and Vascular Biology, 32(5) pp. 1104-1115.

Gialeli, C., Shami, A. and Gonçalves, I. (2021) 'Extracellular matrix: paving the way to the newest trends in atherosclerosis.' Current Opinion in Lipidology, 32(5)

Gifre-Renom, L., Daems, M., Luttun, A. and Jones, E. A. V. (2022) 'Organ-Specific Endothelial Cell Differentiation and Impact of Microenvironmental Cues on Endothelial Heterogeneity.' International Journal of Molecular Sciences, 23(3) p. 1477.

Gocheva, V., Naba, A., Bhutkar, A., Guardia, T., Miller, K. M., Li, C. M.-C., Dayton, T. L., Sanchez-Rivera, F. J., et al. (2017) 'Quantitative proteomics identify Tenascin-C as a promoter of lung cancer progression and contributor to a signature prognostic of patient survival.' Proceedings of the National Academy of Sciences, 114(28) pp. E5625-E5634.

Godeau, A. L., Delanoë-Ayari, H. and Riveline, D. (2020) 'Generation of fluorescent cell-derived-matrix to study 3D cell migration.' In Methods in Cell Biology. Elsevier, pp. 185-203. [Accessed on 2023-06-06T10:09:44]

Golebiewska, E. M. and Poole, A. W. (2015) 'Platelet secretion: From haemostasis to wound healing and beyond.' Blood Rev, 29(3) pp. 153-162.

Grandoch, M., Kohlmorgen, C., Melchior-Becker, A., Feldmann, K., Homann, S., Müller, J., Kiene, L. S., Zeng-Brouwers, J., et al. (2016) 'Loss of Biglycan Enhances Thrombin Generation in Apolipoprotein E-Deficient Mice: Implications for Inflammation and Atherosclerosis.' Arterioscler Thromb Vasc Biol, 36(5) pp. e41-50.

Greenwel, P., Tanaka, S., Penkov, D., Zhang, W., Olive, M., Moll, J., Vinson, C., Di Liberto, M., et al. (2000) 'Tumor Necrosis Factor Alpha Inhibits Type I Collagen Synthesis through Repressive CCAAT/Enhancer-Binding Proteins.' Molecular and Cellular Biology, 20(3) pp. 912-918.

Greineder, C. F., Johnston, I. H., Villa, C. H., Gollomp, K., Esmon, C. T., Cines, D. B., Poncz, M. and Muzykantov, V. R. (2017) 'ICAM-1–targeted thrombomodulin mitigates tissue factor–driven inflammatory thrombosis in a human endothelialized microfluidic model.' Blood Advances, 1(18) pp. 1452-1465.

Grover, S. P. and Mackman, N. (2020) 'How useful are ferric chloride models of arterial thrombosis?' Platelets, 31(4) pp. 432-438.

Gui, L., Muto, A., Chan, S. A., Breuer, C. K. and Niklason, L. E. (2009) 'Development of decellularized human umbilical arteries as small-diameter vascular grafts.' Tissue Eng Part A, 15(9), Sep, pp. 2665-2676.

Guidetti, G., Bertoni, A., Viola, M., Tira, E., Balduini, C. and Torti, M. (2002) 'The small proteoglycan decorin supports adhesion and activation of human platelets.' Blood, 100(5) pp. 1707-1714.

Guo, X., Li, W., Ma, M., Lu, X. and Zhang, H. (2017) 'Endothelial cell-derived matrix promotes the metabolic functional maturation of hepatocyte via
integrin-Src signalling.' Journal of Cellular and Molecular Medicine, 21(11), 2017-11-01, pp. 2809-2822.

Gutmann, C., Siow, R., Gwozdz, A. M., Saha, P. and Smith, A. (2020) 'Reactive Oxygen Species in Venous Thrombosis.' International Journal of Molecular Sciences, 21(6), 2020-03-11, p. 1918.

Guyette, J. P., Gilpin, S. E., Charest, J. M., Tapias, L. F., Ren, X. and Ott, H. C. (2014) 'Perfusion decellularization of whole organs.' Nat Protoc, 9(6) pp. 1451-1468.

Hajal, C., Offeddu, G. S., Shin, Y., Zhang, S., Morozova, O., Hickman, D., Knutson, C. G. and Kamm, R. D. (2022) 'Engineered human blood–brain barrier microfluidic model for vascular permeability analyses.' Nature Protocols, 17(1) pp. 95-128.

Hamilos, M., Petousis, S. and Parthenakis, F. (2018) 'Interaction between platelets and endothelium: from pathophysiology to new therapeutic options.' Cardiovasc Diagn Ther, 8(5) pp. 568-580.

Hansson, G. K., Libby, P. and Tabas, I. (2015) 'Inflammation and plaque vulnerability.' Journal of Internal Medicine, 278(5) pp. 483-493.

Hansson, K. M., Nielsen, S., Elg, M. and Deinum, J. (2014) 'The effect of corn trypsin inhibitor and inhibiting antibodies for FXIa and FXIIa on coagulation of plasma and whole blood.' Journal of Thrombosis and Haemostasis, 12(10) pp. 1678-1686.

Hao, E., Pang, G., Du, Z., Lai, Y.-H., Chen, J.-R., Xie, J., Zhou, K., Hou, X., et al. (2019) 'Peach Kernel Oil Downregulates Expression of Tissue Factor and Reduces Atherosclerosis in ApoE knockout Mice.' International Journal of Molecular Sciences, 20(2) p. 405.

Harada, H. and Takahashi, M. (2007) 'CD44-dependent Intracellular and Extracellular Catabolism of Hyaluronic Acid by Hyaluronidase-1 and -2.' Journal of Biological Chemistry, 282(8) pp. 5597-5607.

Hayes, C., Kitahara, S. and Tcherniantchouk, O. (2014) 'Decreased Threshold of Aggregation to Low-Dose Epinephrine is Evidence of Platelet Hyperaggregability in Patients with Thrombosis.' Hematology Reports, 6(3) p. 5326.

He, F., Chen, X. and Pei, M. (2009) 'Reconstruction of an In Vitro Tissue-Specific Microenvironment to Rejuvenate Synovium-Derived Stem Cells for Cartilage Tissue Engineering.' Tissue Engineering Part A, 15(12) pp. 3809-3821.

He, L., Giri, T. K., Vicente, C. P. and Tollefsen, D. M. (2008) 'Vascular dermatan sulfate regulates the antithrombotic activity of heparin cofactor II.' Blood, 111(8) pp. 4118-4125.

Heemskerk, J. W. M., Sakariassen, K. S., Zwaginga, J. J., Brass, L. F., Jackson, S. P. and Farndale, R. W. (2011) 'Collagen surfaces to measure thrombus formation under flow: possibilities for standardization.' Journal of Thrombosis and Haemostasis, 9(4) pp. 856-858.

Hennan, J. K., Huang, J., Barrett, T. D., Driscoll, E. M., Willens, D. E., Park, A. M., Crofford, L. J. and Lucchesi, B. R. (2001) 'Effects of Selective Cyclooxygenase-2 Inhibition on Vascular Responses and Thrombosis in Canine Coronary Arteries.' Circulation, 104(7), 2001-08-14, pp. 820-825.

Herbig, B. A., Yu, X. and Diamond, S. L. (2018) 'Using microfluidic devices to study thrombosis in pathological blood flows.' Biomicrofluidics, 12(4), 2018-07-01, p. 042201.

Hielscher, A. C., Qiu, C. and Gerecht, S. (2012) 'Breast cancer cell-derived matrix supports vascular morphogenesis.' Am J Physiol Cell Physiol, 302(8), Apr 15, 20120125, pp. C1243-1256.

Hisada, Y. and Mackman, N. (2018) 'Mouse models of cancer-associated thrombosis.' Thrombosis Research, 164, 2018-04-01, pp. S48-S53.

Holinstat, M. (2017) 'Normal platelet function.' Cancer and Metastasis Reviews, 36(2), 2017-06-01, pp. 195-198.

Holme, P. L. A., Ørvim, U., Hamers, M. J. A. G., Solum, N. O., Brosstad, F. R., Barstad, R. M. and Sakariassen, K. S. (1997) 'Shear-Induced Platelet Activation and Platelet Microparticle Formation at Blood Flow Conditions as in Arteries With a Severe Stenosis.' Arteriosclerosis, Thrombosis, and Vascular Biology, 17(4), 1997-04-01, pp. 646-653.

Honda, K., Matoba, T., Antoku, Y., Koga, J.-i., Ichi, I., Nakano, K., Tsutsui, H. and Egashira, K. (2018) 'Lipid-Lowering Therapy With Ezetimibe Decreases Spontaneous Atherothrombotic Occlusions in a Rabbit Model of Plaque Erosion.' Arteriosclerosis, Thrombosis, and Vascular Biology, 38(4), 2018/04/01, pp. 757-771.

Hosokawa, K., Ohnishi, T., Kondo, T., Fukasawa, M., Koide, T., Maruyama, I. and Tanaka, K. A. (2011) 'A novel automated microchip flow-chamber system to quantitatively evaluate thrombus formation and antithrombotic agents under blood flow conditions.' Journal of Thrombosis and Haemostasis, 9(10), 2011-10-01, pp. 2029-2037.

Hosokawa, K., Ohnishi, T., Fukasawa, M., Kondo, T., Sameshima, H., Koide, T., Tanaka, K. A. and Maruyama, I. (2012) 'A microchip flow-chamber system for quantitative assessment of the platelet thrombus formation process.' Microvasc Res, 83(2), Mar, 20111206, pp. 154-161.

Hosseini, V., Mallone, A., Nasrollahi, F., Ostrovidov, S., Nasiri, R., Mahmoodi, M., Haghniaz, R., Baidya, A., et al. (2021) 'Healthy and diseased in vitro models of vascular systems.' Lab on a Chip, 21(4), 2021-01-01, pp. 641-659.

Hu, M., Ling, Z. and Ren, X. (2022) 'Extracellular matrix dynamics: tracking in biological systems and their implications.' Journal of Biological Engineering, 16(1), 2022-12-01,

Huang, E. S., Strate, L. L., Ho, W. W., Lee, S. S. and Chan, A. T. (2011) 'Long-Term Use of Aspirin and the Risk of Gastrointestinal Bleeding.' The American Journal of Medicine, 124(5), 2011-05-01, pp. 426-433.

Hwang, J.-Y., Johnson, P. Y., Braun, K. R., Hinek, A., Fischer, J. W., O'Brien, K. D., Starcher, B., Clowes, A. W., et al. (2008) 'Retrovirally mediated overexpression of glycosaminoglycan-deficient biglycan in arterial smooth muscle cells induces tropoelastin synthesis and elastic fiber formation in vitro and in neointimae after vascular injury.' The American journal of pathology, 173(6) 2008/11/06, pp. 1919-1928.

Iglesias-De La Cruz, M. C., Ruiz-Torres, P., Alcamí, J., Díez-Marqués, L., Ortega-Velázquez, R., Chen, S., Rodríguez-Puyol, M., Ziyadeh, F. N., et al. (2001) 'Hydrogen peroxide increases extracellular matrix mRNA through TGF-β in human mesangial cells.' Kidney International, 59(1), 2001-01-01, pp. 87-95.

Iozzo, R. V. and Schaefer, L. (2015) 'Proteoglycan form and function: A comprehensive nomenclature of proteoglycans.' Matrix Biol, 42, Mar, 2015/02/24, pp. 11-55.

Iozzo, R. V., Moscatello, D. K., McQuillan, D. J. and Eichstetter, I. (1999) 'Decorin Is a Biological Ligand for the Epidermal Growth Factor Receptor.' Journal of Biological Chemistry, 274(8) pp. 4489-4492.

Ivey, M. E. and Little, P. J. (2008) 'Thrombin regulates vascular smooth muscle cell proteoglycan synthesis via PAR-1 and multiple downstream signalling pathways.' Thrombosis Research, 123(2), 2008/12/01/, pp. 288-297.

Jalilian, I., Muppala, S., Ali, M., Anderson, J. D., Phinney, B., Salemi, M., Wilmarth, P. A., Murphy, C. J., et al. (2023) 'Cell derived matrices from bovine corneal endothelial cells as a model to study cellular dysfunction.' Experimental Eye Research, 226, 2023/01/01/, p. 109303.

Jia, H., Abtahian, F., Aguirre, A. D., Lee, S., Chia, S., Lowe, H., Kato, K., Yonetsu, T., et al. (2013) 'In vivo diagnosis of plaque erosion and calcified nodule in patients with acute coronary syndrome by intravascular optical coherence tomography.' J Am Coll Cardiol, 62(19), Nov 5, 2013/07/03, pp. 1748-1758.

Jooss, N. J., De Simone, I., Provenzale, I., Fernández, D. I., Brouns, S. L. N., Farndale, R. W., Henskens, Y. M. C., Kuijpers, M. J. E., et al. (2019) 'Role of Platelet Glycoprotein VI and Tyrosine Kinase Syk in Thrombus Formation on Collagen-Like Surfaces.' International Journal of Molecular Sciences, 20(11), 2019-06-07, p. 2788.

Jurk, K. and Kehrel, B. E. (2005a) 'Platelets: Physiology and Biochemistry.' Seminars in Thrombosis and Hemostasis, 31(04), 2005-08-01, pp. 381-392.

Jurk, K. and Kehrel, B. E. (2005b) 'Platelets: Physiology and Biochemistry.' Seminars in Thrombosis and Hemostasis, 31(04), 2005-08-01, pp. 381-392.

Kaczmarek, E., Koziak, K., Sévigny, J., Siegel, J. B., Anrather, J., Beaudoin, A. R., Bach, F. H. and Robson, S. C. (1996) 'Identification and Characterization of CD39/Vascular ATP Diphosphohydrolase.' Journal of Biological Chemistry, 271(51) pp. 33116-33122.

Kaira, B., Slater, A., McCrae, K., Dreveny, I., Sumya, U., Mutch, N., Searle, M and Emsley, J. (2020) ‘Factor XII and kininogen asymmetric assembly with gC1qR/C1QBP/P32 is governed by allostery.’ Blood, 136(14) pp. 1685-1697.

Kamińska, A., Enguita, F. J. and Stępień, E. Ł. (2018) 'Lactadherin: An unappreciated haemostasis regulator and potential therapeutic agent.' Vascular Pharmacology, 101, 2018/02/01/, pp. 21-28.

Karel, M., Hechler, B., Kuijpers, M. and Cosemans, J. (2020) 'Atherosclerotic plaque injury-mediated murine thrombosis models: advantages and limitations.' Platelets, 31(4), 2020-05-18, pp. 439-446.

Kattoor, A. J., Pothineni, N. V. K., Palagiri, D. and Mehta, J. L. (2017) 'Oxidative Stress in Atherosclerosis.' Current Atherosclerosis Reports, 19(11), 2017-11-01,

Kaur, R., Kaur, M. and Singh, J. (2018) 'Endothelial dysfunction and platelet hyperactivity in type 2 diabetes mellitus: molecular insights and therapeutic strategies.' Cardiovascular Diabetology, 17(1), 2018-12-01,

Kawashima, H., Hirose, M., Hirose, J., Nagakubo, D., Plaas, A. H. K. and Miyasaka, M. (2000) 'Binding of a Large Chondroitin Sulfate/Dermatan Sulfate Proteoglycan, Versican, to L-selectin, P-selectin, and CD44.' Journal of Biological Chemistry, 275(45) pp. 35448-35456.

Keene, D. R., San Antonio, J. D., Mayne, R., McQuillan, D. J., Sarris, G., Santoro, S. A. and Iozzo, R. V. (2000) 'Decorin binds near the C terminus of type I collagen.' J Biol Chem, 275(29), Jul 21, 2000/05/24, pp. 21801-21804.

Khodabandehlou, K., Masehi-Lano, J. J., Poon, C., Wang, J. and Chung, E. J. (2017) 'Targeting cell adhesion molecules with nanoparticles using in vivo and flow-based in vitro models of atherosclerosis.' Experimental Biology and Medicine, 242(8), 2017-04-01, pp. 799-812.

Kim, Y. S., Majid, M., Melchiorri, A. J. and Mikos, A. G. (2019) 'Applications of decellularized extracellular matrix in bone and cartilage tissue engineering.' Bioengineering & Translational Medicine, 4(1), 2019-01-01, pp. 83-95.

Kirkby, N. S., Lundberg, M. H., Wright, W. R., Warner, T. D., Paul-Clark, M. J. and Mitchell, J. A. (2014) 'COX-2 Protects against Atherosclerosis Independently of Local Vascular Prostacyclin: Identification of COX-2 Associated Pathways Implicate Rgl1 and Lymphocyte Networks.' PLoS ONE, 9(6), 2014-06-02, p. e98165.

Klarhöfer, M., Csapo, B., Balassy, C., Szeles, J. C. and Moser, E. (2001) 'High-resolution blood flow velocity measurements in the human finger.' Magnetic Resonance in Medicine, 45(4), 2001-04-01, pp. 716-719.

Kohda, D., Morton, C. J., Parkar, A. A., Hatanaka, H., Inagaki, F. M., Campbell, I. D. and Day, A. J. (1996) 'Solution structure of the link module: a hyaluronan-binding domain involved in extracellular matrix stability and cell migration.' Cell, 86(5), Sep 6, 1996/09/06, pp. 767-775.

Kohli, S., Shahzad, K., Jouppila, A., Holthöfer, H., Isermann, B. and Lassila, R. (2022) 'Thrombosis and Inflammation—A Dynamic Interplay and the Role of Glycosaminoglycans and Activated Protein C.' Frontiers in Cardiovascular Medicine, 9

Kolodgie, F. D., Burke, A. P., Wight, T. N. and Virmani, R. (2004) 'The accumulation of specific types of proteoglycans in eroded plaques: a role in coronary thrombosis in the absence of rupture.' Current Opinion in Lipidology, 15(5)

Kolodgie, F. D., Burke, A. P., Farb, A., Weber, D. K., Kutys, R., Wight, T. N. and Virmani, R. (2002) 'Differential accumulation of proteoglycans and hyaluronan in culprit lesions: insights into plaque erosion.' Arterioscler Thromb Vasc Biol, 22(10), Oct 1, 2002/10/16, pp. 1642-1648.

Koshiishi, I., Shizari, M. and Underhill, C. B. (1994) 'CD44 can mediate the adhesion of platelets to hyaluronan.' Blood, 84(2), Jul 15, 1994/07/15, pp. 390-396.

Koupenova, M., Clancy, L., Corkrey, H. A. and Freedman, J. E. (2018) 'Circulating Platelets as Mediators of Immunity, Inflammation, and Thrombosis.' Circulation Research, 122(2), 2018-01-19, pp. 337-351.

Krautter, F., Hussain, M. T., Zhi, Z., Lezama, D. R., Manning, J. E., Brown, E., Marigliano, N., Raucci, F., et al. (2022) 'Galectin-9: A novel promoter of atherosclerosis progression.' Atherosclerosis, 363, 2022-12-01, pp. 57-68.

Kroll, M. H. and Schafer, A. I. (1989) 'Biochemical Mechanisms of Platelet Activation.' Blood, 74(4), 1989/09/01/, pp. 1181-1195.

Kroon, J., Heemskerk, N., Kalsbeek, M. J. T., De Waard, V., Van Rijssel, J. and Van Buul, J. D. (2017a) 'Flow-induced endothelial cell alignment requires the RhoGEF Trio as a scaffold protein to polarize active Rac1 distribution.' Molecular Biology of the Cell, 28(13), 2017-07-01, pp. 1745-1753.

Kroon, J., Heemskerk, N., Kalsbeek, M. J. T., De Waard, V., Van Rijssel, J. and Van Buul, J. D. (2017b) 'Flow-induced endothelial cell alignment requires the RhoGEF Trio as a scaffold protein to polarize active Rac1 distribution.' Molecular Biology of the Cell, 28(13), 2017-07-01, pp. 1745-1753.

Kular, J. K., Basu, S. and Sharma, R. I. (2014) 'The extracellular matrix: Structure, composition, age-related differences, tools for analysis and applications for tissue engineering.' J Tissue Eng, 5 20141220, p. 2041731414557112.

Kunde, S. S. and Wairkar, S. (2021) 'Platelet membrane camouflaged nanoparticles: Biomimetic architecture for targeted therapy.' International Journal of Pharmaceutics, 598, 2021/04/01/, p. 120395.

Kuznetsova, S. A., Issa, P., Perruccio, E. M., Zeng, B., Sipes, J. M., Ward, Y., Seyfried, N. T., Fielder, H. L., et al. (2006) 'Versican-thrombospondin-1 binding in vitro and colocalization in microfibrils induced by inflammation on vascular smooth muscle cells.' J Cell Sci, 119(Pt 21), Nov 1, 2006/10/19, pp. 4499-4509.

Kölm, R., Schaller, M., Roumenina, L. T., Niemiec, I., Kremer Hovinga, J. A., Khanicheh, E., Kaufmann, B. A., Hopfer, H., et al. (2016) 'Von Willebrand Factor Interacts with Surface-Bound C1q and Induces Platelet Rolling.' J Immunol, 197(9), Nov 1, 2016/10/05, pp. 3669-3679.

Lakota, K., Mrak-Poljsak, K., Rozman, B. and Sodin-Semrl, S. (2009) 'Increased Responsiveness of Human Coronary Artery Endothelial Cells in Inflammation and Coagulation.' Mediators of Inflammation, 2009, 2009-01-01, pp. 1-8.

Lang, I., Pabst, M. A., Hiden, U., Blaschitz, A., Dohr, G., Hahn, T. and Desoye, G. (2003) 'Heterogeneity of microvascular endothelial cells isolated from human term placenta and macrovascular umbilical vein endothelial cells.' European Journal of Cell Biology, 82(4), 2003/04/01/, pp. 163-173.

Lauer, M. E., Glant, T. T., Mikecz, K., DeAngelis, P. L., Haller, F. M., Husni, M. E., Hascall, V. C. and Calabro, A. (2013) 'Irreversible heavy chain transfer to hyaluronan oligosaccharides by tumor necrosis factor-stimulated gene-6.' The Journal of biological chemistry, 288(1) 2012/11/19, pp. 205-214.

Lavigne, D., Guerrier, L., Gueguen, V., Michel, J.-B., Boschetti, E., Meilhac, O. and Letourneur, D. (2010) 'Culture of human cells and synthesis of extracellular matrix on materials compatible with direct analysis by mass spectrometry.' The Analyst, 135(3), 2010-01-01, p. 503.

Lemire Joan, M., Braun Kathleen, R., Maurel, P., Kaplan Elizabeth, D., Schwartz Stephen, M. and Wight Thomas, N. (1999) 'Versican/PG-M Isoforms in Vascular Smooth Muscle Cells.' Arteriosclerosis, Thrombosis, and Vascular Biology, 19(7), 1999/07/01, pp. 1630-1639.

Lepäntalo, A., Beer, J. H., Siljander, P., Syrjälä, M. and Lassila, R. (2001) 'Variability in platelet responses to collagen--comparison between whole blood perfusions, traditional platelet function tests and PFA-100.' Thromb Res, 103(2), Jul 15, pp. 123-133.

Li, J., Wu, F., Zhang, K., He, Z., Zou, D., Luo, X., Fan, Y., Yang, P., et al. (2017) 'Controlling Molecular Weight of Hyaluronic Acid Conjugated on Amine-rich Surface: Toward Better Multifunctional Biomaterials for Cardiovascular Implants.' ACS Applied Materials & Interfaces, 9(36), 2017/09/13, pp. 30343-30358.

Li, M., Qian, M., Kyler, K. and Xu, J. (2018) 'Endothelial-Vascular Smooth Muscle Cells Interactions in Atherosclerosis.' Front Cardiovasc Med, 5 20181023, p. 151.

Liang, J., Jiang, D. and Noble, P. W. (2016) 'Hyaluronan as a therapeutic target in human diseases.' Advanced Drug Delivery Reviews, 97, 2016/02/01/, pp. 186-203.

Lin, C., Pan, C., Wang, C., Liu, S., Hsiao, L. and Yang, C. (2015) ‘Tumor necrosis factor-alpha induces VCAM-1-mediated inflammation via c-Src-dependent transactivation of EGF receptors in human cardiac fibroblasts.’ Journal of Biomedical Science, 22(1) pp. 53-55.

Lin, C.-H., Hsia, K., Ma, H., Lee, H. and Lu, J.-H. (2018) 'In Vivo Performance of Decellularized Vascular Grafts: A Review Article.' International Journal of Molecular Sciences, 19(7) p. 2101.

Lindsey, M. L., Jung, M., Hall, M. E. and Deleon-Pennell, K. Y. (2018) 'Proteomic analysis of the cardiac extracellular matrix: clinical research applications.' Expert Review of Proteomics, 15(2), 2018-02-01, pp. 105-112.

Litwiniuk, M., Krejner, A., Speyrer, M. S., Gauto, A. R. and Grzela, T. (2016) 'Hyaluronic Acid in Inflammation and Tissue Regeneration.' Wounds, 28(3), Mar, 2016/03/16, pp. 78-88.

Liu, G., Alzoubi, K., Chatterjee, M., Walker, B., Münzer, P., Luo, D., Umbach, A. T., Elvira, B., et al. (2016) 'CD44 sensitivity of platelet activation, membrane scrambling and adhesion under high arterial shear rates.' Thromb Haemost, 115(1), Jan, 2015/09/12, pp. 99-108.

Liu, M. and Gomez, D. (2019) 'Smooth Muscle Cell Phenotypic Diversity.' Arteriosclerosis, Thrombosis, and Vascular Biology, 39(9), 2019-09-01, pp. 1715-1723.

Liu, R., Chen, L., Wu, W., Chen, H. and Zhang, S. (2016) 'Extracellular matrix turnover in coronary artery ectasia patients.' Heart and Vessels, 31(3), 2016-03-01, pp. 351-359.

Liu, Y., Lin, J., Wu, X., Guo, X., Sun, H., Yu, B., Shen, J., Bai, J., et al. (2019) 'Aspirin-Mediated Attenuation of Intervertebral Disc Degeneration by Ameliorating Reactive Oxygen Species In Vivo and In Vitro.' Oxidative Medicine and Cellular Longevity, 2019, 2019-11-06, pp. 1-20.

Liu, Z. L., Bresette, C., Aidun, C. K. and Ku, D. N. (2022) 'SIPA in 10 milliseconds: VWF tentacles agglomerate and capture platelets under high shear.' Blood Adv, 6(8), Apr 26, pp. 2453-2465.

Livak, K. J. and Schmittgen, T. D. (2001) 'Analysis of Relative Gene Expression Data Using Real-Time Quantitative PCR and the 2−ΔΔCT Method.' Methods, 25(4), 2001/12/01/, pp. 402-408.

Lord, M. S. and Whitelock, J. M. (2013) 'Recombinant production of proteoglycans and their bioactive domains.' FEBS Journal, 280(10), 2013-05-01, pp. 2490-2510.

Lu, P., Takai, K., Weaver, V. M. and Werb, Z. (2011) 'Extracellular Matrix Degradation and Remodeling in Development and Disease.' Cold Spring Harbor Perspectives in Biology, 3(12), 2011-12-01, pp. a005058-a005058.

Luo, X., Zhao, C., Wang, S., Jia, H. and Yu, B. (2022) 'TNF-α is a Novel Biomarker for Predicting Plaque Rupture in Patients with ST-Segment Elevation Myocardial Infarction.' Journal of Inflammation Research, Volume 15, 2022-03-01, pp. 1889-1898.

Ma, Z., Mao, C., Jia, Y., Fu, Y. and Kong, W. (2020) 'Extracellular matrix dynamics in vascular remodeling.' American Journal of Physiology-Cell Physiology, 319(3), 2020/09/01, pp. C481-C499.

Machha, V. R., Tischer, A., Moon-Tasson, L. and Auton, M. (2017) 'The Von Willebrand Factor A1–Collagen III Interaction Is Independent of Conformation and Type 2 Von Willebrand Disease Phenotype.' Journal of Molecular Biology, 429(1), 2017-01-01, pp. 32-47.

Mackman, N. (2016) 'Mouse models of venous thrombosis are not equal.' Blood, 127(21) pp. 2510-2511.

Malakpour-Permlid, A., Buzzi, I., Hegardt, C., Johansson, F. and Oredsson, S. (2021) 'Identification of extracellular matrix proteins secreted by human dermal fibroblasts cultured in 3D electrospun scaffolds.' Scientific Reports, 11(1), 2021-03-23,

Manning, B. D. and Toker, A. (2017) 'AKT/PKB Signaling: Navigating the Network.' Cell, 169(3) pp. 381-405.

Mansour, A., Krautter, F., Zhi, Z., Iqbal, A and Recio, C. (2022) 'The interplay of galectins-1, -3, and -9 in the immune-inflammatory response underlying cardiovascular and metabolic disease.' Cardiovascular Diabetology, 21(1) pp.253-255

Mastenbroek, T. G., van Geffen, J. P., Heemskerk, J. W. M. and Cosemans, J. M. E. M. (2015) 'Acute and persistent platelet and coagulant activities in atherothrombosis.' Journal of Thrombosis and Haemostasis, 13(S1), 2015/06/01, pp. S272-S280.

Mathur, T., Tronolone, J. J. and Jain, A. (2021) 'Comparative Analysis of Blood-Derived Endothelial Cells for Designing Next-Generation Personalized Organ-on-Chips.' Journal of the American Heart Association, 10(22), 2021-11-16,

Matsuzawa, Y., Kimura, K., Yasuda, S., Kaikita, K., Akao, M., Ako, J., Matoba, T., Nakamura, M., et al. (2021) 'Antithrombotic Therapy for Atrial Fibrillation and Coronary Artery Disease in Patients With Prior Atherothrombotic Disease: A Post Hoc Analysis of the AFIRE Trial.' Journal of the American Heart Association, 10(21), 2021-11-02,

Maurer, S., Kopp, H.-G., Salih, H. R. and Kropp, K. N. (2020) 'Modulation of Immune Responses by Platelet-Derived ADAM10.' Frontiers in Immunology, 11

Mauri, L., Kereiakes, D. J., Yeh, R. W., Driscoll-Shempp, P., Cutlip, D. E., Steg, P. G., Normand, S.-L. T., Braunwald, E., et al. (2014) 'Twelve or 30 Months of Dual Antiplatelet Therapy after Drug-Eluting Stents.' New England Journal of Medicine, 371(23), 2014-12-04, pp. 2155-2166.

Mazzucato, M., Cozzi, M. R., Pradella, P., Perissinotto, D., Malmström, A., Mörgelin, M., Spessotto, P., Colombatti, A., et al. (2002) 'Vascular PG-M/versican variants promote platelet adhesion at low shear rates and cooperate with collagens to induce aggregation.' The FASEB Journal, 16(14), 2002/12/01, pp. 1903-1916.

McGuire, E. A. and Tollefsen, D. M. (1987) 'Activation of heparin cofactor II by fibroblasts and vascular smooth muscle cells.' J Biol Chem, 262(1), Jan 5, 1987/01/05, pp. 169-175.

Mega, J. L. and Simon, T. (2015) 'Pharmacology of antithrombotic drugs: an assessment of oral antiplatelet and anticoagulant treatments.' The Lancet, 386(9990), 2015/07/18/, pp. 281-291.

Meng, F., Cheng, H., Qian, J., Dai, X., Huang, Y. and Fan, Y. (2022) 'In vitro fluidic systems: Applying shear stress on endothelial cells.' Medicine in Novel Technology and Devices, 15, 2022/09/01/, p. 100143.

Michels, A., Dwyer, C. N., Mewburn, J., Nesbitt, K., Kawecki, C., Lenting, P., Swystun, L. L. and Lillicrap, D. (2020) 'von Willebrand Factor Is a Critical Mediator of Deep Vein Thrombosis in a Mouse Model of Diet-Induced Obesity.' Arteriosclerosis, Thrombosis, and Vascular Biology, 40(12), 2020-12-01, pp. 2860-2874.

Miller, R. M., Jordan, B. T., Mehlferber, M. M., Jeffery, E. D., Chatzipantsiou, C., Kaur, S., Millikin, R. J., Dai, Y., et al. (2022) 'Enhanced protein isoform characterization through long-read proteogenomics.' Genome Biology, 23(1)

Montague, S. J., Hicks, S. M., Lee, C. S. M., Coupland, L. A., Parish, C. R., Lee, W. M., Andrews, R. K. and Gardiner, E. E. (2020) 'Fibrin exposure triggers αIIbβ3-independent platelet aggregate formation, ADAM10 activity and glycoprotein VI shedding in a charge-dependent manner.' Journal of Thrombosis and Haemostasis, 18(6) pp. 1447-1458.

Moro, M. A., Russel, R. J., Cellek, S., Lizasoain, I., Su, Y., Darley-Usmar, V. M., Radomski, M. W. and Moncada, S. (1996) 'cGMP mediates the vascular and platelet actions of nitric oxide:

confirmation using an inhibitor of the soluble guanylyl cyclase.' Proceedings of the National Academy of Sciences of the United States of America, 93(4) pp. 1480-1485.

Mosher, D., Maurer, L. and Carlson, C. (2008) ‘Secreted thrombospondin-1 controls platelet sensitivity to NO.’ Blood, 111(2) pp. 473-474

Murthi, P., Faisal, F. A., Rajaraman, G., Stevenson, J., Ignjatovic, V., Monagle, P. T., Brennecke, S. P. and Said, J. M. (2010) 'Placental Biglycan Expression is Decreased in Human Idiopathic Fetal Growth Restriction.' Placenta, 31(8) pp. 712-717.

Méndez-Barbero, N., Gutiérrez-Muñoz, C. and Blanco-Colio, L. (2021) 'Cellular Crosstalk between Endothelial and Smooth Muscle Cells in Vascular Wall Remodeling.' International Journal of Molecular Sciences, 22(14) p. 7284.

Münzel, T. and Daiber, A. (2020) 'Novel Concept for the Regulation of eNOS (Endothelial Nitric Oxide Synthase) Activity.' Arteriosclerosis, Thrombosis, and Vascular Biology, 40(7), 2020-07-01, pp. 1608-1610.

Naso, M. F., Zimmermann, D. R. and Iozzo, R. V. (1994) 'Characterization of the complete genomic structure of the human versican gene and functional analysis of its promoter.' Journal of Biological Chemistry, 269(52) pp. 32999-33008.

Neeves, K. B., Maloney, S. F., Fong, K. P., Schmaier, A. A., Kahn, M. L., Brass, L. F. and Diamond, S. L. (2008) 'Microfluidic focal thrombosis model for measuring murine platelet deposition and stability: PAR4 signaling enhances shear-resistance of platelet aggregates.' Journal of Thrombosis and Haemostasis, 6(12), 2008-12-01, pp. 2193-2201.

Neeves, K. B., Onasoga, A. A., Hansen, R. R., Lilly, J. J., Venckunaite, D., Sumner, M. B., Irish, A. T., Brodsky, G., et al. (2013) 'Sources of Variability in Platelet Accumulation on Type 1 Fibrillar Collagen in Microfluidic Flow Assays.' PLoS ONE, 8(1), 2013-01-23, p. e54680.

Neishabouri, A., Soltani Khaboushan, A., Daghigh, F., Kajbafzadeh, A.-M. and Majidi Zolbin, M. (2022) 'Decellularization in Tissue Engineering and Regenerative Medicine: Evaluation, Modification, and Application Methods.' Frontiers in Bioengineering and Biotechnology, 10

Ng, W. H., Ramasamy, R., Yong, Y. K., Ngalim, S. H., Lim, V., Shaharuddin, B. and Tan, J. J. (2019) 'Extracellular matrix from decellularized mesenchymal stem cells improves cardiac gene expressions and oxidative resistance in cardiac C-kit cells.' Regenerative Therapy, 11, 2019/12/01/, pp. 8-16.

Nielsen, V. G. (2009) 'Corn trypsin inhibitor decreases tissue-type plasminogen activator-mediated fibrinolysis of human plasma.' Blood Coagul Fibrinolysis, 20(3), Apr, pp. 191-196.

Nisar, S. P., Lordkipanidzé, M., Jones, M. L., Dawood, B. B., Murden, S., Cunningham, M. R., Mumford, A. D., Wilde, J. T., et al. (2014) 'A novel thromboxane A2 receptor N42S variant results in reduced surface expression and platelet dysfunction.' Thrombosis and Haemostasis, 112(05), 2014-01-01, pp. 923-932.

O'Brien, K. D., Lewis, K., Fischer, J. W., Johnson, P., Hwang, J. Y., Knopp, E. A., Kinsella, M. G., Barrett, P. H., et al. (2004) 'Smooth muscle cell biglycan overexpression results in increased lipoprotein retention on extracellular matrix: implications for the retention of lipoproteins in atherosclerosis.' Atherosclerosis, 177(1), Nov, 2004/10/19, pp. 29-35.

Okhota, S., Melnikov, I., Avtaeva, Y., Kozlov, S. and Gabbasov, Z. (2020) 'Shear Stress-Induced Activation of von Willebrand Factor and Cardiovascular Pathology.' International Journal of Molecular Sciences, 21(20), 2020-10-21, p. 7804.

Olie, R. H., van der Meijden, P. E. J. and Ten Cate, H. (2018) 'The coagulation system in atherothrombosis: Implications for new therapeutic strategies.' Res Pract Thromb Haemost, 2(2), Apr, 2018/07/27, pp. 188-198.

Osman, N., Getachew, R., Thach, L., Wang, H., Su, X., Zheng, W. and Little, P. J. (2014) 'Platelet-derived growth factor-stimulated versican synthesis but not glycosaminoglycan elongation in vascular smooth muscle is mediated via Akt phosphorylation.' Cellular Signalling, 26(5), 2014/05/01/, pp. 912-916.

Otsuka, F., Yasuda, S., Noguchi, T. and Ishibashi-Ueda, H. (2016) 'Pathology of coronary atherosclerosis and thrombosis.' Cardiovasc Diagn Ther, 6(4), Aug, 2016/08/09, pp. 396-408.

Ott, H. C., Matthiesen, T. S., Goh, S.-K., Black, L. D., Kren, S. M., Netoff, T. I. and Taylor, D. A. (2008) 'Perfusion-decellularized matrix: using nature's platform to engineer a bioartificial heart.' Nature Medicine, 14(2), 2008/02/01, pp. 213-221.

Packham, M. A. and Mustard, J. F. (2005) 'Platelet aggregation and adenosine diphosphate/adenosine triphosphate receptors: a historical perspective.' Semin Thromb Hemost, 31(2), Apr, pp. 129-138.

Paderi, J. E., Stuart, K., Sturek, M., Park, K. and Panitch, A. (2011) 'The inhibition of platelet adhesion and activation on collagen during balloon angioplasty by collagen-binding peptidoglycans.' Biomaterials, 32(10), 2011/04/01/, pp. 2516-2523.

Palacios-Acedo, A.-L., Mege, D., Crescence, L., Panicot-Dubois, L. and Dubois, C. (2020) 'Cancer animal models in thrombosis research.' Thrombosis Research, 191, 2020/07/01/, pp. S112-S116.

Panteleev, M. A., Korin, N., Reesink, K. D., Bark, D. L., Cosemans, J. M. E. M., Gardiner, E. E. and Mangin, P. H. (2021) 'Wall shear rates in human and mouse arteries: Standardization of hemodynamics for in vitro blood flow assays: Communication from the ISTH SSC subcommittee on biorheology.' Journal of Thrombosis and Haemostasis, 19(2), 2021-02-01, pp. 588-595.

Pati, F., Jang, J., Ha, D.-H., Won Kim, S., Rhie, J.-W., Shim, J.-H., Kim, D.-H. and Cho, D.-W. (2014) 'Printing three-dimensional tissue analogues with decellularized extracellular matrix bioink.' Nature Communications, 5(1), 2014-06-02,

Pearson, J. D. (1999) 'Endothelial cell function and thrombosis.' Best Practice & Research Clinical Haematology, 12(3), 1999/09/01/, pp. 329-341.

Pedicino, D., Vinci, R., Giglio, A. F., Pisano, E., Porto, I., Vergallo, R., Russo, G., Ruggio, A., et al. (2018) 'Alterations of Hyaluronan Metabolism in Acute Coronary Syndrome: Implications for Plaque Erosion.' J Am Coll Cardiol, 72(13), Sep 25, 2018/09/22, pp. 1490-1503.

Pedroza, A. J., Koyano, T., Trojan, J., Rubin, A., Palmon, I., Jaatinen, K., Burdon, G., Chang, P., et al. (2020) 'Divergent effects of canonical and non-canonical TGF-β signalling on mixed contractile-synthetic smooth muscle cell phenotype in human Marfan syndrome aortic root aneurysms.' Journal of Cellular and Molecular Medicine, 24(3), 2020-02-01, pp. 2369-2383.

Peerschke, E. I. and Ghebrehiwet, B. (1997) 'C1q augments platelet activation in response to aggregated Ig.' Journal of immunology (Baltimore, Md. : 1950), 159(11), 1997/12//, pp. 5594-5598.

Peerschke, E. I., Reid, K. B. and Ghebrehiwet, B. (1993) 'Platelet activation by C1q results in the induction of alpha IIb/beta 3 integrins (GPIIb-IIIa) and the expression of P-selectin and procoagulant activity.' J Exp Med, 178(2), Aug 1, 1993/08/01, pp. 579-587.

Pei, M. and He, F. (2012) 'Extracellular matrix deposited by synovium-derived stem cells delays replicative senescent chondrocyte dedifferentiation and enhances redifferentiation.' Journal of Cellular Physiology, 227(5), 2012-05-01, pp. 2163-2174.

Petrey, A. C. and de la Motte, C. A. (2014) 'Hyaluronan, a crucial regulator of inflammation.' Frontiers in immunology, 5 pp. 101-101.

Petrey, A. C., Obery, D. R., Kessler, S. P., Flamion, B. and de la Motte, C. A. (2016) 'Hyaluronan Depolymerization by Megakaryocyte Hyaluronidase-2 Is Required for Thrombopoiesis.' The American journal of pathology, 186(9) 2016/07/08, pp. 2390-2403.

Petrey, A. C., Obery, D. R., Kessler, S. P., Zawerton, A., Flamion, B. and de la Motte, C. A. (2019) 'Platelet hyaluronidase-2 regulates the early stages of inflammatory disease in colitis.' Blood, 134(9), Aug 29, 2019/07/03, pp. 765-775.

Pike, J. A., Simms, V. A., Smith, C. W., Morgan, N. V., Khan, A. O., Poulter, N. S., Styles, I. B. and Thomas, S. G. (2021) 'An adaptable analysis workflow for characterization of platelet spreading and morphology.' Platelets, 32(1), 2021-01-02, pp. 54-58.

Pivkin, I. V., Richardson, P. D. and Karniadakis, G. (2006) 'Blood flow velocity effects and role of activation delay time on growth and form of platelet thrombi.' Proceedings of the National Academy of Sciences, 103(46), 2006-11-14, pp. 17164-17169.

Poluzzi, C., Nastase, M.-V., Zeng-Brouwers, J., Roedig, H., Hsieh, L. T.-H., Michaelis, J. B., Buhl, E. M., Rezende, F., et al. (2019) 'Biglycan evokes autophagy in macrophages via a novel CD44/Toll-like receptor 4 signaling axis in ischemia/reperfusion injury.' Kidney International, 95(3), 2019/03/01/, pp. 540-562.

Provenzale, I., De Simone, I., Gibbins, J., Heemskerk, J., van der Meijden, P. and Jones, C. (2023) ‘Regulation of Glycoprotein VI-Dependent Platelet Activation and Thrombus Formation by Heparan Sulfate Proteoglycan Perlecan.’ International Journal of Molecular Science, 24(17) pp. 13352

Pugh, N., Simpson, A. M., Smethurst, P. A., de Groot, P. G., Raynal, N. and Farndale, R. W. (2010) 'Synergism between platelet collagen receptors defined using receptor-specific collagen-mimetic peptide substrata in flowing blood.' Blood, 115(24), Jun 17, 20100329, pp. 5069-5079.

Qin, W., Ho, L., Wang, J., Peskind, E. and Pasinetti, G. M. (2009) 'S100A7, a Novel Alzheimer's Disease Biomarker with Non-Amyloidogenic α-Secretase Activity Acts via Selective Promotion of ADAM-10.' PLoS ONE, 4(1), 2009-01-13, p. e4183.

Quach, M. E., Chen, W. and Li, R. (2018) 'Mechanisms of platelet clearance and translation to improve platelet storage.' Blood, 131(14), Apr 5, 20180223, pp. 1512-1521.

Quillard, T., Franck, G., Mawson, T., Folco, E. and Libby, P. (2017) 'Mechanisms of erosion of atherosclerotic plaques.' Curr Opin Lipidol, 28(5), Oct, 2017/07/07, pp. 434-441.

Rahman, S., Griffin, M., Naik, A., Szarko, M. and Butler, P. E. M. (2018) 'Optimising the decellularization of human elastic cartilage with trypsin for future use in ear reconstruction.' Scientific Reports, 8(1), 2018-02-15,

Raines, E. W. (2001) 'The extracellular matrix can regulate vascular cell migration, proliferation, and survival: relationships to vascular disease.' International Journal of Experimental Pathology, 81(3), 2001-12-25, pp. 173-182.

Randi, A. M., Smith, K. E. and Castaman, G. (2018) 'von Willebrand factor regulation of blood vessel formation.' Blood, 132(2) pp. 132-140.

Reed, E., Fellows, A., Lu, R., Rienks, M., Schmidt, L., Yin, X., Duregotti, E., Brandt, M., et al. (2022) 'Extracellular Matrix Profiling and Disease Modelling in Engineered Vascular Smooth Muscle Cell Tissues.' Matrix Biology Plus, 16, 2022/12/01/, p. 100122.

Robinson, K. A., Sun, M., Barnum, C. E., Weiss, S. N., Huegel, J., Shetye, S. S., Lin, L., Saez, D., et al. (2017) 'Decorin and biglycan are necessary for maintaining collagen fibril structure, fiber

realignment, and mechanical properties of mature tendons.' Matrix Biol, 64, Dec, 2017/09/09, pp. 81-93.

Roffi, M., Patrono, C., Collet, J.-P., Mueller, C., Valgimigli, M., Andreotti, F., Bax, J. J., Borger, M. A., et al. (2016) '2015 ESC Guidelines for the management of acute coronary syndromes in patients presenting without persistent ST-segment elevation: Task Force for the Management of Acute Coronary Syndromes in Patients Presenting without Persistent ST-Segment Elevation of the European Society of Cardiology (ESC).' European Heart Journal, 37(3) pp. 267-315.

Roque, M., Fallon, J. T., Badimon, J. J., Zhang, W. X., Taubman, M. B. and Reis, E. D. (2000) 'Mouse Model of Femoral Artery Denudation Injury Associated With the Rapid Accumulation of Adhesion Molecules on the Luminal Surface and Recruitment of Neutrophils.' Arteriosclerosis, Thrombosis, and Vascular Biology, 20(2), 2000-02-01, pp. 335-342.

Roth, L., Rombouts, M., Schrijvers, D. M., Emini Veseli, B., Martinet, W. and De Meyer, G. R. Y. (2021) 'Acetylsalicylic Acid Reduces Passive Aortic Wall Stiffness and Cardiovascular Remodelling in a Mouse Model of Advanced Atherosclerosis.' International Journal of Molecular Sciences, 23(1), 2021-12-30, p. 404.

Roux, E., Bougaran, P., Dufourcq, P. and Couffinhal, T. (2020) 'Fluid Shear Stress Sensing by the Endothelial Layer.' Frontiers in Physiology, 11

Rubí-Sans, G., Nyga, A., Rebollo, E., Pérez-Amodio, S., Otero, J., Navajas, D., Mateos-Timoneda, M. A. and Engel, E. (2021) 'Development of Cell-Derived Matrices for Three-Dimensional In Vitro Cancer Cell Models.' ACS Applied Materials & Interfaces, 13(37), 2021-09-22, pp. 44108-44123.

Sakariassen, K. S., Aarts, P. A., de Groot, P. G., Houdijk, W. P. and Sixma, J. J. (1983) 'A perfusion chamber developed to investigate platelet interaction in flowing blood with human vessel wall cells, their extracellular matrix, and purified components.' J Lab Clin Med, 102(4), Oct, pp. 522-535.

Sakurai, Y., Hardy, E. T., Ahn, B., Tran, R., Fay, M. E., Ciciliano, J. C., Mannino, R. G., Myers, D. R., et al. (2018) 'A microengineered vascularized bleeding model that integrates the principal components of hemostasis.' Nature Communications, 9(1), 2018-02-06,

Sandmann, R. and Köster, S. (2016) 'Topographic Cues Reveal Two Distinct Spreading Mechanisms in Blood Platelets.' Scientific Reports, 6(1), 2016-03-03, p. 22357.

Sasaki, S., Nishihira, K., Yamashita, A., Fujii, T., Onoue, K., Saito, Y., Hatakeyama, K., Shibata, Y., et al. (2022) 'Involvement of enhanced expression of classical complement C1q in atherosclerosis progression and plaque instability: C1q as an indicator of clinical outcome.' PLOS ONE, 17(1), 2022-01-27, p. e0262413.

Schaefer, L., Beck, K. F., Raslik, I., Walpen, S., Mihalik, D., Micegova, M., Macakova, K., Schonherr, E., et al. (2003) 'Biglycan, a nitric oxide-regulated gene, affects adhesion, growth, and survival of mesangial cells.' J Biol Chem, 278(28), Jul 11, 2003/04/30, pp. 26227-26237.

Schober, A., Manka, D., Von Hundelshausen, P., Huo, Y., Hanrath, P., Sarembock, I. J., Ley, K. and Weber, C. (2002) 'Deposition of Platelet RANTES Triggering Monocyte Recruitment Requires P-Selectin and Is Involved in Neointima Formation After Arterial Injury.' Circulation, 106(12), 2002-09-17, pp. 1523-1529.

Schoeman, R. M., Lehmann, M. and Neeves, K. B. (2017) 'Flow chamber and microfluidic approaches for measuring thrombus formation in genetic bleeding disorders.' Platelets, 28(5), 2017-07-04, pp. 463-471.

Schon, B. S., Hooper, G. J. and Woodfield, T. B. F. (2017) 'Modular Tissue Assembly Strategies for Biofabrication of Engineered Cartilage.' Annals of Biomedical Engineering, 45(1), 2017-01-01, pp. 100-114.

Schultz, G. S. and Wysocki, A. (2009) 'Interactions between extracellular matrix and growth factors in wound healing.' Wound Repair and Regeneration, 17(2), 2009/03/01, pp. 153-162.

Scott, R. A., Ramaswamy, A. K., Park, K. and Panitch, A. (2017) 'Decorin mimic promotes endothelial cell health in endothelial monolayers and endothelial–smooth muscle co-cultures.' Journal of Tissue Engineering and Regenerative Medicine, 11(5), 2017/05/01, pp. 1365-1376.

Seetapun, D. and Ross, J. J. (2017) 'Eliminating the organ transplant waiting list: The future with perfusion decellularized organs.' Surgery, 161(6), 2017-06-01, pp. 1474-1478.

Selvadurai, M. V. and Hamilton, J. R. (2018) 'Structure and function of the open canalicular system – the platelet's specialized internal membrane network.' Platelets, 29(4), 2018-05-19, pp. 319-325.

Semeraro, F., Ammollo, C. T., Morrissey, J. H., Dale, G. L., Friese, P., Esmon, N. L. and Esmon, C. T. (2011) 'Extracellular histones promote thrombin generation through platelet-dependent mechanisms: involvement of platelet TLR2 and TLR4.' Blood, 118(7), Aug 18, 2011/06/16, pp. 1952-1961.

Shao, J., Wu, L., Wu, J., Zheng, Y., Zhao, H., Jin, Q. and Zhao, J. (2009) 'Integrated microfluidic chip for endothelial cells culture and analysis exposed to a pulsatile and oscillatory shear stress.' Lab on a Chip, 9(21), 2009-01-01, p. 3118.

Shao, X., Taha, I. N., Clauser, K. R., Gao, Y. and Naba, A. (2020) 'MatrisomeDB: the ECM-protein knowledge database.' Nucleic Acids Research, 48(D1) pp. D1136-D1144.

Sharma, R., Kumar, P., Prashanth, S. P. and Belagali, Y. (2020) 'Dual Antiplatelet Therapy in Coronary Artery Disease.' Cardiology and Therapy, 9(2), 2020-12-01, pp. 349-361.

Shen, J., Sampietro, S., Wu, J., Tang, J., Gupta, S., Matzko, C. N., Tang, C., Yu, Y., et al. (2017) 'Coordination of platelet agonist signaling during the hemostatic response in vivo.' Blood advances, 1(27) pp. 2767-2775.

Shevchenko, A., Wilm, M., Vorm, O. and Mann, M. (1996) 'Mass spectrometric sequencing of proteins from silver-stained polyacrylamide gels.' Analytical Chemistry, 68(1) pp. 850–858.

Simionescu, M., Simionescu, N. and Palade, G. E. (1976) 'Segmental differentiations of cell junctions in the vascular endothelium. Arteries and veins.' J Cell Biol, 68(3), Mar, pp. 705-723.

Simunovic, F., Winninger, O., Strassburg, S., Koch, H. G., Finkenzeller, G., Stark, G. B. and Lampert, F. M. (2019) 'Increased differentiation and production of extracellular matrix components of primary human osteoblasts after cocultivation with endothelial cells: A quantitative proteomics approach.' Journal of Cellular Biochemistry, 120(1), 2019-01-01, pp. 396-404.

Slevin, M., Krupinski, J., Gaffney, J., Matou, S., West, D., Delisser, H., Savani, R. C. and Kumar, S. (2007) 'Hyaluronan-mediated angiogenesis in vascular disease: uncovering RHAMM and CD44 receptor signaling pathways.' Matrix Biol, 26(1), Jan, 2006/10/24, pp. 58-68.

Sloop, G., Weidman, J. J. and St. Cyr, J. A. (2017) 'Atherothrombosis is a Thrombotic, not Inflammatory Disease.' Cureus, 2017-12-05,

Smith, W. L. and Murphy, R. C. (2008) 'CHAPTER 12 - The eicosanoids: cyclooxygenase, lipoxygenase, and epoxygenase pathways.' In Vance, D. E. and Vance, J. E. (eds.) Biochemistry of Lipids, Lipoproteins and Membranes (Fifth Edition). San Diego: Elsevier, pp. 331-362. https://www.sciencedirect.com/science/article/pii/B9780444532190500143

Song, G., Zheng, C., Liu, Y., Ding, M., Liu, P., Xu, J., Wang, W. and Wang, J. (2021) 'In vitro extracellular matrix deposition by vascular smooth muscle cells grown in fibroin scaffolds, and the regulation of TGF-β1.' Materials & Design, 199, 2021/02/01/, p. 109428.

Sonneveld, M. A. H., de Maat, M. P. M. and Leebeek, F. W. G. (2014) 'Von Willebrand factor and ADAMTS13 in arterial thrombosis: a systematic review and meta-analysis.' Blood Reviews, 28(4), 2014/07/01/, pp. 167-178.

Spagnoli, L. G., Bonanno, E., Sangiorgi, G. and Mauriello, A. (2007) 'Role of Inflammation in Atherosclerosis.' Journal of Nuclear Medicine, 48(11), 2007-11-01, pp. 1800-1815.

Speich, H. E., Grgurevich, S., Kueter, T. J., Earhart, A. D., Slack, S. M. and Jennings, L. K. (2008) 'Platelets undergo phosphorylation of Syk at Y525/526 and Y352 in response to pathophysiological shear stress.' Am J Physiol Cell Physiol, 295(4), Oct, 2008/08/22, pp. C1045-1054.

Starke, R. M., Thompson, J. W., Ali, M. S., Pascale, C. L., Martinez Lege, A., Ding, D., Chalouhi, N., Hasan, D. M., et al. (2018) 'Cigarette Smoke Initiates Oxidative Stress-Induced Cellular Phenotypic Modulation Leading to Cerebral Aneurysm Pathogenesis.' Arteriosclerosis, Thrombosis, and Vascular Biology, 38(3), 2018-03-01, pp. 610-621.

Stern, R. and Jedrzejas, M. J. (2006) 'Hyaluronidases: Their Genomics, Structures, and Mechanisms of Action.' Chemical Reviews, 106(3), 2006/03/01, pp. 818-839.

Stober, V. P., Johnson, C. G., Majors, A., Lauer, M. E., Cali, V., Midura, R. J., Wisniewski, H.-G., Aronica, M. A., et al. (2017) 'TNF-stimulated gene 6 promotes formation of hyaluronan-inter-α-inhibitor heavy chain complexes necessary for ozone-induced airway hyperresponsiveness.' The Journal of biological chemistry, 292(51) 2017/11/09, pp. 20845-20858.

Tamayo-Angorrilla, M., López De Andrés, J., Jiménez, G. and Marchal, J. A. (2022) 'The biomimetic extracellular matrix: a therapeutic tool for breast cancer research.' Translational Research, 247, 2022-09-01, pp. 117-136.

Tammi, M. I., Day, A. J. and Turley, E. A. (2002) 'Hyaluronan and Homeostasis: A Balancing Act.' Journal of Biological Chemistry, 277(7) pp. 4581-4584.

Tao, D. L., Tassi Yunga, S., Williams, C. D. and McCarty, O. J. T. (2021) 'Aspirin and antiplatelet treatments in cancer.' Blood, 137(23), Jun 10, pp. 3201-3211.

Teasdale, J. E., Hazell, G. G. J., Peachey, A. M. G., Sala-Newby, G. B., Hindmarch, C. C. T., Mckay, T. R., Bond, M., Newby, A. C., et al. (2017) 'Cigarette smoke extract profoundly suppresses TNFα-mediated proinflammatory gene expression through upregulation of ATF3 in human coronary artery endothelial cells.' Scientific Reports, 7(1), 2017-01-06, p. 39945.

Ten Cate, H. and Hemker, H. C. (2016) 'Thrombin Generation and Atherothrombosis: What Does the Evidence Indicate?' J Am Heart Assoc, 5(8), Aug 8, 2016/08/10,

Theocharis, A. D., Skandalis, S. S., Gialeli, C. and Karamanos, N. K. (2016) 'Extracellular matrix structure.' Adv Drug Deliv Rev, 97, Feb 1, 2015/11/13, pp. 4-27.

Thygesen, K., Alpert, J. S., Jaffe, A. S., Chaitman, B. R., Bax, J. J., Morrow, D. A., White, H. D. and Group, E. S. C. S. D. (2019) 'Fourth universal definition of myocardial infarction (2018).' European Heart Journal, 40(3) pp. 237-269.

Tiede, K., Melchior-Becker, A. and Fischer, J. W. (2009) 'Transcriptional and posttranscriptional regulators of biglycan in cardiac fibroblasts.' Basic Research in Cardiology, 105(1), 2009/08/23, p. 99.

Tomokiyo, K., Kamikubo, Y., Hanada, T., Araki, T., Nakatomi, Y., Ogata, Y., Jung, S. M., Nakagaki, T., et al. (2005) 'Von Willebrand factor accelerates platelet adhesion and thrombus formation

on a collagen surface in platelet-reduced blood under flow conditions.' Blood, 105(3) pp. 1078-1084.

Toole, B. P. (2004) 'Hyaluronan: from extracellular glue to pericellular cue.' Nat Rev Cancer, 4(7), Jul, 2004/07/02, pp. 528-539.

Tran, N., Garcia, T., Aniqa, M., Ali, S., Ally, A. and Nauli, S. M. (2022) 'Endothelial Nitric Oxide Synthase (eNOS) and the Cardiovascular System: in Physiology and in Disease States.' Am J Biomed Sci Res, 15(2) 20220104, pp. 153-177.

Tsai, M., Kita, A., Leach, J., Rounsevell, R., Huang, J. N., Moake, J., Ware, R. E., Fletcher, D. A., et al. (2012) 'In vitro modeling of the microvascular occlusion and thrombosis that occur in hematologic diseases using microfluidic technology.' Journal of Clinical Investigation, 122(1), 2012-01-03, pp. 408-418.

Tsai, T. T., Ho, P. M., Xu, S., Powers, J. D., Carroll, N. M., Shetterly, S. M., Maddox, T. M., Rumsfeld, J. S., et al. (2010) 'Increased Risk of Bleeding in Patients on Clopidogrel Therapy After Drug-Eluting Stents Implantation.' Circulation: Cardiovascular Interventions, 3(3), 2010-06-01, pp. 230-235.

Turley, E. A., Noble, P. W. and Bourguignon, L. Y. W. (2002) 'Signaling Properties of Hyaluronan Receptors.' Journal of Biological Chemistry, 277(7) pp. 4589-4592.

Van Aelst, B., Feys, H. B., Devloo, R., Vandekerckhove, P. and Compernolle, V. (2016) 'Microfluidic Flow Chambers Using Reconstituted Blood to Model Hemostasis and Platelet Transfusion In Vitro.' Journal of Visualized Experiments, (109), 2016-03-19,

Verheye, S., Markou Christos, P., Salame Mahomed, Y., Wan, B., King Spencer, B., Robinson Keith, A., Chronos Nicolas, A. F. and Hanson Stephen, R. (2000) 'Reduced Thrombus Formation by Hyaluronic Acid Coating of Endovascular Devices.' Arteriosclerosis, Thrombosis, and Vascular Biology, 20(4), 2000/04/01, pp. 1168-1172.

Virmani, R., Burke, A. P., Farb, A. and Kolodgie, F. D. (2006) 'Pathology of the vulnerable plaque.' J Am Coll Cardiol, 47(8 Suppl), Apr 18, 2006/04/25, pp. C13-18.

Vogler, E. A. and Siedlecki, C. A. (2009) 'Contact activation of blood-plasma coagulation.' Biomaterials, 30(10), 2009-04-01, pp. 1857-1869.

Vos, T., Lim, S. S., Abbafati, C., Abbas, K. M., Abbasi, M., Abbasifard, M., Abbasi-Kangevari, M., Abbastabar, H., et al. (2020) 'Global burden of 369 diseases and injuries in 204 countries and territories, 1990–2019: a systematic analysis for the Global Burden of Disease Study 2019.' The Lancet, 396(10258), 2020-10-01, pp. 1204-1222.

Wang, J., Li, H., He, J., Li, B., Bao, Q., Zhang, X., Lv, Z., Zhang, Y., et al. (2015) '20-Hydroxyeicosatetraenoic acid involved in endothelial activation and thrombosis.' Am J Physiol Heart Circ Physiol, 308(11), Jun 1, 20150327, pp. H1359-1367.

Weber, C., Badimon, L., Mach, F. and Van Der Vorst, E. P. C. (2017) 'Therapeutic strategies for atherosclerosis and atherothrombosis: Past, present and future.' Thrombosis and Haemostasis, 117(07), 2017-01-01, pp. 1258-1264.

Weigel, P. H., Fuller, G. M. and LeBoeuf, R. D. (1986) 'A model for the role of hyaluronic acid and fibrin in the early events during the inflammatory response and wound healing.' Journal of Theoretical Biology, 119(2), 1986/03/21/, pp. 219-234.

Weinberg, C. B. and Bell, E. (1985) 'Regulation of proliferation of bovine aortic endothelial cells, smooth muscle cells, and adventitial fibroblasts in collagen lattices.' Journal of Cellular Physiology, 122(3), 1985/03/01, pp. 410-414.

Westein, E., De Witt, S., Lamers, M., Cosemans, J. M. E. M. and Heemskerk, J. W. M. (2012) 'Monitoringin vitrothrombus formation with novel microfluidic devices.' Platelets, 23(7), 2012-11-01, pp. 501-509.

Westrick, R. J., Winn, M. E. and Eitzman, D. T. (2007) 'Murine Models of Vascular Thrombosis.' Arteriosclerosis, Thrombosis, and Vascular Biology, 27(10), 2007-10-01, pp. 2079-2093.

Whelan, M. C. and Senger, D. R. (2003) 'Collagen I Initiates Endothelial Cell Morphogenesis by Inducing Actin Polymerization through Suppression of Cyclic AMP and Protein Kinase A.' Journal of Biological Chemistry, 278(1), 2003-01-01, pp. 327-334.

Whinna, H. C., Choi, H. U., Rosenberg, L. C. and Church, F. C. (1993) 'Interaction of heparin cofactor II with biglycan and decorin.' Journal of Biological Chemistry, 268(6) pp. 3920-3924.

White, S. J., Newby, A. C. and Johnson, T. W. (2016) 'Endothelial erosion of plaques as a substrate for coronary thrombosis.' Thromb Haemost, 115(3), Mar, 2016/01/23, pp. 509-519.

White, S. J., Hayes, E. M., Lehoux, S., Jeremy, J. Y., Horrevoets, A. J. G. and Newby, A. C. (2010) 'Response of the endothelial cell transcriptome to supraphysiological laminar shear stress.' Atherosclerosis, 213(1), 2010-11-01, pp. e8-e9.

White-Adams, T. C., Berny, M. A., Patel, I. A., Tucker, E. I., Gailani, D., Gruber, A. and Mccarty, O. J. T. (2010) 'Laminin promotes coagulation and thrombus formation in a factor XII-dependent manner.' Journal of Thrombosis and Haemostasis, 8(6), 2010-06-01, pp. 1295-1301.

Wight, T. N. (2002) 'Versican: a versatile extracellular matrix proteoglycan in cell biology.' Current Opinion in Cell Biology, 14(5), 2002/10/01/, pp. 617-623.

Wight, T. N. (2017) 'Provisional matrix: A role for versican and hyaluronan.' Matrix Biology, 60-61, 2017-07-01, pp. 38-56.

Wight, T. N. (2017) 'Provisional matrix: A role for versican and hyaluronan.' Matrix Biol, 60-61, Jul, 2016/12/10, pp. 38-56.

Wight, T. N. (2018) 'A Role for Extracellular Matrix in Atherosclerotic Plaque Erosion.' J Am Coll Cardiol, 72(13), Sep 25, 2018/09/22, pp. 1504-1505.

Wight, T. N., Kinsella, M. G., Evanko, S. P., Potter-Perigo, S. and Merrilees, M. J. (2014) 'Versican and the regulation of cell phenotype in disease.' Biochimica et biophysica acta, 1840(8) 2014/01/05, pp. 2441-2451.

Witjas, F. M. R., van den Berg, B. M., van den Berg, C. W., Engelse, M. A. and Rabelink, T. J. (2019) 'Concise Review: The Endothelial Cell Extracellular Matrix Regulates Tissue Homeostasis and Repair.' Stem Cells Transl Med, 8(4), Apr, 20181211, pp. 375-382.

Wittig, C. and Szulcek, R. (2021) 'Extracellular Matrix Protein Ratios in the Human Heart and Vessels: How to Distinguish Pathological From Physiological Changes?' Front Physiol, 12 20210804, p. 708656.

Wu, M.-Y., Li, C.-J., Hou, M.-F. and Chu, P.-Y. (2017) 'New Insights into the Role of Inflammation in the Pathogenesis of Atherosclerosis.' International Journal of Molecular Sciences, 18(10), 2017-09-22, p. 2034.

Wu, Y., Chen, L., Zheng, P. S. and Yang, B. B. (2002) 'beta 1-Integrin-mediated glioma cell adhesion and free radical-induced apoptosis are regulated by binding to a C-terminal domain of PG-M/versican.' J Biol Chem, 277(14), Apr 5, 2002/01/24, pp. 12294-12301.

Xu, J. and Shi, G.-P. (2014) 'Vascular wall extracellular matrix proteins and vascular diseases.' Biochimica et Biophysica Acta (BBA) - Molecular Basis of Disease, 1842(11), 2014-11-01, pp. 2106-2119.

Xu, S., Liu, Y., Ding, Y., Luo, S., Zheng, X., Wu, X., Liu, Z., Ilyas, I., et al. (2021) 'The zinc finger transcription factor, KLF2, protects against COVID-19 associated endothelial dysfunction.' Signal Transduction and Targeted Therapy, 6(1), 2021-07-12,

Xu, X. R., Yousef, G. M. and Ni, H. (2018) 'Cancer and platelet crosstalk: opportunities and challenges for aspirin and other antiplatelet agents.' Blood, 131(16) pp. 1777-1789.

Xu, Y., Yan, M., Gong, Y., Chen, L., Zhao, F. and Zhang, Z. (2014) 'Response of endothelial cells to decellularized extracellular matrix deposited by bone marrow mesenchymal stem cells.' Int J Clin Exp Med, 7(12) 20141215, pp. 4997-5003.

Yadav, S. and Storrie, B. (2017) 'The cellular basis of platelet secretion: Emerging structure/function relationships.' Platelets, 28(2), 2017-02-17, pp. 108-118.

Yahagi, K., Davis, H. R., Arbustini, E. and Virmani, R. (2015) 'Sex differences in coronary artery disease: Pathological observations.' Atherosclerosis, 239(1), 2015/03/01/, pp. 260-267.

Yamaguchi, Y., Mann, D. M. and Ruoslahti, E. (1990) 'Negative regulation of transforming growth factor-beta by the proteoglycan decorin.' Nature, 346(6281), Jul 19, 1990/07/19, pp. 281-284.

Yamamoto, K., de Waard, V., Fearns, C. and Loskutoff, D. J. (1998) 'Tissue distribution and regulation of murine von Willebrand factor gene expression in vivo.' Blood, 92(8), Oct 15, pp. 2791-2801.

Yamauchi, M., Taga, Y., Hattori, S., Shiiba, M. and Terajima, M. (2018) 'Chapter 6 - Analysis of collagen and elastin cross-links.' In Mecham, R. P. (ed.) Methods in Cell Biology. Vol. 143. Academic Press, pp. 115-132.

Yang, Z. H., Von Segesser, L., Bauer, E., Stulz, P., Turina, M. and Lüscher, T. F. (1991) 'Different activation of the endothelial L-arginine and cyclooxygenase pathway in the human internal mammary artery and saphenous vein.' Circulation Research, 68(1) pp. 52-60.

Yang, C., Yang, C., Hsiao, L., Yu, C., Tseng, H., Hsu, C. and Situmorang, J. (2021) 'Upregulation of COX-2 and PGE2 Induced by TNF-α Mediated Through TNFR1/MitoROS/PKCα/P38 MAPK, JNK1/2/FoxO1 Cascade in Human Cardiac Fibroblasts.' Journal of Inflammation Research, 14(1) pp. 2807-2824.

Yau, J. W., Teoh, H. and Verma, S. (2015) 'Endothelial cell control of thrombosis.' BMC Cardiovascular Disorders, 15(1) pp. 55-58

Yin, X., Bern, M., Xing, Q., Ho, J., Viner, R. and Mayr, M. (2013) 'Glycoproteomic analysis of the secretome of human endothelial cells.' Mol Cell Proteomics, 12(4) pp. 956-978.

Zarubin, T. and Han, J. (2005) 'Activation and signaling of the p38 MAP kinase pathway.' Cell Res, 15(1) pp. 11-18.

Zavala, J., Montalvo-Parra, M.-D., Guerrero-Ramírez, G.-I., Rodríguez-Barrientos, C.-A., Treviño, V. and Valdez-García, J. E. (2018) 'Primary explant culture and collagen I substrate enhances corneal endothelial cell morphology.' BMC Research Notes, 11(1) pp. 689-721

Zhang, D. and Dou, K. (2015) 'Coronary Bifurcation Intervention: What Role Do Bifurcation Angles Play?' Journal of Interventional Cardiology, 28(3), 2015-06-01, pp. 236-248.

Zhang, H., Park, Y., Wu, J., Chen, X., Lee, S., Yang, J., Dellsperger, K. C. and Zhang, C. (2009) 'Role of TNF-alpha in vascular dysfunction.' Clin Sci (Lond) pp. 219-230.

Zhang, X., Chen, X., Hong, H., Hu, R., Liu, J. and Liu, C. (2022) 'Decellularized extracellular matrix scaffolds: Recent trends and emerging strategies in tissue engineering.' Bioact Mater, 10, Apr, 20210923, pp. 15-31.

Zhang, X., Dong, Y., Dong, H., Cui, Y., Du, Q., Wang, X., Li, L. and Zhang, H. (2021) 'Telmisartan Mitigates TNF-α-Induced Type II Collagen Reduction by Upregulating SOX-9.' ACS Omega, 6(17), 2021-05-04, pp. 11756-11761.

Zhang, Y. S., Oklu, R. and Albadawi, H. (2017) 'Bioengineered in vitro models of thrombosis: methods and techniques.' Cardiovascular Diagnosis and Therapy, 7(S3), 2017-12-01, pp. S329-S335.

Zhang, Y. S., Davoudi, F., Walch, P., Manbachi, A., Luo, X., Dell'Erba, V., Miri, A. K., Albadawi, H., et al. (2016) 'Bioprinted thrombosis-on-a-chip.' Lab on a Chip, 16(21), 2016-01-01, pp. 4097-4105.

Zheng, P.-S., Reis, M., Sparling, C., Lee, D. Y., La Pierre, D. P., Wong, C.-K. A., Deng, Z., Kahai, S., et al. (2006) 'Versican G3 Domain Promotes Blood Coagulation through Suppressing the Activity of Tissue Factor Pathway Inhibitor-1.' Journal of Biological Chemistry, 281(12) pp. 8175-8182.

Zheng, Y., Chen, J., Craven, M., Choi, N. W., Totorica, S., Diaz-Santana, A., Kermani, P., Hempstead, B., et al. (2012a) 'In vitro microvessels for the study of angiogenesis and thrombosis.' Proceedings of the National Academy of Sciences, 109(24), 2012-06-12, pp. 9342-9347.

Zheng, Y., Chen, J., Craven, M., Choi, N. W., Totorica, S., Diaz-Santana, A., Kermani, P., Hempstead, B., et al. (2012b) 'In vitro microvessels for the study of angiogenesis and thrombosis.' Proceedings of the National Academy of Sciences, 109(24), 2012-06-12, pp. 9342-9347.

Zhi, Z., Jooss, N., Sun, Y., Colicchia, M., Slater, A., Moran, L., Cheung, H., Di, Y., Rayes, J., Poulter, N., Watson, S and Iqbal, A. (2022) ‘Galectin-9 activates platelet ITAM receptors glycoprotein VI and C-type lectin-like receptor-2.’ Journal of Thrombosis and Haemostasis, 20(4) pp.936-950.

Zhou, L., Chen, X., Liu, T., Zhu, C., Si, M., Jargstorf, J., Li, M., Pan, G., et al. (2018) 'SIRT1-dependent anti-senescence effects of cell-deposited matrix on human umbilical cord

mesenchymal stem cells.' Journal of Tissue Engineering and Regenerative Medicine, 12(2), 2018-02-01,

Ziegler, T., Alexander, R. W. and Nerem, R. M. (1995) 'An endothelial cell-smooth muscle cell co-culture model for use in the investigation of flow effects on vascular biology.' Annals of Biomedical Engineering, 23(3), 1995/05/01, pp. 216-225.

Zufferey, A., Schvartz, D., Nolli, S., Reny, J.-L., Sanchez, J.-C. and Fontana, P. (2014) 'Characterization of the platelet granule proteome: Evidence of the presence of MHC1 in alpha-granules.' Journal of Proteomics, 101, 2014/04/14/, pp. 130-140.